Universidad del País Vasco Euskal Herriko Unibertsitatea
MEDIKUNTZA ETA ERIZAINTZA FAKULTATEA
FACULTAD DE MEDICINA Y ENFERMERÍA

Doktorego Tesia / PhD Thesis

E2F1 ETA E2F2 TRANSKRIPZIO FAKTOREEN PARTE-HARTZEA OBESITATEAREKIN LOTURIKO HEPATOKARTZINOMAREN GARAPENEAN

INVOLVEMENT OF THE TRANSCRIPTION FACTORS E2F1 AND E2F2 IN THE DEVELOPMENT OF OBESITY-RELATED HEPATOCARCINOMA

Daniela C. Mestre Congregado

2021

Lan hau burut ahal izateko, Euskal Herriko Unibertsitateko aurre-doktoretza diru-laguntza jaso nuen 2013ko otsailetik 2017ko urtarrilera.

2016an, egonaldi laburra egin nuen Txileko Unibertsitate Pontifizioko Medikuntza Fakultateko Gastroenterologia Departamentuan (Santiago de Chile) Euskal Herriko Unibertsitatearengandik jasotako diru-laguntzari esker

Lan honetako hainbat emaitza hurrengoko artikuluan argitaratu dira:

Gonzalez-Romero, Mestre et al. 2021. E2F1 and E2F2-Mediated Repression of CPT2 Establishes a Lipid-Rich Tumor-Promoting Environment. Cancer research, 81(11), pp. 2874-2887.

Quisiera expresar mi gratitud al Dr. Marco Arrese y su grupo de investigación por su acogida y apoyo durante mi estancia en la Pontificia Universidad Católica de Chile.

También deseo agradecer a la Dra. Ana Zubiaga y su grupo toda la ayuda a nivel práctico y teórico durante la presente Tesis Doctoral; así como a la Dra. María Luz Martínez Chantar y a Virginia Gutiérrez de Juan (CIC BioGUNE, Parque tecnológico de Bizkaia) y la Dra. Irantzu Bernales (Unidad de Expresión Génica, Servicio SGIker de la UPV/EHU) todos los servicios prestados para la determinación de algunos resultados.

Gracias a mis directores. Gracias Patricia, por darme la oportunidad de formar parte de este grupo y descubrirme el mundo de la ciencia. Gracias Igor por acompañarme en este largo camino.

Gracias a todos y cada uno de los Patetales, con vosotros todo se convierte en fácil y divertido. Este trabajo también es vuestro.

Gracias café mañanero y fanta, vosotras habéis vivido el día a día. Siempre soñando con que nos toque el euromillón, pero la verdadera suerte ha sido coincidir en la vida.

Gracias Josean, por toda tu ayuda en el laboratorio y los recorridos por la A8.

Gracias a mis amigos, por las risas, los consejos, los viajes y compartir hasta la última de las espuelas.

Gracias a mi familia, Aita y Ama, por apoyarme y solo soltarme para darme impulso. Ainhoa, eres el mejor regalo que me pudieron hacer. Betidanik eta betirako. Barron, gracias por ser y estar. Os quiero.

AURKIBIDEA/INDEX

AURKIBIDEA/INDEX

LABURDURAK/ABBREVIATIONS

LABURDURAK/ABBREVIATIONS

Aadac Arilazetamida deazetilasa (Arylacetamide deacetylase)

Acaa2 Azetil-KoA aziltransferasa 2(Acetyl-CoA acyltransferase 2)

***Acaca*/ACC** Azetil-KoA karboxilasa genea/proteina (Acetyl-CoA carboxylase gene/protein)

Acadl Azil-KoA deshidrogenasa (Acyl-CoA dehydrogenase)

Acadm Azil-KoA deshidrogenasa, tarteko kateduna (Acyl-CoA dehydrogenase medium chain)

Acadsb Azil-KoA deshidrogenasa, kate adarkatuduna (Acyl-CoA dehydrogenase short/branched) chain

Acsl Azil-KoA deshidrogenasa, kate luzeduna (Acyl-CoA dehydrogenase long chain)

Acsm Azil-KoA sintetasa, tarteko kateduna (Acyl-CoA synthetase medium chain)

Acta2 Alfa 2 aktina (Actin alpha 2)

Actb Beta aktina (Actin beta)

Adgre1 E1 hartzailearekin lotutako adhesiorako G proteína (Ahesion G protein coupled receptor E1)

AEB Ameriketako Estatu Batuak

ALT Alanina aminotransferase (Alanine aminotransferase)

AMP Adenosina monofosfatoa (Adenosine monophosphate)

AMPK AMP bidez aktibatutako proteina kinasa (AMP-activated protein kinase)

ANOVA Bariantzaren analisia (Analysis of the variance)

***Apob*/ApoB/APOB** B apolipoproteína sagu-genea/sagu-proteína/giza-genea (Apolipoprotein B mice gene/mice preotein/human gene)

***Apoe*/ApoE/APOE** E apolipoproteína sagu-genea/sagu-proteína/giza-genea (Apolipoprotein E mice gene/mice preotein/human gene)

ASM Metabolito azido disolbagarriak (Acid soluble metabolites)

ATP Adenosina trifosfatoa (Adenosine triphosphate)

Atp5a1 F1 ATP sintasa, alfa azpiunitatea (ATP synthase F1 subunit Alpha)

Atpif1 ATP sintasaren faktore inhibitzailea, 1 azpiunitatea (ATP synthase inhibitory factor subunit1)

ATZ Azido trikarboxilikoaren zikloa

BAT Brown adipose tissue, euskaraz behatu GEA

BCA Azido bizinkoninikoa (Bicinchoninic acid)

BMI Body mass index, euskaraz behatu GMI

BSA Behi seroalbumina (Bovine seroalbumin)

cAMP Adenosine monofosfato ziklikoa (Cyclic adenosine monophosphate)

***Ccna2*/CycA2** A2 ziklina genea/proteina (Cyclin A2 gene/protein)

***Ccnd3*/CycD3** D3 ziklina genea/proteina (Cyclin D3 gene/protein)

***Ccne1*/CycE1** E1 ziklina genea/proteina (Cyclin E1 gene/protein)

CD Oinarrizko dieta (Chow diet)

***Cd36*/CD36** Plaketen 4 glikoproteina genea/proteina (Platelet glycoprotein 4 gene/protein)

Cdk/CDK Ziklina menpeko kinasa genea/proteina (Cyclin dependent kinase gene/protein)

Cdk1/CDK1 Ziklina menpeko kinasa 1 genea/proteina (Cyclin dependent kinase 1 gene/protein)

Cdk2/CDK2 Ziklina menpeko kinasa 2 genea/proteina (Cyclin dependent kinase 2 gene/protein)

Cdk3/CDK3 Ziklina menpeko kinasa 3 genea/proteina (Cyclin dependent kinase 3 gene/protein)

Cdk4/CDK4 Ziklina menpeko kinasa 4 genea/proteina (Cyclin dependent kinase 4 gene/protein)

Cdk6/CDK6 Ziklina menpeko kinasa 6 genea/proteina (Cyclin dependent kinase 6 gene/protein)

cDNA Azido deoxierribonukleiko osagarria (Complementary deoxyribonucleic acid)

CE Kolesteril ester (Cholesteryl ester)

CHO Kolesterola (Cholesterol)

ChREBP karbohidratoekiko erantzun-elementuei lotzen den proteina (Carbohydrate response element binding protein)

Cidea **Zelula-heriotzak induzitutako DFFA motako A efektorea (**Cell death inducing DFFA like effector A**)**

CKI Cdk kinasa inhibitzailea (Cdk kinase inhibitor)

CL Kardiolipina (Cardiolipin)

CO_2 Karbono dioxidoa (*Carbon dioxide)*

CoA Coenzyme A, euskaraz behatu KoA

Col1a2 Kolagenoa I alfa 2 kate motakoa (Collagen type I alpha 2 chain)

Col3a1 Kolagenoa III alfa 1 kate motakoa (Collagen type III alpha 1 chain)

***Cpt1*/CTP1** Karnitina palmitoiltransferasa 1 genea/proteina (Carnitine palmitoyltransferase 1 gene/protein)

***Cpt2*/CTP2** Karnitina palmitoiltransferasa 2 genea/proteina (Carnitine palmitoyltransferase 2 gene/protein)

cRNA RNA osagarria/complementary RNA

CST Cell Signaling Technology etxe komertziala

CVD Cardiovascular disease, euskaraz behatu GKB

Cyb5a B5 zitokromoa A mota (Cytochrome B5 type A)

DBD DNAra lotzeko domeinua (DNA binding domain)

DEN Dietilnitrosamina (Diethylnitrosamine)

DG Diglizeridoa (Diglyceride)

dH_2O Ur distilatua (Distillated water)

Dhrf dihidrofolato erreduktasa (dihydrofolate reductase)

DMEM *Dulbecco´s modified Eagle* izeneko zelula-hazkuntza medioa (cell-culture medium)

DNA Azido deoxierribonukleikoa (Deoxyribonucleic acid)

DNase Deoxierribonukleasa (Deoxyribonuclease)

DNL *de novo* lipogenesia (*de novo* lipogénesis)

DP1 Dimerizazio-kide 1 proteina (Dimerization partner protein 1)

DP2 Dimerizazio-kide 2 proteina (Dimerization partner protein 1)

DP3 Dimerizazio-kide 3 proteina (Dimerization partner protein 1)

DP4 Dimerizazio-kide 4 proteina (Dimerization partner protein 1)

DTT Ditiotreitola (Dithiothreitol)

***E2f1*$^{-/-}$** *E2f1* knockout sagua/*E2f1* knockout mice

E2f1/E2F1 1 motako E2 faktorearen sagu-proteina / 1 motako E2 faktorearen giza proteina (E2 factor 1 mice protein/ E2 factor 1 human protein)

E2f1/E2F1 1 motako E2 faktorearen sagu-genea/ 1 motako E2 faktorearen giza-genea /E2 factor 1 mice gene/ E2 factor 1 human gene)

***E2f2*$^{-/-}$** *E2f2* knockout sagua/*E2f2* knockout mice

E2f2/E2F2 2 motako E2 faktorearen sagu-proteina / 1 motako E2 faktorearen giza-proteina (E2 factor 2 mice protein/ E2 factor 2 human protein)

E2f2/E2F2 2 motako E2 faktorearen sagu-genea/ 2 motako E2 faktorearen giza genea /E2 factor 2 mice gene/ E2 factor 2 human gene)

E2f3/E2F3 3 motako E2 faktorea (E2 factor 3)

E2f4/E2F4 4 motako E2 faktorea (E2 factor 4)

E2f5/E2F5 5 motako E2 faktorea (E2 factor 5)

E2f6/E2F6 6 motako E2 faktorea (E2 factor 6)

E2f7/E2F7 7 motako E2 faktorea (E2 factor 7)

E2f8/E2F8 8 motako E2 faktorea (E2 factor 8)

EDTA Azido etilenglikol tetraazetikoa (Ethylenglycol tetraacetic acid)

***Elovl6*/ELOVL6** Kate luzeko gantz-azidoen 6 elongasa genea/proteína (Long chain fatty acid elongase 6 gene/protein)

EMEM *Eagle´s minimum essential* izeneko zelula-hazkuntza medioa (cell-culture medium)

ER Erretikulu endoplasmikoa (Endoplasmic reticulum)

FA Fatty acid, euskaraz behatu GA

FADH Flabina adenine dinukleotidoa (Flavin adenine dinucleotide)

FAO Fatty acid oxidation

Fasn/FASN/FAS Gantz azidoen sintasa, sagu-genea/giza-genea/sagu edo giza proteína (Fatty acid synthase mice gene/human gene/mice or human protein)

FATP Gantz-azidoen proteina garraitzailea (Fatty acid transport protein)

FATP5 Gantz-azidoen 5 motako proteina garraitzailea (Fatty acid transport protein 5)

FBS Behi-fetalaren seruma (Fetal bovine serum)

FC Kolesterol askea/Free cholesterol

FDR False discovery rate

G_0 fase ez-ugalkorra (non-proliferative pase)

G_1 Gap1 edo hazkuntza-fasea (Gap1 or growth phase)

G_2 Gap2 fasea (Gap2 phase)

GA Gantz-azidoa

GAO Gantz-azidoen oxidazioa

Gapdh/GAPDH Glizeraldeido-3-fosfato deshidrogenasa genea/proteína (Glyceraldehyde-3-phosphate dehydrogenase gene/protein)

GEA Gantz-ehun arrea

GEZ Gantz-ehun zuria

GIB Giza inmunoeskasiaren birusa

GKB Gaixotasun kardiobaskularra

Gp6pdx/G6PDH Glukosa-6-fosfato deshidrogenasa genea/proteína (Glucose-6-phosphate dehydrogenase gene/protein)

Gt Ahuntz/Goat

GT Giro tenperatura

GZ Gorputz zetonikoak

HbA1c A1c motako hemoglobina (Hemoglobin A1c)

HBMS Hidroximetilbilano sintasa (Hidroxymethylbilane synthase)

HBV B hepatitisaren birusa (Hepatitis B virus)

HCC Kartzinoma hepatozelularra (Hepatocellular carcinoma)

HCV C hepatitisaren birusa (Hepatitis C virus)

HDAC Histona deazetilasa (Histone deacetylase)

HDL Dentsitate altuko lipoproteina (High density lipoprotein)

HDV D hepatitisaren birusa (Hepatitis D virus)

HEPES Azido 2-[4-(2-hidroxietil)piperazina-1-yl]etanosulfonikoa (2-[4-(2-hydroxyethyl)piperazin-1-yl]ethanesulfonic acid**)**

HFD Gantzetan aberatsa den dieta (High-fat diet)

HIV Human immunodeficiency virus, euskaraz behatu GIB

***Hnf4a*/HNF4-α** Gibeleko 4 alfa faktore nuklearraren genea/proteina (Hepatic nuclear factor 4 alpha gene/protein)

HOMA-IR Intsulinaren Erresistentzia Homeostasiaren Ereduaren Ebaluazioa (Homeostatic model assessment-insulin resistance)

Hr Zaldia (Horse)

HRP Errefau minaren peroxidasa (Horseradish peroxidase)

Hs-CRP Sentikortasun altuko C proteina erreaktiboa (High-sensitivity C-reactive protein)

IFC Dynamic array integrated fluidic circuits

IG Immunoglobulina (Immunoglobulin)

***Il1b*/IL-1β**	1β interleukina genea/proteina (Interleukin 1β gene/protein)
***Il6*/IL6**	6 interleukina genea/proteina (Interleukin 6 gene/protein)
IOD	Dentsitate optiko integratua (Integrated optic density)
IR	Intsulinarekiko erresistentzia (Insulin resistance)
KB	Ketone bodies, euskaraz behatu GZ
Kir6.2	KIR6.2 motako potasio kanal barruarazlea (Inwardly Rectifying Potassium Channel KIR6.2)
KoA	A koentzima
LD	Tanta lipidikoa (Lipid droplet)
LDL	Dentsitate txikiko lipoproteina (Low density lipoprotein)
Lipc	Gibeleko C lipase (Lipase C, hepatic type)
***Lpl*/LPL**	Lipoproteina lipase genea/proteína (Lipoprotein lipase gene/protein)
LZ	Leuzina kremailera (Leuzine zipper)
M	Fase mitotikoa (Mitotic phase)
MAFLD	Disfuntzio metabolikoarekin loturiko gibel koipetsuaren gaixotasuna (Metabolic-dysfunction-associated fatty liver disease)
MBM	Markatutako kutxa (Marked box)
Mcm	Minikromosoma mantentzeko konplexuaren atala (Minichromosome maintenance complex component)
ME	Entzima malikoa proteina (Malic enzyme protein)
Me1	1 motako entzima malikoaren genea (Malic enzyme 1 gene)
Me2	2 motako entzima malikoaren genea (Malic enzyme 2 gene)
MeV	Multi experiment viewer
MHO	Metabolikoki osasuntsua den obesitatea (Metabolically healthy obesity)
miR-122	122 mikro-RNA (Micro-RNA 122)
mRNA	RNA mezularia 8Messenger RNA)
MUHNW	Metabolikoki ez osasuntsua, pisu normalduna (Metabolically unhealthy with normal weight)
MUO	Metabolikoki osasuntsua ez den obesitatea (Metabolically unhealthy obesity)
NADH	Nikotinamida adenine dinukleotidoa (Nicotinamide adenine dinucleotide)

$NADP^+$ Nikotinamida adenine dinukleotido fosfato oxidatua (Nicotinamide adenine dinucleotide phosphate oxidized)

NADPH Nikotinamida adenine dinukleotido fosfatoa (Nicotinamide adenine dinucleotide phosphate)

NAFLD Gibel koipetsuaren gaixotasun ez-alkoholikoa (Non-alcoholic fatty liver disease)

NAS NAFLDaren aktibitate maila (NAFLD activity score)

NASH Esteatohepatitis ez-alkoholikoa (Non-alcoholic steatohepatitis)

Ndufs5 NADH:ubikinona oxidoerreduktasa S5 azpiunitatea (NADH:ubiquinone oxidoreductase subunit S5)

Ndufs7 NADH:ubikinona oxidoerreduktasa S7 azpiunitatea (NADH:ubiquinone oxidoreductase subunit S7)

Ndufv1 Erdiko NADH:ubikinona oxidoerreduktasa V1 azpiunitatea (NADH:ubiquinone oxidoreductase core subunit V1)

NES Nukleora esportatzeko seinalea (Nuclear export signal)

NFDM Gantzik gabeko esne hautsa (Non-fat dried milk)

NL Gibel normala (Normal liver)

NLS Nukleoan kokatzeko seinalea (Nuclear localization signal)

OME Munduko Osasun Erakundea

***Orc1*/ORC1** Jatorria ezagutzeko konplexuaren 1 azpiunitatea genea/proteina (Origin recognition complex subunit 1 gene/protein)

Oxphos Fosforilazio oxidatzailea (Oxidative phosphorylation)

P407 Poloxamer P-407 detergentea (Poloxamer P-407 detergent)

PBS Fosfatoarekin indargetutako gatz-disoluzioa (Phosphate buffered saline)

PC Fosfatidilkolina/Phosphatidylcholine

PCR Polimerasaren erreakzio kateatua/Polymerase chain reaction

p-CREB Fosforilatutako CREB (Phosphorylated CREB)

PDK4 Pirubato deshidrogenasa lipoamida kinasa 4 isozima (Pyruvate dehydrogenase lipoamide kinase isozyme 4)

PE Fosfatidiletanolamina (Phosphatidylethanolamine)

PL Fosfolipidoa (Phospholipid)

Plk1 Polo motako kinasa 1 (Polo like kinase 1)

PMSF Fenilmetanosulfonilo fluoridoa (Phenylmethanesulfonyl fluoride)

PNPLA3 Patatina motako fosfolipasa 3 domeinuduna (Patatin like phospholipase domain containing 3)

***Ppara*/Ppara/PPAR-α** Peroxisoma proliferatzaileagatik aktibatutako alfa hartzailea sagu-genea/giza-genea/proteina (Peroxisome proliferator-activated receptor- alfa mice gene/human gene/protein)

***Pparb*/Pparb/PPAR-β** Peroxisoma proliferatzaileagatik aktibatutako beta hartzailea sagu-genea/giza-genea/proteina (Peroxisome proliferator-activated receptor- beta mice gene/human gene/protein)

***Pparg*/Pparg/PPAR-γ** Peroxisoma proliferatzaileagatik aktibatutako gamma hartzailea sagu-genea/giza-genea/proteina (Peroxisome proliferator-activated receptor-gamma mice gene/human gene/protein)

Ppargc1a/PGC-1α 1 alfa motako PPAR-γ koaktibatzailearen genea/proteina (PPAR-γ-coactivator-1-alpha gene/protein)

Ppargc1b/PGC-1β 1 beta motako PPAR-γ koaktibatzailearen genea/proteina (PPAR-γ-coactivator-1-beta gene/protein)

Ppia A ziklofilina (Cyclophilin A)

PPRE Peroxisoma proliferatzaileari erantzueko elementua (Peroxisome proliferator response element)

pRB Fosforilatutako RB/Phosphorylated RB

PS Serum fisiologikoa (Physiological serum)

R Errestrikzio kontrol-puntua (Restriction checkpoint)

R1 1 erreaktiboa (Reagent 1)

R2 2 erreaktiboa (Reagent 2)

RB Untxia (Rabbit)

Rb/Rb1 Erretinoblastoma genea/proteína (Retinoblastoma gene/protein)

RNA Azido erribonukleikoa (Ribonucleic acid)

ROS Oxigeno espezie erreaktiboak (Reactive oxygen species)

RT Room temperature, euskaraz behatu GT

rt-qPCR Denbora errealean kuantifikatzailea den polimerasaren kate-erreakzioa (Real time quantitative PCR)

Rxr/RXR X erretinoidearen hartzailearen genea/proteína (Retinoid X receptor gene/protein)

Rxra alfa motako X erretinoidearen hartzailea (Retinoid X receptor Alpha)

S Sintesiaren edo DNA erreplikazioaren fasea (Synthesis or DNA replication pase)

SC Santa Cruz etxe komertziala (Santa Cruz Trading House)

***Scd1*/SCD1** Estearoil-KoA desaturasa 1 genea/proteína (Stearyl-CoA desaturase 1 gene/protein)

***Scd2*/SCD2** Estearoil-KoA desaturasa 2 genea/proteína (Stearyl-CoA desaturase 2 gene/protein)

Sdha Sukzinato deshidrogenasa konplexuaren flavoproteina A azpiunitatea (Succinate dehydrogenase complex flavoprotein subunit A)

SDS Sodio dodezil sulfatoa (Sodium dodecyl sulphate)

SDS-PAGE SDS-poliakrilamida gelezko elektroforesia (SDS-polyacrylamide gel electrophoresis)

SEM batez bestekoaren errore estandarra (Standard error of the mean)

siC isiltze-kontrola (Control silencing)

si*E2F1* *E2F1* isilarazitako zelulak (*E2F1* silenced-cells)

si*E2F2* *E2F2* isilarazitako zelulak (*E2F2* silenced-cells)

siRNA RNA isilarazlea (Silencing RNA)

Slc27a1 Solute carrier family 27 member 1

Slc27a5 Solute carrier family 27 member 1

Srepb1/SREBP1c Esterolagatik erregulatutako elementura lotzen den 1c sagu/giza proteina (Sterol regulatory element binding protein 1c mice/human)

T2DM Type II diabetes mellitus, euskaraz behatu 2MDM

TAE Tris-azetato-EDTA/Tris-acetate-EDTA

TBP TATA kutxara lotzen den proteina (TATA box binding protein)

TBST Tris-arekin indargetutako gatz soluzioa (Tris-buffered saline supplemented with Tween 20)

TCA Tricarboxylic cycle, euskaraz behatu ATZ

TE Tris-EDTA

TEA Trietanolamina (Triethaholamine)

TG Triglizeridoa (Triglyceride)

***Tgfb1*/TGF-β** beta Hazkuntza-faktore eraldatzailea genea/proteina (Transforming growth factor beta gene/protein)

Tk/TK Timidina kinasa sagu-proteina/giza-proteina (*Thymidine* kinase mice protein/human protein)

TLC Geruza fineko kromatografia (Thin layer chromatography)

TLR Toll motako hartzailea (*Toll*-like receptor)

***Tnf*/TNF-α** gene/protein)	Nekrosi tumoralaren alfa faktorea genea/proteína (Tumoral necrosis factor alpha
Tris	Tris(hidroximetil)aminometanoa (Tris(hydroxymethyl)aminomethane)
USA	United States of America
VLDL	Dentsitate oso txikino lipoproteina (Very-low density lipoprotein)
WAT	White adipose tissue, euskaraz behatu GEZ
WB	Western blotting
WHO	World Health Organization, euskaraz behatu
WT	Sagu basatia (Wild type mice)
2MDM	II motako diabetes mellitus

SUMMARY

SUMMARY

1. Introduction and objectives

According to the World Health Organization (WHO) global database, **obesity** is a risk to health condition characterized by excessive fat accumulation in the body, whose prevalence worldwide has nearly tripled in the last 40 years, both in high-income countries and non-developed nations. It is associated with hepatic metabolic dysregulations that contribute to liver lipid accumulation and non-alcoholic fatty liver disease (NAFLD) progression.

NAFLD is characterized by steatosis or non-alcoholic fatty liver, a situation in which the increased TG content in liver arises from a decompensation between lipid deposition (mainly, serum fatty acid (FA) uptake and *de novo* lipogenesis or DNL) and elimination pathways (mainly, lipid oxidation or FAO and very-low density lipoprotein or VLDL export). Nowadays, NAFLD is a relevant risk factor for hepatocellular carcinoma (HCC). HCC that arises in the setting of steatosis is recognized as **NAFLD-related HCC** and shows differential features (i.e. lipid accumulation and inflammation) when compared to HCC derived from other etiologies. There is a wide variety of genetic drivers in HCC, which could explain the high heterogeneous characteristics of HCC concerning tumor histology, cell signaling pathways and metabolic reprogramming. Regarding the NAFLD-related HCC's phenotype, it should be note that obesity by itself can also contribute to metabolic impairments, since it is related to a metabolic signature which even differs between metabolically healthy obesity (MHO) and metabolically unhealthy obesity (MUO) subjects.

The **E2F transcription factor family**, typically described as cell cycle regulators, is also responsible for metabolic changes in liver pathological conditions and the associated metabolic complications such as obesity and diabetes. Alterations in E2Fs have also been reported in HCC, which points out their relevance in liver cancer. Most of the investigations are focused on E2F1, who is described as oncogene or tumor suppressor depending on the study. In case of E2F2, it has been associated too often with E2F1 functional similarity. However, several works have already shown that although they share several processes, some functions are unique for one or the other. Further investigation is needed to discern common and particular mechanisms between E2F1 and E2F2, as well as to establish their potential impact to NAFLD-related HCC.

Taking all this into account, we proposed that **E2F1 and E2F2 regulate the metabolic pathways involved in obesity-related NAFLD development and its progression to HCC**. In this context, the specific aims of this project were: 1) To investigate if E2F1 and/or E2F2 are involved in obesity-linked NAFLD development and its progression to HCC; 2) to identify the mechanisms by which E2F1 and/or E2F2 drive the metabolic dysregulation involved in NAFLD development and progression to HCC; 3) to validate E2F1 and/or E2F2 as early biomarkers in obesity-related NAFLD.

2. Experimental procedures

Animal models were male *E2f1* knockout (*E2f1*$^{-/-}$), *E2f2* knockout (*E2f2*$^{-/-}$) and their wild type (WT) (129/Sv x C57BL/6) littermates. The hepatic procarcinogen diethylnitrosamine (DEN) was injected intraperitoneally to mice on postnatal day 14 and, after weaning, mice were placed in a high-fat diet (HFD) (referred to them as DEN HFD group) or in chow-diet (CD) (named as DEN CD group) until sacrificed at 3 months old for NAFLD study or at 9 months old for HCC study. Other age-matched groups were administered vehicle alone (physiological serum, PS) combined with CD (named as CD group) or HFD (referred to them as HFD group). Hepatic expression of *E2f1* and *E2f2* genes was analyzed in the different stages of the liver disease in WT mice. In all the groups of study, several body parameters and food consumption were obtained, liver injury was measured, liver and serum lipid profile was analyzed as well as liver histology, fibrosis grade, cell cycle activation and insulin resistance (IR). In 9 month-old *E2f2*$^{-/-}$ mice, a gene expression profiling was assessed and, both in 3 and 9 month-old *E2f2*$^{-/-}$ mice, the metabolic fluxes of the pathways involved in liver lipid acquisition and elimination were also analyzed.

E2F1 and *E2F2* was silenced via siRNA in human hepatoma **HepG2 cell line** to measure triglyceride (TG) content and the metabolic flux of its synthesis and degradation.

Finally, E2F1 and E2F2 expression were assessed in **liver biopsies** of patients previously classified as histologically normal liver (NL) or NAFLD.

3. Results

The measure of body weight and white adipose tissue (WAT) index showed that HFD administration induced obesity in 3 month-old mice, a condition that was exacerbated when mice get older. Of note, body weight increase was not due to a higher consumption of food. Study of the lipid content revealed that this

effect was accompanied by triglyceride (TG), diglyceride (DG) and cholesteryl ester (CE) accumulation in liver and, in fact, by NAFLD development. Exposition just to HFD also promoted the progression to NAFLD-HCC in our mice model of study. By contrary, the results showed that DEN-induced HCC was not linked to obesity or NAFLD development. Exposition only to HFD was the less carcinogenic treatment, nevertheless, feeding a lipid-rich diet exacerbates DEN-induced HCC concerning tumor quantity and size. In accordance with the histopathologic features, liver lipid accumulation in terms of TG and CE was evident in mice exposed to DEN HFD who developed NAFLD-HCC.

The results showed that liver E2f2 was only upregulated in mice with obesity-related NAFLD and NAFLD-HCC, indicating that E2f2 was induced in obesity since the early stages of the liver disease. This is in accordance with the enhanced expression of E2F1 and E2F2 in obese patients, even when they did not present liver disease, which points out its value as a predictor of the liver disease. Of note, E2F2 overexpression was more exacerbated once NAFLD was developed in obese patients, who met criteria to be classified as MUO and would allow to differentiate MUO patients by E2F2 content.

After determining that there was an involvement of E2f1 and E2f2 in obesity-related liver disease, given the effect of the metabolic status in E2F1 and E2F2 levels in liver of obese patients and mice, the role of E2f1 and E2f2 in the instauration and progression of NAFLD and NAFLD-HCC was investigated. We observed that *E2f1*$^{-/-}$ and especially *E2f2*$^{-/-}$ animals showed a nearly complete reduction in development of liver tumors when induced by all the treatments, indicating that the absence in *E2f1* and, especially, in *E2f2* confers protection against the treatment-induced hepatocarcinogenesis. As demonstrated by histochemical analysis and lipid quantification, the lack of *E2f1* or *E2f2* also restrained the development of liver lipid accumulation in response to HCC-induction treatments. Similar metabolic profile was displayed in human HCC cell line when *E2F2* was silenced, but not in case of *E2F1* silencing. Notably, *E2f1* and, especially, *E2f2* deficiency also protected mice from the hepatoesteatosis developed at 3 months old, when cell cycle is not active, evidencing the metabolic role of E2f1 and E2f2. According to the prevention of progressive NAFLD, gene expression and histochemistry analysis revealed that *Tfgb1*-mediated fibrosis and *Il1b*-mediated inflammation presented in our model of obesity-related NAFLD and NAFLD-HCC were also prevented in absence of *E2f1* and *E2f2*.

The involvement of E2f2 in the progression of the obesity-linked liver disease was more relevant than E2f1, then, we investigated the transcriptional program associated with the resistance to NAFLD-related HCC in the absence of *E2f2* and observed that the most significantly upregulated genes were

clustered in lipid catabolism and energy production, both typically induced during HCC, while the downregulated locuses were related to cell cycle, apoptosis and lipid synthesis, which agrees with the observation that absence in *E2f2* protected mice from NAFLD and related HCC.

Based on the microarray data, metabolic pathways involved in liver lipid input and output were analyzed. Concerning lipid elimination pathways, deficiency in E2F2 was found associated to high rates of fatty acid oxidation (FAO) in human tumoral cells and in mice livers, together with increased expression of genes related to several β-oxidation reactions and activation of FAs. Notably, gene and protein expression of CPT2, which participates in the rate limiting process of FAO and is promotor of hepatocarcinogenesis in obesity, was downregulated in mice models of NAFLD and NAFLD-HCC and upregulated when *E2f2* was deficient. Besides, contrary to that observed in NAFLD and NAFLD-HCC, absence in *E2f2* was also linked with upregulation of HNF4-α, a nuclear receptor that induces FAO and has a role in the inhibition of HCC. Hence, the results suggest that enhanced FAO, mediated by an increased channeling of FAs towards the mitochondria, was one of the main mechanism involved in the protection from the liver disease by E2f2. If more ATP is needed by cells, the reducing power obtained from FAO and TCA is derived to oxidative phosphorylation (oxphos). We observed that different genes related to this process had low expression in obesity-derived HCC, while they were induced in *E2f2* deficient mice livers. The expression pattern of PGC-1β, a factor that mediates oxphos and regulates obesity-driven steatosis, was also similar.

Regarding lipid input pathways, increased esterification of [^{3}H]-glycerol and FA, together with upregulated expression of PPAR-γ (gene and protein) and its target-genes involved in lipid transport and storage, indicates that TG biosynthesis was also a pathogenic mechanism promoting NAFLD and its progression to HCC. In *E2f2* depleted mice livers exposed to DEN HFD, all those parameters were decreased, which suggest that the absence in *E2f2* prevented the lipogenesis induced by the treatment. *de novo* lipogenesis (DNL) of TG assessed by [^{3}H]-acetate was not altered in *E2f2*$^{-/-}$ mice exposed to DEN HFD, which indicates that the reduced TG biosynthesis related to the lack of *E2f2* was specifically due to a disruption of the esterification and not to a decreased DNL.

The results also suggest that dyslipidemia had an important role in NAFLD and its progression to HCC, since serum TG and FA were increased in mice exposed to DEN HFD. However, dyslipidemia was not caused by altered hepatic VLDL export, as liver VLDL secretion rate and *Apob* and *Apoe* expression maintained unaltered. WAT lipolysis, responsible for FA supply in liver and other non-adipose tissues if energy is required, was neither a route involved, since WAT index was increased in WT mice with obesity-

related NAFLD as compared to controls. Despite the altered lipid serum profile in mice who developed NAFLD and NAFLD-HCC, increased *Lpl* expression suggests that hepatic catabolism of circulating TG was enhanced, a condition that leads to lipid accumulation in liver and HCC as it has been described elsewhere. Concerning the role of E2F2, the results indicate that absence in *E2f2* protected mice from the dyslipidemia and serum TG removal by liver. Indeed, serum FA and TG were not increased in *E2f2*$^{-/-}$ mice exposed to proesteatotic conditions, although WAT lipolysis was enhanced, WAT index was diminished and liver expression of *Lpl* was downregulated.

Collectively, liver FAO, lipid synthesis and TG uptake, impaired routes in obesity-derived HCC, were also altered in early stages of the liver disease, a condition in which E2F2 was upregulated. Together with the fact that *E2f2* depletion protected mice from the metabolic profile associated to progressive NAFLD *(Figure 1)*, we suggest that E2F2 is orchestrating the adaptive metabolism that precedes the NAFLD-**related HCC**. The relevance of this finding lies in the fact that E2F2 could be used as early biomarker of the obesity-**related** liver disease.

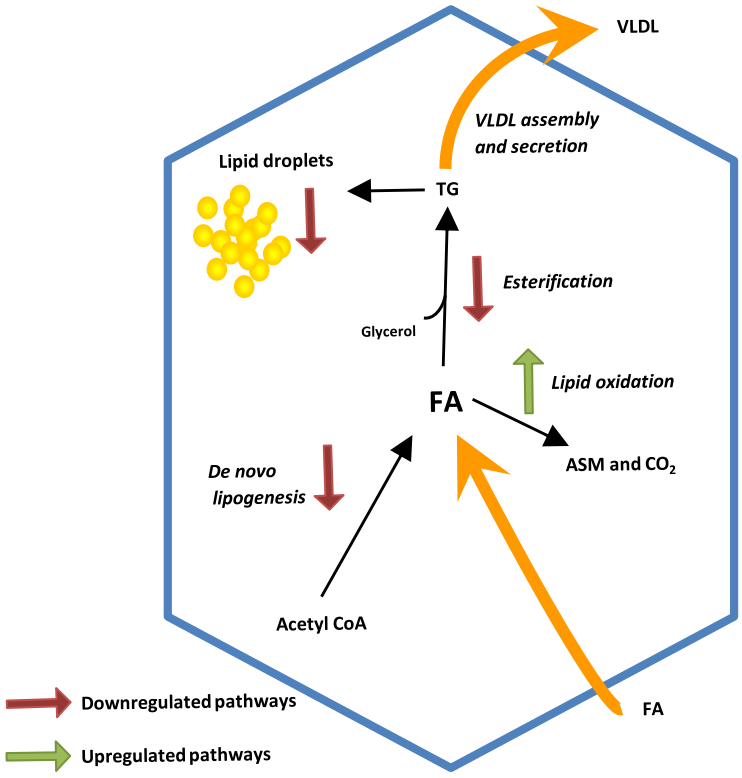

Figure 1. Schematic representation of FA metabolism in *E2f2*$^{-/-}$ mice liver to prevent obesity-related NAFLD and progression to HCC. ASM, Acid soluble metabolites; FA, Fatty acid; HCC, hepatocellular carcinoma; TG, triglyceride; NAFLD, non-alcoholic fatty liver disease.

Finally, metabolic complications of obesity and NAFLD include type II diabetes mellitus (T2DM), a condition that results from insulin resistance (IR) and that increases the risk for HCC development in NAFLD patients. Besides, the role of E2F1 in maintaining the glucose homeostasis and prevention of diabetes has

been already described. Thus, we wondered if the early stages of NAFLD and its progression to HCC would lead to IR and if E2f1 and/or E2f2 could be involved on it. The corresponding tolerance tests revealed that IR was developed in obese WT mice with NAFLD exposed to a short-term HFD combined or not with DEN, suggesting that it is a sole domain of diet-induced obesity. The absence in *E2f1* and *E2f2* prevented the IR associated to NAFLD-induction treatment but did not protect from that related to NAFLD-HCC inductor treatment.

4. Conclusions

1. E2F1 and, especially, E2F2 transcription factors are involved in obesity-related NAFLD development and its progression to HCC.

1.1 Both E2F1 and E2F2 are overexpressed in obese patients with NAFLD and *E2f2* is also overexpressed in mice models of obesity-related NAFLD and NAFLD-related HCC, which implies that these transcription factors are proesteatotic and oncogenic factors in the liver disease.

1.2. Absence in E2f1 and, particularly, in E2f2 prevent the development of obesity-related NAFLD. Mice lacking *E2f1* or *E2f2* do not present the hepatosteatosis neither liver inflammation caused by NAFLD-induction treatments, showing that these transcription factors are required for obesity-related NAFLD.

1.3. *E2f1* and *E2f2* deficiency in mice confers resistance to NAFLD-related HCC development and the associated fibrosis and lipid storage, suggesting that both E2f1 and E2f2 are required in those processes.

2. E2f2 transcription factor coordinates the metabolic reprogramming involved in obesity-related NAFLD development and its progression to HCC.

2.1. E2f2 controls the metabolic pathways involved in liver lipid storage from the early stages of the liver disease. As a protective mechanism, *E2f2* deficiency in mice prevents the dyslipemia and the increased liver TG synthesis and uptake linked to NAFLD and NAFLD-HCC. In addition, increased FAO, mediated by an increased channeling of FAs towards the mitochondria, contributes to the liver resistance to NAFLD and HCC development in *E2f2* knockout mice.

2.2. In addition to the improvement of the lipid profile, *E2f2* deficiency in mice prevents the IR linked to early stages of the obesity-related NAFLD, but not that associated to NAFLD-HCC.

3. E2F1 and, particularly, E2F2 are potential prognostic markers for the obesity-related NAFLD. E2F1 and E2F2 are induced in obesity with and without NAFLD. Besides, the increase in E2F2 liver content is even more exacerbated once NAFLD is developed.

Chapter A. INTRODUCTION

Chapter A. INTRODUCTION

1. The liver

1.1. The liver structure and anatomy

The **liver** is the second largest organ and the biggest gland in the human body and constitutes the 2.5% of the body weight (Juza, Pauli 2014). It occupies the space inferior to the diaphragm, in the upper-right hand abdominal cavity, next to the digestive track and the whole-body blood-flow. The strategic localization allows liver to play its function in the regulation of the organic metabolism.

The **parenchyma** is the functional structure of the liver and it is formed by 4 lobes (right, left, quadrate and caudate or Spiegel lobe) (Arias, Wolkoff et al. 2009, Malarkey, Johnson et al. 2005) *(Figure B1.A)*. Each lobe is separated in hexagonal structural units called **lobules** by the Glisson's capsule, a connective tissue layer that surrounds the parenchyma *(Figure B1.B)*. Lobules contain a central hepatic vein and, in the edge, the portal triad, which is a branch of the portal vein, a branch of the hepatic artery and a branch of the bile duct. The central vein and the portal triad are connected by sinusoids and hepatocytes rows (Remak trabeculaes or cordons), which are in turn separated by endothelium cells and the perisinusoidal space of Disse *(Figure B1.C)*.

The functional and microcirculatory unit of the liver is the **hepatic acinus** *(Figure B1.D)*, a parenchymal space connecting two portal triads that extends outwards the two adjacent central veins. There is an oxygen concentration gradient depending on the distance from the triad, hence, the hepatic acinus is divided into 3 regions: periportal (1), intermediate (2) and perivenous (3).

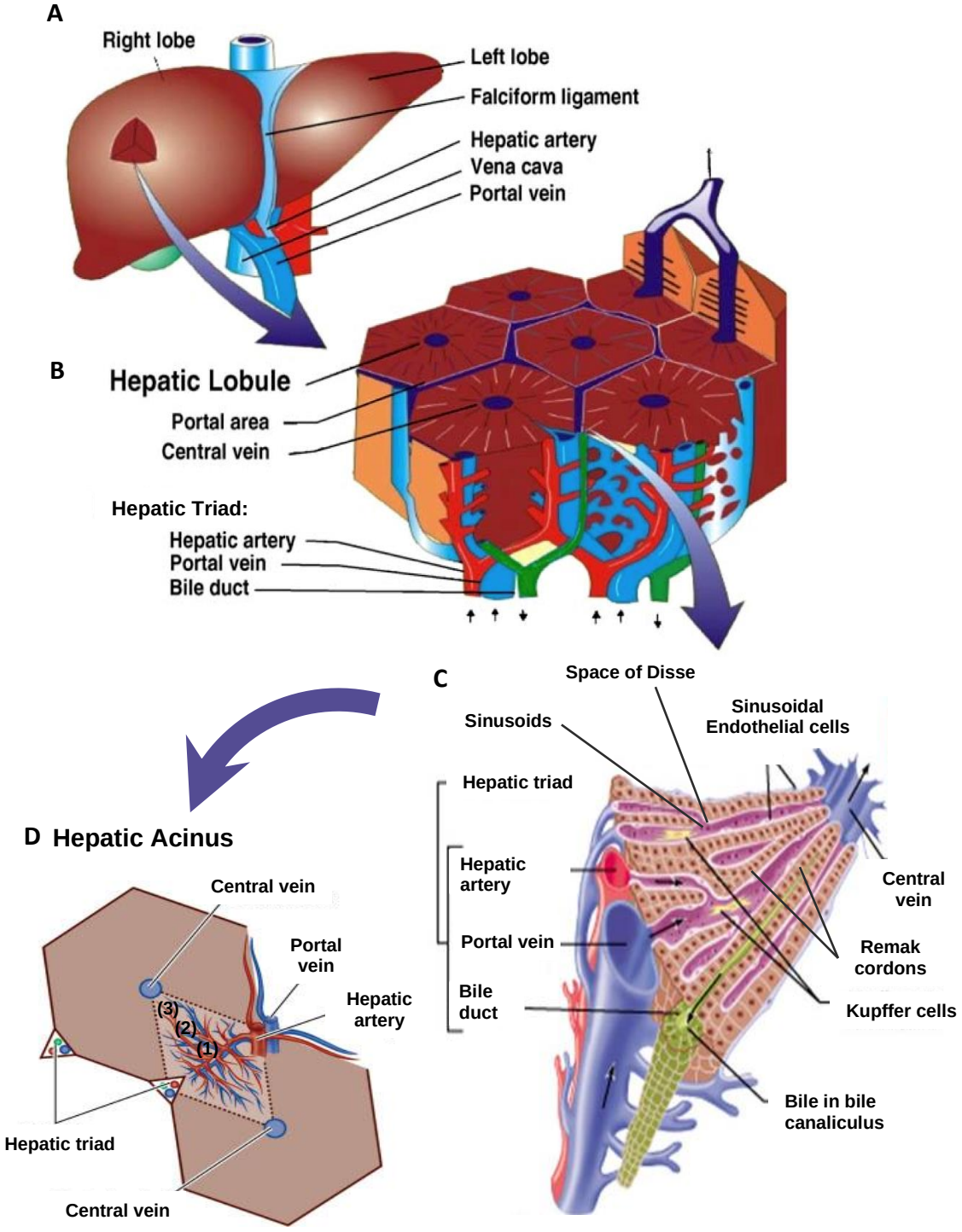

Figure B1. The liver (A) and its structural (B, C) and functional units (D): the lobule and the acinus. The hepatic acinus is represented with a dotted line. The zonation is indicated as (1) periportal, (2) intermediate and (3) perivenous. Images adapted from https://bio.mox.polimi.it/nanomedicine/perfusion-characteristics-liver-tissue/ and https://medicine.academic.ru/99185/hepatic_acinus.

The liver is composed of several **cell populations** that are divided in two groups: the parenchymal cells and the non-parenchymal cells. The parenchymal cells or **hepatocytes** compose the 80% of the total volume of the liver and are the responsible of many synthetic and metabolic functions of the tissue *(Figure B2)*. They are polarized by three molecular specializations. The canalicular or apical domain is specialized in bile excretion, whereas the basolateral o sinusoidal domain is where the exchange of substances occurs between the blood and the hepatocyte, for example, lipid secretion. The lateral domain is the responsible for cellular adhesion. Due to their numerous metabolic functions, hepatocytes contain an important amount of organelles in their cytoplasm.

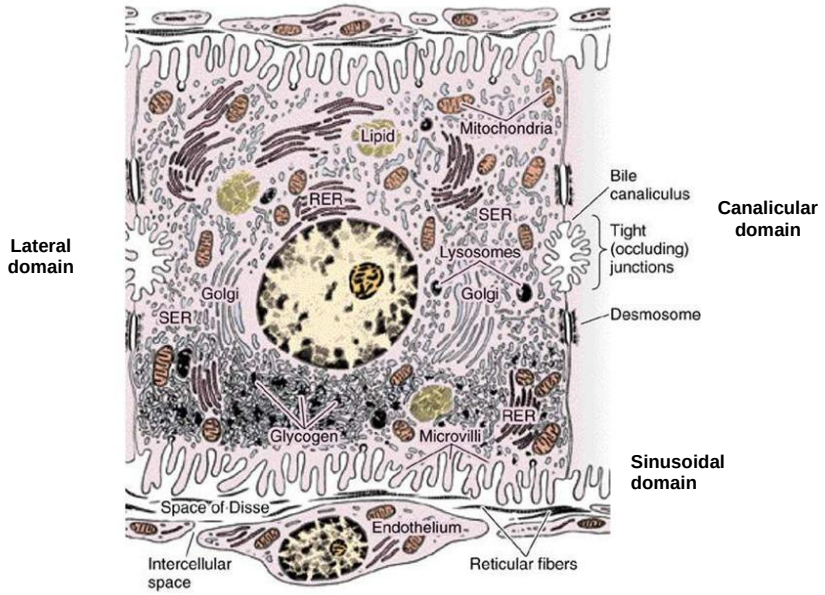

Figure B2. Schematic representation of the hepatocyte. RER, rough endoplasmic reticulum; SER smooth endoplasmic reticulum. Image modified from http://intranet.tdmu.edu.ua/data/kafedra/internal/histolog/classes_stud/en/stomat/ptn/1/17%20Digestive%20system.htm

The non-parenchymal or **sinusoidal cells** are 1) the endothelial cells (involved in the exchange of substances between the portal blood and the hepatocytes), 2) Kupffer cells (phagocytic macrophages involved in the innate immune system), 3) stellate cells or Ito cells (fat storing cells with key function in fibrogenesis as source of extracellular matrix components), 4) lymphoid cells or Pit cells (lymphocytes with natural killing activity) and 5) the biliar epithelium.

Apart from its heterogeneous structure and functional complexity, the liver has the capacity to regenerate, which is a compensatory mechanism to injury (Mao, Glorioso et al. 2014). Multiple **metabolic processes** are also performed in liver: maintenance of the whole body ammonia and bicarbonate

homeostasis, processing of absorbed nutrients and xenobiotics, biliary acid synthesis and bile formation, synthesis of most of the plasma proteins, storage and processing of signal molecules and hormones and involvement in the acute immune response of the organism (Arias, Wolkoff et al. 2009, Malarkey, Johnson et al. 2005).

Moreover, liver plays an essential role in the regulation of **energy metabolism** and acts as a centerpiece that is metabolically connected to other tissues (Betts, Young et al. 2013, Rui 2014). Indeed, liver is the responsible for the synthesis, metabolism, disposal and delivering of proteins, lipids and carbohydrates. In a **positive energy balance** (postprandial state), liver builds up body energy repositories in the forms of glycogen and triglycerides (TG) both in liver and white adipose tissue (WAT). Other enhanced anabolic pathways are the cholesterogenesis and the synthesis of amino acids, where the latter molecules are precursors of proteins and other nitrogen compounds. The energy and reducing equivalents consumption required for these anaplerotic reactions are supported by hepatic oxidation of glucose. By contrast, in a **negative energy balance** (during fasting or exercise), liver secrets glucose and ketone bodies (KB) to provide essential metabolic fuel for extrahepatic tissues like brain, muscles and heart. For that, energy source is obtained from fatty acid (FA) oxidation. Glucose and FAs are not only released from hepatic storages, but they are also newly synthetized in liver from precursors that arise from WAT and muscles. Energy metabolism in liver is strictly regulated by several hormones, neuronal signals and nutrients. Mainly, insulin and glucose drive the reactions in fed state, while glucagon is the responsible for the metabolic coordination in deprivation. Any impairment in the control of energy metabolism could be associated with metabolic diseases such as non-alcoholic fatty liver disease (NAFLD) or type II diabetes mellitus (T2DM) (Jones 2016).

1.2. Lipid metabolism in the liver

As mentioned, the liver is a central organ modulating the whole body metabolism and it plays a key role regulating lipid metabolism. Under physiological conditions, low levels of liver lipid content remain constant, since the balance between lipid sourcing and removal is correctly compensated (Kawano, Cohen 2013). Major routes involved in liver lipid acquisition are serum free FA uptake and de novo lipogenesis (DNL) of TG, whereas those regulating TG disposal are its degradation through FA oxidation and its secretion in very-low density lipoproteins (VLDL) (Figure B3).

Rate of **FA uptake** in liver depends on the serum FA concentration, which is in turn regulated by lipolysis of WAT (Kawano, Cohen 2013). WAT is the essential TG store in eukaryotes and a process called lipolysis takes place in this organ, that is to say, the hydrolysis of TG resulting in free FA and glycerol which are released into the circulation (Duncan 2007). It is mainly enhanced in fasting state, since its product molecules are used to fuel the energetics demands of other tissues. Besides, liver uptake of FA also depends on the capacity that hepatocytes exhibit for it, a process carried out through plasma membrane transporters like fatty acid transport proteins (FATPs) and patelet glycoprotein 4 (CD36) (Kawano, Cohen 2013).

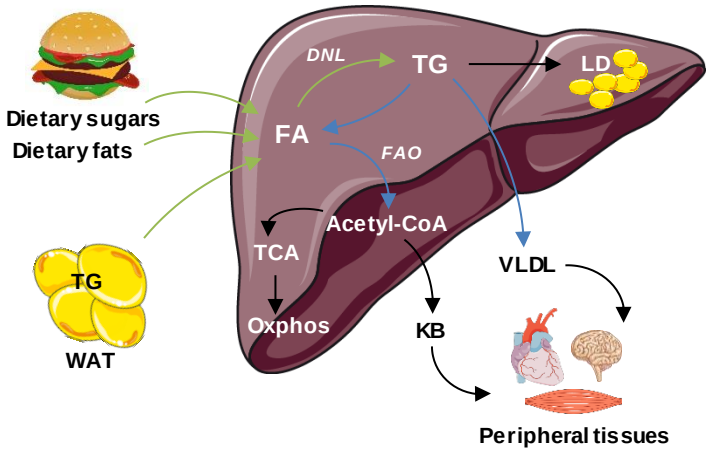

Figure B3. Key mechanisms regulating lipid metabolism in liver. Lipid sourcing routes are indicated with green arrows and pathways involved in lipid elimination are indicated with blue arrows. DNL, *de novo* lipogenesis; FA, fatty acids; FAO, fatty acid oxidation; KB, ketone bodies; LD, lipid droplets; Oxphos, oxidative phosphorylation; TG, triglyceride; TCA, tricarboxylic cycle; VLDL, very-low density lipoproteins; WAT, white adipose tissue.

The second major source of liver lipids is **DNL**. Dietary sugars (i.e. glucose and especially fructose) are used to synthetize new FA. Glucose is catabolized to acetyl-CoA by glycolysis and oxidation of pyruvate (Kawano, Cohen 2013). Acetyl-CoA is then carboxylated by acetyl-CoA carboxylase (ACC), the rate-limiting enzyme, and the resulting malonyl-CoA is converted to palmitate by FA synthase (FAS). After, long chain FA elongase 6 (ELOVL6) and stearyl-CoA desaturases (SCD1, SCD2) brings about the conversion of palmitate to monounsaturated FAs. Finally, acyltransferases carry out several reactions in which three newly synthetized FAs are sequentially esterified with glycerol-3-phosphate and leads to the formation of phosphatidic acid, diglycerides (DG) and triglycerides. The reducing power (NADPH and $FADH_2$) needed for DNL is furnished in the reactions catalyzed by glucose-6-phosphate dehydrogenase (G6PDH) and malic enzyme (ME) (Wise EM 1964). The production of NADPH does not control the synthesis of FA, but DNL is mainly regulated at transcriptional level by carbohydrate response element binding protein (ChREBP) and sterol regulatory element binding protein 1c (SREBP1c), which are induced by glucose and insulin respectively. Besides,

peroxisome proliferator-activated receptor γ (PPAR-γ) also regulates lipogenic genes (Gavrilova, Haluzik et al. 2003).

One of the aforementioned ways regarding the hepatic TG disposal is the catabolism of FA through **mitochondrial β-oxidation** (FAO), a process that provides energy source for ATP production when serum glucose levels are low (Kawano, Cohen 2013). Firstly, FAs must be activated to their coenzyme A derivatives so they gain biological reactiveness. For that, fatty acyl-CoA synthetases (i.e. Acsm1, Acsm2, Acsl1), possibly in collaboration with FATPs, catalyze the conversion of FA to fatty acyl-CoAs. Then, carnitine palmitoyltransferases (CPT1 and CPT2) transport fatty acyl-CoAs into the mitochondrial matrix and, once there, fatty acyl-CoAs enter the FAO cycle, where are broken down to acetyl-CoAs. This cycle requires four types of enzymes: acyl-CoA dehydrogenases (i.e. Acadl, Acadm, Acadsb), 2-enoyl-CoA hydratases, 3-hydroxyacyl-CoA dehydrogenases and 3-oxoacyl-CoA thiolases (i.e. Acaa2). Then, acetyl-CoAs are oxidized in the tricarboxylic (TCA) cycle and the resultant NADH and $FADH_2$ are used to produce ATP in the oxidative phosphorylation (Oxphos) process. Acetyl-CoA overload is rerouted to the synthesis of KBs, which are an alternative fuel for highly oxidative extrahepatic tissues (particularly brain and heart) in fasting (Puchalska, Crawford 2017).

In a postprandial state, FAO is inhibited by the effect of insulin (Kawano, Cohen 2013). Contrary, glucagon promotes FAO during fasting through regulation of the key enzymes AMP-activated protein kinase (AMPK), ACC and CPT (Kawano, Cohen 2013, Schreurs, Kuipers et al. 2010). Regarding the transcriptional regulation, a major role of PPAR-α has been largely described (Kawano, Cohen 2013). Active PPAR-α assembles with retinoid X receptor (RXR) to form heterodimers and binds to peroxisome proliferator response elements (PPREs). PPAR-α also interacts with PPAR-γ-coactivator (PGC) 1α and 1β, both involved in promotion of FAO, oxphos and mitochondrial biogenesis in liver (Finck, Kelly 2006).

Hepatic lipid content can also be balanced by **TG export in VLDL** particles (Kawano, Cohen 2013, Ipsen, Lykkesfeldt et al. 2018). VLDL is composed by a hydrophobic core rich in TG and cholesteryl esters surrounded by a hydrophilic monolayer of phospholipids and free cholesterol. Each VLDL particle is associated with one molecule of apolipoprotein B (ApoB), so it can be mobilized out of the liver. Apart from that, apolipoprotein E (ApoE) particles are assembled in VLDL as well, in order to regulate VLDL secretion and clearance from blood (Getz, Reardon 2009). Once in plasma, VLDL particles are used to supply peripheral tissues like skeletal muscle, adipose tissue and heart. For that, TG is hydrolyzed by the action of lipoprotein lipase (Lpl). Remnant VLDL particles go back to liver and hepatic Lpl regulates its uptake (Liu, G., Xu et al. 2016).

2. Non-alcoholic fatty liver disease (NAFLD)

NAFLD is characterized by steatosis or non-alcoholic fatty liver, that is, excessive fat accumulation in at least 5% of the hepatocytes that is not secondary to alcohol/medication consumption and other diseases (i.e. viral hepatitis, lipodystrophy). It covers a broad spectrum of conditions that ranges from the potentially non-progressive steatosis to the potentially progressive steatohepatitis or NASH. NASH is determined by the concomitant presence of inflammation and cell injury (hepatocyte ballooning). Varying degrees of fibrosis can also coexist. In its more exacerbated stages, liver disease can progress into cirrhosis or hepatocellular carcinoma (HCC) (Al-Dayyat, Rayyan et al. 2018). A representation of a healthy liver together with main states of NAFLD pathogenesis are shown in Figure B4.

Figure B4. Representation of a healthy liver and the different states of NAFLD pathogenesis. HCC, hepatocellular carcinoma; NAFLD, non-alcoholic fatty liver disease. Based on (Baffy 2015).

In order to a better conceptualization, an international consensus expert panel has recently suggested the renaming of the disorder to metabolic-dysfunction-associated fatty liver disease (**MAFLD**) (Eslam, Newsome et al. 2020). MAFLD is considered the hepatic manifestation of a multisystem disease which is based on the organic dysregulation of metabolism. In addition to the hepatic steatosis, a positive diagnosis of MAFLD includes one of the following criteria: overweight/obesity, T2DM or metabolic dysregulation in non-obese patients (Figure B5) (Eslam, Newsome et al. 2020). The concept of metabolic dysregulation is further described in section 2.2.1, Table B1. MAFLD can coexist with another hepatic disorders such as inflammation, cell injury (hepatocyte ballooning) or fibrosis (Eslam, Newsome et al. 2020). Unlike to NAFLD, the new definition of MAFLD does not exclude concomitant diseases or alcohol consumption (Eslam, Sanyal et al. 2020). Anyway, patients with predominant alcoholic cirrhosis are not included in trials.

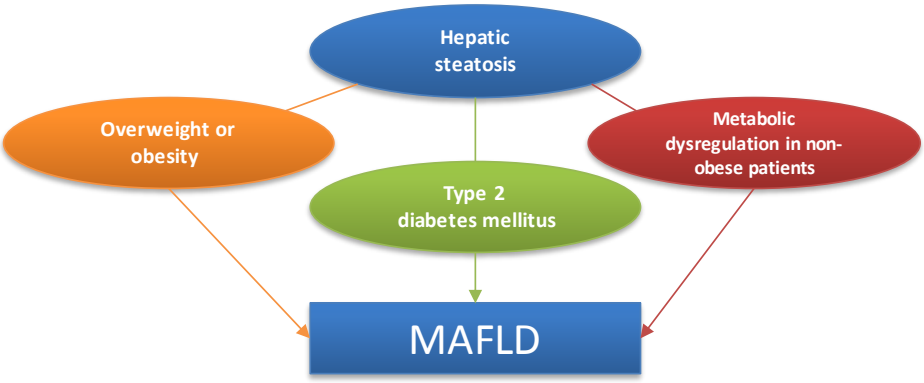

Figure B5. Diagram for the diagnosis of MAFLD. MAFLD, metabolic-dysfunction-associated fatty liver disease. Based on Eslam M. *et al.*, 2020(Eslam, Newsome et al. 2020).

There is an ongoing debate about the redefinition. In the one hand, it is considered that the new term highlights the role of metabolism, comprises the heterogeneity of the disease (Fouad, Elwakil et al. 2021) and has a clinical utility in different patient cohorts (Eslam, Newsome et al. 2020). By contrast, other experts seem that it is still an ambiguous term that does not serve to a better understanding of the pathogenesis of the disease and could even hinder its awareness in healthcare providers and policy makers, which concomitantly, could negatively affect to the management of the disease regarding diagnosis methods and drug discovery (Younossi et al. 2021). Until further clarification, we decided to use the NAFLD term in this work.

Fat deposition in NAFLD can be reliably **diagnosed** with noninvasive techniques (imaging, blood biomarkers) or with histological analysis, which requires liver biopsy. However, liver biopsy is the only available tool to distinguish precisely between hepatosteatosis and NASH in NAFLD patients so far. Then, the activity grade or NAFLD activity score (NAS score) is determined by a pathologist and for it the steatosis degree, inflammation, hepatocyte ballooning and fibrosis are taken into account (Lindenmeyer, McCullough 2018, Kleiner, Brunt et al. 2005).

As previously mentioned, steatosis can be accompanied by **cell injury**, a condition known as **NASH** (Noureddin, Sanyal 2018). Liver damage can be induced by several parallel events. Lipotoxicity is one of the main drivers, since elevated concentration of certain lipids (FA, ceramides, lysophosphatidylcholine, free cholesterol) results in endoplasmic reticulum (ER) stress and mitochondrial dysfunction with the subsequent generation of reactive oxygen species (ROS). Then, oxidative stress and inflammation are induced. Activation of the inflammasome, a multiprotein cytoplasmic complex that responds to danger-associated molecular patterns, leads to activation of proinflammatory cytokines like interleukin (IL) 1β and tumoral necrosis factor α (TNF-α) and induces cell apoptosis (Szabo, Csak 2012). Activation of this protein complex is associated with

NASH, but not with the steatotic condition *per se*. Liver inflammation can also be driven by external factors (Noureddin, Sanyal 2018). For instance, in NASH-related metabolic disorders, insulin resistance (IR) in WAT leads to the release of IL6 or adipokines; besides, altered gut microbiome is also linked with the induction of proinflammatory effects in liver. In fact, inflammation caused by intestinal dysbiosis facilitates chronic liver injury in NAFLD patients (Fukui 2019).

Liver damage and inflammation by itself target tumoral growth factor β (TGF-β) signaling, which results in the activation of Kupffer cells and, in turn, differentiation of stellate cells into myofibroblast (Fabregat, Moreno-Caceres et al. 2016). Then, extracellular matrix is produced in excess and accumulated in liver, leading to **fibrosis** and establishment of **cirrhosis**. Finally, cirrhosis can predispose patients to **HCC** development or liver failure (Kumar, Priyadarshi et al. 2020).

It is well stated that steatosis is a pre-requisite for NAFLD development (Lindenmeyer, McCullough 2018). Historically, it was believed a benign state, since it is a reversible condition and most of the patients remain asymptomatic for decades with no important clinical consequences However, recent meta-analysis reported that NAFLD affects to the 25% of the total adult population worldwide, then, it is the most common chronic liver disease and is a major health problem (Kumar, Priyadarshi et al. 2020). It is also a risk factor for irreversible liver diseases such as cirrhosis and HCC. The majority of the cases never present inflammatory damage or only exhibit it for a certain time, nonetheless, 20% of the patients with steatosis are classified as NASH (Estes, Razavi et al. 2018). Some of NASH cases show a rapid evolution of fibrosis, while others not. It has been described that patients with inflammation or fibrosis are more susceptible to develop cirrhosis and liver cancer, but only 10% of patients with steatosis present cirrhosis (Kumar, Priyadarshi et al. 2020). In addition, hepatocarcinogenesis can also progress in steatotic livers in absence of cirrhosis (Eslam, Sanyal et al. 2020, Reeves, Zaki et al. 2016), which points out the oncogenic potential of liver lipid accumulation (further described in section 2.3.1.).

2.1. Imbalance of lipid metabolism in NAFLD

As described before, liver lipid metabolism is strictly controlled. Then, an imbalance in the processes that regulate it can produce excess lipid storage and lead to NAFLD. In particular, the increased TG content in liver arises from a decompensation between lipid deposition and elimination.

It is described that 60% of the hepatic TG are derived from **serum FA** in NAFLD pathogenesis (Donnelly, Smith et al. 2005). Under a pathogenic state such as obesity or over-nutrition, body fatty mass is increased and IR together with inflammation are usually present. These conditions promote an increased TG lipolysis in WAT and the subsequent release of FA into the bloodstream, which is attributable to the elevated serum FA levels in NAFLD patients (Fabbrini, Mohammed et al. 2008), whose hepatic expressions of FATPs and CD36 are also enhanced (Greco, Kotronen et al. 2008).

Although it is not a main route involved in liver lipid supply, 14% of the hepatic TG in NAFLD patients comes directly from **dietary fats** (Donnelly, Smith et al. 2005). Intestinally absorbed lipids are transported in lipoproteins called chylomicrons through circulation to provide peripheral tissues. The remnants are removed from the circulation by the liver.

DNL is a process that is enhanced in NAFLD individuals and furnishes until the 26% of the hepatic TG pool (Donnelly, Smith et al. 2005). As PPAR-γ regulates lipogenic genes, it contributes to NAFLD development as well (Gavrilova, Haluzik et al. 2003)

Controversial results have been found concerning the contribution of **lipid oxidation** to the liver disease (Ipsen, Lykkesfeldt et al. 2018). FAO studies in patients with steatosis or NASH reported that this metabolic pathway can be increased, not altered or even decreased. In addition to the impaired FAO, alterations in mitochondrial structure and function are characteristic of NAFLD subjects (Friedman, Neuschwander-Tetri et al. 2018).

Finally, inadequate **VLDL** assembly and secretion results in the instauration of hepatic steatosis (Ipsen, Lykkesfeldt et al. 2018). On the contrary, overproduction of VLDL, a characteristic of NAFLD patients, or the secretion of richer-TG-VLDL particles is related to hypertriglyceridemia. It is also a common finding in NAFLD patients to have genetic alterations in APOB.

2.2. Risk factors for NAFLD

NAFLD is closely related to some **extrahepatic illnesses** such as metabolic syndrome and its components: obesity, dyslipidemia, hypertension and T2DM (Al-Dayyat, Rayyan et al. 2018). In fact, the prevalence of NAFLD in obese subjects or hyperlipidemia cases is 90%, whereas the 50% of individuals with hypertension present NAFLD (Friedman, Neuschwander-Tetri et al. 2018). Up to the 70% of the subjects suffering from T2DM also have NAFLD (Al-Dayyat, Rayyan et al. 2018). Besides, the global rates of NAFLD are

concurrently increasing with the raising prevalence of obesity or T2DM, the sedentary lifestyle and the lack of physical activity. This scenario drives NAFLD patients to have enhanced risk of liver-related, cardiovascular or all-cause mortality (Younossi, Tacke et al. 2019). Importantly, metabolically unhealthy phenotype has also been described in individuals with normal weight (MUHNW) according to body mass index (BMI) (Schulze 2019). Indeed, 10% of the NAFLD patients are lean and the prevalence of NAFLD in non-obese subjects is 16% (Shi, Wang et al. 2020).

Both clinical presentation and progression of NAFLD are heterogeneous and depends on the wide variety of **factors** that contribute to them (Figure B6). Moreover, genetic predisposition, environmental factors and elements of metabolic syndrome interact with each other and the increased number and severity of those factors exacerbates the clinical course of NAFLD (Pais, Maurel 2021). For instance, metabolic homeostasis is influenced by dietary intake and microbiota. Diet, especially high fat/high fructose "western diet", is associated to metabolic dysregulation (Carrera-Bastos, Fonte et al. 2011) and increased risk of NAFLD

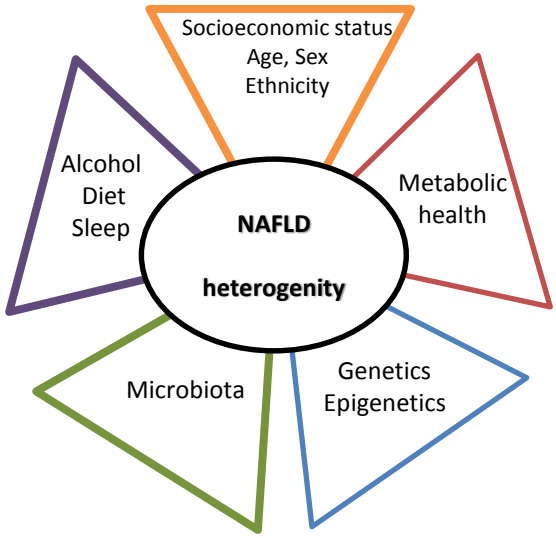

Figure B6. Framework of the factors contributing to the clinical course of NAFLD. NAFLD, non-alcoholic fatty liver disease. Based on (Pais, Maurel 2021).

progression (Berna, Romero-Gomez 2020). In fact, it can rapidly modify gut flora and intestinal permeability, regulating bile acid metabolism (David, Maurice et al. 2014) and, as a consequence, glucose and lipid metabolism as well as energy homeostasis (Arab, Karpen et al. 2017).

There is a great diversity of gene loci associated to NAFLD susceptibility and progression and most of them encode proteins related to liver lipid metabolism (Eslam, Valenti et al. 2018). The better replicated genetic variant involved in NAFLD is the I148M polymorphism in PNPLA3, a gene associated to lipid droplet

(LD) remodeling. Variations in APOB or UCP2 locuses have also been described in the predisposition towards NAFLD. Regarding epigenetic changes, among others, downregulation of miR-122 is linked to NASH and its progression to HCC.

Nowadays, there is not specific therapeutics for NAFLD treatment and management strategies for patients are based on lifestyle modifications together with pharmacologic treatment for associated comorbidities such as insulin sensitizers or statins (Mazhar K. 2019).

2.2.1. Obesity: the most prevalent risk factor for NAFLD

As determined by the World Health Organization (WHO), **obesity** is a risk to health condition characterized by excessive fat accumulation in the body. Nowadays, BMI is the tool used to classify overweight and obesity in adults and is given by the body weight divided by the square of the height (kg / m^2). Hence, overweight is defined as BMI ≥ 25, while obesity is determined as BMI ≥ 30.

Rates of obesity and overweight has reached epidemic proportions and its global **prevalence** has approximately tripled between 1975 and 2016 as specified by the WHO database. In 2016, 39% of the adults aged 18 and older were overweight and 13% were obese (Figure B7) (World Health Organization data repository. <ahref='https://www.who.int/topics/obesity;'target='_blank'>https://www.who.int/topics/obesity; accesed 30 April 2020.). In Spain, the proportion of obese people increased to 21% in 2015 (Aranceta-

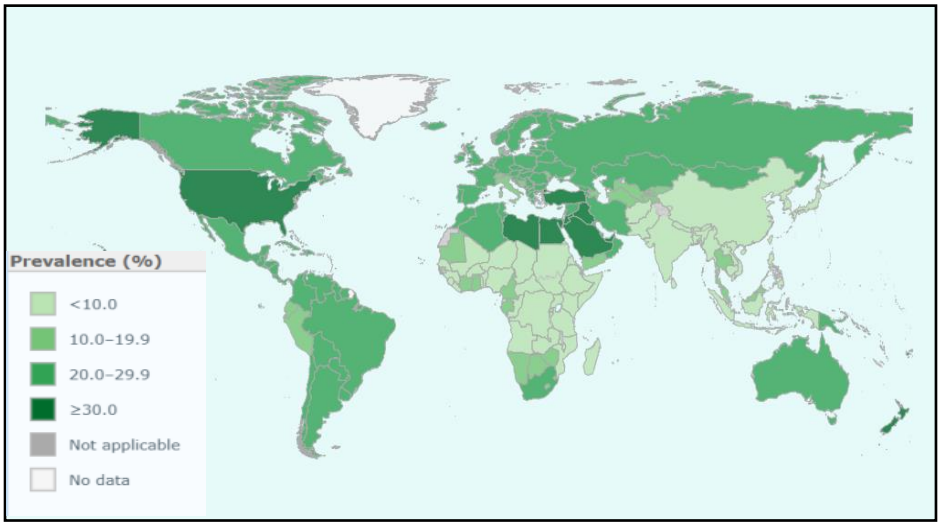

Figure B7. Prevalence of obesity in adults worldwide. Percentage of adults aged 18 and over defined as obese by country in 2016. Image modified from the World Health Organization(World Health Organization data repository. https://www.who.int/topics/obesity; accesed 30 April 2020.).

Bartrina, Perez-Rodrigo et al. 2016). It also constitutes a health issue in terms of incidence. Indeed, it is stated that 50% of the global population will be overweight in 2030 if the trend of incidence continues like that (Tremmel, Gerdtham et al. 2017). This health concern implies an important economic burden too, since the impact of obesity was estimated to be the 2.8% of the global gross domestic product in 2014.

So far, obesity was considered to affect only to developed nations, however, overweight and obesity rates are now rising in low and middle-income countries as well (World Health Organization data

Table B1. Criteria defining the risk of suffering from metabolic dysregulation. Modified from Eslam M. *et al.*, 2020(Eslam, Newsome et al. 2020).

The presence of <u>at least two</u> of the following conditions
• Waist circumference ≥ 102/88 cm in Caucasian men/women or ≥ 90/80 cm in Asian men/women. • Blood pressure ≥ 130/85 mmHg or specific drug treatment. • Plasma TG ≥ 150 mg/dl or specific drug treatment. • Plasma CHO-HDL < 40/50 mg/l for men/women or specific drug treatment. • Prediabetes: fasting glucose levels from 100 to 125 mg/dl, two-hour postload glucose levels of 140 to 199 mg/dl or HbA1c 5.7 % to 6.4 %. • HOMA-IR score ≥ 2.5. • Plasma hs-CRP level > 2 mg/l.

CHO, Cholesterol; HbA1c; hemoglobin A1c; HDL, high density lipoprotein; HOMA-IR, homeostatic model assessment-insulin resistance; hs-CRP, high-sensitivity C-reactive protein; TG, triglycerides.

repository. https://www.who.int/topics/obesity; accesed 30 April 2020.). Globally, the main causes promoting this health issue are the increased high fat diet intake and the decreased physical activity linked to sedentary lifestyle. Biological, environmental and society factors also influence the susceptibility to develop them (Blüher 2019).

Obesity is associated with an increased risk of death due to **comorbidities** such as T2MD, cardiovascular disease (CVD), NAFLD and cancer (Abdelaal, le Roux et al. 2017). Importantly, there is a subgroup of obese individuals having a metabolic healthy status (Stefan, Haring et al. 2013). That is, they do not have a higher risk of CVD when compared to normal weight subjects due to an appropriate body fat distribution mainly in the abdominal region.

Since BMI cannot provide information about the patterns of fat deposition, obesity definition could be misleading. In this context, obesity can be **stratified** in the further two groups: metabolically healthy obesity (MHO) and metabolically unhealthy obesity (MUO) (Tsatsoulis, A & Paschou, SA 2020). MHO includes obese subjects with absent risk of CVD. It is considered a transient condition that evolves to MUO depending on the lifestyle and aging. MUO phenotype usually presents adipose tissue dysfunction and IR, which are encompassed in the metabolic syndrome. Although the concept of metabolic health still remains controversial, it is defined by the presence of at least two metabolic risk conditions specified in Table B1 (Eslam, Newsome et al. 2020).

2.3. NAFLD-related hepatocellular carcinoma

Globally, **liver cancer** is a major cause of morbidity and mortality. According to Global Cancer Statistics, it was the sixth most common neoplasm and the fourth cause of death by cancer in 2018 (Bray, Ferlay et al. 2018). 841 000 new cases are estimated per year, being responsible for 782 000 deaths. By 2030, liver cancer incidence is expected to increase by 137%, while the prevalence is projected to reach the 146% (Estes, Razavi et al. 2018). Besides, incidence and mortality rates of hepatocarcinogenesis are 2- or 3-fold higher in men than in women (Bray, Ferlay et al. 2018). Among different types of liver cancer, **HCC** represents the 90% of the primary malignancies.

In addition to having a poor prognosis, HCC development presents low survival (median survival is 11 months and 5-year rate survival is 18%) mainly due to tumor recurrence and metastasis (Berkan-Kawinska, Piekarska 2020, Sun, Zhang 2020). **Etiological triggers** of HCC are diverse and include viral (hepatitis B, C and D viruses; HBV, HCV and HDV respectively) as well as non-infectious factors: toxic (alcohol, smoking, aflatoxin), immune (autoimmune hepatitis and primary biliary hepatitis) and metabolic diseases (diabetes, hemochromatosis and NAFLD) (De Matteis, Ragusa et al. 2018). Historically, HBV and HCV have mainly contributed to HCC (Bertot, Adams 2019). However, the improvement of HCV therapy together with the increased prevalence of NAFLD points out that NAFLD-associated HCC is overcoming the HCC cases attributable to other etiologies. Then, NAFLD is one of the principal etiologies causing HCC. Indeed, 32% of the HCC cases in United States of America are developed in the background of NAFLD, while the 20% are attributable to hepatitis C virus.

HCC that arises in the setting of steatosis is recognized as steatohepatitic HCC (SH-HCC) or **NAFLD-related HCC** and shows differential features when compared to HCC derived from other etiologies (Salomao,

Remotti et al. 2012). As expected, it has been related to metabolic syndrome, since obesity, T2DM, dyslipemia and hypertension prevalence is higher in NAFLD-HCC patients than in conventional HCC cases (Dhamija, Paul et al. 2019, Shibahara, Ando et al. 2014, Salomao, Remotti et al. 2012, Salomao, Yu et al. 2010). In addition, HCC evolves in older patients in a background of NAFLD (Campani, Bensi et al. 2020).

Concerning histopathology, tumors in NAFLD-HCC are mainly characterized by lipid accumulation in form of large LD, inflammation, Mallory-Denk inclusion bodies and ballooning (Park, Lee et al. 2010, Shibahara, Ando et al. 2014, Salomao, Remotti et al. 2012, Salomao, Yu et al. 2010, Lee, Yoo et al. 2017) (Figure B8). Due to the different morphological criteria used for diagnosis, there are varying proportions of prevalence, tumor size and differentiation, presence of fibrosis as well as cancer aggressiveness when compared to other HCC subclasses (Nahon, Allaire et al. 2020). Despite liver cirrhosis is a major risk factor for HCC development, 23-65% of HCC cases occur in non-cirrhotic patients with NAFLD (Bertot, Adams 2019, Paradis, Zalinski et al. 2009).

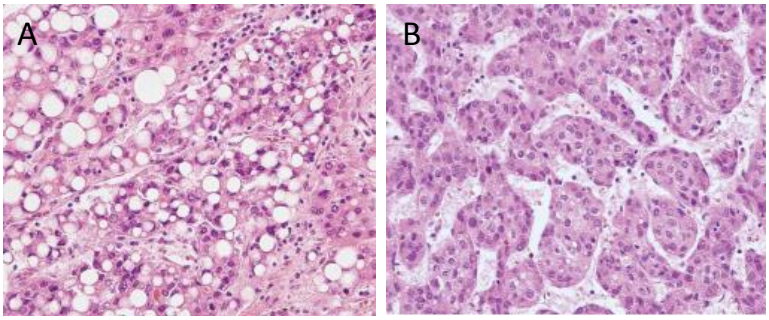

Figure B8. Histological features of SH-HCC (A) and conventional HCC (B). HCC, hepatocellular carcinoma; SH-HCC, steatohepatitic HCC. Adapted from (Lee, J. S., Yoo et al. 2017)**.**

Related to the aforementioned poor prognosis, HCC is usually diagnosed at advanced stages. Then, treatment options are limited and main of the patients have no successfully chances for liver transplantation, resection or any other treatment, and only receive supportive care (Golabi, Rhea et al. 2019). In case of HCC derived from NAFLD, the fact that no consensus definition is established for the moment (Nahon, Allaire et al. 2020) hampers even more its detection. That is why, new definition criteria are necessary (Jamwal, Krishnan et al. 2020).

2.3.1. Metabolic reprogramming in hepatocellular carcinoma

Liver is the responsible organ in the body for the regulation of organic glucose and lipid metabolism. Alterations in metabolic pathways are largely observed in liver pathological conditions such as NAFLD. Since HCC can arise in steatotic livers without cirrhosis (Zarrinpar 2017), the relevance of the metabolic disorders is

increased in hepatocarcinogenesis. However, the mechanisms by which obesity and/or NAFLD promotes HCC are not fully understood because few data are available about the metabolic profile for the moment.

Apart from the oncogenic events that involve activation of oncogenes and loss of tumor suppressors, there are some microenvironmental and metabolic factors in the tumor that induce hepatocarcinogenesis and are common with NAFLD development: IR-mediated hyperinsulinemia, elevated proinflammatory cytokines induced by oxidative and ER stress, dysregulation of adipokines and altered gut microbiota (Nakagawa, Hayata et al. 2018). Besides, **metabolic reprogramming**, that is to say, the metabolic changes that occur in cancerous cells innately, contributes to carcinogenesis in obesity (Ward, Thompson et al. 2012). Metabolism in proliferating cells differs from that in quiescent cells, since uncontrolled cell proliferation in tumors needs of energy, biomass and redox balance maintenance. All these requirements are supplied by the metabolic reprogramming. Furthermore, metabolites produced in the metabolic adaptations also play functions in cancer induction by regulating signaling pathways, epigenetic states and cellular differentiation.

Regarding **glucose metabolism**, the most analyzed adaptive event of cancer cells is the Warburg effect or aerobic glycolysis, in which glucose is rerouted to lactate production instead of being metabolized to TCA cycle and oxphos (Vander Heiden, Cantley et al. 2009). This phenomenon occurs even in presence of oxygen or functional mitochondria. Together with an increased glucose uptake, aerobic glycolysis is observed in HCC patients (De Matteis, Ragusa et al. 2018). Moreover, Bjornson *et al*. reported that gluconeogenesis is suppressed during hepatocarcinogenesis, since key enzymes of this process were downregulated (Bjornson, Mukhopadhyay et al. 2015).

Recent studies have also uncovered the relevance of **adaptive lipid metabolism** in cancer cells. Apart from being energy reservoirs and storage compounds, lipids exert structural functions and can modulate membrane fluidity and protein dynamics depending on their composition and abundance (Beloribi-Djefaflia, Vasseur et al. 2016). Lipids also play several functions during carcinogenesis, since they drive signaling cascades involved in different malignant processes such as cell growth, migration or metastasis. Nowadays, lipid metabolism is considered a hallmark of hepatocarcinogenesis, particularly when derived from steatosis, a condition that constitutes a lipid-rich environment.

Nakagawa and cols showed that **DNL** is universally enhanced in HCC (Nakagawa, Hayata et al. 2018). Expression profile of HCC shows upregulation of key genes involved in lipid biosynthesis when compared to non-cancerous liver tissue (Bjornson, Mukhopadhyay et al. 2015). Furthermore, FASN overexpression is associated with a poor prognosis of HCC (De Matteis, Ragusa et al. 2018), SCD network is linked with

hepatocarcinogenesis and patient outcome (De Matteis S., Ragusa A., Marisi G. et al. 2018) and activation of the SREBP1-mediated lipogenesis is described in HCC (Nakagawa, Hayata et al. 2018). Enzymes related to NADPH production like G6PDH and ME are also upregulated in this type of liver malignancy (De Matteis, Ragusa et al. 2018). Of note, there are different chemicals inhibitors of DNL in preclinical and clinical trials for cancer therapy, including HCC treatment (Nakagawa, Hayata et al. 2018).

Despite non-proliferative cells usually exert via exogenous lipids, increased **uptake of circulating FA** by hepatic LPL may be another major route contributing to HCC development (Cao, Song et al. 2017). Indeed, Cao and cols reported that enhanced LPL expression is the responsible for the serum FA consumption in HCC. In addition, FA translocases (CD36), transporters (FATP2, FATP5) and some members from FABP family (1, 4, 5) are involved in FA acquisition and transport to liver in HCC (Hu, Lin et al. 2020). As mentioned before, this is especially relevant in case of over-nutrition-driven obesity, a condition in which FA sourced from WAT lipolysis and diet increases its concentration in bloodstream (Fabbrini, Mohammed et al. 2008).

Concerning the key routes involved in liver **lipid disposal**, conflicting data have been reported on their involvement in HCC. The behavior of these pathways could be related to FA origin (Berndt, Eckstein et al. 2019). It is reported that upregulated expression of PPAR-α and CTP2, with a concomitant increased rate of **FAO** is the fuel of β-catenin driven HCC (Senni, Savall et al. 2019, Hu, Lin et al. 2020). By contrast, other studies demonstrated a suppression of FAO by Cpt2 downregulation in HCC as an adaptation to a lipid-rich environment (Nakagawa, Hayata et al. 2018, Berndt, Eckstein et al. 2019). Anyway, mitochondrial impairments are considered to be a soon constituent of HCC (De Matteis, Ragusa et al. 2018).

As mentioned above, disruption of **VLDL secretion** also contributes to liver lipid accumulation. In HCC, important genes involved in VLDL export are downregulated when compared to noncancerous liver tissue (Bjornson, Mukhopadhyay et al. 2015). Specifically, APOB ablation in HCC is related to poor outcome in patients (Lee, Jeong et al. 2018). However, increased rates of VLDL export have been described in patients with HCC (Berndt, Eckstein et al. 2019). Nothing is described about the hepatic mobilization of TG in NAFLD-HCC subclass particularly.

In essence, metabolic reprogramming is necessary in HCC for tumor growth and progression. Hence, the control of the altered pathways during hepatocarcinogenesis could have important clinical implications (De Matteis, Ragusa et al. 2018). So far, it was thought that mutations in tumor suppressors or proto-oncogenes firstly regulate cell cycle, sustain proliferation and avoid growth suppression and/or cell death (Ward, Thompson et al. 2012). Then, the adaptive metabolism in cancer cells was considered a passive

response to those alterations. However, evidences support an unconventional concept in which proto-oncogenes and tumor suppressors are evolved to control metabolism and this is precisely the primary role they play in carcinogenesis.

Cancer driver genes modify the type of HCC, what supports a unique tumoral biology (Molina-Sanchez, Ruiz de Galarreta et al. 2020). Alterations in the expression levels and their activity as well as their cooperation patterns confer intertumor heterogeneity concerning histology, immune phenotype, transcriptome and response to therapy. Notably, the risk of HCC progression in NAFLD can be stratified and predicted by some alleles in PNPLA3 gene, always in combination with other determined factors of HCC (male gender, older age and obesity) (Nahon, Allaire et al. 2020). However, specific exome, genome and RNA sequencing studies have not uncovered any particular genome pattern associated to NAFLD-HCC. The E2F transcription factors, as important regulators of the cell cycle, can play a role in all this process, since they participate in the control of physiological and pathological metabolism (further described in section 3.3).

3. The cell cycle and E2F transcription factors

3.1. The cell cycle and its regulation

The **cell cycle** is a highly conserved process that leads to cellular proliferation. During cell proliferation, a cell is divided into two genetically identical daughter cells. This mechanism is essential in cell growth, development and differentiation of eukaryotic organisms (Wenzel, Singh 2018, Vermeulen, Van Bockstaele et al. 2003). It is also closely related to cell death, as both processes are the responsible for tissue homeostasis in adults (Zhivotovsky, Orrenius 2010). Hence, altered regulation throughout the cell cycle leads to several pathologies such as cancer (Wenzel, Singh 2018, Vermeulen, Van Bockstaele et al. 2003), metabolic disorders or cardiovascular and neurodegenerative diseases (Zhivotovsky, Orrenius 2010).

Cellular division comprises four sequential **phases**: Gap1 (G_1) or growth phase, synthesis (S) or DNA replication phase; Gap2 (G_2) phase, in which the cell is prepared for mitosis, and the mitotic phase (M), when cell is divided (Wenzel, Singh 2018) *(Figure B9)*. Cells in G_1 can enter in a non-proliferative phase called G_0. Contrary to senescent cells, the resting state is reversible for quiescent cells, as they can re-enter the cell cycle to proliferate in response to physiological growth factors (Yao 2014). The period prior to mitosis is known as interphase (G_1, S, G_2) and around 95% of the cell cycle is spent in it (Cooper 2000).

Genomic integrity and accurate duplication must be accomplished in daughter cells. For that, there are rigorous control mechanisms termed as **checkpoints** *(Figure B9)*. Checkpoints ensure that cell cycle is unidirectional and make execution of the later events dependent of the successful completion of preceding ones, resulting in the ordered transition of the cell cycle (Rhind, Russell 2012). G_1/S or restriction checkpoint (R) is the most important one and ascertains that the cell is committed to division (Gerard, Goldbeter 2009). It is a point of no return and, once overtaken, cell division occurs irrevocably without requiring any growth factor. There are another three checkpoints: intraS, G_2/M and M or mitotic spindle checkpoint (Barnum, O'Connell 2014). All these regulatory circuits comprise positive and negative signals that mainly control the cell size, the response to DNA damage and the chromosome segregation. Until the defects are properly repaired, activation of the checkpoints allows the cell cycle arrest. If unsuccessful repair occurs, cell would enter senescence or undergo apoptosis (Malumbres, Barbacid 2009).

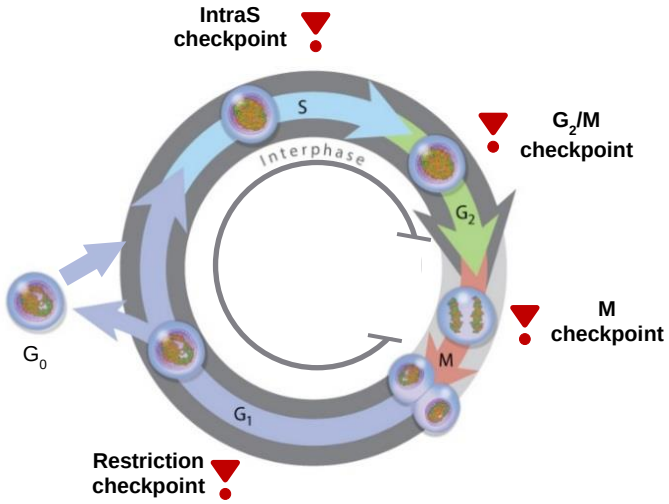

Figure B9. Schematic representation of the cell cycle. Cell cycle phases and regulation checkpoints are shown. G_0, non-proliferative phase; G1, Gap1 phase; G2, Gap2 phase; M mitotic phase; S, synthesis phase. Adapted from O'Connor et al., 2008.

Cyclin dependent kinases (Cdk) are serine/threonine kinases who control the dynamic of the cell cycle by sequential and transient activation (Malumbres, Barbacid 2005). Despite their constitutive expression, the biological activity of Cdks requires the binding of cyclins, the regulatory subunits. Contrary to Cdks, cyclins are synthetized and destroyed in a cyclical fashion during cell cycle. Cdk kinase activity is also regulated by binding to inhibitors (CKI), phosphorylation/dephosphorylation, folding and cellular location.

Specific heterodimeric complexes of Cdk-cyclins operate in each phase of the cell division and phosphorylate key substrates that allow **cell cycle progression** (Malumbres, Barbacid 2005). During early G_1, Cdk 4,6/Cyclin D inactivates the retinoblastoma tumor suppressor protein (Rb) by phosphorylation. Inactivation of Rb is then completed by Cdk 2/Cyclin E. Cdk 3/Cyclin C is also thought to phosphorylate Rb in the G_0/G_1 transition of quiescent cells. Inactive Rb, leads to the liberation of functional **E2F transcription factor**, which allows cells to crossover the restriction checkpoint and entry the S phase (Nevins 1992, Weinberg 1995). Cdk 2/Cyclin E complexes are also relevant in G_1/S transition. Finally, S phase completion and exit is mediated by Cdk 2/Cyclin A, while Cdk 1/Cyclin A, B are involved in S/G_2 and G_2/M transition.

3.2. The E2F family of transcription factors

E2 factor (E2F) was firstly identified as a cellular factor required for the activation of the adenoviral promoter E2 (Kovesdi, Reichel et al. 1986a, Kovesdi, Reichel et al. 1986b). Since then, the E2F family has been constantly expanding in mammals by addition of new members (Dimova, Dyson 2005).

E2F is a family of **transcription factors** that plays pivotal role in the **cell cycle progression**. Several key regulators of the cell cycle (Cyclin E, Cyclin A, Rb) are induced by E2F, as well as those related to biosynthesis of nucleotides (Tk, Ts, Dhrf), DNA replication (Orc1, Cdc6 and some Mcm members) (Dyson 1998) or mitosis (Plk1) (Martin, Strebhardt 2006). In addition, other E2F targets include genes involved in DNA repair, apoptosis, differentiation and development (Bracken, Ciro et al. 2004).

To date, eight E2F **chromosomal loci** (E2F1-8) are found in mammals, that encode 10 different gene products (E2F1, E2F2, E2F3a, E3F3b, E2F4, E2F5, E2F6, E2F7a, E2F7b, E2F8) (DeGregori, Johnson 2006, Chen, Tsai et al. 2009) *(Figure B10)*. Two distinct promoters are used to produce E2F3a and E2F3b, while E2F7a and E2F7b are the result of the alternative splicing of the primary transcript (Di Stefano, Jensen et al. 2003).

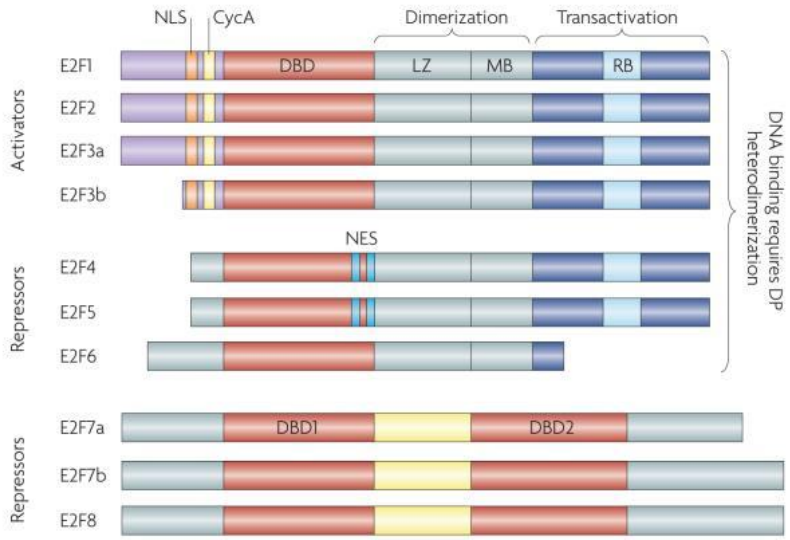

Figure B10. Schematic representation of the E2F proteins in mammals. CycA, Cyclin A binding-site; DBD, DNA binding domain; NES, nuclear export signal, NLS, nuclear localization signal; MB, marked box; RB, LZ, Leuzine zipper; Rb biding-domain. Image from Chen, Tsai et al. 2009.

All E2F family members contain at least one conserved winged-helix **DNA binding domain** (DBD) (Chen, Tsai et al. 2009). The high homology degree between E2F partners remains in this domain, which allows the binding to the consensus motif 5'-TTTSSCGC-3', where S is either a G or a C. E2F1-6 also have a **dimerization domain**, a binding site for the dimerization partner proteins (DP). Heterodimerization of E2F with DP (DP1, DP2 and DP3/4 in *Homo sapiens*) modulates the affinity to DNA binding and transcriptional activity (Helin, Wu et al. 1993, Bandara, Buck et al. 1993, Huber, Edwards et al. 1993, Krek, Livingston et al. 1993), and occurs through the leuzine zipper (LZ) and marked box (MB) motifs. E2F7-8 do not content this domain and bind to DNA as homodimers in a DP-independent manner (Chen, Tsai et al. 2009). The **carboxyl-terminal** of E2F1-5 contains a transactivation domain, which allows the specific interaction with Rb family

members or pocket proteins (Rb, p107, p130). E2F6-8 lack the transactivation domain, then, they act in an Rb-independent fashion. On the other hand, Cyclin A/Cdk 2 binding site and nuclear localization signal (NLS) are located in the **amino-terminal** of E2F1-3, where E2F4-5 contain a bipartite nuclear export signal (NES).

Based on their homology and the subsequent *in vitro* functional properties, E2F family members are traditionally divided into activators (E2F1-3a), which are regulated during cell growth and cell cycle, or into repressors (E2F3b-6) and atypical repressors (E2F7-8), which are constitutively expressed (Kong, Chang et al. 2007). However, several studies revealed more complex roles, since activators can also act as repressors and vice versa depending on the cell context (Mitxelena, Osinalde et al. 2012). Nowadays, that classification is considered inaccurate and oversimplified (Huntington, Tang et al. 2016).Due to their similarity, E2f members have overlapping **functions**, as organism survival is ensured with a compensation of other partners when loss of function of an individual member occurs (Kong, Chang et al. 2007). By regulation of specific gene sets, each member also has its own and unique roles. For example, E2F1-3 are required for S-phase entry (Wu, Timmers et al. 2001, Kong, Chang et al. 2007), but only E2F3 is necessary for successive cell cycle entry in growing cells (Kong, Chang et al. 2007) and E2F1 is the only one who induces apoptosis in absence of proliferative stimuli (Hallstrom, Nevins 2003). DNA binding to the consensus motif seems not to be the only mechanism involved in the **transcriptional control specificity** of target genes, since most of the E2F binding sites *in vivo* do not contain that consensus motif (Rabinovich, Jin et al. 2008, Cao, Rabinovich et al. 2011). In addition, E2F1 usually binds to a GC-rich sequence present in most of the human promoters and can be recruited directly or by protein-protein interaction (Cao, Rabinovich et al. 2011). Another E2F partners have also been described to interact with several transcription factors and proteins of the transcriptional machinery (Mitxelena, Osinalde et al. 2012). Hence, the binding specificity arises in the cooperation of E2F with other transcription factors in the promoters of each target gene (Mitxelena, Osinalde et al. 2012). The combinatorial gene regulation allows distinct E2F members to have particular functional roles by regulation of different target genes, including other E2Fs (Freedman, Chang et al. 2009).

Functional specificity also emerges by regulation of E2F synthesis (Chen, Tsai et al. 2009) or degradation by ubiquitin-proteasome machinery (Hateboer, Kerkhoven et al. 1996), binding to particular Rb partners (Chen, Tsai et al. 2009), direct phosphorylation by Cdks (Morris, Allen et al. 2000) or epigenetic changes (Chen, Tsai et al. 2009). As mentioned before, E2F family can also be autoregulated, as they contain E2F binding sites in their own promoters (Johnson, Ohtani et al. 1994, Hsiao, McMahon et al. 1994, Neuman, Flemington et al. 1995). In addition, its function is dependent upon their subcellular localization (Verona, Moberg et al. 1997).

3.3. E2F transcription factors as metabolic regulators

The metabolic adaptations that occur in cell progression and cancer establish a link between cell cycle and metabolism. Apart from the traditional functions, the involvement of several cell cycle regulators in the metabolic control has been uncovered in the last decade, even in physiological or pathological conditions. That is why, it is proposed that cell cycle modulators are the responsible of the metabolic switch in cancer.

3.3.1. Role of the CDK-E2F axis in physiological metabolic regulation

Cell cycle regulators contribute to the global metabolic homeostasis participating in the development and differentiation of important metabolic organs like pancreas, adipose tissue, muscle or liver (Denechaud, Lopez-Mejia et al. 2016). Supporting role of the cell cycle modulators in the control of metabolism is the observation of the phenotype in mutant mice (Aguilar, Fajas 2010). For instance, genetic aberrations in different genes regulating the cell cycle (i.e. cyclin D1, some Cdks or CKIs) promote alterations in the **body size**. However, *E2f1*$^{-/-}$ and *E2f2*$^{-/-}$ mice has a normal development probably due to compensation by other members (Denechaud, Lopez-Mejia et al. 2016).

It has been extensively demonstrated that certain members of the E2F family are involved in **adipogenesis**. E2f1 and E2f3 activate *Pparg* expression and induce adipocyte differentiation (Fajas, Landsberg et al. 2002). Particularly, E2f1 binds to the *Pparg* promoter *in vivo*. Contrary to the aforementioned, E2f4 negatively regulates adipogenesis by specific union to *Pparg* promoter (Fajas, Landsberg et al. 2002).

In **liver**, Cdk 4-Rb-E2f1 pathway activates DNL in response to insulin and E2f1 shows functional occupancy for *Fasn*, *Scd1* and *Srebp1* promoters, key lipogenic genes (Denechaud, Lopez-Mejia et al. 2016). In addition, E2f1 maintains cholesterol homeostasis in liver, since its knock-down leads to an increased LDL uptake concomitant with a cholesterol accumulation (Lai, Giralt et al. 2017). Conversely, studies in mouse embryonic fibroblasts have demonstrated that the inactivation of Rb increases FA synthesis and changes FA composition throughout the transcriptional regulation of *Elovl6* and *Scd1* coordinated by E2f and Srbp1 (Muranaka, Hayashi et al. 2017).

In addition to lipid metabolism, E2F family has also been involved in the control of glucose homeostasis by regulation of **pancreatic β-cell proliferation**. It is described that β-cell number is decreased in *E2f1* deficient mice, which impairs the glucose-dependent insulin secretion (Fajas, Annicotte et al. 2004).

Nevertheless, they do not exhibit diabetes, since insulin sensitivity is increased in peripheral tissues (Fajas, Annicotte et al. 2004).

E2f1 also participate in modulating the **function of β-cells** by triggering the metabolic response to glucose and insulin. Notably, E2f1 induces glucose-stimulated insulin secretion through activation of Kir6.2 gene expression in pancreatic islets, an ATP-sensitive potassium channel (Annicotte, Blanchet et al. 2009). Indeed, glucose enhances Cdk 4-Cyclin D2 activity, which results in the inactivation of Rb and the concomitant activation of E2f1. The pathway is also induced via the autocrine effect of insulin. Other evidences suggest that E2f1 could regulate glucose synthesis in liver. Particularly, hepatic gluconeogenesis is impaired in *E2f1*$^{-/-}$ mice (Giralt, Denechaud et al. 2018), who also showed a decreased glycolytic flux due to reduced glycogen content in liver (Denechaud, Lopez-Mejia et al. 2016).

There are studies demonstrating that cell cycle modulators control **oxidative metabolism** as well. Particularly, Rb inactivation enhances anaerobic glycolysis (Clem, Chesney 2012) and increases mitochondrial activity and number in adipocytes (Aguilar, Fajas 2010). This suggests that Rb can modulate the switch from oxidative to glycolytic metabolism, a hallmark of cancer cells. Conversely, other studies report that Rb deletion augmented the mitochondrial activity in heart and impaired oxphos in muscle (Denechaud, Lopez-Mejia et al. 2016). Rb-E2f1 pathway also promotes myocardial glucose oxidation by activation of pyruvate dehydrogenase lipoamide kinase isozyme 4 (PDK4), a key nutrient sensor overexpressed in diabetes and obesity (Hsieh, Das et al. 2008). In addition, Rb-E2f1 induces the oxidative metabolism in BAT and skeletal muscles in response to exercise, cold conditions and reduced nutrient availability (Blanchet, Annicotte et al. 2011). Current investigations evidence that the control of oxidative metabolism by Rb-E2f axis depends on the context.

It is to be noted that there are certain functions of E2f1 in which Rb does not participate. For example, E2F1 is physically repressed by BIN1 to attenuate the cell cycle (Folk, Kumari et al. 2019) or by KAP1 to prevent apoptosis in response to DNA damage (Wang, Rauscher et al. 2007).

So far, all these highlights support that the E2f family of transcription factors and, specially, E2f1 modulate cell physiology apart from the control of the cell cycle, in an Rb-dependent or independent fashion. It is involved in the maintenance of lipid and glucose homeostasis as well as in the regulation of energy expenditure in high metabolic tissues.

3.3.2. Involvement of cell cycle regulators in the metabolic complications of liver disease and hepatocellular carcinoma

As already mentioned, it is stated that the E2F family of transcription factors is indeed responsible for several metabolic changes even when cancer is not developed. These new proposals are based on the observations like impairments in cell cycle modulators are related to liver pathological conditions and the associated metabolic complications, mainly including obesity and diabetes.

There are many evidences that report the involvement of cell cycle regulators in **obesity**. For example, specific inactivation of Rb in adipocytes also protects mice from dietary obesity by enhancing energy expenditure and WAT browning (Dali-Youcef, Mataki et al. 2007). Consistently, *E2f1*$^{-/-}$ mice exhibit resistance to diet-induced obesity (Fajas, Landsberg et al. 2002) and its absence reduces the hyperglycemia in diabetic mice models (Giralt, Denechaud et al. 2018). Furthermore, *E2F1* is overexpressed in the visceral adipose tissue of obese patients (BMI > 30) that suffer from abdominal adiposity, elevated serum free FA and IR (Haim, Bluher et al. 2015). E2F1 expression is also increased in liver samples of patients with BMI > 40 and glucose intolerance (Denechaud, Lopez-Mejia et al. 2016).

Concerning the role of E2Fs in the **liver disease**, it is described that *E2f1* deficiency ameliorates the steatosis developed in diabetic mice models, although does not protect them from the related obesity or hyperglycemia (Denechaud, Lopez-Mejia et al. 2016). E2F1 may relate to fibrosis as well, since it is upregulated in human cirrhotic-NASH patients and mice models (Zhang, Xu et al. 2014).

E2f1, 2, 7 and 8 regulation by PPAR-β is required for the correct progression in **liver regeneration** (Liu, Fang et al. 2013). However, previous studies demonstrated that E2f1 is dispensable in liver regeneration (Lukas, Bartley et al. 1999). On the other hand, it is known that E2f2 contributes to the normal liver growth after partial hepatectomy (Delgado, Fresnedo et al. 2011), probably due to its function in maintaining the phosphatidylcholine (PC) and phosphatidylethanolamine (PE) homeostasis (Maldonado, Delgado et al. 2014).

Given the relevance on the cell cycle progression, mutations in the Rb-E2F pathway are found in several types of **cancer** (Chen, Tsai et al. 2009). Based on the traditional view, the Rb-E2F pathway induces tumorigenesis by genetic alterations leading to Rb loss and subsequent E2F stimulation, which results in the deregulation of cell proliferation. Thus, E2F activators are expected to behave as oncogenes and their alterations would include gain-of-function mutations, amplification and overexpression. Conversely, E2F

repressors may proceed as tumor suppressors and be related to loss-of-function mutations, chromosomal deletions and epigenetic silencing in cancer. Nevertheless, it has been reported that same E2Fs could act as oncogenes or tumor suppressors depending on the environment and tissue (Chen, Tsai et al. 2009).

In **HCC**, functional inactivation of Rb is due to genetic, epigenetic and viral mechanisms and occurs by direct mutations or through altered CDK activity (Huntington, Tang et al. 2016). Indeed, low levels of pRb are described in most cases of human HCC, which is associated with poor prognosis (Palaiologou, Koskinas et al. 2012).

Alterations in E2Fs have also been reported in HCC, although their behavior changes depending on the study. Mainly, investigations are focused on E2F1, the most studied member. Important evidence that support the oncogenic role of **E2f1** is the fact that its absence protects mice from DEN-induced carcinogenesis (Kent, Bae et al. 2017). Moreover, in patients with early or advanced HCC, *E2F1* expression is found to be increased and copy number gain in *E2f1* promotes spontaneous HCC development in mice by transcriptional activation of target genes involved in maintaining DNA integrity (Kent, Bae et al. 2017). Besides, overexpression of *E2F1* in high glucose environment, which resembles the Warburg effect, is linked with enhanced proliferation and metastasis in human HCC cell line (He, Huang et al. 2020). It is also reported that E2F1 is an antiapoptotic factor in human and mice HCC (Zhan, Huang et al. 2014). By the contrary, other studies revealed that E2f1 can act as tumor suppressor, since it promotes apoptosis in HCC (Palaiologou, Koskinas et al. 2012).

Far less is known about the involvement of the other E2F members in HCC. Particularly in case of **E2F2**, it has been associated with E2F1 roles due to their functional similarity. In fact, E2F2 gene expression is increased in HCC cohorts and HCC cell lines, which is related with a poor outcome (Zhan, Huang et al. 2014, Hong, Eun et al. 2019). By contrast, the loss of copy number in *E2F2* observed in human HCC reflects that it can also act as tumor suppressor (Kent, Bae et al. 2017).

Except for E2F8, which also have a dual role, rest of the E2F family partners (E2F3-6) are supposed to contribute to liver oncogenesis because they are upregulated in HCC (Zhan, Huang et al. 2014, Kent, Bae et al. 2017, Huang, Ning et al. 2019).

Appropriated cell cycle progression and whole-body homeostasis is given by E2F family, hence, disorders in this network leads to tumorigenesis and metabolic diseases. However, the canonical view of E2F activators and repressors does not correlate with the observed complex function of E2F, particularly in case

of E2F1 and E2F2 and HCC development. Then, further investigation is needed to discern common and particular mechanisms between E2F1 and E2F2, as well as to establish their potential impact to obesity-related HCC.

Chapter B. OBJECTIVES

Chapter B. OBJECTIVES

According to the World Health Organization (WHO) global database, the prevalence of obesity worldwide has nearly tripled in the last 40 years. This public health concern not only affects to high-income countries, but overweight and obesity rates are now increasing in non-developed nations as well.

Obesity is associated with hepatic metabolic dysregulations that contribute to liver lipid accumulation and non-alcoholic fatty liver disease (NAFLD) progression (Alzahrani, Iseli et al. 2014). Indeed, up to 90% of obese patients suffer from NAFLD (Kumar, Priyadarshi et al. 2020). Epidemiological studies revealed that obesity also constitutes a risk factor for development of cancer in different organs, including the liver (Lauby-Secretan, Scoccianti et al. 2016). Hepatocarcinoma (HCC), the primary liver cancer, is the sixth most common malignancy globally and is a major cause of obesity-related cancer deaths (Michelotti, Machado et al. 2013). In western countries, between 4-22% of HCC cases arise in NAFLD patients (Michelotti, Machado et al. 2013). However, the mechanisms that promote HCC in NAFLD remain unclear, which restricts the early diagnosis of the disease.

Tumor formation and development occur due to an uncontrolled division of cells, which is in turn allowed by genetic alterations involving 1) gain of function of oncogenes or 2) loss of function of tumor suppressor genes (Grander 1998). As described elsewhere (Schulze, Imbeaud et al. 2015, Cancer Genome Atlas Research Network. Electronic address: http://wheeler@bcm.edu, Cancer Genome Atlas Research Network 2017, Totoki, Tatsuno et al. 2011), there is a wide variety of genetic drivers in HCC, which explains, at least in part, the high heterogeneous characteristics of HCC. Changes in their expression level, activity as well as in the combination of alterations set off an intertumor heterogeneity concerning tumor histology or cell signaling pathways (Molina-Sanchez, Ruiz de Galarreta et al. 2020). Regarding the NAFLD-related HCC's phenotype, it should be taken into account that obesity by itself can also contribute to metabolic impairments. Indeed, it is related to a metabolic signature, which even differs between MHO and MUO subjects (Rangel-Huerta, Pastor-Villaescusa et al. 2019). Once the tumor is formed, metabolism is reprogrammed in cancer cells in order to fulfill the demands of energy and biosynthetic-precursors (Grander 1998).

The E2F transcription factor family is critical for cell cycle progression and, depending on the cell context and cell type, plays a function as oncogene or as a tumor suppressor (Huntington, Tang et al. 2016).

There is a high expression of E2Fs in tumoral liver tissue, which points out their relevance in liver cancer (Huang, Ning et al. 2019). Moreover, concerning E2F1, there are increasing studies that uncovered its role in metabolism, independent to cell cycle. However, there is no insight about the involvement of E2F1 or E2F2 in the development of the liver disease and the induction of carcinogenesis in NAFLD.

Taking all this into account, we proposed that **E2F1 and E2F2 regulate the metabolic pathways involved in obesity-related NAFLD development and its progression to HCC**.

In this context, the specific aims of this project were:

Aim 1. To investigate if E2F1 and/or E2F2 are involved in NAFLD development and progression to HCC.

1.1. To identify if E2F1 and/or E2F2 are overexpressed in obesity-related liver samples and if so, if it is associated with NAFLD development.

1.2. To investigate if E2F1 and/or E2F2 deficiency protects from obesity-related NAFLD and HCC.

Aim 2. To identify the mechanisms by which E2F1 and/or E2F2 drive the metabolic dysregulation involved in obesity-related NAFLD development and progression to HCC.

2.1. To investigate whether E2F1 and/or E2F2 deficiency prevents the adaptive lipid metabolism in obesity-driven NAFLD and HCC.

2.2. To investigate if E2F1 and/or E2F2 deficiency prevents the insulin resistance of obesity-driven NAFLD and HCC.

Aim 3. To validate E2F1 and/or E2F2 as early biomarkers in obesity-related NAFLD.

Chapter C. MATERIALS AND METHODS

1. Materials

1.1 Buffers and medias

1.1.1. Buffers for cytochemistry and histochemistry

- **Citrate buffer for inmunohistochemistry.** 0.37% (w/v) citric acid monohydrate and 0.29% (w/v) sodium citrate dehydrate in distillated water (dH_2O); pH 6.
- **Sirius red staining solution I.** 0.01% (w/v) Fast Green FCF in saturated picric acid (Panreac, Spain).
- **Sirius red staining solution II**. 0.04% (w/v) Fast Green FCF, 0.1% (w/v) Sirius red in saturated picric acid (Panreac, Spain).
- **Oil red solution.** 0.5% (w/v) Direct Red in isopropanol (Scharlau Chemicals, Spain).

1.1.2. Buffers for gene expression

- **Loading buffer for RNA electrophoresis (6 x).** 40% (w/v) sucrose; 0.25% (w/v) bromophenol blue; 0.25% (w/v) xylene cyanol.
- **Tris-Acetate-EDTA (TAE) buffer.** 0.4% (v/v) glacial acetic acid (Panreac, Spain); 10 mM EDTA; 40 mM Tris-HCl in miliQ-H_2O; pH 8.5.

1.1.3. Buffers and mediums for metabolic activities

[^{3}H]-oleate esterification into TG:

- **Medium**. 5 µCi/ml [^{3}H]-oleic acid (PerkinElmer, USA) with 20 µM cold oleic acid in 1 g/L glucose containing Eagle's minimum essential medium (EMEM) from ATCC (USA) supplemented with 2 mM L- glutamine and 0.5% (w/v) fatty acid (FA) free bovine seroalbumin (BSA) (Roche, Switzerland).

β-oxidation rate assay:

- **Homogenization buffer.** 25 mM Tris-HCl, 500 nM sucrose (Panreac, Spain), 1 mM EDTA-Na_2 (Merck-Millipore, Germany); pH 7.4.

- **Medium for β-oxidation assay in cell culture.** 0.5 μCi/ml [1-^{14}C]-palmitate (PerkinElmer, USA) and 0.2 mM palmitic acid in 1 g/L glucose containing EMEM supplemented with 0.5% (w/v) FA free BSA.
- **Medium for β-oxidation assay in liver tissue**. 0.5 μCi/ml [1-^{14}C]-palmitate (PerkinElmer, USA) and 0.2 mM palmitic acid containing 115 mM NaCl, 2.8 mM KCl, 10 mM Tris-HCl, 1.2 mM KH_2PO_4, 10 mM $NaHCO_2$, 0.2 mM EDTA-Na_2, 0.3% (w/v) FA free BSA, 2 mM L-carnitine, 5 mM ATP, 0.5 mM malate, 0.1 mM CoA.

***De novo* lipogenesis (DNL):**

- **Medium for DNL in cell culture.** 20 μCi/ml [^{3}H]-acetic acid (PerkinElmer, USA) with 20 μM cold sodium acetate in 2 g/L glucose containing EMEM supplemented with 2 mM L- glutamine and 84 nM insulin.
- **Medium for DNL in liver tissue.** 20 μCi/ml [^{3}H]-acetic acid (PerkinElmer, USA) and 20 μM cold sodium acetate (Merck-Millipore, Germany) in 1 g/L Dulbecco's Modified Eagle Medium (DMEM) containing 4 g/L glucose and 150 nM insulin (Novo Nordisc, Denmark).

Glucose-6-phosphate dehydrogenase (G6PDH) and malic enzyme (ME) activities:

- **Homogenization buffer.** 150 mM KCl, 1 mM $MgCl_2$, 0.5 mM dithiothreitol (DTT; Roche, Switzerland), 10 mM N-acetylcysteine; pH 7.6.
- **G6PDH incubation buffer.** 100 mM glycylglycine, 10 mM $NADP^+$ (Merck-Millipore, Germany); 150 mM $MgSO_4$; 30 mM glucose-6-phosphate; 2.4 mM NADPH (Merck-Millipore, Germany); pH 8.
- **ME incubation buffer**. 0.4 M triethanolamine (TEA), 3.4 mM $NADP^+$ (Merck-Millipore, Germany); 0.12 M $MnCl_2$; pH 7.4.

Lipolysis:

- **Lipolysis medium.** 1 g/L DMEM containing 4% (w/v) FA free BSA and supplemented (for stimulated lipolysis) or not (for basal lipolysis) with 20 μM of isoproterenol bitartrate.

1.1.4. Buffers for western blotting

- **Buffer for protein transference into nitrocellulose membrane.** 76.8 mM glycine, 0.04 % (w/v) SDS, 10 mM Tris-HCl, 20% (v/v) methanol (Panreac, Spain).
- **Homogenization buffer**. 10 mM NaF, 1% (v/v) NP-40, 2 mM Na_3VO_4, 150 mM NaCl, 50 mM 4-(2-hydroxyethyl)-1-piperazineethanesulfonic acid (HEPES), 10% (v/v) glycerol (Merck-Millipore, Germany), 10

mM $Na_4P_2O_7$, 2 mM EDTA-Na_2, 2 mM phenylmethanesulfonyl fluoride (PMSF), 0.1 mM leupeptin (Fisher Scientific, USA); pH 7.4.

- **Loading buffer for SDS-PAGE (5 x)**. 300 mM Tris-HCl, 50% (v/v) glycerol; 10% (w/v) SDS; 25% (v/v) 2-mercaptoethanol, 0.04 (w/v) bromophenol blue; pH 6.8
- **SDS-PAGE buffer.** 25 mM Tris-HCl; 192 mM glycine, 0.1% (w/v) SDS; pH 8.3
- **Tris-buffered saline supplemented with Tween 20 (TBST)**. 0.15 M NaCl, 20 mM Tris-HCl, 0.05% (v/v) Tween 20 in dH_2O; pH 7.5.

1.1.5. Other buffers

- **Bradford reagent mixture.** 0.01% (w/v) Coomassie Brilliant Blue G, 5% (v/v) ethanol (Panreac, Spain), 10% (w/v) H_3PO_4 in dH_2O.
- **Chromic mixture.** 50% (v/v) H_2SO_4 (Fluka Chemical, USA), 0.5% (w/v) $K_2Cr_2O_7$ (Probus, Spain).
- **Phosphate buffered saline (PBS).** 0.14 mM NaCl, 3 mM KCl, 10 mM Na_2HPO_4, 1.2 mM KH_2PO_4 in miliQ H_2O; pH 7.4
- **Physiological serum (PS).** 0.9% (w/v) NaCl in dH_2O.

1.1.6. Other medias

- **Medium for cell maintenance.** 1 g/L glucose containing EMEM supplemented with 100 IU/ml penicillin, 100 µg/ml streptomycin, 2 mM L-glutamine and 10% (v/v) fetal bovine serum (FBS) from ATCC (USA).
- **Medium for gene silencing.** 1 g/L glucose containing EMEM supplemented with 2 mM L- glutamine and 10% (v/v) FBS.

Unless otherwise specified, all reagents are from Sigma-Aldrich, USA.

1.2. Equipment

Automated cell counter	Bio-Rad TC 20™
Centrifuge	Sorvall RT 7 (rotor RTH-750)
Chamber for electrotransference	Bio-Rad Trans-Blot Cell
Class II Biological Safety Cabinets	Thermo Scientific MSC-Advantage
Concentrator-evaporator	Thermo Scientific Savant SC250EXP
Confocal microscope	Olympus Fluoviwe FV500
Densitometer	Bio-Rad GS-800 and Molecular Imager FX
Electrophoresis Power Supply	Bio-Rad Power 1000
Exposure cassette	FUJI EC-AWU (18 x 24 cm^2)
Glucometer	Arkray Glucocard M
Gavage needle	Instech Laboratories 20 GA 25 mm stainless feeding tube
Heater	P Selecta Theroven (200 °C)
Homogenizers	Kinematica Polytron PT 1200 C and B.Braun Biotech International and Elvejhem Potter S
Horizontal electrophoresis	Bio-Rad Sub-Cell GT agarose Gel Electrophoresis System
Incubator of CO_2	Thermo Scientific HeraCell 150
Microcentrifuges	Heraeus Biofuge primoR and Biofuge Fresco
Microtome	Equipment of the sterilization service from the Department of Cellular Biology and Histology, Faculty of Medicine and Nursing, UPV/EHU
Optic microscope	Carl Zeiss AG, Nikon Eclipse 50i and Jenoptik ProgRes® CapturePro camera
pHmeter	Crison GLP 21
Scintillation liquid analyzer	PerkinElmer Tri-Carb 2810 TR
Shakers	Heidolph REAX 2000 and Duomax 1030
Sonicator	Soniprep 150
Spectophotometers	Nanodrop ND-1000 Spectophotometer and a plate reader Biotek Synergy™ HT

Sterilization	Equipment of the sterilization service from the Department of Cellular Biology and Histology, Faculty of Medicine and Nursing, UPV/EHU
Thermocycler	Biometra T-Gradient Thermoblock
Thermostatic bath with shaker	P-Selecta Unitronic 320 OR
TLC chamber	Desaga
Ultracentrifuge	Beckman Coulter Optima™ L-100 XP
Ultracentrifuge rotors	Beckman Coulter 50.4 Ti
Vertical electrophoresis	Bio-Rad Mini Protean II
Weighing scales	Mettler PJ400 and Mettler AT231 Delta rang

2. Models of study

2.1. Human samples

2.1.1. Clinical and laboratory assessment in human samples

This study comprised 80 liver samples. 18 samples were from liver donors who died from stroke and were provided by Dr. Javier Crespo from Marqués de Valdecilla University Hospital, Santander, Spain. Analysis of liver biopsies proved that livers were histologically normal (NL) and there was no evidence of hepatitis B virus (HBV), hepatitis C virus (HCV) and human immunodeficiency virus (HIV). Body mass index (BMI) in these donors was lower than 30 kg/m^2.

62 patients were obese patients with a BMI higher than 30 kg/m^2 who underwent to liver biopsy with a diagnostic purpose. 15 of them had histologically NL and 47 patients were diagnosed with non-alcoholic fatty liver disease (NAFLD) according to Kleiner's criteria (Kleiner, Brunt et al. 2005). Inclusion criteria for obese patients were also based on the absence of alcohol (< 20 g per day) or potentially hepatotoxic drugs intake. They showed negative serum tests for HBV, HCV and HIV and none of them suffered from autoimmune medical conditions.

The study was performed in agreement with the Declaration of Helsinki and with local and national laws. The Human Ethics Committee of each hospital and the University of the Basque Country approved the study procedures and a written informed consent was obtained before inclusion in the study.

2.2. Animal models

3 or 9 month-old male *E2f1* knockout (*E2f1*$^{-/-}$), *E2f2* knockout (*E2f2*$^{-/-}$) and their wild type (WT) (129/Sv x C57BL/6) littermates were produced in the animal facility of the University of Basque Country UPV/EHU, in Dr. Ana Zubiaga's laboratory (Department of Genetics, Physical Anthropology and Animal Physiology, Faculty of Science and Technology, UPV/EHU). *E2f1* and *E2f2* knock-down was validated by western blotting (see procedure in Materials and Methods, section 3.9) (Figure D1).

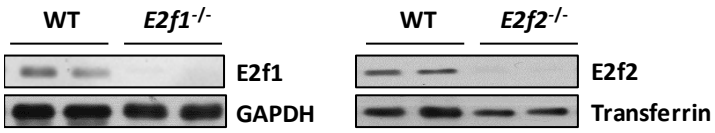

Figure D1. Validation of *E2f* knock-down in livers of 3-month-old *E2f*$^{-/-}$ mice. *E2f1* knockout (*E2f1*$^{-/-}$), *E2f2* knockout (*E2f2*$^{-/-}$) and their wild type (WT) mice were used. They were sacrificed at 3 months old and liver was collected. E2f1 and E2f2 liver content was assessed by immunoblotting using glyceraldehyde-3-phosphate dehydrogenase (GAPDH) or transferrin as loading control (n=8 per group) (see the procedure in Materials and Methods, section 3.9). Representative immunoblots are shown.

5-6 mice were placed in each cage. They were housed at 22 °C with an artificial 12 hours light (8:00 to 20:00)/12 hours dark cycle. Food and tap water were provided *ad libitum*. Body weight and food intake were measured every two weeks. Food intake was determined as consumed grams per day and mouse.

Animal procedures were approved by the Ethics Committee for Animal Welfare of the University of the Basque Country UPV/EHU, in accordance with the European Union Directives for animal experimentation.

2.2.1. Induction of hepatocellular carcinoma and non-alcoholic fatty liver disease

Hepatocellular carcinoma (HCC) was induced by administration of the hepatic procarcinogen diethylnitrosamine (DEN) combined with high-fat diet (60% fat calories mouse diet, F3282, Bio-Serv, USA) (HFD) or chow diet (20% Protein Mouse Control Diet F4031; Bio-Serv, USA) (CD) as described (Park, Lee et al. 2010) (Figure D2). DEN (25 mg/kg of mice, Sigma-Aldrich, USA) was injected to mice intraperitoneally on postnatal day 14. After weaning at 1 month old, mice were placed in HFD (referred to them as DEN HFD group) or in CD (named as DEN CD group) for 32 weeks and sacrificed at 9 months old (9m). Other age-matched groups were administered vehicle alone (physiological serum, PS) combined with CD (named as CD group) or HFD (referred to them as HFD group).

Non-alcoholic fatty liver disease was studied in 3 month-old mice (3m). For that, DEN or PS was administered as describe above and mice were fed with CD or HFD for 10 weeks.

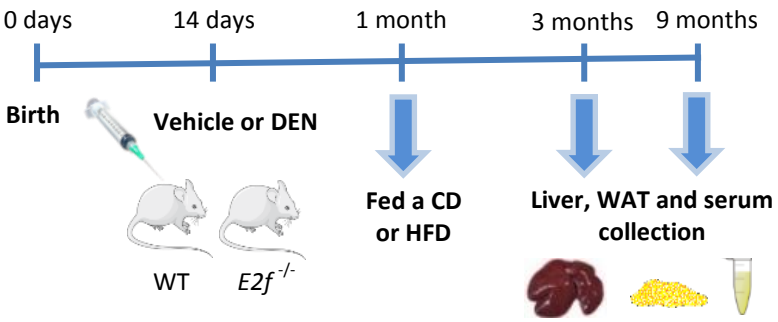

Figure D2. Schematic representation of treatments for HCC and NAFLD induction in mice. 25 mg/kg of mice of the hepatic procarcinogen diethylnitrosamine (DEN) or the vehicle were administered intraperitoneally in 2-week-old male *E2f1* knockout (*E2f1*$^{-/-}$), *E2f2* knockout (*E2f2*$^{-/-}$) and wild type (WT) mice. Animals were weaned two weeks later and were kept on a chow diet (CD) or a high-fat diet (HFD) until sacrificed at 3 or 9 months old. Then, serum, liver and WAT were collected. HCC, hepatocarcinoma; NAFLD, non-alcoholic liver disease; WAT, white adipose tissue.

2.2.2. Tissue and serum collection

Otherwise specified, mice were fasted for 4 hours and were euthanized with sodium pentobarbital (Abbott Laboratorios, Spain) injected intraperitoneally (60 mg/kg of mice in PS).

Blood was drawn by puncture in the inferior vena cava or in the tail vein and was allowed to clot at RT for 30 minutes. For serum, blood was centrifuged at 2,000 xg for 30 minutes at 4 °C. For elimination of any cellular fraction, the resultant supernatant was centrifuged again at 10,000 xg for 10 minutes at 4 °C. Serum was collected and stored at -80 °C for subsequent analysis.

Liver and white adipose tissue (WAT) were collected and washed in cold PBS. Tissues were rapidly weighed and tumors in liver were counted and measured with a caliper. Then, tissues were divided immediately into different pieces to be used in metabolic assays, to be fixed with formalin (Sigma-Aldrich, USA) or Tissue-Tek® O.C.T. Compound (VWR-Avantor, USA) for histological analysis and to be frozen in liquid nitrogen and stored at -80 °C until biochemical analysis.

2.3.Cell lines

The human hepatoma cell line HepG2 was purchased from ATCC. Cells were cultured in maintenance medium (Materials and Methods section 1.1.6) at 37 °C and 5% CO_2.

3.2.1.*E2F1* or *E2F2* knock-down

Knock-down experiments were performed by siRNA oligonucleotide reverse transfection. Validated anti-*E2F1* siRNA (si*E2F1*) and pre-designed anti-*E2F2* siRNA (si*E2F2*) (all from Ambion, USA) were used. Negative controls were included in each assay by using Silencer™ Select Negative Control siRNA (siC) (Ambion, USA). Nucleotide sequences for each specific siRNA are detailed in Table D1.

Table D1. siRNA sequences used for gene silencing in HepG2 cells.

siRNA	Species	Sense	Antisense
si*E2F1*	*Homo sapiens*	5'-GUCACGCUAUGAGACCUCATT-3'	5'-UGAGGUCUCAUAGCGUGACTT-3'
si*E2F2*	*Homo sapiens*	5'-GCCUCAUGGUUCUAGUAAATT-3'	5'-UUUACUAGAACCAUGAGGCCT-3'

Lyophilized siRNAs were resuspended in nuclease-free sterile water (Ambion, USA) at 50 mM. These stock solutions were stored at -20 °C. Work solutions were prepared for immediate use at 1 mM.Cells were seeded in the suitable dishes for each subsequent assay. Conditions are detailed in Table D2. siRNA, OptiMEM Reduced Serum (Gibco, USA) and RNAiMAX lipofectamine (Invitrogen, USA) were incubated in the corresponding plates for 20 minutes at RT. Afterwards, HepG2 cells in medium for gene silencing (section 1.1.6.) were added to siRNA-containing plates and cultured for 48 hours. Metabolic studies were carried out as described in each section.

Table D2. Conditions for siRNA reverse transfection in HepG2 cells.

	Cytochemistry	WB mRNA expression	TG content measure Radioisotope assays
Plate	24-well	6-well	60 mm diameter
nM siRNA	12	12	18
ul siRNA work solution	6	30	53
ul Lipofectamine RNAiMAX	1	5	9
ul OptiMEM	100	500	875
Cells	7.5×10^4 cells in 0.4 ml medium	4×10^5 cells in 2 ml medium	7.5×10^5 cells in 2 ml medium

Gene silencing efficiency was confirmed by RNA expression analysis as described in section 3.11 (Figure D5).

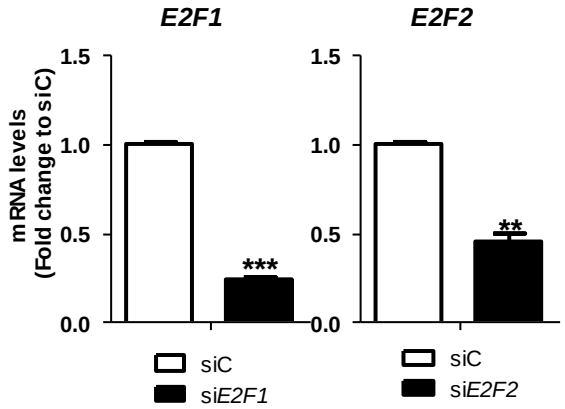

Figure D5. Validation of *E2F1* or *E2F2* knock-down in human tumoral cells. *E2F1* (si*E2F1*) or *E2F2* (si*E2F2*) were silenced in HepG2 cell line by reverse transcription of specific siRNAs. Negative controls (siC) were included in each assay. mRNA expression of *E2F1* and *E2F2* was analyzed by rt-q-PCR. Procedure is described in Materials and Methods section 3.11. Values are means ± SEM of 5 experiments per group. Significant differences between si*E2F* and siC are indicated as **p<0.001 and *** p<0.0001).

3.Experimental procedures

3.1. Histochemistry and cytochemistry

3.1.1. Liver sample preparation

Unless otherwise specified, fresh liver pieces were fixed in 10% (v/v) non-buffered formalin (Sigma-Aldrich, USA) for 24 hours at 4 °C and were kept in 50% (v/v) ethanol (Scharlau Chemicals, Spain) until they were paraffinized.

The paraffin blocks were prepared and cut in 5 µm-thick sections with the microtome. They were picked up in poly-lysine treated microscope slides (Thermo Scientific, USA) and fixed overnight at 37 °C.

3.1.2. Hematoxylin and eosin staining

Paraffin embedded section was deparaffinized in xylene (Sigma-Aldrich, USA), rehydrated with decreasing ethanol solutions (Scharlau Chemicals, Spain) and washed with distilled water (dH_2O). After that, it was stained with Shandon™ Harris Hematoxylin (Thermo Scientific, USA) for 2.5 minutes and washed with dH_2O. Sample was decolorized by immersion in 0.5% (v/v) HCl (Merck-Millipore, Germany) and washed with dH_2O. Then, tissue was counterstained with Eosin-Y Alcoholic (Thermo Scientific, USA) for 25 seconds, washed and dehydrated with increasing ethanol solutions. Finally, samples were mounted using DPX mounting medium (Sigma-Aldrich, USA).

Representative micrographs were taken under 20 x objective from upright optical microscope.

3.1.3. Sirius Red staining

Fibrogenesis was assessed staining collagen fibers with Sirius Red (Yata, Gotwals et al. 2002).

Paraffin embedded section was deparaffinized and rehydrated. Once hydrated, section was placed in Sirius red staining solution I (section 1.1.1) for 15 minutes and in Sirius red staining solution II (section 1.1.1) for another 15 minutes. Then, it was dehydrated in ethanol 100 % (Scharlau Chemicals, Spain) and washed with Histo-Clear (National Diagnostics, USA). Finally, section was mounted using DPX mounting medium (Sigma-Aldrich, USA).

Micrographs were digitally taken under 20 x objective as described above. Stained collagen area was quantified with FRIDA software in randomly chosen 5 fields for each liver section.

3.1.4. Oil red O staining

Hepatic steatosis was analyzed in liver tissue by Oil red O staining, which visualizes neutral lipids (Mehlem, Hagberg et al. 2013).

8 µm-thick OCT-frozen tissue sections were cut and fixed with 10% (v/v) non-buffered formalin (Sigma-Aldrich, USA) for 2 minutes. Section was rinsed in 60% (v/v) isopropanol (Scharlau Chemicals, Spain) and stained with freshly prepared and filtered Oil Red O solution (section 1.1.1). Afterwards, samples were placed in 60% (v/v) isopropanol (Scharlau Chemicals, Spain) and counterstained with Mayer Hematoxylin (Sigma-Aldrich, USA) for 1 minute. Finally, they were mounted with aqueous mounting media (Dako, Denmark).

Representative micrographs were taken under 40 x objective as described before.

3.1.5. Immunohistochemical analysis of Ki67, E2F1 and E2F2

In all the immunostaining types, liver sections were deparaffinized, rehydrated and washed with PBS. Then, they were subjected to antigen retrieval with citrate buffer (section 1.1.4) for 20 minutes at 97 °C and non-boiling conditions. Once the antigen was unmasked, sections were blocked with 3% H_2O_2 in PBS for 10 minutes at RT. To reduce background, sections were re-blocked for 30 minutes at RT. Then, samples were incubated with primary antibody in a humid chamber. Re-blocking and incubation conditions for each antibody are detailed in Table D3. Afterwards, sections were incubated with ImmPRESS™ anti-rabbit HRP conjugated secondary antibody (Vector laboratories, USA) for 30 minutes at RT. Colorimetric detection was performed with Vector VIP purple chromogen (Vector laboratories, USA). Finally, samples were counterstained with Mayer Hematoxylin (Sigma-Aldrich, USA), washed with tap water, dehydrated and mounted with DPX mounting media (Sigma-Aldrich, USA) as described before.

Micrographs were digitally taken under 40 x objective. Ki67 staining, which evaluates cell cycle progression to S phase (Gerdes, Lemke et al. 1984), was quantified with CellProfiler software counting the number of positive stained nuclei in randomly chosen 5 fields for each liver section. E2f1 or E2f2 stained nuclear area was calculated with FRIDA software, in randomly chosen 5 fields for each patient.

Table D3. References, re-blocking solutions and incubation conditions for the primary antibodies used in immunohistochemical analysis.

	Trading house	Catalog No.	Re-blocking solutions	Antibody incubation conditions	Host
Ki67	Abcam	AB66155	10% goat serum in PBS	1:2000 (v/v) in 2% (w/v) BSA-PBS 1 hour at RT	Rabbit
E2f1	Abcam	AB94888	5% ImmPRESS™ goat serum (Vector)	1:100 (v/v) in antibody diluent (Dako) Overnight at 4 °C + 1 hour at 37 °C	Rabbit
E2f2	Invitrogen	PA5-41473	5% ImmPRESS™ goat serum (Vector)	1:100 (v/v) in antibody diluent (Dako) 2 hours at 37 °C	Rabbit

PBS, phosphate buffered saline; BSA, bovine seroalbumine; RT, room temperature; Invitrogen, Invitrogen (USA); Vector, Vector Laboratories (USA); Dako, Dako (Denmark).

3.1.6. Cytochemistry of neutral lipids

7.5 x 10^4 cells were seeded in sterilized circular coverslips in 24-well plates as described in section 2.3.1. After silencing, cells were washed three times with PBS and were fixed with formaldehyde 3.7% (v/v) (Panreac, Spain) in PBS. For cell permeabilization, sample was incubated in 0.25% (v/v) Triton (Sigma-Aldrich, USA) in PBS for 5 minutes at RT. Afterwards, three washes were realized and cells were blocked with 10% (v/v) FBS (Biochrom, UK) in PBS for 15 minutes at RT.

Neutral lipid droplets were stained with Bodipy 493/503 green fluorescent dye (1:200 in PBS) (Invitrogen, USA) for 2 hours at RT. Subsequently, coverslips were washed three times in order to remove the remaining dye and cell nucleus were dyed with DAPI blue fluorescent probe (Sigma-Aldrich, USA) (1:1000 in PBS) for 5 minutes at RT. Finally, coverslips were mounted with aqueous mounting media (Dako, Denmark).Optical images were taken with Olympus Fluoviwe FV500 confocal microscopy in the SGIker Microscopy Service from the UPV/EHU.

3.2. Serum analysis

Depending on the parameter aimed to measure, blood was drawn in mice from the tail vein or the inferior vena cava. Then, serum was isolated as indicated in section 2.2.2.

3.2.1. Quantification of transaminase, lipids and glucose

Serum transaminase alanine aminotransferase (ALT), total triglyceride (TG), fatty acids (FA) and glucose were quantified with colorimetric method assays by commercially available kits. For that, 96-well plates were used and samples were applied in duplicate.

ALT was measured in serum obtained from the inferior vena cava of mice sacrificed after 4 hours of food deprivation following the commercial kit instructions. In brief, 12 µl of serum were diluted to a volume of 15 µl with dH_2O. Then, the sample was mixed with 200 µl of reagent (R1:R2, 4:1) (Spinreact, Spain) and incubated for 1 minute at 37 °C. Absorbance was read at 340 nm in 1 minute intervals during 30 minutes. The interval from 10 to 20 minutes was chosen to calculate ALT concentration. The standard range used for the calibration curve was from 129 to 1548 µU. Data are represented as international units per serum liter.

Serum **TG** measurement was performed in blood drawn of the tail vein of mice after 13 hours of fasting as detailed in commercial available kits. In brief, 7 µl of serum were diluted to a volume of 15 µl with dH_2O. Then, 200 µl of reagent (Menarini Diagnostics, Italy) were added to sample and incubated for 5 minutes at 37 °C. Absorbance was measured at 500 nm. The calibration curve was built with a multicalibrator (1.2 to 35.2 µg of TG) (Menarini Diagnostics, Italy) and the results obtained are expressed as mg of TG per serum dL.

FA determination was performed following the instructions of a commercial kit. In brief, 3 µl of serum from 13 hours fasted state were used in a volume of 15 µl. 160 µl of R1 reagent (Wako Life Sciences, USA) were added to serum and were incubated for 2 minutes at 37 °C. Blank measurement was performed at 546 nm. Then, 80 µl of R2 reagent were added and absorbance was read after 4 minutes of incubation period at 37 °C. FA concentration was calculated substracting the blank read. The standard range used for the calibration curve was from 0.5 to 15 nmol. Results are represented as µM of FA.

Glucose concentration was measured with a glucometer (Arkray Factory, Japan) in blood obtained from the mice tail vein. Data are expressed as mg of glucose per serum dL.

3.3. Tolerance tests

Insulin resistance (IR) was evaluated in mice by glucose, insulin and pyruvate tolerance tests.

3.3.1. Glucose tolerance test (GTT)

After 4 hours of fasting, mice received a glucose solution (2 g/kg of mice) dissolved in tap water by oral gavage with a suitable needle (Instech Laboratories, USA) (Andrikopoulos, Blair et al. 2008). Blood glucose levels were measured (as indicated in section 3.2.1.) before and 15, 30, 60 and 120 minutes postgavage.

3.3.2. Insulin tolerance test (ITT)

For insulin sensitivity studies, mice were fasted for 4 hours. Then, mice received an intraperitoneal injection of 0.75 U insulin/kg of mice dissolved in PBS (Sun, Miller et al. 2012). Glucose levels were monitored as described before in GTT.

3.3.3. Pyruvate tolerance test

Pyruvate tolerance test was performed to determine the activation of gluconeogenesis, more specifically, the biosynthesis of glucose from pyruvate. Mice were fasted for 13 hours and injected intraperitoneally a sodium pyruvate (2 g/kg of mice) solution dissolved in PBS (Song, Kim et al. 2013). Glucose levels were monitored as described above GTT and ITT.

3.4. Quantification of lipids in liver and cells

3.4.1. Sample preparation

For lipid extraction in **liver**, 30 mg of tissue were mechanically homogenized in 10 volumes of cold PBS with a Potter Elvehjem Glass homogenizer by 20 strokes of a glass pestle at 700 rev/minutes in an ice bath at 4 °C. Then, as detailed in section 3.10.1, protein concentration was measured.

For lipid extraction in **cells** were washed twice with PBS and scraped in 1 ml of PBS. They were centrifuged at 2,000 xg for 5 minutes at 4 °C and resuspended in 1 ml of dH_2O. Samples were subjected to 2 freeze-thaw cycles to ensure cell lysis. Afterwards, protein concentration was measured (see section 3.10.1).

3.4.2. Lipid extraction

Lipids were extracted following the Folch method (FOLCH, LEES et al. 1957) from 1.5 mg of protein of liver homogenate or from 1 mg of cellular suspension. Glass material was used, previously cleaned with chromic mixture to avoid biological contamination.

Samples were diluted to 1.5 ml with dH_2O and 8 ml chloroform:methanol:HCl (1:2:0.0075, v/v/v) (Scharlau Chemicals, Spain) solution was added. Tubes were shaken vigorously in a shaker for 2 minutes. After that, they were centrifuged at 2,000 xg for 12 minutes at 4 °C to separate the aqueous phase (the upper one) and the organic phase (the lower one). Lipid containing chloroformic phase (lower phase) was transferred to another tube using a glass Pasteur pipette. Then, the remaining lipids were reextracted from the aqueous phase. For that, 4 ml chloroform:methanol:HCl (1:2:0.0075, v/v/v) were added and tubes were shaken and centrifuged as described before. The separated organic phase was collected and mixed with the previous one. To remove the aqueous contaminant, organic phase was washed by adding 0.88% (w/v) KCl solution in one third of the final volume. Tubes were vigorously shaken with a vortex for 1 minute and were centrifuged at 2,000 xg for 12 minutes at 4 °C. The lower phase was then transferred to another tube.

Finally, samples were evaporated to dryness with a concentrator-evaporator at 45 °C for 1.5 hours. Lipid extract coming from liver o cell samples was dissolved in 100 µl toluene (Scharlau Chemicals, Spain) and was stored in N_2 atmosphere in glass vials at -20 °C until it was analyzed.

3.4.3. Lipid separation by thin layer chromatography

Lipid extract was separated by thin layer chromatography (TLC) with six developments (Ruiz, Ochoa 1997).

First of all, 20 x 20 cm silica-gel plates (Pre-coated TLC-plates SIL-G25, Macherey-Nagel, Germany) were pre-treated with 1 mM EDTA-Na_2 for at least 5 hours and left drying overnight. After that, impurities

were removed washing the plates with chroloform:methanol:dH_2O (60:40:10, v/v/v) overnight. Plates were activated at 100 °C for 30 minutes the day the TLC was going to carry out.

3 µl of pure lipid standards (Avanti Polar Lipids and Sigma-Aldrich, USA) and 3 µl of the lipid extracts were spotted at 1.5 cm from the lower edge of the plate. Then, six different chromatographic developments were consecutively carried out in solutions of decreasing polarity as presented in the Table D4. After each chromatographic development, plates were dried using hot air.

Table D4. Mixture of solvents used in the six chromatographic developments for neutral lipids and phospholipids separation by thin layer chromatography.

Mobile phase composition	Proportion (v:v)	Distance from the edge (cm)
Chloroform:methanol:dH_2O	60:40:10	1.8
Chloroform:methanol:dH_2O	65:40:5	2.3
Ethyl acetate:ethanol:isopropanol: methanol:chloroform:KCl at 0.25%	35:20:5:15:22:9	5.5
Toluene:diethyl ether:ethanol	60:40:3	8.5
n-heptane:diethyl ether	94:8	12
n-heptane	100	13

3.4.4. Lipid visualization and quantification

When all the chromatographic separations were performed, lipids were charred by dipping the plate in a solution of 10% $CuSO_4$ (w/v) in 8% H_3PO_4 (v/v) for 10 seconds. Subsequently, the plate was dried with hot air until the first lipid dots became evident and was immediately heated at 200 °C for 3 minutes.

An image of the TLC plate was digitalized with GS-800 densitometer (Bio-Rad Laboratories, USA) (Figure D2) and quantification was performed with Quantity One software (Bio-Rad Laboratories, USA). The integrated optic density (IOD) of each lipid spot, after substraction of the background, was interpolated in the IOD values of the calibration curves. Lipid quantity ranges (nmol) for calibration were the following ones: CE (0.09-1.45), TG (0.27-17), DG (0.15-3), FC (0.36-3.6), CL (0.02-0.3), PE (0.33-3.91), PI (0.1-1.72), PS (0.13-2.22) and PC (0.63-7.63). The obtained results were expressed in nmol per mg of protein.

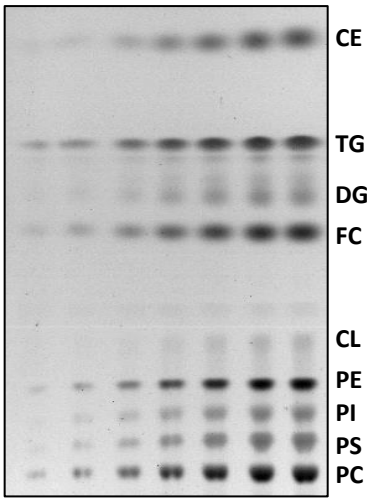

Figure D2. A representative image of a TLC with the 9 different pure lipid standards. CE, cholesteryl ester; CL, cardioliphin; DG, diacylglyceride; FC, free cholesterol; PC, phosphatidylcholine; PE, phosphatidylethanolamine; PI, phosphatidylinositol; PS, phosphatidylserine and TG, triacylglyceride.

3.4.5. Triglyceride concentration measurement

For liver or cellular TG quantification, the enzymatic assay detailed in section 3.2.1 was used.

Lipids were extracted (section 3.4.2) and dissolved in 100 µl of isopropanol (Scharlau Chemicals, Spain). A microassay was performed with 5 µl of lipid extract from liver homogenate or 20 µl of sample from cellular suspension. The corresponding volume of isopropanol was added to the calibration curve. The obtained results were expressed in nmol per mg of protein.

3.5. Analysis of liver triglyceride secretion rate

Liver TG secretion, indicative of the production rate of very-low density lipoprotein (VLDL) by the liver, was measured in mice *in vivo*. For that, animals were fasted for two hours before the experiment was carried out, which avoids circulating chylomicrons in blood stream.

VLDL catabolism was then inhibited by intraperitoneal injection of Pluronic F-127 (Poloxamer P-407) (Invitrogen, USA), a lipoprotein lipase inhibitor, in physiological serum (PS) (section 1.1.5) at 1 g/kg of mice (Millar, Cromley et al. 2005). Immediately prior to injection and 6 hours following injection, blood samples were drawn and TG concentration was measured by commercially available kit (section 3.2.1).

The hepatic VLDL secretion rate was calculated from the difference in serum TG levels over the 6 hours following Poloxamer injection. The obtained results were expressed as mM per hour.

3.6. Analysis of metabolic fluxes using radioisotopes

Metabolic fluxes were quantified by radioisotope incorporation. These experiments were performed *in vitro* in HepG2 cells, *in vivo* in mice and *ex vivo* in liver tissues.

3.6.1. Synthesis of triglyceride

Synthesis of TG was assessed in two different ways, depending on the step aimed to study. Esterification of glycerol and FAs was analyzed by measuring the [^{14}C]-glycerol or [^{3}H]-oleate incorporated into TG and *de novo* synthesis of TG was analyzed measuring the [^{3}H]-acetate incorporated into TG (Figure D3).

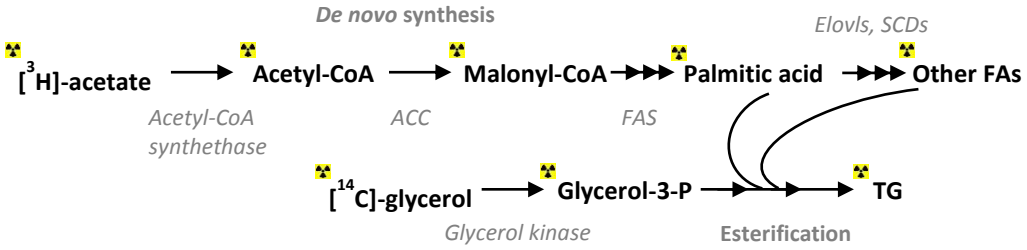

Figure D3. The radioactive track from [^{3}H]-acetate or from [^{14}C]-glycerol into TG for measurement of its synthesis. ACC, acetyl-CoA carboxilase; Elovls, fatty acyl-CoA elongases; FA, fatty acids; FAS, FA synthase; SCDs, stearoyl-CoA desaturases; TG, triacylglyceride.

3.6.1.1. *In vivo* esterification of [^{14}C]-glycerol into triglyceride

After two hours of food deprivation, animals were administered the corresponding [^{14}C]-glycerol medium (section 1.1.3) intraperitoneally (Niebergall, Jacobs et al. 2011). 2 hours later, liver was collected and used for lipid extraction and separation.

750 mg of liver were homogenized as described in section 3.4.1. Lipids were extracted from each of the prepared homogenate. Lipid extract was then dissolved in 200 µl of toluene (Scharlau Chemicals, Spain) and lipids were separated by TLC (section 3.4.3) with slight modifications. In this case, 30 µl of each sample were applied in non-pre-treated plates and TLC was carried out with four developments. This chromatographic method was able to separate the following lipids: PC, PE, FC, DG, TG and CE. Solvent mixtures for each development are indicated in Table D5.

Table D5. Mixture of solvents used in the four chromatographic developments for neutral lipids and phospholipids separation by TLC.

Mobile phase composition	Proportion (v:v)	Distance from the front (cm)
Chloroform:methanol:dH_2O	60:40:10	1.8
Chloroform:methanol:dH_2O	65:40:5	2.3
Ethyl acetate:ethanol:isopropanol: methanol:chloroform:KCl at 0.25 %	35:20:5:15:22:9	5.5
n-heptane:diisopropylether:acetic acid	70:30:3	15
n-heptane	100	16

After performing the TLC, lipids were dyed with iodine vapors. For that, a chromatographic chamber containing iodine crystals was used. The plate was maintained in there until the yellow bands of lipids appeared. The silica-band corresponding to TG was scraped and transferred into vials with 4 ml of Coctail BioGreen 3 scintillation liquid (Scharlau Chemicals, Spain). The radioactivity was measured in a scintillation liquid analyzer. Finally, results obtained were represented as dpm per grams of liver tissue.

3.6.1.2. Esterification of [^{3}H]-oleate into triglyceride in cell culture

Synthesis of TG from oleate was assessed with [^{3}H]-oleate in HepG2 cells (Aspichueta, Perez et al. 2005). After E2F2 RNA knock-down (section 2.3.1.) cells were incubated with 1.5 ml of the corresponding media containing [^{3}H]-oleic acid (section 1.1.3.) for 120 minutes at 37 °C and 5% CO_2. Afterwards, cells were washed 5 times with cold PBS and scraped in 1 ml of PBS. 100 µl of cell suspension were used for total protein measure as described in section 3.10.1.

Lipids were extracted from the rest of the sample (section 3.4.2.) and separated by TLC (section 3.4.3) with slight modifications. All lipid extract was resuspended in 50 µl of toluene (Scharlau Chemicals, Spain) and applied in non-pre-treated plates. In order to ensure the recollection of lipids another 30 µl of toluene were added to sample containing vials and applied in the plates. Three chromatografic developments were carried out, which separates the following main classes of lipids: phospholipids (PL), FC, DG, TG and EC. Solvent mixtures for each development are indicated in Table D6.

Table D6. Mixture of solvents used in the three chromatographic developments for neutral lipids and phospholipids separation by TLC.

Mobile phase composition	Proportion (v:v)	Distance from the front (cm)
Chloroform:methanol:dH_2O	60:40:10	1.8
n-heptane:diisopropylether:acetic acid	70:30:3	15
n-heptane	100	16

The radioactivity incorporated from [^{3}H]-oleate into TG was quantified as described in section 3.6.1.1. The results obtained were expressed as dpm per grams of cellular protein.

3.6.1.3. *De novo* lipogenesis of triglyceride

De novo lipogenesis (DNL) of lipids was assessed as described by Aspichueta et al (Aspichueta, Perez et al. 2005) in cell culture or in liver tissue.

When DNL was measured in **cells**, previously silenced **HepG2 cells** (section 2.3.1.) were incubated with 1.5 ml of the corresponding media containing the labelled substrate (section 1.1.3.) for 120 minutes at 37 °C and 5% CO_2. Afterwards, as indicated in section 3.6.1.2, cells were recollected and washed, total protein was measured and lipids were extracted.

To analyze DNL **in livers,** mice were fasted for 3 hours before sacrifice for liver extraction. 40 mg of freshly isolated tissue slices were incubated in 700 µl of DNL media containing [^{3}H]-acetic acid (section 1.1.3) for 4 hours at 37 °C. Tissue slices were then washed five times in cold PBS, freeze immediately with liquid nitrogen and stored at -80 °C until further analysis. Tissue was homogenized (section 3.4.1) and lipids were extracted from all the homogenate (section 3.4.2).

In both cases, lipids were separated by TLC as described in section 3.6.1.2.

The [^{3}H] label incorporated into TG was measured as described in section 3.6.1.1. The results obtained were represented as dpm per grams of cellular protein or dpm per grams of liver tissue.

3.6.2. Fatty acid β-oxidation rate

The rate of fatty acid β-oxidation was determined by measuring the complete oxidation of [^{14}C]-palmitate into CO_2 and its incomplete oxidation into soluble acid metabolites (ASM) (Huynh, Green et al.

2014) (Figure D4). ASM include the following molecules: acetyl-CoA, acetyl-carnitines, ketone bodies and tricarboxylic acid (TCA) cycle intermediates.

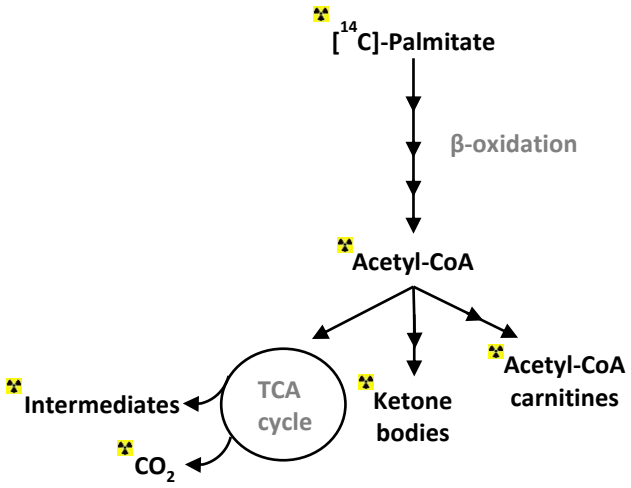

Figure D4. The radioactive track from [^{14}C]-palmitate into acid soluble metabolites and CO_2. TCA; trycarboxylic acid.

When the assay was performed *ex vivo* in **liver sections**, mice were fasted for 3 hours before sacrifice. 60 mg of fresh liver pieces were homogenized with cold homogenization buffer (section 1.1.2) in a Potter Elvehjem Glass homogenizer by 5 strokes (section 3.4.1). Thereafter, homogenates were sonicated at 6 microns of potency for 10 seconds in an ice bath and were centrifuged at 500 xg for 10 minutes at 4 °C. 500 µg of protein from the homogenate supernatants were used for the assay in a volume of 200 µl. The reaction was started by adding 400 µl of the assay mixture containing [1-^{14}C]-palmitic acid (section 1.1.3). Samples were incubated for 1 hour at 37 °C in 1.5 ml tubes with a Whatman chromatography paper disc (GE Healthcare, UK) in the cap. Reaction was stopped by adding 300 µl of 3 M perchloric acid (Scharlau Chemicals, Spain). In this way, ASM remain soluble and unoxidized-bound palmitate precipitates out of the solution. Just before stopping the reaction, paper discs were impregnated with 1 M NaOH (Sigma-Aldrich, USA), which allowed capturing the CO_2 released from the acetyl-CoA oxidized in the TCA cycle. Samples were incubated for 2 hours at RT.

For cell cultures, previously silenced **HepG2 cells** (section 2.3.1.) were incubated with 1.5 ml of the corresponding media (section 1.1.3.) for 4 hours at 37 °C and 5% CO_2. Afterwards, medium was collected and centrifuged at 5000 xg for 5 minutes. 1000 µl of the supernatant were transferred into another tubes.

A paper disc impregnated with 1 M NaOH was put in each cap and the reaction was stopped as describe above. Then, samples were incubated for 2 hours at 37 °C with a gentle shaking.

After the corresponding time of incubation, in both cases, paper discs were transferred into glass vials containing 4 ml of Optiphase HISAFE 2 scintillation liquid (PerkinElmer, USA). The remaining acid solution was centrifuged at 21,000 xg for 10 minutes at 4 °C. 400 µl of the supernatant were transferred to plastic vials containing 4 ml of Hionic Fluor scintillation liquid (PerkinElmer, USA). The radioactivity associated to CO_2 and ASM was measured in a scintillation liquid analyzer. [^{14}C]-palmitate label was also quantified in non-incubated reaction mixture with 4 ml of Coctail BioGreen 3 scintillation liquid (Scharlau Chemicals, Spain), in order to calculate the specific activity of the reaction. The oxidized moles of [1-^{14}C]-palmitate were determined with the value of the specific activity. Results obtained were represented as nmol oxidized [1-^{14}C]-palmitate per gram of liver and hour.

3.7. Lipolysis of white adipose tissue

The capability of white adipose tissue (WAT) to hydrolyze TG into free fatty acids (FA) and glycerol was measured in freshly dissected WAT from mice fasted for 3 hours as described before (Gao, van der Veen et al. 2015).

In brief, 20 mg of WAT slices were incubated in 100 µl of the corresponding lipolysis medium (section 1.1.3) for 2 hours. Then, culture media was renewed with fresh media and incubated for another 2 hours. Cultured mediums were collected and the released FA and glycerol were determined with commercially available kits. 10 µl of medium were used for FA measurement (section 3.2.1) and 15 µl for glycerol determination by the commercially available TG quantification kit used in section 3.2.1, which measures **free glycerol**. For that purpose, the calculated values were corrected following the manufacturer's instructions and data are expressed as µmol per grams of WAT.

3.8. Analysis of glucose-6-phosphate dehydrogenase and malic enzyme activity

Glucose-6-phosphate dehydrogenase (G6PDH) (Betke, Brewer et al. 1967) and malic enzyme (ME) (Hsu RY 1967) activities were measured by spectrophotometry quantifying the NADPH produced in the reactions catalyzed by the enzymes as shown below:

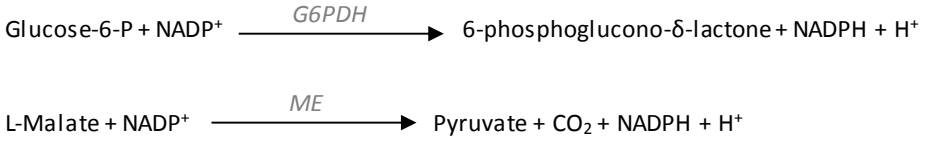

For these measurements, 40 mg of liver were homogenized (section 3.4.1) in the specific homogenization buffer (section 1.1.3). Then, homogenate was centrifuged at 105,000 xg for 1 hour at 4 °C and the supernatant, corresponding to the cytosolic fraction, was collected (Buque, Martinez et al. 2010). For G6PDH and ME activity measurements, 60 and 250 µg of protein from the cytosolic extract adjusted to 1 µg/µl were used respectively. Total protein of the sample was quantified by Bradford assay (section 3.10.2).

The assay tubes containing 900 µl of G6PDH incubation buffer and 400 µl of ME incubation buffer (section 1.1.3) were pre-incubated for 5 minutes at 37 °C. The reaction was started by addition of the corresponding sample quantity to the assay tubes. After 5 minutes of incubation at 37 °C in agitation, the reaction was stopped introducing the tubes on ice. Finally, produced NADPH+H^+ was measured at 340 nm.

The standard range used for the calibration curve was from 19 to 84 nmol of NADPH for G6PDH assay and from 28.8 to 180 nmol for ME assay. The blank was done with dH_2O instead of the sample and without adding NADPH. Activities were represented as nmol of produced NADPH per mg of protein and minutes.

3.9. Western blotting

The liver tissue was homogenized as described in section 3.4.1 with the corresponding homogenization buffer (section 1.1.4). Homogenates were maintained shaking on ice for 30 minutes to dissolve proteins. Afterwards, samples were centrifuged at 16,000 xg for 30 minutes at 4 °C and the supernatant was kept. Total protein was measured in supernatants (section 3.10.1) and samples were stored at -20 °C until subsequent analysis.

Samples were diluted to 2 µg/µl with loading buffer (section 1.1.4) and dH_2O and were denaturalized by heating at 95 °C for 5 minutes. 20 µg of protein extract was separated by sodium dodecyl sulphate-polyacrylamide gel electrophoresis (SDS-PAGE) at 10% in denature and reducing conditions (Laemmli 1970)

using a vertical Mini Protean II electrophoresis equipment (Bio-Rad, USA) at 100 v of voltage. PageRuler Plus Protein Ladder (ThermoFisher Scientific, USA) was used as molecular weight marker. The separated proteins were transferred and immobilized onto nitrocellulose membranes (Amersham™ Protran™, 0.2 µm, GE HealthCare, UK) by wet eletroblotting using Mini Trans-Blot cell (Bio-Rad, USA) for 2 hours at 100 v of voltage.

Membranes were then blocked with blocking buffer for 1 hour at RT and incubated with commercial primary antibody overnight at 4 °C. Optimal incubation conditions are specified in Table D7. Next day, membranes were washed three times with tris-buffered saline supplemented with Tween 20 (TBST) (section 1.1.4) and were incubated in 5% (w/v) BSA in TBST containing secondary antibody conjugated to horseradish peroxidase (HRP) for 1 hour at RT (Table D7). After another three washes, immunoreactive proteins were detected by ECL Western blotting detection chemiluminiscence Reagent (GE Healthcare, UK). They were exposed to RX-N X-Ray film (Fujifilm, Japan) using an exposure cassette. Subsequently, the film was developed and fixed with photography liquids (AGFA, Belgium). Finally, quantification was performed after

Table D7. References and incubation conditions for the antibodies employed in Western blotting.

	Target	Trading house	Catalog No.	Blocking buffer	Antibody dilution	Host
Primary antibodies	**E2f1**	SC	Sc-251	5% NFDM in TBST	1:1,000	Ms
	E2f2	SC	Sc-9967	5% NFDM in TBST	1:1,000	Ms
	PPAR-α	SC	Sc-9000	5% NFDM in TBST	1:1,000	Rb
	PPAR-γ	SC	Sc-7273	5% NFDM in TBST	1:1,000	Ms
	PGC-1α	SC	Sc-13067	5% NFDM in TBST	1:1,000	Rb
	PGC-1β	Abcam	Ab176328	5% NFDM in TBST	1:1,000	Rb
	CPT2	Abcam	Ab181114	5% BSA in TBST	1:1,000	Rb
	HNF4-α	Abcam	Ab201460	5% BSA in TBST	1:1,000	Rb
	GAPDH	Abcam	Ab8245	5% BSA in TBST	1:20,000	Ms
	Transferrin	SC	sc-22597	5% NFDM in TBST	1:1,000	Gt
Secondary antibodies (HRP-linked)	**Anti-mouse IgG**	CST	7076	5% BSA in TBST	1:2,000	Hr
	Anti-rabbit IgG	CST	7074	5% BSA in TBST	1:2,000	Hr
	Anti-goat IgG	Thermo	31400	5% BSA in TBST	1:10,000	Ms

E2f1, E2F transcription factor 1; E2f2, E2F transcription factor 2; PPAR-α, peroxisome proliferator activated receptor alpha; PPAR-γ, peroxisome proliferator activated-receptor gamma; PGC-1α, PPAR-γ coactivator alpha; PGC-1β, PPAR-γ coactivator beta; CPT2, Carnitine palmitoyltransferase 2; HNF4-α, Hepatic nuclear factor 4 alpha; GAPDH, glyceraldehyde-3-phosphate dehydrogenase; Ig, immunoglobulin; HRP, Horseradish peroxidase; CST, Cell Signaling Technology; SC, Santa Cruz; Thermo, Thermo Fisher Scientific; BSA, bovine seroalbumin, NFDM, non-fat dried milk; TBST; Tris-buffered saline supplemented with Tween-20; Rb, rabbit; Ms, mouse; Gt, goat; Hr, Horse.

digitalization by two-dimensional densitometry using a GS-800 densitometer and Quantity One software (Bio-Rad, USA).

3.10. Determination of total protein concentration

Total protein concentration was measured by colorimetric detection. Depending on the following technique to be applied, bicinchoninic acid-based method or Bradford assay was used. In both cases, microassays were performed by duplicate in 96-well plates.

3.10.1. Bicinchoninic acid-based method

A commercially available Bicinchoninic Acid (BCA) Reagent (ThermoFisher Scientific, USA) was used and the manufacturer's instructions were followed.

When samples directly came from liver homogenates, they were previously treated with ultrasound for complete disruption of the tissue. For that, Soniprep-150 ultrasonic-probe was used at 6 microns of potency (3 cycles, 30 seconds ON + 15 seconds OFF) and samples were maintained on an ice bath at 4 °C to avoid heating.

In the assay, 0.15 µl of liver homogenate or 10 µl of cell suspension were used. Samples were diluted with H_2O in volume of 100 µl. Then, 100 µl of A and B reagents mixture (50:1) from the kit were added. The reaction was incubated in darkness at 37 °C for 30 minutes and the absorbance was measured at 562 nm.

The protein concentration of the sample was calculated interpolating the value of the absorbance in the calibration curve built with BSA (0-15 µg).

3.10.2. Bradford assay

In G6PDH or ME activity analysis (section 3.8), total protein concentration in liver tissue was quantified by Bradford microassay after homogenization, as the homogenization buffers contain substances that interfere with BCA kit.

For this, 2 µl of sample in a volume of 25 µl were applied in duplicate. 250 µl of Bradford reagent mixture (section 1.1.5) were added and incubated in darkness for 10 minutes at RT. Absorbance was measured at 595 nm and the standard range used for calibration curve was from 0 to 7.5 µg of BSA.

3.11. Analysis of gene expression

3.11.1. RNA extraction

Total RNA was extracted using Trizol Reagent (Invitrogen, USA) and according to the manufacturer's instructions. All the material was previously decontamined with RNaseZap® RNA decontamination solution (Invitrogen, USA).

For liver samples, 30 mg of tissue were homogenized in 1 ml of Trizol Reagent with Polytron PT 1200 homogenizer in an ice bath for 30 seconds at speed 5. For cellular samples, silenced HepG2 cells were directly scrapped in 1 ml of Trizol Reagent.

In both cases, RNA was extracted and subjected to DNase treatment (Invitrogen, USA) to avoid DNA contamination. Its concentration was determined measuring the absorbance at 260 nm in the Nanodrop ND-1000 spectrophotometer. Absorbance at 280 nm, indicative of protein contamination, was also measured. Pure RNA sample was considered when 260/280 ratio was higher than 1.85.

RNA quality was also assessed by electrophoresis. 1 µg of RNA mixed with loading buffer (section 1.1.2) was separated in an agarose (Laboratorios CONDA, Spain) gel of 1% (w/v) dissolved in tris-acetate-EDTA (TAE) (section 1.1.2) buffer in a horizontal electrophoresis equipment (Bio-Rad, USA). RNA was visualized with Sybr safe™ DNA gel stain (ThermoFisher Scientific, USA) at 1:25 (v/v).

3.11.2. Microarray analysis

To gain biological insight about the pathways altered by HCC induction treatment in mice, a gene expression profiling was realized by a microarray in livers of 9 month-old *E2f2*$^{-/-}$ and WT mice exposed to DEN HFD or control treatment (n=4 for each condition).

For this purpose, RNA samples were used. Firstly, RNA integrity was assessed again on a Agilent 2100 Bioanalyzer with Agilent RNA 6000 Nano chips (Agilent Technologies, USA), which estimates the 28S/18S (ribosomic RNAs) ratio and the RNA integrity number (RIN value).

RNA samples were labeled and hybridized following standard Protocol “One-Color Microarray-Based Gene Expression analysis (Low Input Quick Amp Labeling)" Version 6.5 (Agilent Technologies, USA). For that, 50 ng of total RNA were retrotranscribed with AffinityScript Reverse Transcriptase (Agilent Technologies, USA), using Oligo dT primers coupled to T7 promoter. To generate amplified and labeled cRNA, double stranded cDNA synthesized by AffinityScript RT was in vitro transcribed by T7 RNA pol in the presence of Cy3-CTP. Labeled samples were then purified with silica-based RNeasy spin columns (Qiagen, Germany). Yield and specific activity of each reaction was determined by quantifying the cRNA in the NanoDrop 1000 spectrophotometer. A valid sample was consider when yield was > 0.825 µg and specific activity was 3 < 6 pmol/µg.

Samples were then analyzed using Agilent SurePrint G3 Mouse GE 8x60K (Design ID 028005) (Agilent Technologies, USA), in which 55,681 mouse features are represented. 600 ng of labeled cRNA samples were hybridized at 65 ℃ for 20 hours. Arrays were scanned on a G2565CA DNA microarray scanner and images were processed using Agilent Feature Extraction Software (vs. 10.7.3.1).

Raw data from Feature Extraction software was subsequently processed on GeneSpring GX 12.5 (Agilent Technologies, USA). Data were normalized by quantile normalization and mean centering, which makes comparable the gene expression from all microarrays. There were excluded the data with non-uniform features, population outliers or features whose intensities were not significantly above the background signal of all samples in 1 out of any 4 conditions.

Differential gene expression between both mice strains was analyzed with LIMMA statistical package (Smyth 2004) using MultiExperiment Viewer (MeV) vs. 4.7.1 (http://www.tm4.org/mev/) application. The adjusted p-values (adj-p-value) were obtained applying Benjamini-Hochberg method (False discovery rate, FDR) for multiple test correction. Then, a multi-class comparison was realized between both genotypes for DEN HFD and CD treatments.

3.11.3. Functional analysis of the microarray

The biological relevance of the gene expression profile was assessed by a pathway enrichment analysis using the ClueGO (v2.3.3) application (Bindea, Mlecnik et al. 2009), a plugin of the Cytoscape platform (Shannon, Markiel et al. 2003) (http://www.cytoscape.org, v3.4.0). Reactome databases

(http://www.reactome.org) was used for gene clustering in biological pathways (Croft, O'Kelly et al. 2011). Inclusion criteria for the genes whose expression changed were adj-p-value < 0.05 and fold change > 1.35.

Microarray analysis, including data preprocessing and bioinformatic analysis, were performed in the SGIker Gene Expression Unit of the Genomics Facility Service from the UPV/EHU.

3.11.4. cDNA synthesis and real time-quantitative polymerase chain reaction (RT-qPCR)

Microarray results were then validated by RT-qPCR. For that, a retrotranscription (RT) was performed from 1.8 µg RNA extract with SuperScript III First-Strand Synthesis System for RT-PCR kit (Invitrogen, USA) and following the commercial protocol. To avoid RNA contamination in the sample, first strand cDNA was synthesized in the presence of random primers and RNase OUT.

The expression of the selected genes (some overexpressed, some downregulated and others with no change) was measured by RT-qPCR in the SGIker Gene Expression Unit of the Genomics Facility Service from the UPV/EHU, using the BioMarkTM HD system in combination with Dynamic Array Integrated Fluidic Circuits (IFC) (Fluidigm Corporation, USA). The protocol used was Fluidigm's Fast Gene Expression Analysis using EvaGreen on the BioMark HD System version D1.

Target genes were specifically preamplificated with Multiplex PCR Master (Qiagen, Germany) (95 ˚C 15 minutes, 14 cycles of 95 ˚C for 15 seconds and 60 °C for 4 minutes). 50 nM of primers were used. Afterwards, remaining primers were removed with Exo I (Thermo Scientific, USA) following the manufacturer's instructions. Samples were diluted 1:5 with 0.1 mM EDTA containing tris-EDTA buffer and were loaded onto 96.96 Dynamic Array IFC. SsoFastTM EvaGreen® Supermix with Low ROX (Bio-Rad, USA) was used for amplification. GE Fast 96x96 PCR + Melt v2 protocol was followed for PCR.

Candidate genes were run in duplicate. Serial dilutions of control sample cDNA were also run for the standard curve, which was used for evaluation of the PCR amplification. Finally, the stability of selected genes for normalization was assessed with NormFinder and GeNorm algorithms (De Spiegelaere, Dern-Wieloch et al. 2015) using GenEx software (MultiD 5.2 version). For mice samples, glyceraldehyde-3-phosphate dehydrogenase (*Gapdh*), TATA-Box binding protein (*Tbp*), cyclophilin A (*Ppia*) and actin (*Actb*) expression were used to calculate the normalization factor. For cells, TATA-Box binding protein (*TBP*) and hidroxymethylbilane synthase (*HBMS*) were used as normalization genes. Primers were designed using

Primer3 software and were synthetized by Invitrogen (USA). The primers used to analyze the target genes are detailed in Table D8.

Table D8. Oligonucleotides used for RT-qPCR analysis.

Pathway	Gene	Species	Accession number	Oligonucleotide Sequence (5'- 3')	
DNA synthesis	***Tk***	*M. musculus*	NM_009387.2	F	CCACACATGATCGGAACACC
				R	GCCATCATTTCACAGAAATCCA
	Orc	*M. musculus*	NM_011015.2	F	TGGCCCTGTTCAGGTAGTGG
				R	GGCAGTGGTGCAAAGTCCTT
Mitosis	***Plk1***	*M. musculus*	NM_011121.4	F	TGTAGTTTTGGAGCTCTGTCG
				R	TCCCTGTGAATGACCTGATTG
E2F	***E2f1***	*M. musculus*	L21973.1	F	TGCCAAGAAGTCCAAGAATCA
				R	GCTTACCAATCCCCACCAT
	E2F1	*H. sapiens*	NM_005225.2	F	ATGTTTTCCTGTGCCCTGAG
				R	AGATGATGGTGGTGGTGACA
	E2f2	*M. musculus*	BC062101.1	F	AGGAGCTGAAGGAGCTGATG
				R	GGGAGCAACTCTGAATGAGC
	E2F2	*H. sapiens*	NM_004091.3	F	AGGCAGGGGAATGTTTGA
				R	TGCTCCGTGTTCATCAGC
Cyclins	***Ccnd3***	*M. musculus*	U43844.2	F	ACTGGATGCTGGAGGTGTGTG
				R	CAATTGCGCCTTTCGGG
	Ccna2	*M. musculus*	NM_009828.3	F	GTTTCTCTTCTCAACCCACCAGA
				R	AAACTAAAACCCGACATAAAAACTGTACA
	Ccne1	*M. musculus*	NM_007633.2	F	GAAGGTGGCTCCGACCTTTC
				R	CATCCCAGGGCTGACTGCT
Lipid oxidation	***Ppara***	*M. musculus*	NM_011144.6	F	GCAGTGCCCTGAACATCGAG
				R	CGTCTGATGAGCATGTCACTGTG
	Ppargc1a	*M. musculus*	NM_008904.2	F	AATGCAGCGGTCTTAGCACT
				R	ACGTCTTTGTGGCTTTTGCT
	Ppargc1b	*M. musculus*	NM_133249.2	F	CCTACCCACAAGGACAGCAT
				R	CTTTTACAGGACGCCAGGTC
	Rxra	*M. musculus*	NM_001290481.1	F	GTCAAGCAGCAGACAAGCAG
				R	TATGGAGCGGTGGGAGAA
	Acsl1	*M. musculus*	NM_007981.4	F	AGTGTGGGGTGGAAATCATC
				R	TTTGGGGTTGCCTGTAGTTC
	Acsm1	*M. musculus*	NM_054094.5	F	TGTGGCTTCTGAGTGTCCTG
				R	AGTATGGTCTGGGGATGCTG
	Acsm3	*M. musculus*	NM_212441.2	F	GGACACAAAACACGACGAGA
				R	ATCGGAGGCTATCAAATCCA
	Cpt1	*M. musculus*	NM_013495.2	F	TCGAAAGCCCATGTTGTACAGC
				R	CATCAGTGGCCTCACAGACTCC
	Cpt2	*M. musculus*	NM_009949.2	F	AATCCCTCAGAAATCCAGGCAC
				R	CTGCCCAGACATCTCGGTTC
	Acadl	*M. musculus*	NM_007381.4	F	GTAAGAACGAACGCCAAAAGA
				R	TGATGAACACCTTGCTTCCA
	Acasb	*M. musculus*	NM_025826.4	F	CGTTGCTCCTCTGGTTTCC
				R	CACCGATTTCTCCATTTTTGAG
	Acaa2	*M. musculus*	NM_177470.3	F	CTTTTGCCCCTCAGTTCTTG
				R	GCCTCCACTCACATTGGTTT
Oxphos	***Ndufv1***	*M. musculus*	NM_133666.3	F	ACGACAGCACCCAAGAAAAC
				R	TACCAGTCACCCCGTCTCA
	Ndufs7	*M. musculus*	NM_029272.3	F	GCACGCTTACCAACAAGATG
				R	GTCACAGCCACGAACAACC
	Ndufs5	*M. musculus*	NM_001030274.1	F	TCAAGAAACAGCGGGAGAAG
				R	TGAGGTGGAGGGGTGTATTT
	Sdha	*M. musculus*	NM_023281.1	F	TATTGCTACTGGGGGCTACG
				R	TGGGGTGGAACTGAACAAAT
	Cyb5a	*M. musculus*	NM_025797.4	F	CCTGGTGGAGAAGAAGTCCTAA
				R	TCCCCGATGATGTATGTTTTG

	Atpif1	*M. musculus*	NM_007512.4	F R	TCGGTGTCTGGGGTATGAAG TCAGCCTTTTCTCGTTTTCC
	Atp5a1	*M. musculus*	NM_007505.2	F R	TTTAGAGACAACGGCAAGCA CAGGCGGGAGTGTAGGTAGA
Lipogenesis	***Pparg***	*M. musculus*	AB644275	F R	CACTCGCATTCCTTTGACATC CGCACTTTGGTATTCTTCGAG
	Cd36	*M. musculus*	NM_001159558.1	F R	CCCTCCAGAATCCAGACAAC CACAGGCTTTCCTTCTTTGC
	G6pdx	*M. musculus*	NM_008062.2	F R	GGGAAGAGTTGTACCAGGGTG TTCAGGTAGAAGGCCATCCCG
	Scd1	*M. musculus*	NM_009127.4	F R	TGGCTGGGCAGGAACTAGTG TGTTCCCCAAGGGCTTCATC
	Scd2	*M. musculus*	NM_009128.2	F R	TTTGTACTATGTAATCAGCGCCC AGCCGTGCCTTGTATGTTCT
	Cidea	*M. musculus*	BC096649.1	F R	CTCGGCTGTCTCAATGTCAA GGAACTGTCCCGTCATCTGT
	Acaca	*M. musculus*	NJ5MYKM201R	F R	TGGTGCAGAGGTACCGAAGTG GTCGTAGTGGCCGTTCTGAAAG
	Fasn	*M. musculus*	NJ5SCE0G016	F R	GATCCTGGAACGAGAACACGATC GACATTTCCTGAAGTTTCCGCA
	Me2	*M. musculus*	NJ5TPBG1014	F R	TGCGACTTTTGAAGATGCAG TGGCTTTGATTACACCGTGA
	Me3	*M. musculus*	NJ5UDPPE016	F R	ATACTGGGCTTGGGAGACCT TAGCAGGACAGGAAGGCACT
Lipolysis	***Aadac***	*M. musculus*	AF306788.1	F R	CGTCTGATGAGCATGTCACTGTG TGAGAGCCATTGACTTTCTTTTGG
	Lipc	*M. musculus*	AY228765.1	F R	GGAAATCCCCTCCAAATCTCC CTCTGTTCCCACGCCTTGCT
FA transport	***Slc27a1***	*M. musculus*	BC028937.1	F R	CAGTGCCACCAACAAGAAGA CAGCTCGTCCATCACTAGCA
	Slc27a5	*M. musculus*	NM_009512.2	F R	TCATTGCTGACCCCCTCTAC TCCAGGTTCCTTCACACACA
VLDL metabolism	***Apob***	*M. musculus*	NM_009693.2	F R	GTGATCCCCACAGCAATAAGCA AGATTCCCAGGACCATGGAAAA
	Apoe	*M. musculus*	NM_009696.3	F R	TGGAGGCTAAGGACTTGTTTCG CTCGGCTAGGCATCCTGTCA
	Lpl	*M. musculus*	NM_008509.2	F R	GCCCAGCAACATTATCCAGT GGTCAGACTTCCTGCTACGC
Inflammation	***Tnf***	*M. musculus*	NM_001278601.1	F R	ACGGCATGGATCTCAAAGAC GTGGGTGAGGAGCACGTAGT
	Il1b	*M. musculus*	NM_008361.4	F R	CAGGCAGGCAGTATCACTCA AGGTGCTCATGTCCTCATCC
	Il6	*M. musculus*	DQ788722.1	F R	TCCTTCCTACCCCAATTTCC GCCACTCCTTCTGTGACTCC
	Adgre1	*M. musculus*	NM_010130.4	F R	GAGCTTACGATGGAATTCTCCTTGTAT CACAGCAGGAAGGTGGCTATG
Fibrosis	***Tgfb1***	*M. musculus*	NM_011577.2	F R	CGCCATCTATGAGAAAACCA CCAAGGTAACGCCAGGAAT
	Acta2	*M. musculus*	NM_007392.3	F R	CCACCGCAAATGCTTCTAAGTC AGGAACTGGAGGCGCTGATC
	Col1a2	*M. musculus*	NM_007743.3	F R	AGGACACAGTGGTATGGATGG ACCTGGAGTTCCATTCTCTCC
	Col3a1	*M. musculus*	NM_009930.2	F R	AGAATGGGGAGACTGGACCT TGCCTTGTAATCCTTGTGGA
Normalization genes	***Actb***	*M. musculus*	NM_007393	F R	ATCGCTGACAGGATGCAGAAG TCAGGAGGAGCAATGATCTTGA
	Gapdh	*M. musculus*	NM_001289726	F R	TATGACTCCACTCACGGCAAATT TCGCTCCTGGAAGATGGTGAT
	Tbp	*M. musculus*	NM_001004198	F R	AGCGGTTTGCTGCAGTCATC TCACTCTTGGCTCCTGTGCAC
	TBP	*H. sapiens*	BT019657.1	F R	TTCCGGGAGTCATGGCACCCT TCTTTGCAGTGACCCAGCAGCATC
	Ppia	*M. musculus*	NM_00890	F R	CCAAGACTGAGTGGCTGGATG GCTCCATGGCTTCCACAATG

	HBMS	*H. sapiens*	M95623.1	F R	CACCCACACACAGCCTACTT ACACTGTCCGTCTGTATGCG

3.12. Statistical analysis

The results were represented as the arithmetical mean ± standard error of the mean (SEM) of "n" animals per group. Statistical analysis of the data was performed with different tests using GraphPad software. Differences between two groups were tested using the unpaired Student t test. Two-way variance (ANOVA) analysis and Bonferroni's post-test were used when more than two groups were compared.

The statistical significance is expressed as:

- *E2f1*$^{-/-}$ vs WT: * p<0.05, ** p<0.01 and *** p<0.001
- *E2f2*$^{-/-}$ vs WT: * p<0.05, ** p<0.01 and *** p<0.001

- DEN HFD vs CD: # p<0.05, ## p<0.01 and ### p<0.001
- DEN CD vs CD: # p<0.05, ## p<0.01 and ### p<0.001
- HFD vs CD: # p<0.05, ## p<0.01 and ### p<0.001

- si*E2F1* vs siC: * p<0.05, ** p<0.01 and *** p<0.001
- si*E2F2* vs siC: * p<0.05, ** p<0.01 and *** p<0.001

- Non-obese NL vs obese NL: * p<0.05, ** p<0.01 and *** p<0.001
- Non-obese NL vs obese NAFLD: * p<0.05, ** p<0.01 and *** p<0.001
- Obese NL vs obese NAFLD: * p<0.05, ** p<0.01 and *** p<0.001

Chapter D. RESULTS

Chapter D. RESULTS

1. E2F1 and E2F2 transcription factors are required for HCC development and the associated metabolic dysregulation

Obesity, considered a chronic and pandemic disease by the World Health Organization (WHO), is one of the greatest public health challenges of our time. Together with non-alcoholic fatty liver disease (NAFLD), obesity is a risk factor for many types of cancer, including hepatocellular carcinoma (HCC) (Lauby-Secretan, Scoccianti et al. 2016). Since HCC cases arising in NAFLD patients are raising, epidemiological studies identify NAFLD as the most rapidly increasing cause of HCC (Younes, Bugianesi 2017). Notwithstanding, it remains unclear the reason by which only some of the NAFLD patients develop HCC. While HCC is the primary malignancy in liver, liver cancer is the sixth most prevalent cancer around the world and it is a main cause of death by cancer (Bray, Ferlay et al. 2018). Evidences suggest that altered metabolism could be both a cause and a consequence of the hepatic carcinogenesis (Kim, Shariff et al. 2016), hence, there are emerging ideas about the existence of common modulators of cell cycle and metabolism.

E2F1 and E2F2 transcription factors are key regulators of the cell cycle. Their role in carcinogenesis is controversial, since they can act as proto-oncogenes or as tumor suppressor genes depending on the cell type and context (Huntington, Tang et al. 2016). Moreover, recent studies have demonstrated that E2F1 can regulate metabolism in several tissues in which cell cycle is not active (Fajas, Annicotte et al. 2004, Annicotte, Blanchet et al. 2009, Fajas, Landsberg et al. 2002, Blanchet, Annicotte et al. 2011, Denechaud, Lopez-Mejia et al. 2016, Giralt, Denechaud et al. 2018). However, nothing has been described about their relevance in the development of NAFLD-driven HCC.

Taking all this into consideration, we wondered if E2f1 and/or E2f2 are involved in the obesity-driven HCC and the associated metabolic dysregulation. For this purpose, *E2f1* knockout (*E2f1*$^{-/-}$), *E2f2* knockout (*E2f2*$^{-/-}$) and their control littermates (WT) were used. As dietary obesity is a bona fide HCC promoter (Park, Lee et al. 2010a), we induced NAFLD-related HCC in mice by a single administration of the hepatic procarcinogen diethylnitrosamine (DEN) at 14 days old followed by a long term of high-fat diet (HFD) feeding regimen for 32 weeks (named as DEN HFD group). Mice that were injected with DEN and fed a chow diet (CD) (named as DEN CD group) (Park, Lee et al. 2010a) and other group of mice fed a CD or a HFD in which the vehicle was injected were also included.

Concerning the effects of the treatments in WT mice along the 32 weeks, the results showed that body weight increased gradually in CD-fed mice *(Figure E1.A)*. As expected, mice fed a HFD-regimen reached higher body weight than their respective CD-fed control littermates *(Figure E1.A)*. Administration of DEN induced a slight decrease in body weight in CD-fed mice *(Figure E1.A)*. However, the decrease was more marked when mice were fed a HFD after the administration of DEN, where the body weight loss was pronounced from week 18 so that the DEN HFD mice reached the CD-fed mice body weight by the end of treatment *(Figure E1.A)*.

In *E2f1*$^{-/-}$ mice, body weight was lower than in WT mice when fed CD in presence or absence of DEN *(Figure E1.B)*. Body weight in *E2f1*$^{-/-}$ mice was also reduced till week 12 when exposed to a HFD combined or not with DEN, but reached similar body weight to WT mice at 9 months old *(Figure E1.B)*. In *E2f2*$^{-/-}$ mice, body weight was diminished in comparison to WT animals when exposed to each of the treatments *(Figure E1.B)*.

We then measured the food intake during the 32 weeks of regimen to verify that differences in body weight between genotypes were not due to variations in the feeding amount. Food consumption in *E2f1*$^{-/-}$ mice was similar to control mice when treated with DEN HFD, DEN or CD *(Figure E1.C)*. However, *E2f1*$^{-/-}$ mice administered HFD showed reduced food intake in comparison to WT animals *(Figure E1.C)*. Regarding *E2f2*$^{-/-}$ mice, food consumption was higher than in WT mice when mice were fed CD or HFD *(Figure E1.C)*; though, there was no change in the food intake of *E2f2*$^{-/-}$ mice treated with DEN CD or DEN HFD when compared to their WT counterparts *(Figure E1.C)*.

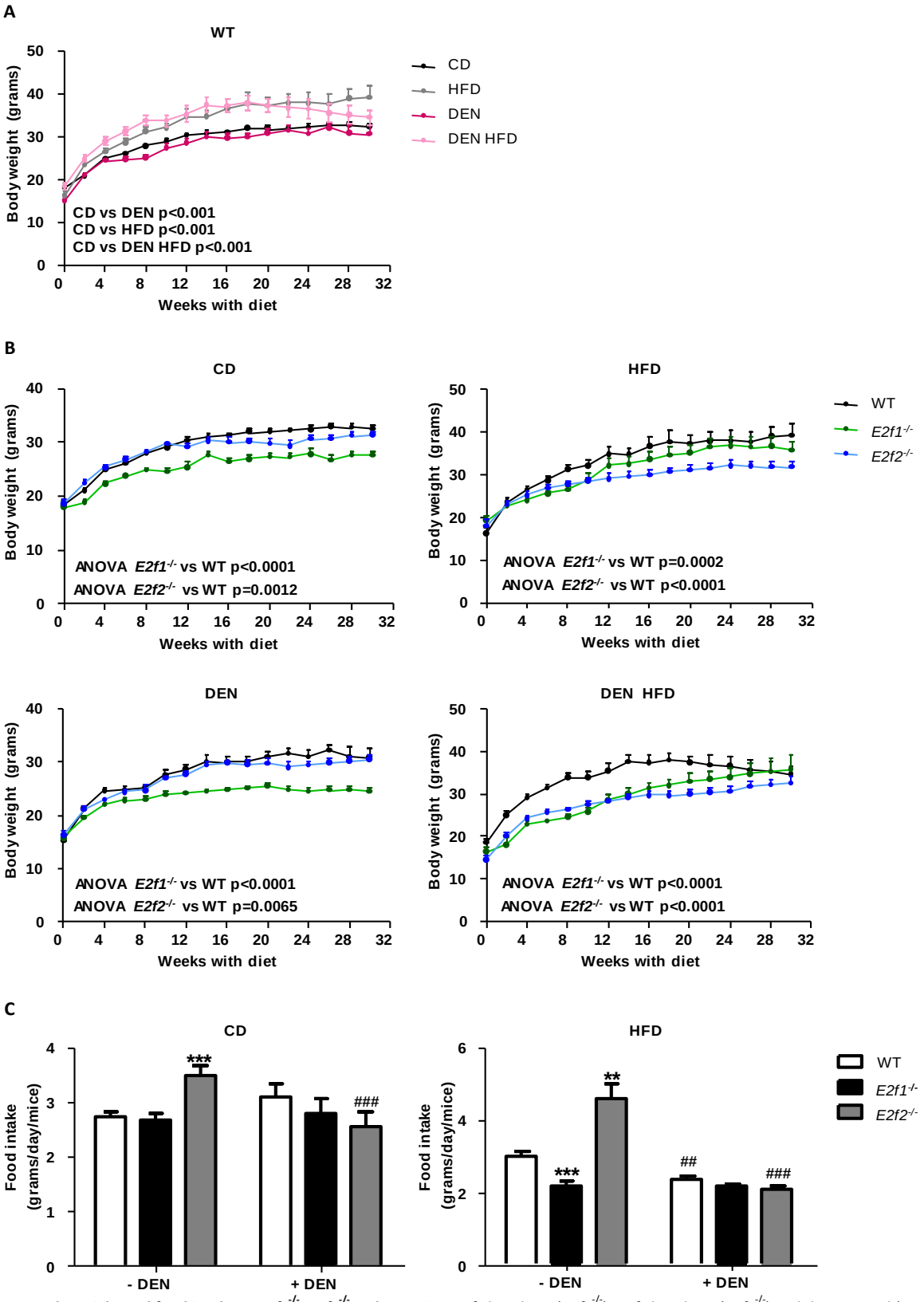

Figure E1. **Body weight and food intake in *E2f1*$^{-/-}$, *E2f2*$^{-/-}$ and WT mice.** *E2f1* knockout (*E2f1*$^{-/-}$), *E2f2* knockout (*E2f2*$^{-/-}$) and their control (WT) mice were injected the procarcinogenic compound diethylnitrosamine (DEN) (25 mg/kg of mice) or vehicle when they were 14 days old. After weaning, mice were kept on a high-fat diet (HFD) or a chow diet (CD) until they were sacrificed at 9 months old. (A and B) Body weight and (C) food intake were measured every two weeks. Values are means ± SEM of n=17-18 animals in CD groups and n=7-12 animals per group in the other conditions. Two-way ANOVA was performed to analyze differences in body weight. Statistical analysis of food intake was assessed by Student's two-tailed t-test. Significant differences between *E2f1*$^{-/-}$ or *E2f2*$^{-/-}$ and WT mice are indicated as *p <0.05, **p <0.01 and ***p <0.001 and differences between DEN CD and CD or DEN HFD and HFD are denoted by $^{\#}$p <0.05, $^{\#\#}$p <0.01 and $^{\#\#\#}$p <0.001.

Next, liver injury was evaluated by the percentage of liver-to-body weight ratio (liver index) and serum alanine aminotransferase (ALT) levels. We observed that the HFD did not induce changes in the liver index in 9 month-old WT mice in comparison to CD-fed mice, while slightly increased serum ALT levels (Table E1). Moreover, liver index and serum ALT levels were elevated in 9 month-old WT mice after being exposed to DEN and, mainly, to DEN HFD. These results show that combination of DEN plus HFD causes liver damage in WT mice (Table E1). On the contrary, the percentage of liver to body and serum ALT levels were lower in *E2f1*$^{-/-}$ and *E2f2*$^{-/-}$ mice than in WT animals and were not augmented after treatment to DEN and/or HFD (Table E1). These data suggest that *E2f1* and, more markedly, *E2f2* deficiency in mice result in protection from liver injury caused by exposition to HFD, DEN and DEN HFD treatments.

Table E1. Liver index and serum ALT in 9 month-old *E2f1*$^{-/-}$, *E2f2*$^{-/-}$ and WT mice treated with diethylnitrosamine (DEN) or the vehicle combined with high-fat diet (HFD) or chow diet (CD).

		CD	HFD	DEN CD	DEN HFD
Liver index (%)	WT	4.25 ± 0.07	4.68 ± 0.25	5.59 ± 0.17 $^{\#}$	7.79 ± 1.17 $^{\#\#\#}$
	E2f1$^{-/-}$	3.84 ± 0.10 **	3.03 ± 0.10 *** $^{\#\#\#}$	3.56 ± 0.08 **	3.36 ± 0.17 **
	E2f2$^{-/-}$	4.17 ± 0.05	3.81 ± 0.11 * $^{\#\#\#}$	4.16 ± 0.10	3.98 ± 0.11 **
ALT (U/L)	WT	22.35 ± 1.60	54.00 ± 11.75 $^{\#}$	104.44 ± 27.98 $^{\#\#}$	100.06 ± 21.79 $^{\#\#}$
	E2f1$^{-/-}$	29.01 ± 12.63	45.81 ± 10.97	28.64 ± 12.08	60.94 ± 13.39
	E2f2$^{-/-}$	23.78 ± 2.8	16.76 ± 4.55 *	15.41 ± 3.26 **	8.61 ± 3.34 *** $^{\#\#}$

E2f1 knockout (*E2f1*$^{-/-}$), *E2f2* knockout (*E2f2*$^{-/-}$) and their control (WT) mice were injected the procarcinogenic compound diethylnitrosamine (DEN) (25 mg/kg of mice) or vehicle when they were 14 days old. After weaning, mice were kept on a high-fat diet (HFD) or a chow diet (CD) until they were sacrificed at 9 months old and livers were collected. Liver index is determined by dividing the liver weight to the body weight. Values are means ± SEM of n=17-18 animals in vehicle-treated CD groups and n=7-12 mice per group in the other conditions for body weight and liver index. For alanine aminotransferase (ALT), an n of 5-8 animals was used in each group. Statistical analysis was realized by Student's two tailed t-test. Significant differences between *E2f1*$^{-/-}$ or *E2f2*$^{-/-}$ and WT mice are indicated by *p <0.05, **p <0.01 and ***p <0.001 and differences between HFD, DEN CD or DEN HFD and CD treatments are denoted by $^{\#}$p <0.05, $^{\#\#}$p <0.01 and $^{\#\#\#}$p <0.001.

1.1 Obesity-driven HCC promotes *E2f2* upregulation in mice livers

Previous studies showed that both *E2F1* (Kent, Bae et al. 2017) and *E2F2* (Huang, Ning et al. 2019, Hong, Eun et al. 2019) mRNA expression was increased in human HCC. Moreover, *E2f2* overexpression was demonstrated in c-myc/TGFα-induced hepatocarcinogenesis in transgenic mice (Santoni-Rugiu, Jensen et al. 1998). Thus, we aimed to investigate if *E2f1* and *E2f2* gene expression was elevated in livers of 9 month-old WT mice, including those fed a HFD, where HCC was developed.

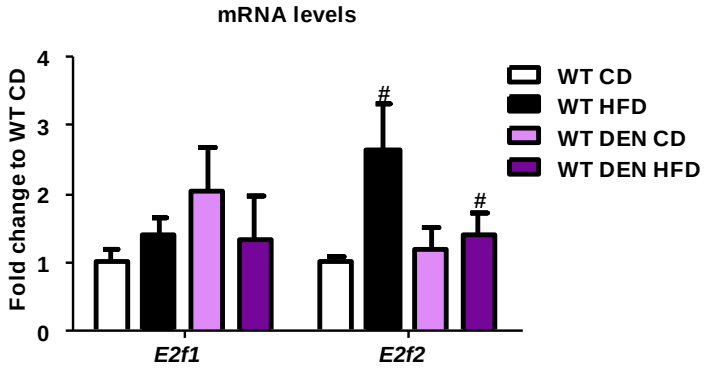

Figure E2. *E2f1* and *E2f2* gene expression in livers of 9 month-old WT mice. Wild type (WT) mice were injected the procarcinogenic compound diethylnitrosamine (DEN) (25 mg/kg of mice) or vehicle when they were 14 days old. After weaning, mice were kept on a high-fat diet (HFD) or a chow diet (CD) until they were sacrificed at 9 months old and livers were collected. Hepatic mRNA of *E2f1* and *E2f2* were measured by rt-qPCR. Values are means ± SEM of 6-10 animals per group. Statistical analysis was realized by Student's two tailed t-test. Significant differences between DEN HFD, DEN CD, HFD and CD are indicated as $^{\#}p < 0.05$, $^{\#\#}p < 0.01$ and $^{\#\#\#}p < 0.001$.

The results showed that hepatic *E2f1* gene expression maintained unaltered in WT mice treated with HFD, DEN CD or DEN HFD *(Figure E2)*. However, hepatic mRNA levels of *E2f2* were increased in control mice fed HFD treated or not with DEN *(Figure E2)*, showing that *E2f2* gene expression in liver is induced by dietary obesity.

1.2. *E2f1* or *E2f2* deficiency in mice confers resistance to hepatocarcinogenesis

Kishida *et al.* demonstrated that the combined treatment of DEN HFD resulted in HCC within 20 weeks(Kishida, Matsuda et al. 2016). We observed that 9 month-old WT mice exposed to just a HFD feeding regimen for 32 weeks developed small HCCs *(Figure E3.A)*. More and bigger tumors were induced when WT mice were administered DEN *(Figure E3.B, C)*. According to Park *et al.* (Park, Lee et al. 2010b), obesity-related HCC, developed after the combined treatment of DEN HFD *(Figure E3.A, B, C)*, induced higher number of bigger tumors, as we have also observed here *(Figure E3.A, B, C)*. The results here showed that *E2f1*$^{-/-}$ mice

and, more markedly, *E2f2*$^{-/-}$ mice were resistant to treatment-induced hepatocarcinogenesis, as nearly complete reduction of liver tumors induced by HFD, DEN or DEN HFD was observed in these mice compared with controls *(Figure E3.A, B, C)*.

Consistently with HCC development, the hepatic percentage of Ki67 positive cells, a cell proliferation marker, was increased in WT mice exposed to DEN or DEN HFD as compared to the control treatment *(Figure E4.A)*. That effect was prevented when *E2f1*$^{-/-}$ and *E2f2*$^{-/-}$ mice were exposed to the hepatocarcinogenic treatments *(Figure E4.A)*. Besides, the DEN HFD induced the overexpression of some (*Ccna2, Plk1*), but not all, E2F target-genes involved in cell cycle progression when compared to control treatment *(Figure E4.B)*. In *E2f1* or *E2f2* depleted mice livers, the overexpression of the cell-cycle genes caused by DEN HFD was avoided *(Figure E4.B)*. Notably, the liver expression of those genes was diminished in absence of *E2f1* and/or *E2f2* even in CD-fed mice *(Figure E4.B)*.

Altogether, these results indicate that the absence in *E2f1* and, especially, in *E2f2* confers protection against the hepatocarcinogenesis caused by HFD, DEN and DEN HFD treatments.

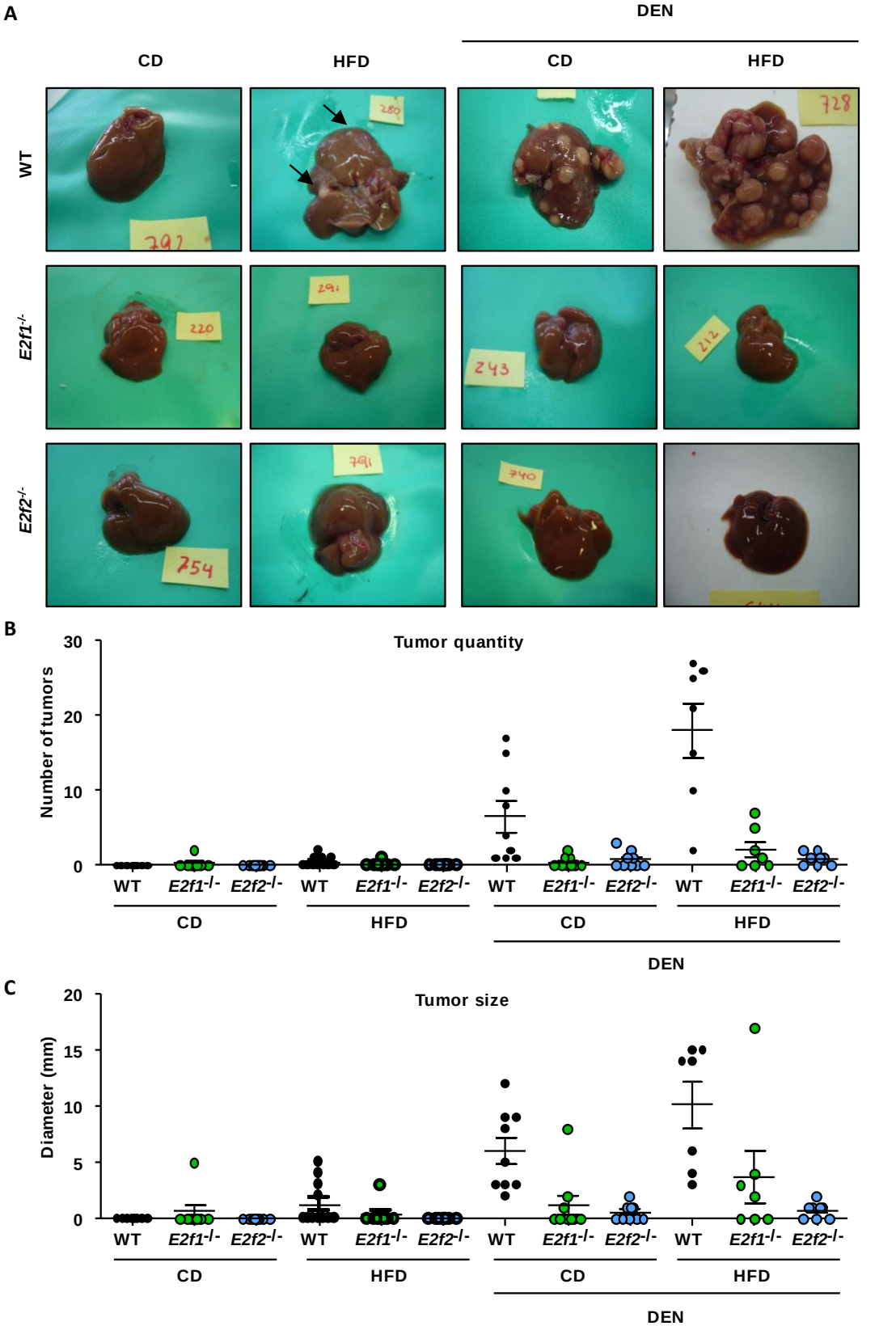

Figure E3. The absence in *E2f1* and more markedly in *E2f2* confers resistance to DEN and/or HFD-induced hepatocarcinogenesis in mice of 9 months old. *E2f1* knockout (*E2f1*$^{-/-}$), *E2f2* knockout (*E2f2*$^{-/-}$) and their control (WT) mice were injected the procarcinogenic compound diethylnitrosamine (DEN) (25 mg/kg of mice) or vehicle when they were 14 days old. After weaning, mice were kept on a high-fat diet (HFD) or a chow diet (CD) until they were sacrificed at 9 months old and livers were collected. (A) Representative photographs of mice livers. Tumors were (B) counted and (C) measured with a calipe. (n=7-9 animals per group).

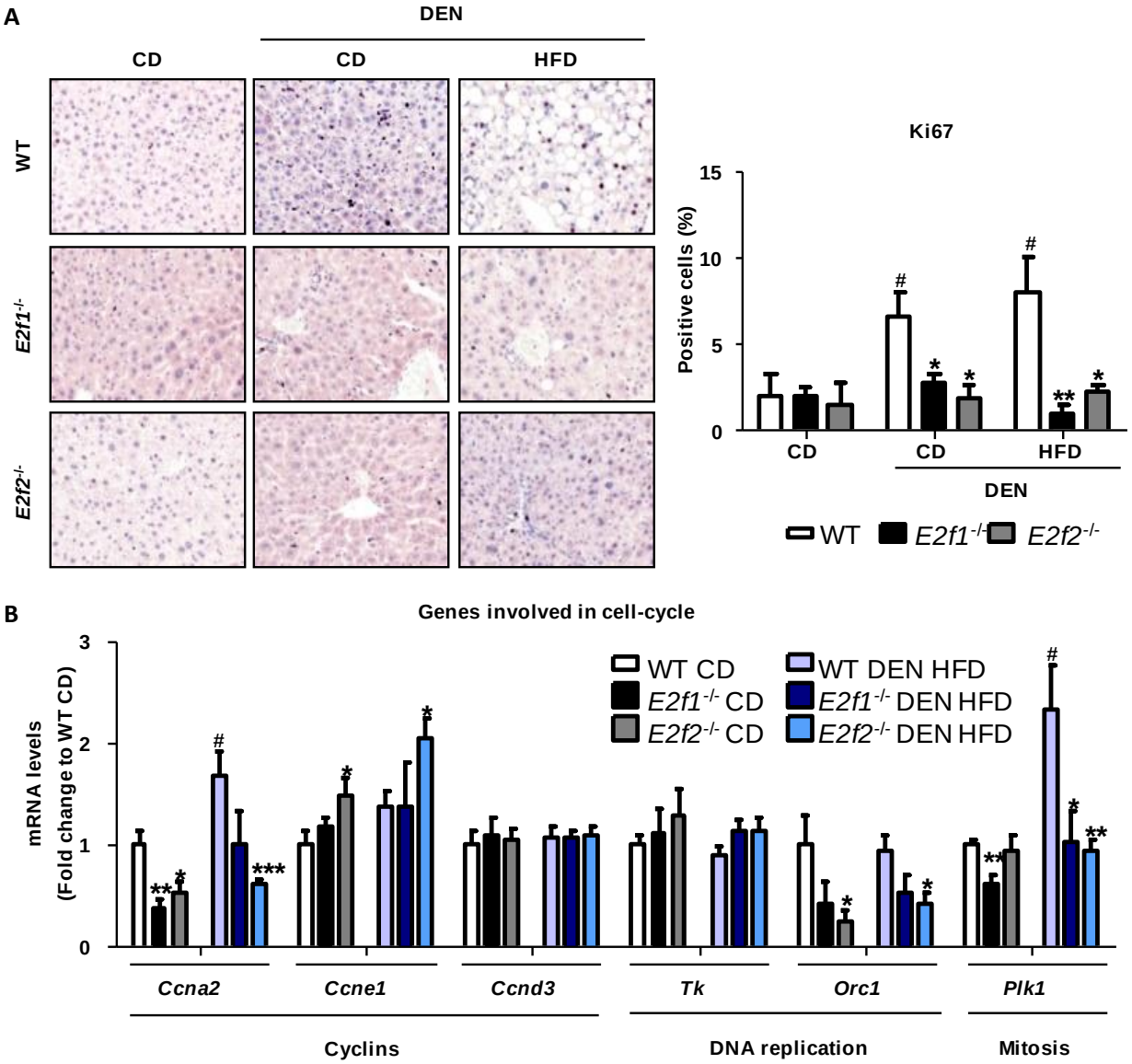

Figure E4. *E2f1* or *E2f2* deficiency prevents cell-cycle progression in 9 month-old mice livers exposed to the DEN HFD hepatocarcinogenic treatment. *E2f1* knockout (*E2f1*$^{-/-}$), *E2f2* knockout (*E2f2*$^{-/-}$) and their control (WT) mice were injected the procarcinogenic compound diethylnitrosamine (DEN) (25 mg/kg of mice) or vehicle when they were 14 days old. After weaning, mice were kept on a high-fat diet (HFD) or a chow diet (CD) until they were sacrificed at 9 months old and livers were collected. (A) Ki67 immunohistochemistry was performed as described in Materials and Methods (n=4-5 per condition). The percentage of Ki67+ cells was quantified by counting the number of positive nuclei in 5 randomly chosen 40 x magnified fields per section and mouse. Representative microscope images of *E2f1*$^{-/-}$, *E2f2*$^{-/-}$ and WT mice livers are shown. (B) Hepatic mRNA levels of genes involved in cell cycle progression were measured by rt-qPCR (n=7-8 per group). Values are means ± SEM and statistical analysis was assessed by Student's two-tailed t-test. Significant differences between *E2f1*$^{-/-}$ or *E2f2*$^{-/-}$ and WT mice are indicated as *p <0.05, **p <0.01 and ***p <0.001 and differences between DEN CD or DEN HFD and CD are denoted by $^{\#}$p <0.05, $^{\#\#}$p <0.01 and $^{\#\#\#}$p <0.001.

1.3. Deletion of *E2f1* or *E2f2* in mice prevents the progression of the disease induced by the long-term DEN HFD treatment

1.3.1. Fibrosis is not developed in *E2f1*$^{-/-}$ and *E2f2*$^{-/-}$ mice

Hepatic inflammation and fibrosis are key features of the long-term non-alcoholic steatohepatitis (NASH) and predispose liver to establish cirrhosis (Eslam, Sanyal et al. 2020). Although it is reported that cirrhosis is not a requirement for progression of hepatocarcinogenesis(Reeves, Zaki et al. 2016, Eslam, Sanyal et al. 2020), these steatohepatitic characteristics are linked with an increased risk of HCC development (Eslam, Sanyal et al. 2020). Then, we evaluated if *E2f1* or *E2f2* deficiency in mice could prevent liver inflammation and/or fibrosis. For that, extracellular matrix was measured by Sirius Red staining and expression of major genes related to fibrosis and inflammation were assessed in 9 month-old *E2f1*$^{-/-}$, *E2f2*$^{-/-}$ and WT mice livers exposed to HCC-promoter treatments.

The results showed that the percentage of collagen area in liver was increased only when obesity-related HCC was induced in 9 month-old WT mice by administration of DEN HFD *(Figure E5)*. By contrast,

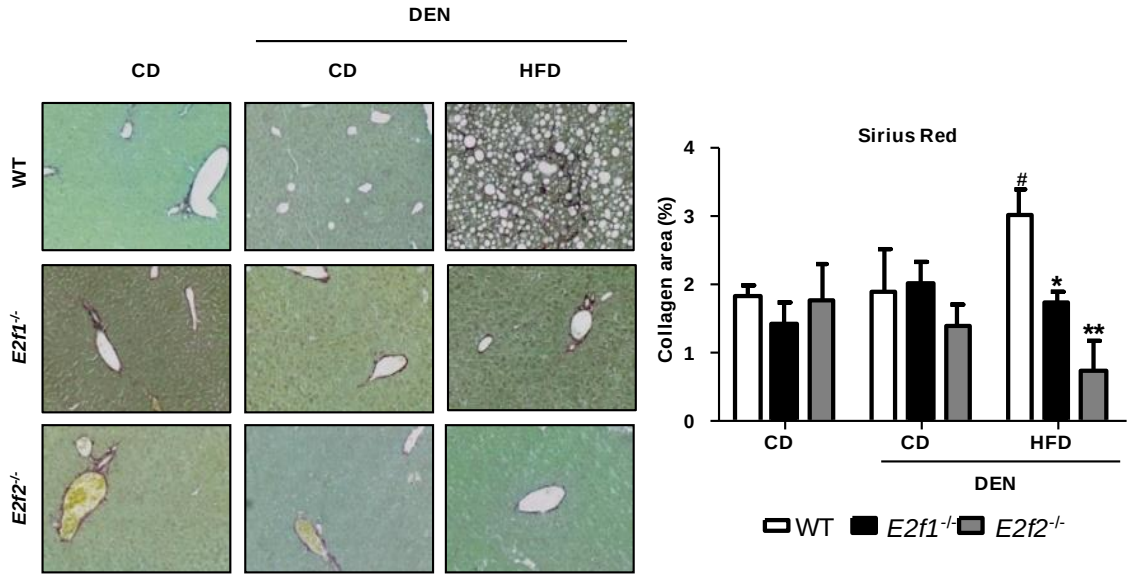

Figure E5. The fibrogenesis associated to long-term carcinogenic treatments is prevented in 9 month-old *E2f1*$^{-/-}$ and *E2f2*$^{-/-}$ mice. *E2f1* knockout (*E2f1*$^{-/-}$), *E2f2* knockout (*E2f2*$^{-/-}$) and their control (WT) mice were injected the procarcinogenic compound diethylnitrosamine (DEN) (25 mg/kg of mice) or vehicle when they were 14 days old. After weaning, mice were kept on a high-fat diet (HFD) or a chow diet (CD) until they were sacrificed at 9 months old and livers were collected. Fibrogenesis was evaluated with the percentage of collagen area, determined by Sirius Red staining (n=4-5 per group). The percentage of collagen was quantified in 5 randomly chosen 20 x magnified fields per section and mouse. Representative micrographs of *E2f1*$^{-/-}$, *E2f2*$^{-/-}$ and WT mice livers are shown. Values are means ± SEM and statistical analysis was assessed by Student's two-tailed t-test. Significant differences between *E2f1*$^{-/-}$ or *E2f2*$^{-/-}$ and WT mice are denoted as *p <0.05, **p <0.01 and ***p <0.001 and differences between DEN CD or DEN HFD and CD are indicated by $^{\#}$p <0.05, $^{\#\#}$p <0.01 and $^{\#\#\#}$p <0.001.

collagen deposition was not observed in *E2f1*$^{-/-}$ and *E2f2*$^{-/-}$ mice livers exposed to DEN HFD treatment when compared to controls *(Figure E5)*.

According to that observed in Sirius Red staining, gene expression of central mediators of liver fibrosis (*Tfgb1, Acta2, Col1a2*) *(Figure E6.A)* and proinflammatory cytokine interleukin-1-β (*Il1b*) was enhanced in WT mice who developed obesity-related HCC *(Figure E6.B)*. However, mRNA levels of other genes involved in inflammation were not altered (*Tnf, Adgre1*) or even diminished (*Il6*) in WT mice treated with DEN HFD as compared to their controls *(Figure E6.B)*. In *E2f1* and especially in *E2f2* deficient mice, mRNA levels of genes involved in fibrogenesis (*Tgfb1, Col1a2, Col3a1*) and inflammation (*Tnf, Il1b, Il6, Adgre1*) were lower as compared to their WT counterparts, even when exposed DEN HFD treatment *(Figure E6.A, B)*.

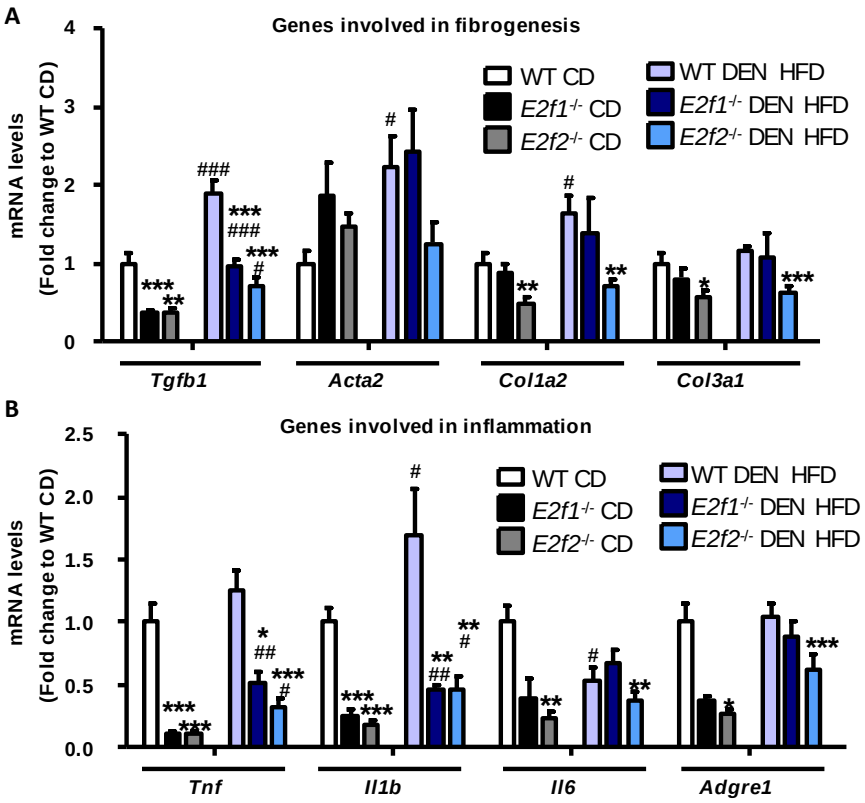

Figure E6. Expression of genes related to fibrosis and inflammation in 9 month-old *E2f1*$^{-/-}$ and *E2f2*$^{-/-}$ mice. *E2f1* knockout (*E2f1*$^{-/-}$), *E2f2* knockout (*E2f2*$^{-/-}$) and their control (WT) mice were injected the procarcinogenic compound diethylnitrosamine (DEN) (25 mg/kg of mice) or vehicle when they were 14 days old. After weaning, mice were kept on a high-fat diet (HFD) or a chow diet (CD) until they were sacrificed at 9 months old and livers were collected. (A) Hepatic mRNA levels of genes involved in fibrogenesis and (B) inflammation were measured by rt-qPCR (n=7-8 per condition). Values are means ± SEM and statistical analysis was assessed by Student's two-tailed t-test. Significant differences between *E2f1*$^{-/-}$ or *E2f2*$^{-/-}$ and WT mice are denoted as *p <0.05, **p <0.01 and ***p <0.001 and differences between DEN CD or DEN HFD and CD are indicated by $^{\#}$p <0.05, $^{\#\#}$p <0.01 and $^{\#\#\#}$p <0.001.

These results showed that our model of obesity-related HCC is associated with liver fibrosis and inflammation. In addition, the absence in *E2f1* or *E2f2* restrains the development of both processes.

1.3.2. E2f1 and E2f2 regulate liver lipid storage during hepatocarcinogenesis

Adaptive events in highly proliferative cells involve energy generation provided by lipids to satisfy their needs for cell division (Beloribi-Djefaflia, Vasseur et al. 2016). Neutral lipids like triglyceride (TG) and cholesteryl esters (CE) are stored in lipid droplets (LD), cytoplasmic organelles now considered a signature of cancer aggressiveness (Beloribi-Djefaflia, Vasseur et al. 2016). Lipogenic phenotype of cancer cells also leads to the production of complex lipids involved in membrane synthesis such as free cholesterol (FC) (Ribas, Garcia-Ruiz et al. 2016).

We have already showed that administration of the procarcinogen agent DEN in combination with a long-term HFD regimen induced HCC with higher number of tumors and increased diameter than the DEN alone *(see Results section 1.2)*. Since cancer cells require high energy stores, obesity-driven liver tumors show lipid accumulation (Park, Lee et al. 2010a). As *E2f1*$^{-/-}$ and *E2f2*$^{-/-}$ mice escaped from HCC development, we proposed that *E2f1* and, particularly, *E2f2* deficiency could also prevent the HCC-related rewiring of lipid metabolism. Hence, we determined the liver lipid concentration in all the mice models of study.

1.3.2.1. E2f1 and E2f2 are involved in the liver lipid storage related to HCC development

Lipid content was assessed by histochemical analysis in livers from 9 month-old *E2f1*$^{-/-}$, *E2f2*$^{-/-}$ and WT mice exposed to DEN, HFD or DEN HFD treatments. Hematoxylin-eosin and Oil Red O stainings showed that liver tumors in WT mice exhibited lipid storage, mainly in obese mice exposed to HFD and DEN HFD *(Figure E7.A)*. By contrast, 9 month-old *E2f1*$^{-/-}$ and, particularly, *E2f2*$^{-/-}$ mice showed reduced liver lipid content as compared to their WT counterparts independently to the treatment administered *(Figure E7.A)*.

Lipid quantification confirmed that liver TG increased in WT mice after the HCC-induction treatments, especially in obese mice exposed to HFD and DEN HFD, in which liver DG was also increased *(Figure E7.B)*. Levels of hepatic CE were enhanced only after exposition to DEN HFD, a condition in which the number of lipid droplets were markedly increased *(Figure E7.B)*.

By contrast, 9 month-old DEN HFD *E2f1*$^{-/-}$ and, particularly, *E2f2*$^{-/-}$ mice showed decreased levels of neutral lipids in liver when compared to their WT littermates *(Figure E7.B)*. In addition, liver content in TG and CE were also reduced in *E2f2*$^{-/-}$ mice when compared to WT mice fed a CD, a HFD or treated with DEN CD, while maintained unaltered in *E2f1*$^{-/-}$ mice *(Figure E7.B)*.

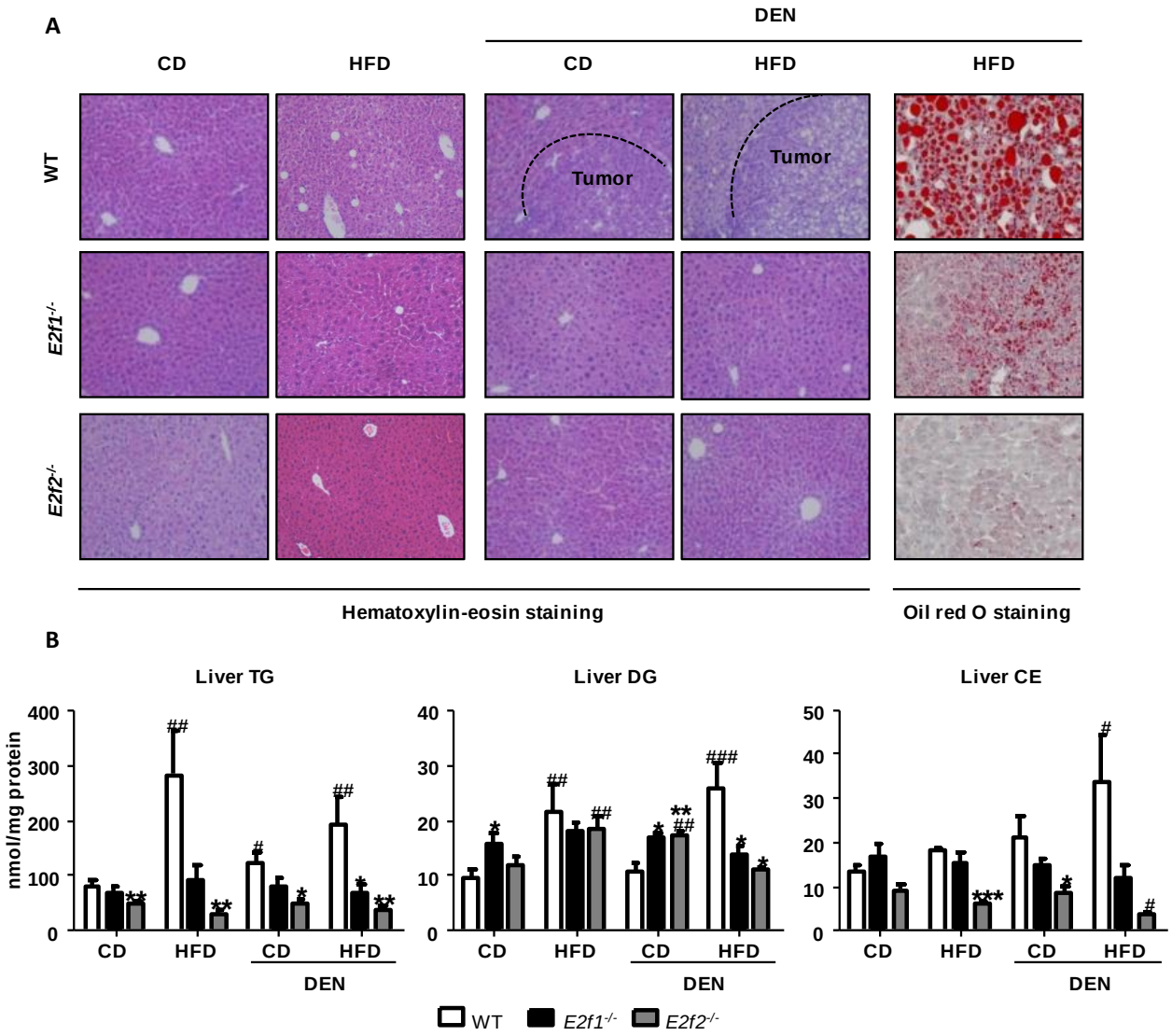

Figure E7. The lack of *E2f1* and mainly of *E2f2* prevents the liver lipid storage associated to the hepatocarcinogenic treatments in 9-month-old mice. *E2f1* knockout (*E2f1*$^{-/-}$), *E2f2* knockout (*E2f2*$^{-/-}$) and their control (WT) mice were injected the procarcinogenic compound diethylnitrosamine (DEN) (25 mg/kg of mice) or vehicle when they were 14 days old. After weaning, mice were kept on a high-fat diet (HFD) or a chow diet (CD) until they were sacrificed at 9 months old and livers were collected. (A) Collected livers were prepared for histochemistry. Representative sections of hematoxylin-eosin (40 x magnification) and Oil red O stainings (20 x magnification) are shown. (B) Lipids were extracted from liver homogenate. Neutral lipids, involved in energy storage, were separated and quantified as described in Materials and Methods (n=7-9 for HFD, DEN CD and DEN HFD groups, n=18 for CD groups). Values are means ± SEM and statistical analysis was assessed by Student's two-tailed t-test. Significant differences between *E2f1*$^{-/-}$ or *E2f2*$^{-/-}$ and WT mice are denoted as *p <0.05, **p <0.01 and ***p <0.001 and differences between DEN CD or DEN HFD and CD are determined by $^{\#}$p <0.05, $^{\#\#}$p <0.01 and $^{\#\#\#}$p <0.001. DG, diglyceride; CE, cholesteryl ester; TG, triglyceride.

Collectively, these results show that E2f1 and, more markedly, E2f2 are involved in the increased NAFLD-related HCC lipid storage.

1.3.2.2. E2f1 and E2f2 regulate cholesterol metabolism in liver

In concordance with the changes observed in liver CE, liver free cholesterol (FC) concentration was only increased in the DEN HFD WT mice, while maintained unaltered in HFD WT and in DEN CD WT mice *(Figure E8.D)*. In addition, the concentration of FC did not increase in *E2f1*$^{-/-}$ nor *E2f2*$^{-/-}$ mice treated with DEN when compared to their WT littermates, even when combined with HFD *(Figure E8.D)*. These results here suggest that E2f1 and E2f2 not only control neutral lipid metabolism, but also cholesterol metabolism.

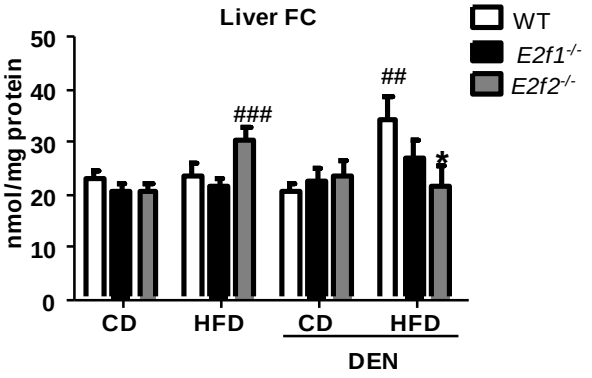

Figure E8. Liver cholesterol content in 9 month-old mice. *E2f1* knockout (*E2f1*$^{-/-}$), *E2f2* knockout (*E2f2*$^{-/-}$) and their control (WT) mice were injected the procarcinogenic compound diethylnitrosamine (DEN) (25 mg/kg of mice) or vehicle when they were 14 days old. After weaning, mice were kept on a high-fat diet (HFD) or a chow diet (CD) until they were sacrificed at 9 months old. Liver was collected and lipids were extracted from liver homogenate. Free cholesterol (FC) were separated and quantified as described in Materials and Methods (n=18 for CD groups and n=7-9 for the rest of the groups). (C) PC/PE ratio was also calculated. Values are means ± SEM and statistical analysis was assessed by Student's two-tailed t-test. Significant differences between *E2f1*$^{-/-}$ or *E2f2*$^{-/-}$ and WT mice are indicated as *p <0.05, **p <0.01 and ***p <0.001 and differences between DEN CD or DEN HFD and CD are denoted by $^{\#}$p <0.05, $^{\#\#}$p <0.01 and $^{\#\#\#}$p <0.001.

1.3.2.3. *E2F2* knock-down in human tumoral cells reduces lipid accumulation

Next, we aimed to know if the decreased liver lipid content in 9 month-old mice lacking *E2f1* or *E2f2* was a liver-specific effect and not an adaptive response mediated by peripheral tissues. To this end, *E2F1* or *E2F2* were silenced in the HepG2 cell line and cellular lipid content was analyzed.

Fluorescence staining of lipid droplets showed that lipid storage barely diminished in *E2F1* knockout cells as compared to controls *(Figure E9.A)* while was reduced when *E2F2* was knocked down *(Figure E9.A)*. Accordingly, the TG quantification showed that cellular content in TG was reduced only when *E2F2* was silenced *(Figure E9.B)*. These experiments suggest that *E2F2* controls lipid metabolism in liver tumor cells, independently from cancer development.

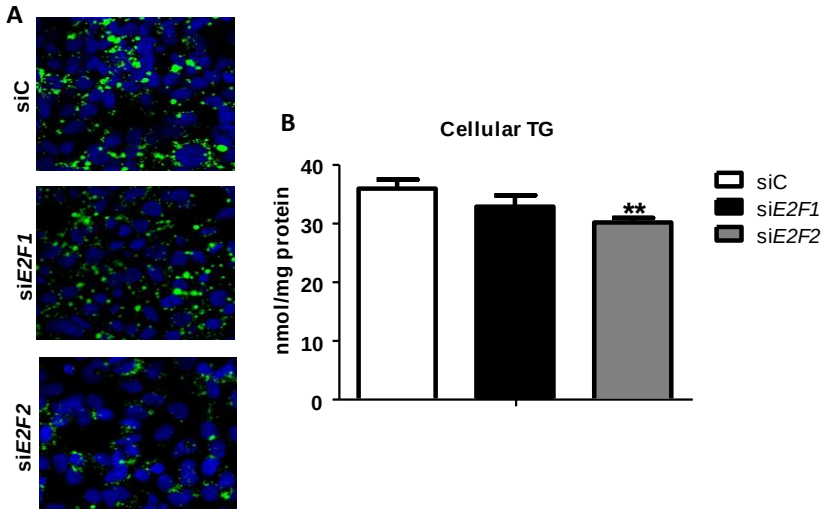

Figure E9. *E2F2* knock-down in human tumoral liver cells diminishes lipid storage. *E2F1* and *E2F2* transcription factors were silenced in HepG2 cell line by reverse transcription of specific siRNAs (si*E2F1* and si*E2F2* respectively). Controls treated with a negative control siRNA (siC) were included in each assay. (A) For immunofluorescence staining of neutral lipid droplets, silenced cells were fixed and permeabilized. Then, lipids were labelled with Bodipy Green lipophilic fluorescent dye and cell nucleus were dyed with DAPI blue fluorescent probe. Representative confocal micrographs are shown. (B) Cellular triglyceride (TG) was quantified in cell homogenates as indicated in Materials and Methods. Values are means ± SEM of 2 independent experiments each one with n=4 per group. Statistical analysis was assessed by Student's two-tailed t-test. Significant differences between si*E2F1* or si*E2F2* and siC are indicated as *p <0.05, **p <0.01 and ***p <0.001.

2. E2F1 and E2F2 transcription factors control obesity-related NAFLD development

We had previously observed that *E2f2* overexpression was linked to hepatocarcinogenesis in obese mice at 9 months old. In addition, absence in *E2f1* and, especially, in *E2f2* prevented the HCC development linked or not to obesity. Loss of *E2f1* or *E2f2* also protected mice from the DEN HFD induced fibrogenesis and lipid storage. Thus, we proposed that E2f1 and E2f2 were involved in the metabolic reorganization that occurs even before the HCC is developed, when cell cycle is still not active.

Then, early stage of the liver disease was induced in *E2f1*$^{-/-}$, *E2f2*$^{-/-}$ and WT mice. For that, animals were injected with DEN or the vehicle when they were 14 days old. Once weaned, they were placed in a short-term regimen of HFD or CD for 10 weeks and sacrificed at 3 months old. In addition, liver samples of obese patients were used to assess the relevance of E2F1 and E2F2 in human physiopathology of NAFLD.

2.1. E2F1 and E2F2 liver content is enhanced in obese patients

We wondered whether the liver disease could be linked with variations in E2F1 and E2F2 levels in liver samples from obese patients. For that, a cohort of 62 obese patients was analyzed histologically and classified in normal liver (NL) (n=15 patients) and non-alcoholic fatty liver disease (NAFLD) (n=47 patients) following NAS score evaluation as outlined by Kleiner *et al* (Kleiner, Brunt et al. 2005). Liver samples from non-obese donors (BMI < 30 Kg/m^2) with NL were used as controls.

Obese patients with NAFLD presented elevated circulating TG and insulin concentrations comparing to NL-obese subjects *(Table E2)*. They also showed higher serum HOMA-IR as well as ALT and AST activities *(Table E2)*. Nevertheless, they were not identified as individuals with metabolically unhealthy obesity (MUO) in their medical history, because serum values of cholesterol (CHO and CHO-HDL), glucose, insulin and transaminases were kept within the reference values specified by the WHO *(Table E2)*.

Table E2. Baseline characteristics of obese patients (BMI > 30 Kg/m^2) with or without non-alcoholic fatty liver disease (NAFLD).

Characteristics	Overall (n=62)	NL (n=15)	NAFLD (n=47)
Age	49.2 (24-69)	48.8 (24-63)	49.3 (26-69)
Male gender	22 (35.5 %)	4 (26.7 %)	18 (38.3 %)
BMI (kg/m^2)	43.6 (33.4-53.2)	43 (36,5-53)	49.3 (33.4-53.1)
TG (mg/dl)	149.3 (57-412)	105 (57-211)	164 (63-412)**
CHO (mg/dl)	160.6 (79-250)	153.3 (115-226)	163.1 (79-250)
CHO-HDL (mg/dl)	36 (20-53)	36.9 (25-53)	35.7 (20-53)
Glucose (mg/dl)	93.4 (66-203)	81.5 (67-140)	97.3 (66-203)
Insulin (µIU/ml)	13.8 (2-54.2)	9.3 (2.7-16.5)	15.3 (2-54.2)*
HOMA-IR	3.2 (0.4-13.7)	2 (0.4-5.4)	3.7 (0.5-13.7)*
ALT (IU/l)	37.3 (13-106)	26.5 (13-95)	40.8 (13-106)*
AST (IU/l)	29.4 (11-116)	22.3 (11-50)	31.8 (14-116)*
Alkaline Phosphatase (IU/l)	65.2 (13-120)	58.2 (29-84)	67.6 (13-120)
Esteatosis			
Grade 0	15 (24.2 %)	15 (100 %)	
Grade 1	28 (45.2 %)		28 (59.6 %)
Grade 2	12 (19.4 %)		12 (25.5 %)
Grade 3	7 (11.3 %)		7 (14.9)

Liver samples from obese patients (n=62) were obtained by liver biopsy and were classified in NL (n=15) and metabolic-dysfunction-associated fatty liver disease (NAFLD) (n=47) following NAS score evaluation as outlined by Kleiner *et al*. Data are shown as mean (range) or n (%). Statistical analysis was assessed by Student's two-tailed t-test. Significant differences between NAFLD and NL are determined by *p <0.05, **p <0.01 and ***p <0.001. BMI, body mass index; TG, Triglyceride; CHO, Cholesterol; HDL, high density lipoprotein; HOMA-IR, homeostatic model assessment-insulin resistance score; ALT, alanine aminotransferase; AST, aspartate aminotransferase.

Immunohistochemistry analysis revealed that liver E2F1 *(Figure E10.A)* and E2F2 *(Figure E10.B)* levels increased in obese patients as compared to lean donors, even when diagnosed as NL. Contrary to E2F1, E2F2 content also enhanced in livers of obese patients with NAFLD when compared to obese patients with NL *(Figure E10.B)*.

Altogether, these results suggested that E2F1 and E2F2 are induced in obesity even in the absence of liver disease. Moreover, high E2F2 liver content is linked to obesity-driven NAFLD development, which points out its value as a predictor of the liver disease.

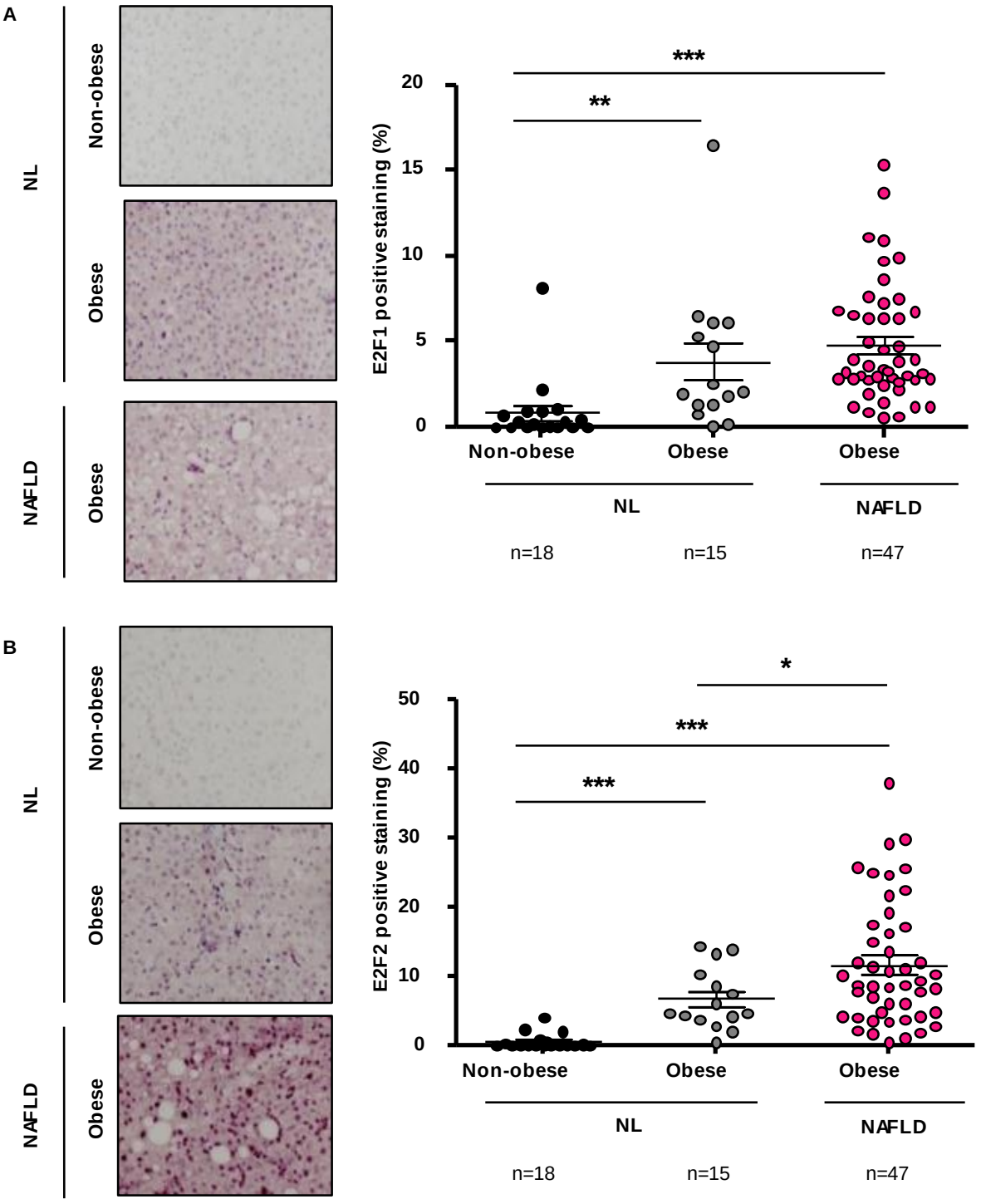

Figure E10. E2F1 and E2F2 liver content in individuals with NL and NAFLD patients. Liver samples from obese patients (n=67) were obtained by liver biopsy and were classified in NL (n=15 patients) and non-alcoholic fatty liver (NAFL) (n=47 patients) following NAS score evaluation as outlined by Kleiner *et al*. Samples from non-obese donors (n=18) with NL were used as controls. (A) E2F1 or (B) E2F2 liver content was determined by immunohistochemistry as described in Materials and Methods. Positive stained nuclear area was quantified in 5 randomly chosen 40 x magnified fields per section and liver sample. Representative slides are shown. Values are shown as means ± SEM. Statistical analysis was assessed by Student's two-tailed t-test. Significant differences are determined by *p <0.05, **p <0.01 and ***p <0.001.

2.2. Obesity-related NAFLD promotes *E2f2* gene expression in mice

Since E2F1 and E2F2 levels were higher in obese patients with NAFLD *(see Results section 2.1.)*, we hypothesized that E2f1 and E2f2 could also be involved in the obesity-related hepatosteatosis instauration in mice. Hence, the metabolic phenotype of 3 month-old *E2f1*$^{-/-}$, *E2f2*$^{-/-}$ and WT animals exposed to HFD, DEN CD or DEN HFD was studied.

The results showed that exposition to a HFD feeding regimen for 10 weeks, combined or not with DEN, induced an increase in the body weight and WAT index of WT mice when compared to controls *(Table E3)*. This effect was not accompanied by hepatomegaly, although serum ALT levels were higher, mainly when mice were exposed to DEN HFD treatment *(Table E3)*. Exposition only to DEN did not modify body weight nor WAT index in WT mice when compared to the control treatment *(Table E3)*. Although liver percentage to body weight also maintained unaltered, DEN induced liver damage in WT mice as the serum ALT levels showed when compared to controls *(Table E3)*.

Table E3. Body weight, liver index, WAT index and serum ALT in 3 month-old *E2f1*$^{-/-}$, *E2f2*$^{-/-}$ and WT mice treated with diethylnitrosamine (DEN) or the vehicle combined with high-fat diet (HFD) or chow diet (CD).

		CD	HFD	DEN CD	DEN HFD
Body weight (gr)	WT	26.80 ± 0.65	35.50 ± 1.40 $^{###}$	25.95 ± 0.89	35.85 ± 1.22 $^{###}$
	E2f1$^{-/-}$	24.46 ± 0.49 **	25.95 ± 0.74 ***	23.89 ± 0.49 *	27.04 ± 0.95 *** $^{##}$
	E2f2$^{-/-}$	27.78 ± 0.77	28.77 ± 0.51 ***	27.17 ± 0.49	27.21 ± 0.76 ***
WAT index (%)	WT	1.54 ± 0.08	2.30 ± 0.17 $^{###}$	1.29 ± 0.17	2.99 ± 0.18 $^{###}$
	E2f1$^{-/-}$	1.78 ± 0.10	2.03 ± 0.28	1.71 ± 0.12	2.29 ± 1.41
	E2f2$^{-/-}$	1.56 ± 0.07	2.01 ± 0.16 $^{##}$	1.50 ± 0.11	2.11 ± 0.15 *** $^{###}$
Liver index (%)	WT	4.29 ± 0.16	4.15 ± 0,17	4.91 ± 0.08	4.40 ± 0.10
	E2f1$^{-/-}$	3.91 ± 0.08 *	3.65 ± 0.10 * $^{#}$	3.80 ± 0.07 ***	4.13 ± 0.16
	E2f2$^{-/-}$	4.02 ± 0.06	4.00 ± 0.08	4.29 ± 0.19 $^{#}$	3.91 ± 0.19 **
ALT (U/L)	WT	25.15 ± 2.19	39.72 ± 4.70 $^{#}$	37.12 ± 5.40 $^{##}$	56.08 ± 6.63 $^{###}$
	E2f1$^{-/-}$	48.38 ± 4.35 ***	43.11 ± 7.53	23.72 ± 4.70 $^{##}$	45.80 ± 3.18
	E2f2$^{-/-}$	31.74 ± 2.45	17.71 ± 2.70 ** $^{##}$	14.88 ± 1.68 *** $^{###}$	16.56 ± 3.12 *** $^{###}$

E2f1 knockout (*E2f1*$^{-/-}$), *E2f2* knockout (*E2f2*$^{-/-}$) and their control (WT) mice were injected the procarcinogenic compound diethylnitrosamine (DEN) (25 mg/kg of mice) or vehicle when they were 14 days old. After weaning, mice were kept on a high-fat diet (HFD) or a chow diet (CD) until they were sacrificed at 3 months old and livers were collected. Liver and white adipose tissue (WAT) index is determined by dividing the liver and the WAT weight to the body weight, respectively. Values are means ± SEM. (n=21-26 animals in CD groups and n=12-13 animals in the rest of the groups for body weight, liver index and WAT index. For alanine aminotransferase (ALT) an n of 5-19 animals per group was used). Statistical analysis was assessed by Student's two-tailed t-test. Significant differences between *E2f1*$^{-/-}$ or *E2f2*$^{-/-}$ and WT mice are indicated by *p <0.05, **p <0.01 and ***p <0.001 and differences between HFD, DEN CD or DEN HFD and CD are denoted by $^{#}$p <0.05, $^{##}$p <0.01 and $^{###}$p <0.001.

Conversely to WT animals, 3 month-old *E2f1*$^{-/-}$ and *E2f2*$^{-/-}$ mice did not show increased body weight after exposition to the short term HFD regimen when combined or not with DEN in comparison to their CD-counterparts *(Table E3)*. Reduction in the body weight was not accompanied by lower WAT and liver percentage or serum ALT levels in E2F1 deficient mice *(Table E3)*. The increase of WAT and liver index and in ALT values was prevented in *E2f2*$^{-/-}$ animals, especially when it was mediated by DEN HFD treatment *(Table E3)*.

The above findings demonstrated that *E2f1* and, especially, *E2f2* deficiency protected mice from the obesity and liver injury associated to a short term of HFD feeding regimen when combined or not with DEN.

Then, we aimed to know if NAFLD-induction treatments lead to E2f1 and E2f2 upregulation in WT mice. mRNA analysis showed that *E2f1* gene expression maintained unaltered in 3 month-old WT mice exposed to HFD, DEN or DEN HFD *(Figure E11.A)*. However, mRNA levels of *E2f2* were enhanced in WT mice after feeding HFD combined or not with DEN *(Figure E11.A)*. Exposition only to DEN did not alter *E2f2* gene expression comparing to the control treatment, which indicated that *E2f2* gene is induced in obesity *(Figure E11.A)*. Accordingly, DEN HFD treatment also increased E2f2 protein levels *(Figure E11.B)*.

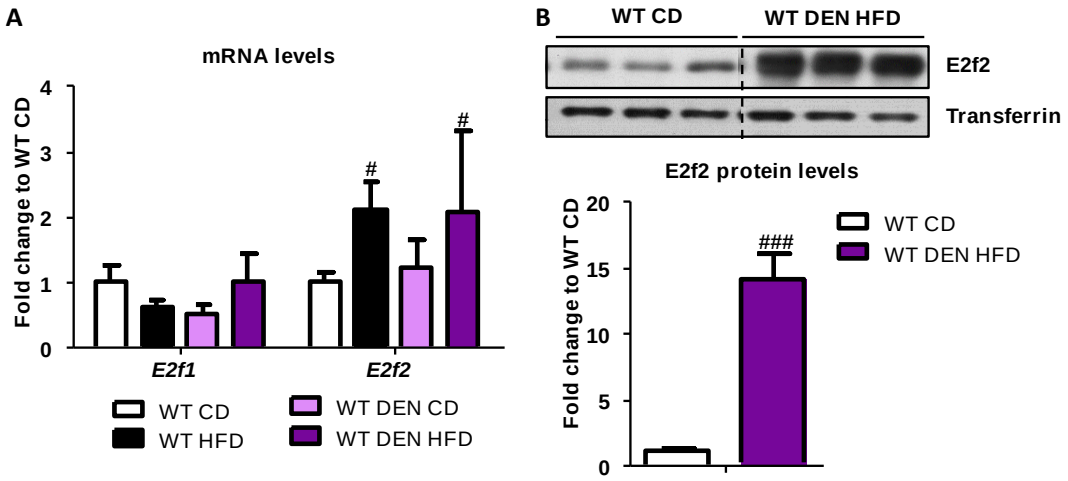

Figure E11. *E2f1* and *E2f2* expression in livers of 3 month-old WT mice. Wild type (WT) mice were injected the procarcinogenic compound diethylnitrosamine (DEN) (25 mg/kg of mice) or vehicle when they were 14 days old. After weaning, mice were kept on a high-fat diet (HFD) or a chow diet (CD) until they were sacrificed at 3 months old and livers were collected. (A) Hepatic mRNA of *E2f1* and *E2f2* were measured by rt-qPCR. (B) E2f2 protein was assessed by immunoblotting in liver extracts. Transferrin was used as loading control. Representative Immunoblots are shown. Values are means ± SEM of 7-8 animals per group. Statistical analysis was assessed by Student's two-tailed t-test. Significant differences between DEN HFD, DEN CD, HFD and CD are indicated as $^{\#}p < 0.05$, $^{\#\#}p < 0.01$ and $^{\#\#\#}p < 0.001$.

2.3. E2f1 and E2f2 regulate liver lipid content from early stages of the obesity-related liver disease

2.3.1. *E2f1* or *E2f2* deficiency in mice protects from hepatosteatosis

We next investigated if 3 month-old *E2f1*$^{-/-}$ and *E2f2*$^{-/-}$ mice were also resistant to NAFLD development induced by dietary obesity when combined or not with DEN.

Hematoxylin-eosin and Oil red O staining showed that HFD administration caused accumulation of neutral lipids in WT mice livers, mainly in combination with DEN *(Figure E12.A)*. In contrast, exposition only to DEN did not induce liver lipid storage in WT mice *(Figure E12.A)*. *E2f1*$^{-/-}$ and *E2f2*$^{-/-}$ mice showed decreased lipid accumulation in liver after each of the treatments *(Figure E12.A)*.

Accordingly, liver content in TG increased in WT mice exposed to HFD and mainly to DEN HFD, in which hepatic DG amount was also enhanced *(Figure E12.B)*. Notably, exposition only to DEN did not enhance TG accumulation in WT mice as compared to their CD counterparts *(Figure E12.B)* and liver CE concentration did not increase in WT mice after exposition to any of the treatments *(Figure E12.B)*. *E2f1*$^{-/-}$ and *E2f2*$^{-/-}$ mice showed resistance to liver TG accumulation after administration of HFD, DEN or DEN HFD treatments *(Figure E12.B)*. In addition, DEN HFD *E2f1*$^{-/-}$ and especially *E2f2*$^{-/-}$ mice maintained lower levels of liver CE than their corresponding WT animals *(Figure E12.B)*. These data indicated that *E2f1* or *E2f2* deficiency in mice avoids obesity-linked NAFLD development. Liver quantity in neutral lipids was also diminished in *E2f2*$^{-/-}$ mice administered the control treatment as compared to WT animals *(Figure E12.B)*, suggesting that the inability to storage lipid was more marked in absence of *E2f2* than *E2f1*.

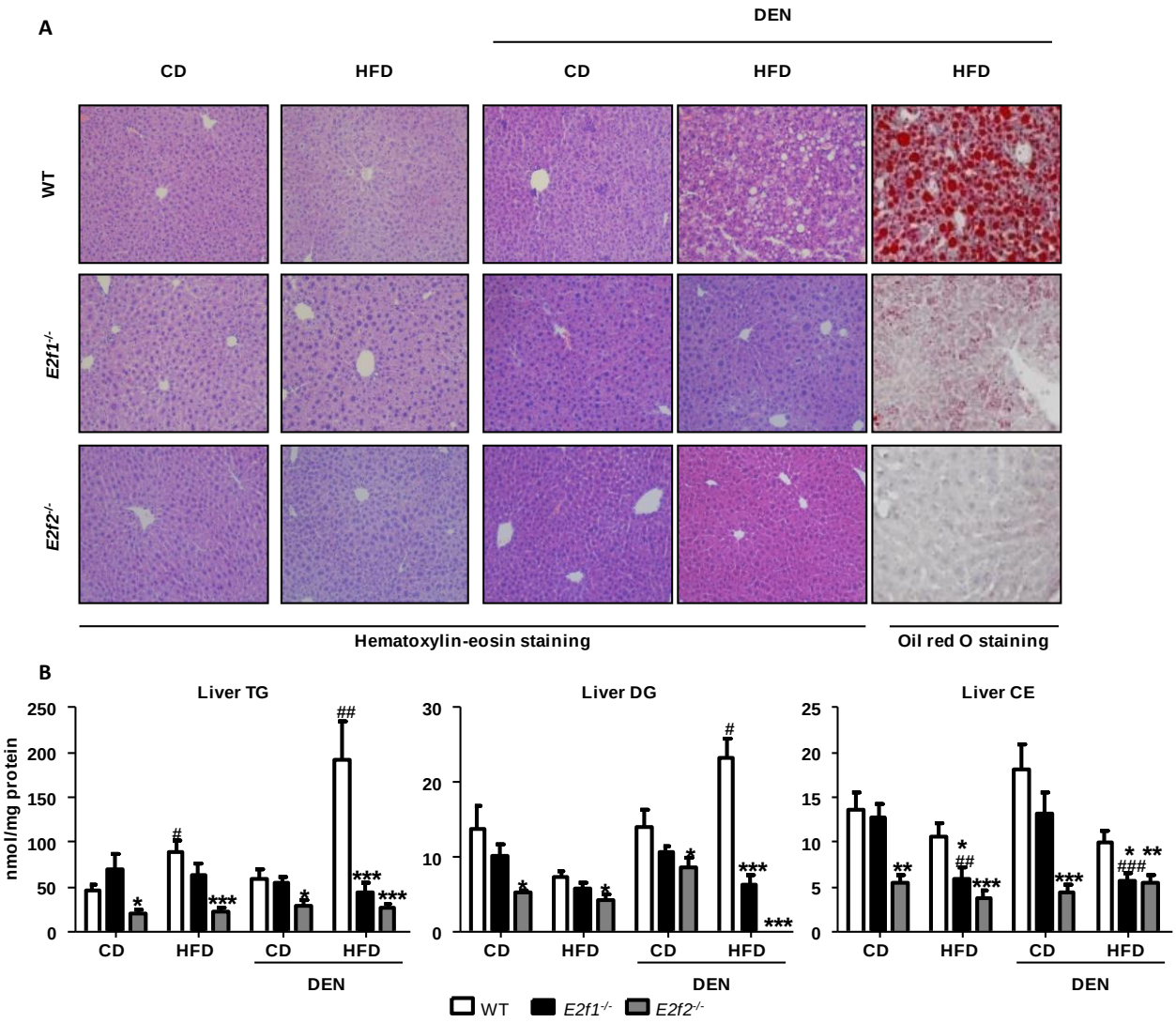

Figure E12. The lack of *E2f1* or *E2f2* avoids the hepatosteatosis associated with 3 month-old obese mice. *E2f1* knockout (*E2f1*$^{-/-}$), *E2f2* knockout (*E2f2*$^{-/-}$) and their control (WT) mice were injected the procarcinogenic compound diethylnitrosamine (DEN) (25 mg/kg of mice) or vehicle when they were 14 days old. After weaning, mice were kept on a high-fat diet (HFD) or a chow diet (CD) until they were sacrificed at 3 months old. (A) Collected livers were prepared for histochemistry. Representative sections of hematoxylin-eosin (40 x magnification) and Oil red O staining (20 x magnification), which stains neutral lipids, are shown. (B) Lipids were extracted from liver homogenates. Neutral lipids, involved in energy storage, were separated and quantified as described in Materials and Methods. Values are means ± SEM of n=6-12 animals per group and statistical analysis was assessed by Student's two tailed t-test. Significant differences between *E2f1*$^{-/-}$ or *E2f2*$^{-/-}$ and WT mice are denoted as *p <0.05, **p <0.01 and ***p <0.001 and differences between DEN CD or DEN HFD and CD are determined by $^{\#}$p <0.05, $^{\#\#}$p <0.01 and $^{\#\#\#}$p <0.001. TG, triglyceride; DG, diglyceride; CE, cholesteryl ester.

2.3.2. Free cholesterol content in livers from 3 month-old mice

Regarding liver FC, only the HFD treatment diminished its content in WT mice when compared to the controls *(Figure E13.D)*. In *E2f1*$^{-/-}$ and *E2f2*$^{-/-}$ mice, liver quantity of FC maintained barely unaltered as compared to their WT littermates, even after exposition to the NAFLD-induction treatments *(Figure E13.D)*.

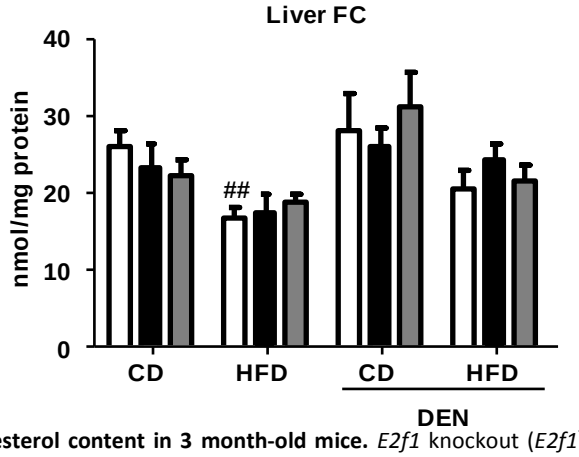

Figure E13. Liver free cholesterol content in 3 month-old mice. *E2f1* knockout (*E2f1*$^{-/-}$), *E2f2* knockout (*E2f2*$^{-/-}$) and their control (WT) mice were injected the procarcinogenic compound diethylnitrosamine (DEN) (25 mg/kg of mice) or vehicle when they were 14 days old. After weaning, mice were kept on a high-fat diet (HFD) or a chow diet (CD) until they were sacrificed at 3 months old and livers were collected. Lipids were extracted from liver homogenates. Free cholesterol (FC) was separated and quantified as described in Materials and Methods. Values are means ± SEM of n=6-12 animals per group and statistical analysis was assessed by Student's two-tailed t-test Significant differences between *E2f1*$^{-/-}$ or *E2f2*$^{-/-}$ and WT mice are indicated as *p <0.05, **p <0.01 and ***p <0.001 and differences between DEN CD or DEN HFD and CD are denoted by $^{\#}$p <0.05, $^{\#\#}$p <0.01 and $^{\#\#\#}$p <0.001.

Altogether, the findings above suggested that diminished amount of liver CE in *E2f1* or *E2f2* depleted mice *(see Results section 2.3.1, Figure E12)* is not related to alterations in FC content. Thus, a reduction of liver fatty acid (FA) content could be associated with changes in CE concentration of *E2f1*$^{-/-}$ and *E2f2*$^{-/-}$ mice livers after the control or the NAFLD-induction treatments.

2.4. At 3 months old, absence in *E2f1* or *E2f2* protects mice from the liver inflammation linked to DEN HFD treatment

Previous results demonstrated that the lack of *E2f1* or *E2f2* in mice prevented from liver fibrosis, inflammation *(see Results section 1.3.1)* and cell-cycle progression associated with HCC-inductor treatments *(see Results section 1.2)*. Then, we analyzed whether the hepatic steatosis caused by DEN HFD treatment in

3 month-old mice was accompanied by fibrogenesis or cell-cycle progression and whether E2f1 or E2f2 were involved on it.

Sirius red staining showed that DEN HFD treatment did not induce liver fibrosis in 3 month-old WT, *E2f1*$^{-/-}$ or *E2f2*$^{-/-}$ mice *(Figure E14.A)*. Accordingly, mRNA levels of several genes involved in fibrogenesis (*Acta2, Col1a2, Col3a1*) did not increase in none of mice strains after exposition to DEN HFD treatment when compared to controls *(Figure E14.B)*. Notably, the initiation of inflammation mediated by the NAFLD-induction treatment in WT mice was not observed in E2f1$^{-/-}$ and E2f2$^{-/-}$ mice, as demonstrated by the mRNA levels of the proinflammatory cytokine *Il1b* *(Figure E14.C)*.

Concerning the cell-cycle, the percentage of Ki67 positive cells was not increased in WT mice exposed to DEN HFD when compared to controls *(Figure E15.A)*, which suggests that the combined treatment does not promote cell proliferation at 3 months old. As expected, expression of E2F target genes (C*cna2, Ccne1, Ccnd3, Tk, Orc1, Plk1*) maintained unaltered in WT mice after the obesity-related NAFLD induction treatment *(Figure E15.B)*.

Altogether, these results demonstrated that the hepatic steatosis developed by exposition to DEN HFD presented inflammation, but not fibrosis or cell-cycle progression. In addition, the lack of *E2f1* or *E2f2* in mice protects liver from inflammatory process mediated by the NAFLD-inductor treatment

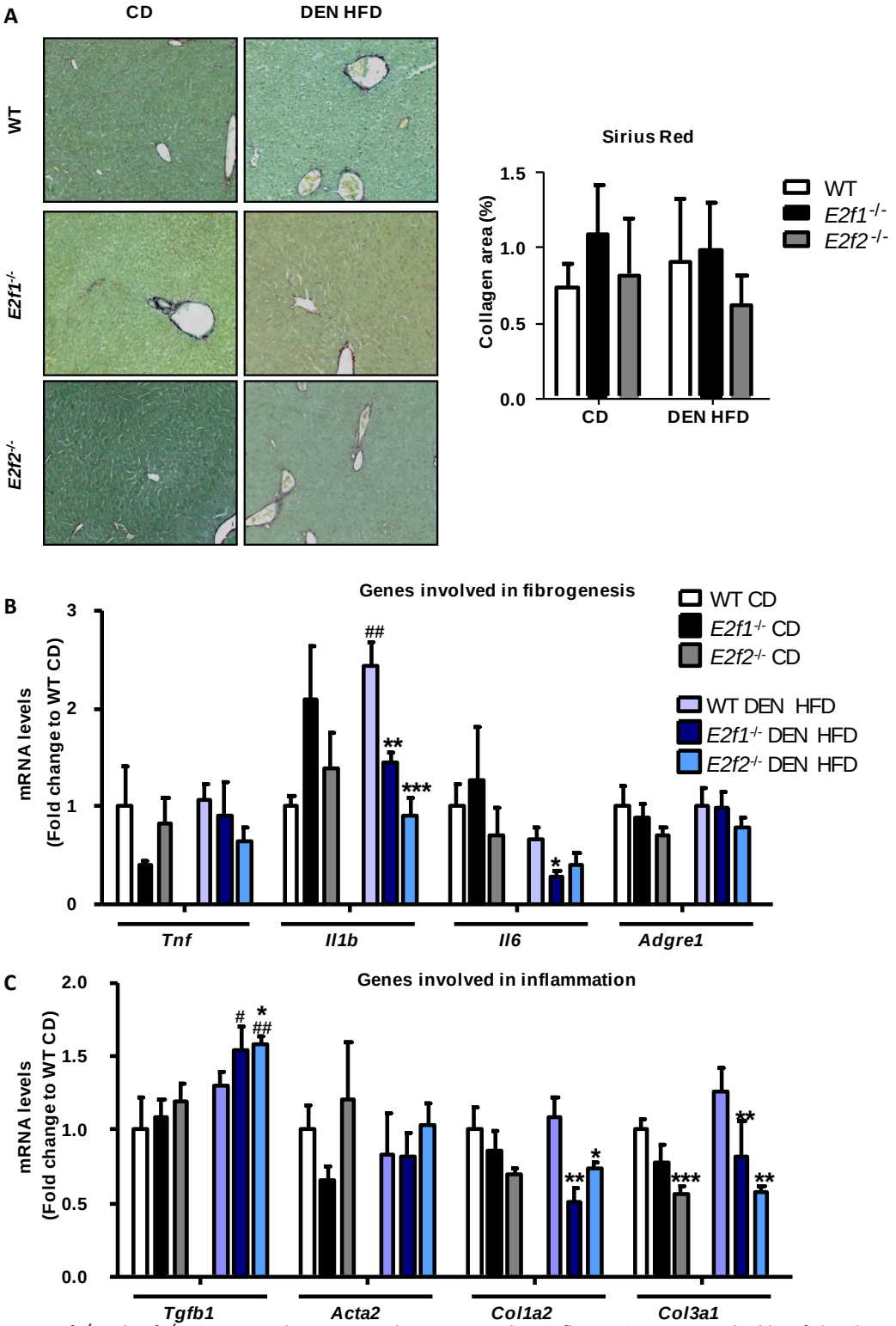

Figure E14. *E2f1*$^{-/-}$ and *E2f2*$^{-/-}$ mice exposed to DEN HFD do not present liver inflammation at 3 month-old. *E2f1* knockout (*E2f1*$^{-/-}$), *E2f2* knockout (*E2f2*$^{-/-}$) and their control (WT) mice were injected the procarcinogenic compound diethylnitrosamine (DEN) (25 mg/kg of mice) or vehicle when they were 14 days old. After weaning, mice were kept on a high-fat diet (HFD) or a chow diet (CD) until they were sacrificed at 3 months old and livers were collected. (A) Fibrogenesis was evaluated with the percentage of collagen area, determined by Sirius Red staining (n=4-5 per condition). The percentage of collagen was quantified in 5 randomly chosen 20 x magnified fields per section and mouse. Representative micrographs of *E2f1*$^{-/-}$, *E2f2*$^{-/-}$ and WT mice livers are shown. (B) Hepatic mRNA levels of genes involved in fibrogenesis and (C) inflammation were measured by rt-qPCR (n=7-8 per condition). Values are means ± SEM and statistical analysis was assessed by Student's two-tailed t-test. Significant differences between *E2f1*$^{-/-}$ or *E2f2*$^{-/-}$ and WT mice are denoted as *p <0.05, **p <0.01 and ***p <0.001 and differences between DEN HFD and CD are indicated by $^{\#}$p <0.05, $^{\#\#}$p <0.01 and $^{\#\#\#}$p <0.001.

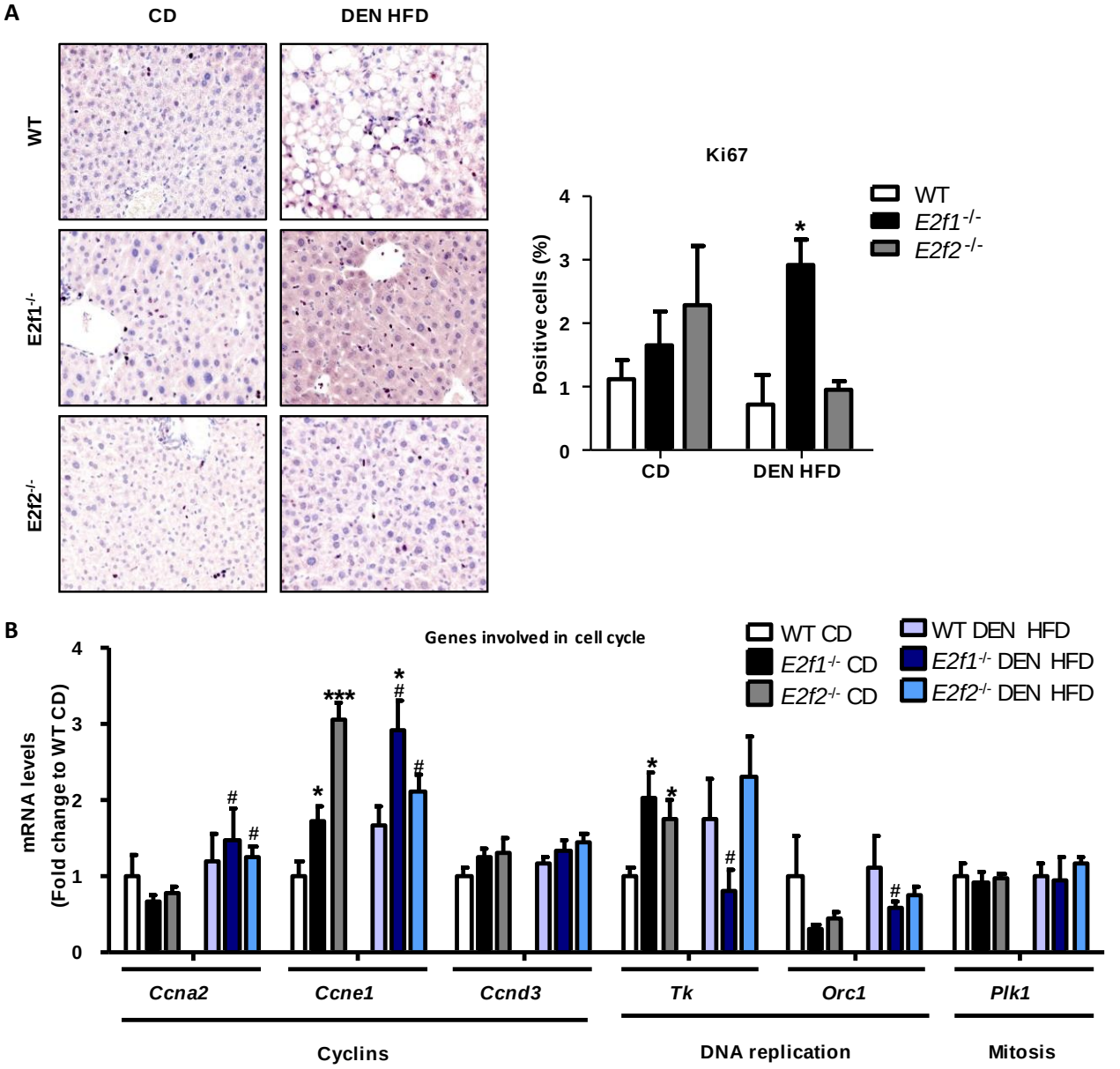

Figure E15. The DEN HFD treatment does not induce cell-cycle activation in livers from 3 month-old mice. *E2f1* knockout (*E2f1*$^{-/-}$), *E2f2* knockout (*E2f2*$^{-/-}$) and their control (WT) mice were injected the procarcinogenic compound diethylnitrosamine (DEN) (25 mg/kg of mice) or vehicle when they were 14 days old. After weaning, mice were kept on a high-fat diet (HFD) or a chow diet (CD) until they were sacrificed at 3 months old and livers were collected. (A) Ki67 immunohistochemistry was performed as described in Materials and Methods (n=4-5 per condition). The percentage of Ki67+ cells was quantified by counting the number of positive nuclei in 5 randomly chosen 40 x magnified fields per section and mouse. Representative microscope images of *E2f1*$^{-/-}$, *E2f2*$^{-/-}$ and WT mice livers are shown. (B) Hepatic mRNA levels of genes involved in cell cycle progression were measured by rt-qPCR (n=7-8 per group). Values are means ± SEM and statistical analysis was determined by Student's two-tailed t-test. Significant differences between *E2f1*$^{-/-}$ or *E2f2*$^{-/-}$ and WT mice are indicated as *p <0.05, **p <0.01 and ***p <0.001 and differences between DEN HFD and CD are denoted by $^{\#}$p <0.05, $^{\#\#}$p <0.01 and $^{\#\#\#}$p <0.001.

3. *E2f2 transcription factor drives the metabolic dysregulation involved in lipid storage during obesity-related liver disease*

Our former findings demonstrated that, in obesity, the involvement of E2F2 in the progression of the liver disease was more relevant than E2F1, as changes in gene and protein expression were more accused in NAFLD-HCC mice models *(see Results section 1.1, Figure E.2 and section 2.2, Figure E.11)* and NAFLD patients *(see Results section 2.1, Figure E10)*. Metabolic reorganization in NAFLD encompassed liver lipid accumulation *(see Results section 1.3.2.1, 2.3.1)*, which was associated with fibrosis and cell-cycle activation in the latest stages of the liver disease *(see Results section 1.2 and 1.3.1)*. *E2f2* deficiency in mice avoided better than *E2f1* the phenotype linked with obesity-linked NAFLD development and its progression to HCC. Within this framework, we decided to go deeper into the metabolic adaptations mediated only by E2f2. To this end, we used 9 and 3 month-old *E2f2*$^{-/-}$ and WT mice exposed to DEN HFD treatment. Age-matched groups were administered the vehicle of DEN and a CD feeding regimen and used as controls.

Hepatosteatosis occurs when fatty acid pool increases due to an imbalance between the input and output pathways. Hence, serum FA uptake (released from diet and WAT lipolysis), *de novo* synthesis of FA (DNL), its esterification to TG and the subsequent TG storage could be increased, while FA oxidation (FAO) and export as TG-very-low density lipoprotein (VLDL) could be decreased (Fabbrini, Sullivan et al. 2010). As the major metabolic changes were observed at 9 months old, the metabolic fluxes involved in liver lipid homeostasis were analyzed firstly at this age.

3.1. E2f2 regulates liver lipid synthesis and oxidation in NAFLD-driven HCC

3.1.1. *E2f2* deficiency induces a new metabolic transcriptome to prevent NAFLD-driven HCC

To define the transcriptional program associated with the resistance to NAFLD-related HCC in the absence of E2f2, a gene expression profiling was performed in livers of 9 month-old *E2f2*$^{-/-}$ mice versus WT mice exposed to DEN HFD. 2210 probes were identified with significantly altered gene expression in *E2f2*$^{-/-}$ mice when compared to control mice, 1027 of them were upregulated and 1183 were downregulated (NCBI's Gene Expression Omnibus (GEO) database, accession number GSE117420).

In order to gain about the biological relevance of this expression profile, the genes whose expression was altered were clustered in pathways. Reactome database analysis revealed that upregulated genes were assigned into 69 processes in *E2f2*$^{-/-}$ mice (GEO database, accession number GSE117420). Among them, the more significantly altered ones were related to lipid catabolism and energy production *(Figure E16.A)*. Genes encoded by downregulated probes were clustered into 230 pathways (GEO database, accession number GSE117420). As expected, the more significantly changed processes were patelet functioning, Toll-like receptors (TLR) cascades, cell cycle, apoptosis and lipid synthesis *(Figure E16.A)*. The results suggested that multiple pathways involved in liver lipid metabolism are modified when obesity-linked HCC development is avoided in *E2f2*$^{-/-}$ mice.

The transcriptional profile of 9 month-old *E2f2*$^{-/-}$ mice livers in control conditions was also analyzed and discovered that 1982 genes had altered expression in comparison to WT mice (GEO database, accession number GSE117420). Those upregulated (634 probes) were clustered in 12 pathways, while those downregulated (1348 probes) were grouped in 222 processes (GEO database, accession number

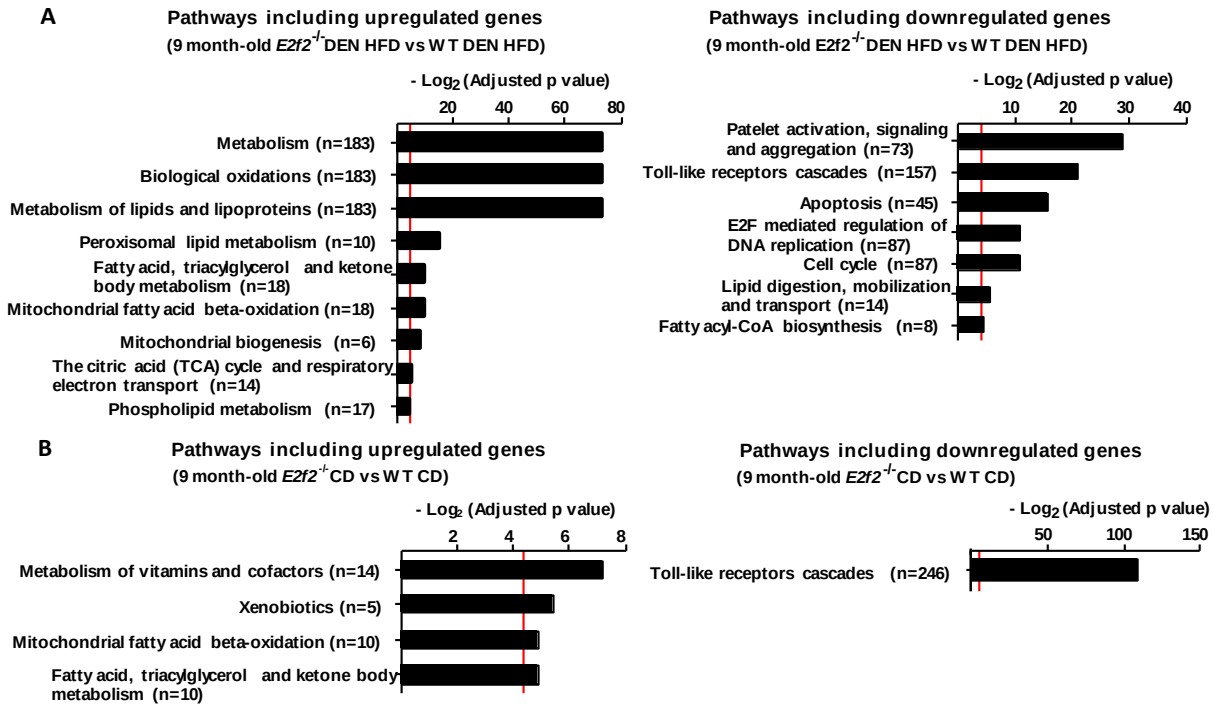

Figure E16. *E2f2* deficiency induces a new transcriptome in 9 month-old mice treated with DEN HFD. *E2f2* knockout (*E2f2*$^{-/-}$) and their control (WT) mice were injected the procarcinogenic compound diethylnitrosamine (DEN) (25 mg/kg of mice) or vehicle when they were 14 days old. After weaning, mice were kept on a high-fat diet (HFD) or a chow diet (CD) until they were sacrificed at 9 months old and livers were collected. RNA was extracted from liver homogenates and a microarray was carried out (n=4 per condition). Differential gene expression between both genotypes was analyzed with Limma statistic package and the adjusted p-value was obtained applying the Benjamini-Hochberg method. Significant probes were assigned into pathways with Reactome database. There are shown the most representative biological pathways modified in *E2f2*$^{-/-}$ mice treated with (A) DEN HFD or (B) CD and, in parenthesis, the number of genes clustered in each pathway. p=0,05 is indicated with a red line. Microarray was then validated with real time quantitative PCR (rt-qPCR) in cDNA synthetized by retrotranscription (n=8).

GSE117420). Consistent with the reduced liver lipid content in *E2f2*$^{-/-}$ mice when administered the control treatment *(see Results section 1.3.2.1)*, genes related to lipid oxidation processes were upregulated *(Figure E16.B)*. Among the downregulated genes, those involved in TLR cascades were changed to the established significance in the steady-state of *E2f2*$^{-/-}$ mice livers *(Figure E16.B)*.

3.1.2. Fatty acid β-oxidation is enhanced in *E2f2* knockout mice

Based on the microarray data, the rate of mitochondrial FAO was analyzed in livers of 9 month-old *E2f2*$^{-/-}$ and WT mice, a critical pathway by which FA are metabolized for energy production (McGarry, Foster 1980). In particular, we determined the conversion of [^{14}C]-palmitate to CO_2 and acid soluble metabolites (ASM), substances representing the complete and incomplete products of FAO respectively.

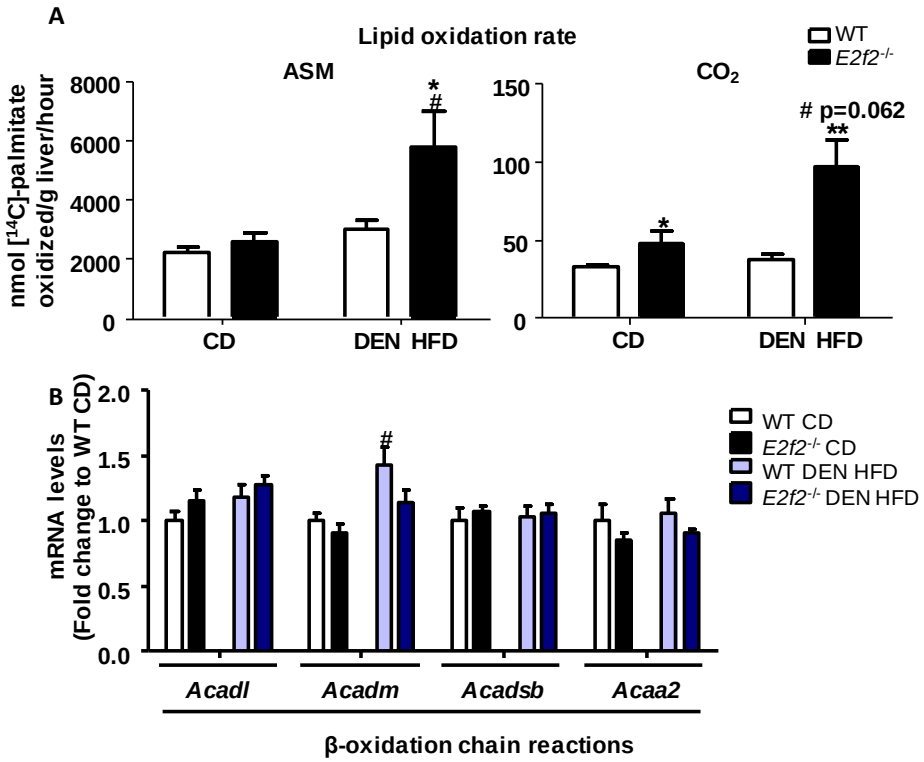

Figure E17. The absence in *E2f2* enhances liver lipid oxidation in 9 month-old mice. *E2f2* knockout (*E2f2*$^{-/-}$) and their control (WT) mice were injected the procarcinogenic compound diethylnitrosamine (DEN) (25 mg/kg of mice) or vehicle when they were 14 days old. After weaning, mice were kept on a high-fat diet (HFD) or a chow diet (CD) until they were sacrificed at 9 months old and livers were collected. (A) Lipid oxidation rate was determined in liver homogenate by measuring the amount of [^{14}C]-CO_2 (complete oxidation of [^{14}C]-palmitate) and [^{14}C] labeled acid-soluble metabolites (ASM) (incomplete oxidation of [^{14}C]-palmitate) (n=8 per group). (B) Hepatic mRNA levels of genes involved in β-oxidation chain reactions were measured by rt-qPCR (n=7-8 per condition). Values are means ± SEM and statistical analysis was determined by Student's two-tailed t-test. Significant differences between *E2f2*$^{-/-}$ and WT mice are denoted as *p <0.05, **p <0.01 and ***p <0.001 and differences between DEN HFD and CD are determined by $^{\#}$p <0.05, $^{\#\#}$p <0.01 and $^{\#\#\#}$p <0.001. HCC, hepatocellular carcinoma.

The results showed that the [^{14}C] track in released ASM and CO_2 maintained unaltered in WT mice after DEN HFD treatment when compared to controls, indicating that hepatic FAO was not enhanced during NAFLD-related HCC development *(Figure E17.A)*. On the contrary, complete and incomplete oxidation of palmitate, in terms of ASM and CO_2, were higher in livers of *E2f2*$^{-/-}$ mice exposed to DEN HFD when compared to WT animals *(Figure E17.A)*. Consequently, liver expression of genes involved in multiple steps of FAO (*Acadl, Acadm, Acadsb, Acaa2*) was also increased in *E2f2*$^{-/-}$ mice treated with DEN HFD comparing to their WT littermates *(Figure E17.B)*. These data suggested that E2F2 absence in mice increased FAO as a response to the NAFLD-related HCC induction treatment at 9 months old.

mRNA levels of important transcription factors regulating lipid catabolism (*Ppara, Ppargc1b*) were decreased in WT mice who developed NAFLD-HCC, while others' expression was not altered (*Ppargc1a, Hnf4a, Rxra*) *(Figure E18.A)*. According to the increased FAO rate, *Ppara, Pparc1b, Hnf4a* and *Rxra* were overexpressed in *E2f2* depleted mice administered the HCC-inductor treatment as compared to WT animals *(Figure E18.A)*. Moreover, mRNA levels of *Rxra* were increased in *E2f2*$^{-/-}$ mice even in control conditions *(Figure E18.A)*.

Prior to lipid degradation, FAs have to be firstly activated by conversion to fatty acyl-CoAs (Watkins 1997). Besides, its transport into the mitochondrial matrix via the carnitine shuttle is the rate limiting step of FAO (Bremer 1983). We observed that the expression of most of the genes involved in FA activation (*Acsm1, Acsm3, Acsl1*) or transport (*Cpt1*) was not changed in WT mice with NAFLD-HCC *(Figure E18.B)*. Notably, *Cpt2* expression was downregulated in WT mice who developed obesity-related HCC at 9 months old *(Figure E18.B)*. By contrast, *E2f2*$^{-/-}$ mice exposed to DEN HFD exhibited higher mRNA levels of the genes responsible for FA activation (*Acsm1, Acsm3, Acsl1*) and transport (*Cpt1, Cpt2*) than their WT counterparts *(Figure E18.B)*.

We then evaluated the protein expression of those genes who were mainly altered and observed that, consistent with the gene expression, protein levels of PGC-1β, HNF4-α and CPT2 were enhanced in *E2f2*$^{-/-}$ mice after exposition to the HCC-induction treatment *(Figure E18.C)*. Surprisingly, protein expression of PPAR-α was decreased in *E2f2*$^{-/-}$ mice exposed to DEN HFD when compared to WT mice and PGC-1α did not change *(Figure E18.C)*. The results indicated that increased FAO in *E2f2* deficient mice who escaped from obesity-related HCC is associated with upregulated expression of PGC-1β, HNF4-α and CPT2.

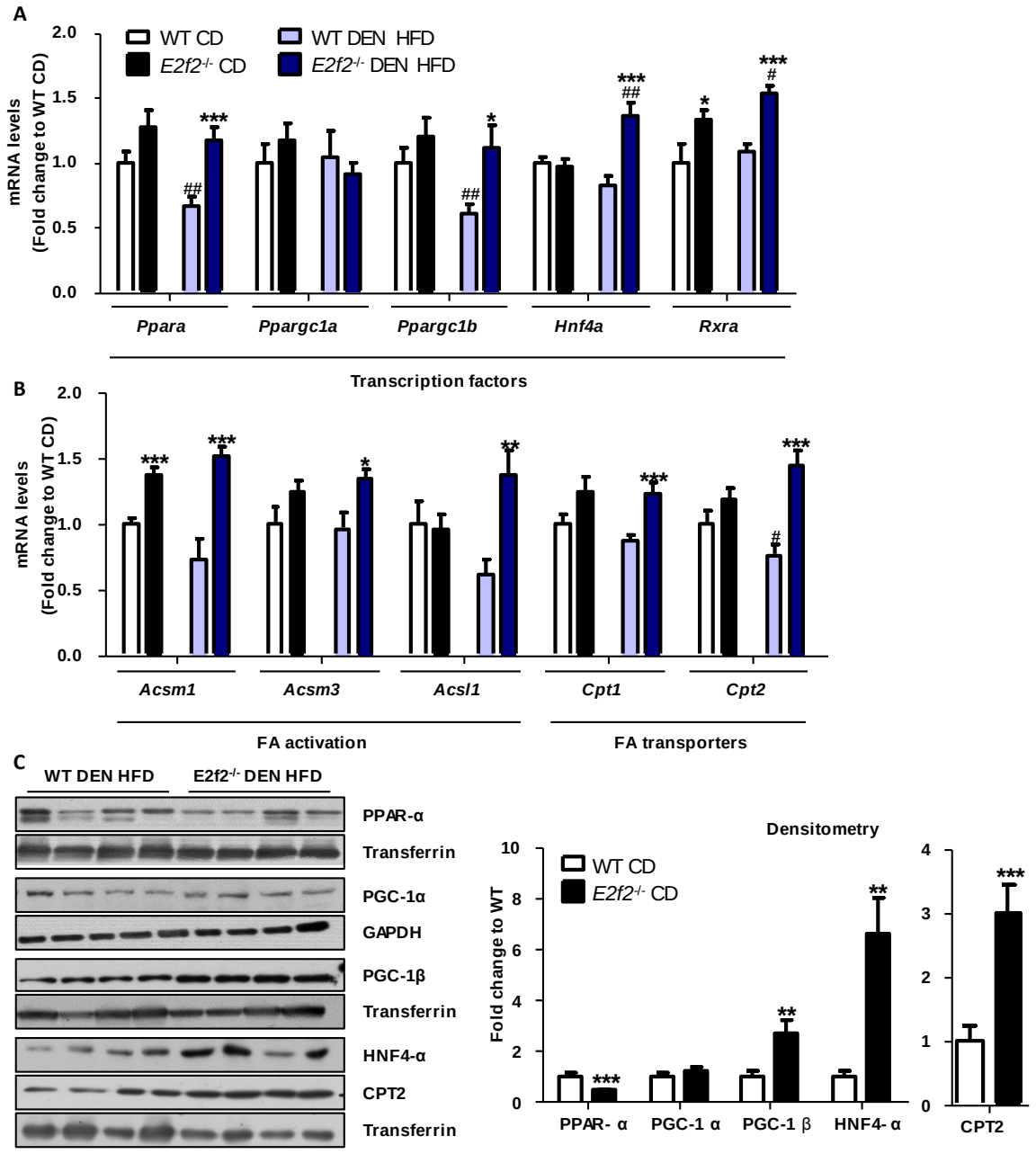

Figure E18. *E2f2* deficiency enhances PGC-1β, HNF4-α and CPT2 expression in 9-month-old mice as a response to the NAFLD-related HCC induction. *E2f2* knockout (*E2f2*$^{-/-}$) and their control (WT) mice were injected the procarcinogenic compound diethylnitrosamine (DEN) (25 mg/kg of mice) or vehicle when they were 14 days old. After weaning, mice were kept on a high-fat diet (HFD) or a chow diet (CD) until they were sacrificed at 9 months old and livers were collected. (A and B) Hepatic mRNA levels of genes involved in the regulation of the lipid oxidation were measured by rt-qPCR (n=7-8 per condition). (C) PPAR-α, PGC-1-α and PGC-1-β, HNF4-α and CPT2 proteins were assessed by immunoblotting in liver extracts (n=8 per condition). Transferrin was used as loading control. Representative immunoblots are shown. Values are means ± SEM and statistical analysis was determined by Student's two-tailed t-test. Significant differences between *E2f2*$^{-/-}$ and WT mice are denoted as *p <0.05, **p <0.01 and ***p <0.001 and differences between DEN HFD and CD are determined by $^{\#}$p <0.05, $^{\#\#}$p <0.01 and $^{\#\#\#}$p <0.001. FA, Fatty acid; HCC, hepatocarcinoma, PPAR-α, peroxisome proliferator-activated receptor alpha; PGC-1α, peroxisome proliferator-activated receptor gamma coactivator-1 alpha; PGC-1β, peroxisome proliferator-activated receptor gamma coactivator-1 beta; HNF4-α, hepatocyte nuclear factor 4-alpha; CPT2, carnitine-O-palmitoyltransferase 2; NAFLD, non-alcoholic fatty liver disease.

The reducing power (NADH and FADH) provided from FAO and TCA can then be used in the oxidative phosphorylation (oxphos) to produce more ATP (Carracedo, Cantley et al. 2013). The results showed that gene expression of enzymes involved in several complexes of oxphos (*Ndufs5, Ndufv1, Atp5a1*) was decreased in WT mice with NAFLD-HCC comparing to controls. Accordingly, mRNA levels of *Atpif1*, inhibitor of the complex V, were enhanced in WT animals exposed to DEN HFD *(Figure E19)*, which suggests that HCC development in obesity is linked with downregulated oxphos. By contrast, genes related to oxphos (*Ndufs5, Ndufs7, Ndufv1, Sdha, Cyb5a, Atp5a1*) were overexpressed while expression of *Atpif1* was decreased in *E2f2*$^{-/-}$ mice as compared to their WT littermates after HCC-induction treatment *(Figure E19)*, indicating that oxphos is promoted.

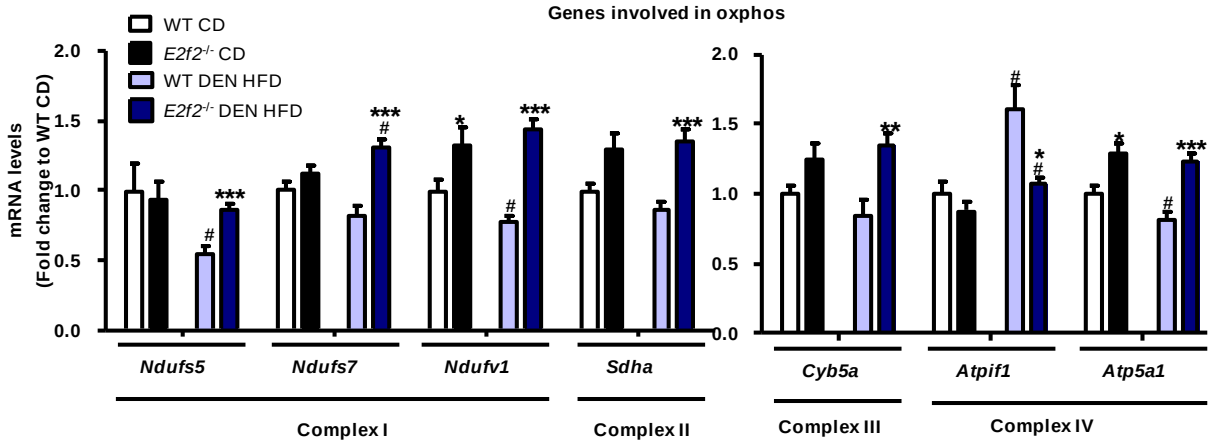

Figure E19. Oxphos is increased in 9-month-old *E2f2*$^{-/-}$ mice exposed to the NAFLD-related HCC induction treatment. *E2f2* knockout (*E2f2*$^{-/-}$) and their control (WT) mice were injected the procarcinogenic compound diethylnitrosamine (DEN) (25 mg/kg of mice) or vehicle when they were 14 days old. After weaning, mice were kept on a high-fat diet (HFD) or a chow diet (CD) until they were sacrificed at 9 months old and livers were collected. Hepatic mRNA levels of genes involved in oxidative phosphorylation (oxphos) were measured by rt-qPCR (n=7-8 per condition). Values are means ± SEM and statistical analysis was determined by Student's two-tailed t-test. Significant differences between *E2f2*$^{-/-}$ and WT mice are denoted as *p <0.05, **p <0.01 and ***p <0.001 and differences between DEN HFD and CD are determined by $^{\#}$p <0.05, $^{\#\#}$p <0.01 and $^{\#\#\#}$p <0.001. HCC, hepatocarcinoma.

All these data suggest that hepatic FAO and oxphos are enhanced in 9 month-old *E2f2* deficient mice livers as a response to the NAFLD-HCC induction treatment. Hence, lipid could not being stored, which results in the prevention of obesity-driven HCC development.

3.1.3. *E2f2* deficiency in mice protects from the dyslipidemia linked with NAFLD-HCC induction treatment

Dyslipidemia is another pathophysiological mechanism involved in obesity and NAFLD (Katsiki, Mikhailidis et al. 2016). Thus, we wanted to know whether obesity-related HCC development in WT mice altered serum lipid profile and whether E2f2 deficiency could be involved on it. For this purpose, circulating TG and FA concentrations we determined in 9 month-old WT and *E2f2*$^{-/-}$ mice.

DEN HFD treatment increased serum concentration of TG and FA in WT mice when compared to the control treatment *(Figure E20.A)*, indicating that HCC development when feeding a HFD is associated to high levels of circulating TG and FA. By contrast, *E2f2* deficiency in mice conferred protection against the dyslipemia mediated by exposition to the NAFLD-HCC inductor treatment, since serum concentration of TG and FA did no change in *E2f2*$^{-/-}$ mice after exposition to DEN HFD treatment and were lower than in WT mice *(Figure E20.A)*. Even in control conditions, circulating FA levels maintained diminished in *E2f2* depleted mice when compared to WT animals *(Figure E20.A)*.

High serum TG concentration could be due to an increased liver export of TG in terms of VLDL (Julius 2003), hence, the hepatic VLDL secretion rate was determined by inhibition of the VLDL catabolism. The results showed that, after inhibition of VLDL catabolism, circulating TG levels did not enhance in WT mice exposed to DEN HFD as compared to their controls *(Figure E20.B)*. This suggests that the dyslipidemia associated to NAFLD-HCC is not caused by an increased liver VLDL secretion. Hepatic TG secretion rate also maintained unaltered in *E2f2*$^{-/-}$ mice *(Figure E20.B)*.

Consistently, mRNA levels of proteins involved in VLDL structure (*Apob, Apoe*) did not change in WT mice livers after NAFLD-HCC induction treatment *(Figure E20.C)*. It is reported that overexpression of *Lpl*, pivotal enzyme in catabolism of circulating TG, promotes liver lipid accumulation and diabetes (Kim, Fillmore et al. 2001) and is related to HCC (Cao, Song et al. 2017). Analysis of mRNA levels showed that DEN HFD treatment induced a great increase in liver *Lpl* expression of WT mice *(Figure E20.C)*. This effect could be linked to the enhanced lipid storage in HCC *(see Results section 1.3.2)*. Absence in *E2f2* protected mice from the increased mRNA levels of *Lpl* mediated by the HCC-induction treatment *(Figure E20.C)*.

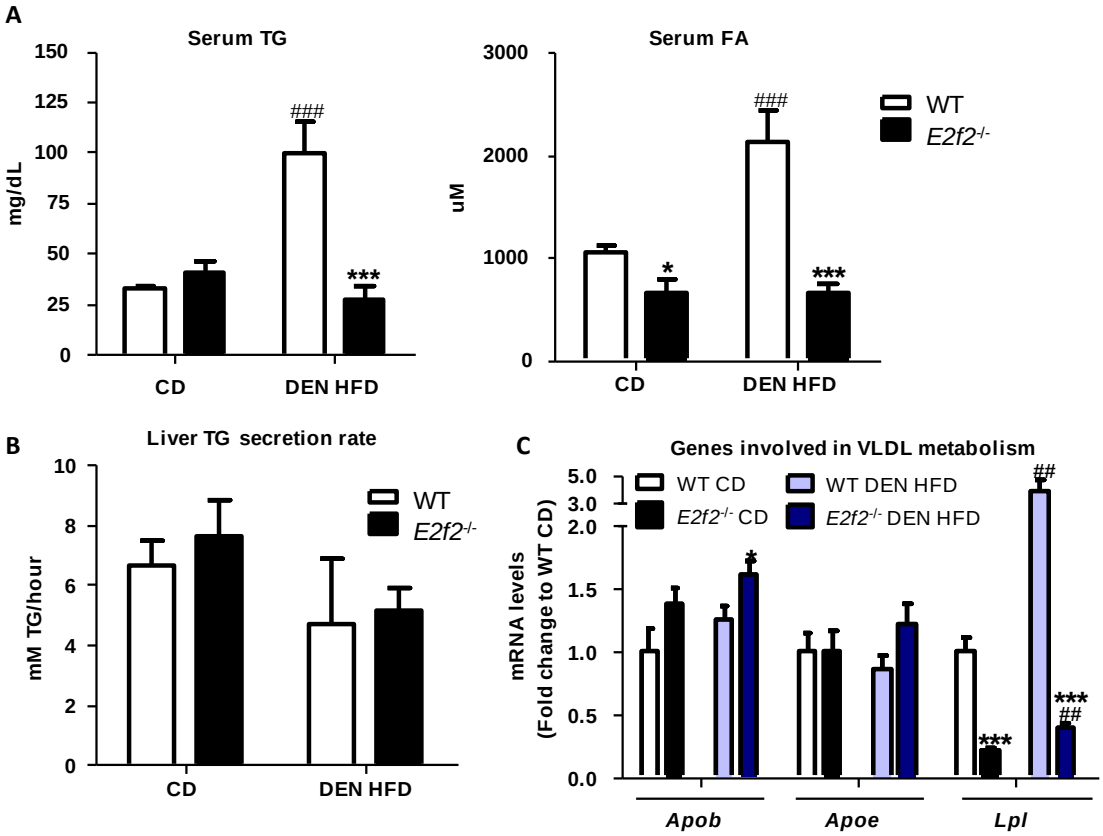

Figure E20. The lack of *E2f2* prevents the dyslipidemia mediated by NAFLD-HCC induction treatment in 9 month-old mice. *E2f2* knockout (*E2f2*$^{-/-}$) and their control (WT) mice were injected the procarcinogenic compound diethylnitrosamine (DEN) (25 mg/kg of mice) or vehicle when they were 14 days old. After weaning, mice were kept on a high-fat diet (HFD) or a chow diet (CD) until they were sacrificed at 9 months old. Livers and serum were collected. (A) Circulating triglycerides (TG) and fatty acids (FA) were measured in serum obtained from mice in fed state as indicated in Materials and Methods (n=8 per condition). (B) Liver TG secretion, indicative of hepatic very-low density lipoproteins (VLDL) secretion, was calculated from the difference in serum of TG levels over the 6 hours following VLDL metabolism inhibition with P-407 (1 g/kg of mice) (n=4-5 per group). (C) Hepatic mRNA levels of genes involved in VLDL metabolism were determined by rt-qPCR (n=7-8 per condition). Values are means ± SEM and statistical analysis was assessed by Student's two-tailed t-test. Significant differences between *E2f2*$^{-/-}$ and WT mice are indicated as *p <0.05, **p <0.01 and ***p <0.001 and differences between DEN HFD and CD are denoted by $^{\#}$p <0.05, $^{\#\#}$p <0.01 and $^{\#\#\#}$p <0.001.

Altogether, these findings suggest that VLDL export is not the main route leading to the dyslipidemia in the obesity-linked HCC development. In addition, *E2f2* deficiency in mice improves the circulating lipid profile.

3.1.4. Lack of *E2f2* in mice reduces TG biosynthesis contributing to the decreased lipid storage

Microarray analysis revealed that genes related to lipid synthesis were the most significantly downregulated ones in livers of 9 month-old *E2f2*$^{-/-}$ mice exposed to NAFLD-HCC induction treatment *(see Results section 3.1.1)*. Thus, we determined the flux of TG biosynthesis by assessing the esterification of [^{14}C]-glycerol and FA into TG.

The results showed that the [^{14}C]-glycerol incorporated into TG was lower in *E2f2*$^{-/-}$ mice exposed to DEN HFD treatment when compared to their WT littermates *(Figure E25.A)*, indicating that the overall TG synthesis was decreased in *E2f2* depleted mice livers. Concomitantly, protein expression of the lipogenesis mediator PPAR-γ (Pettinelli, Videla 2511) was diminished in *E2f2* deficient mice exposed to HCC induction treatment when compared to their WT counterparts *(Figure E25.B)*.

In WT mice, NAFLD-HCC inductor treatment increased the mRNA levels of *Pparg*, as well as the expression of its target genes involved in lipid synthesis (*Scd2*), storage (*Cidea*) and uptake (*Cd36*) *(Figure E21.C)*. The reduced flux of TG synthesis in *E2f2* deficient mice was accompanied by decreased mRNA levels of *Pparg* and its target genes (*Scd1, Scd2, Cidea, Cd36*) *(Figure E21.C)*.

Surprisingly, DNL was not increased in WT mice who developed NAFLD-HCC, as demonstrated by the mRNA levels of key genes related to DNL of FA (*Acaca, Fasn*) and some supplier of the reducing power required for lipogenesis (*Me2, Me3*) *(Figure E21.D)*. Absence in *E2f2* neither altered liver DNL in 9 month-old mice exposed to the NAFLD-HCC inductor treatment, since no major changes were observed in the gene expression of *Acaca* and *Fasn* *(Figure E21.D)*.

Altogether, NAFLD-HCC development is associated with an increased synthesis of TG that is not a consequence of enhanced DNL. Besides, these experiments confirmed that *E2f2* absence in mice reduces the biosynthesis of TG, which could contribute to the protection against obesity-related HCC development in 9 month-old *E2f2*$^{-/-}$ mice exposed to DEN HFD treatment.

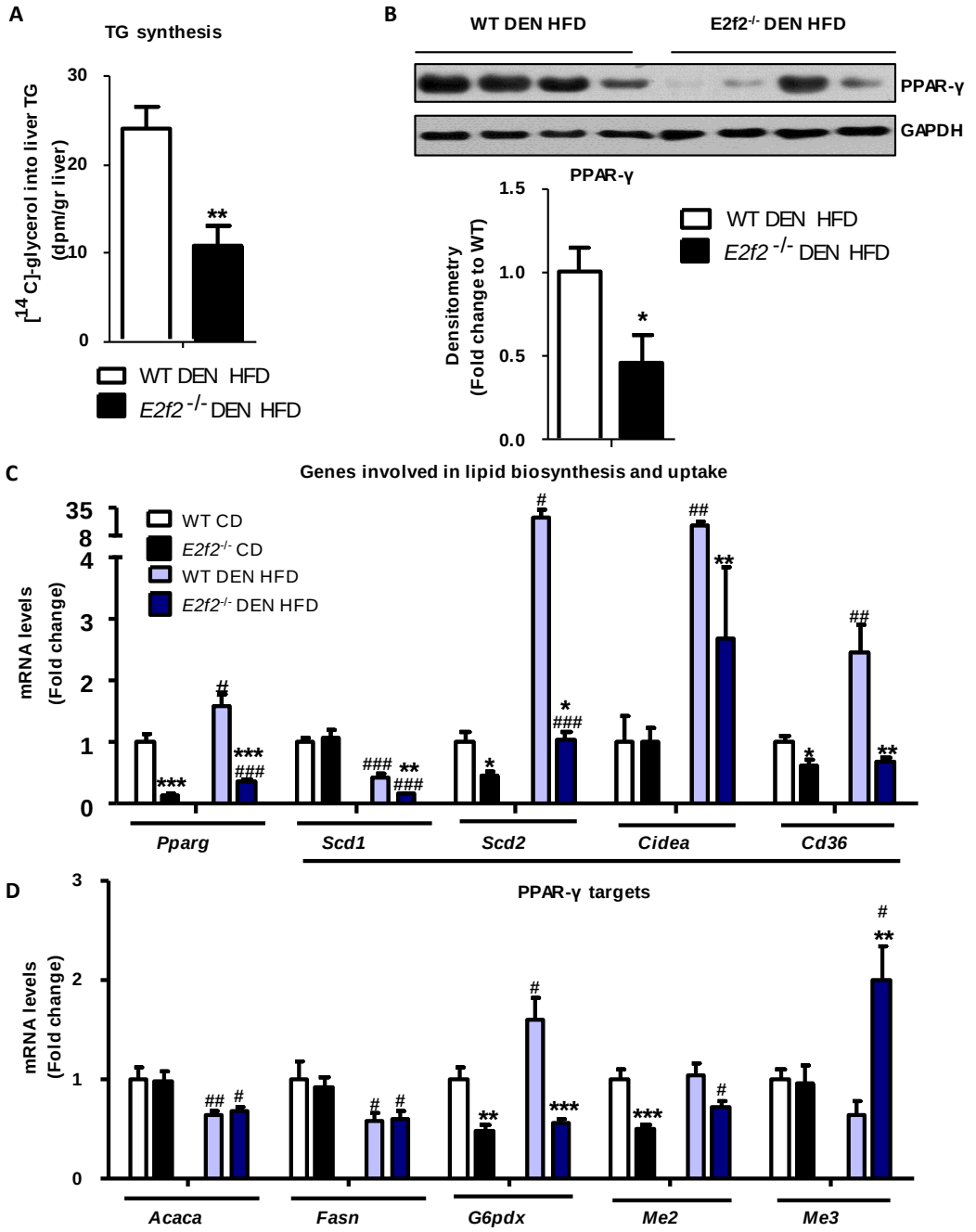

Figure E21. Liver synthesis of TG is decreased in 9 month-old *E2f2*$^{-/-}$ mice. *E2f2* knockout (*E2f2*$^{-/-}$) and their control (WT) mice were injected the procarcinogenic compound diethylnitrosamine (DEN) (25 mg/kg of mice) or vehicle when they were 14 days old. After weaning, mice were kept on a high-fat diet (HFD) or a chow diet (CD) until they were sacrificed at 9 months old and livers were collected. (A) Biosynthesis of liver triglyceride (TG) was measured by the amount of [^{14}C]-glycerol incorporated *in vivo* into TG (n=4 per condition). (B) Peroxisome proliferator-activated receptor gamma (PPAR-γ) liver content was assessed by immunoblotting using glyceraldehyde-3-phosphate dehydrogenase (GAPDH) as loading control (n=8). Representative immunoblots are shown. (C) Hepatic mRNA levels of genes involved in lipid synthesis and (D) *de* novo lipogenesis were determined by rt-qPCR (n=7-8 per condition). Values are means ± SEM and statistical analysis was determined by Student's two-tailed t-test. Significant differences between *E2f2*$^{-/-}$ and WT mice are indicated as *p <0.05, **p <0.01 and ***p <0.001 and differences between DEN HFD and CD are denoted by $^{\#}$p <0.05, $^{\#\#}$p <0.01 and $^{\#\#\#}$p <0.001.

3.1.5. *E2F2* deficiency in human hepatoma cells increases fatty acid oxidation and reduces TG synthesis

Previous findings showed that *E2F2* knock-down also resulted in a reduction of the lipid storage in human tumoral cells *(see Results section 1.3.2.3)*. Thereupon, the major metabolic pathways involved in cellular lipid catabolism and anabolism were assessed in *E2F2*-silenced HepG2 cell line.

[^{14}C]-ASM and [^{14}C]-CO_2 amount demonstrated that both complete and incomplete FAO increased when *E2F2* was knocked down in cells as compared to controls *(Figure E22.A)*.

Next, we wondered if the reduced TG content in absence of *E2F2* was also due to a decreased TG anabolism. The results showed that TG synthesis from [^{3}H]-oleate decreased in *E2F2*-silenced cells *(Figure E22.B)*. Since the metabolic precursor of FA is acetate, we assessed DNL by measuring the [^{3}H]-acetate incorporation into TG. *De novo* synthesis of TG was also reduced when *E2F2* was knocked down in HepG2 cells *(Figure E22.A)*. Overall, *E2F2* is involved in the TG metabolism in human cancer cells. These results were consistent with those found in our mice models of study.

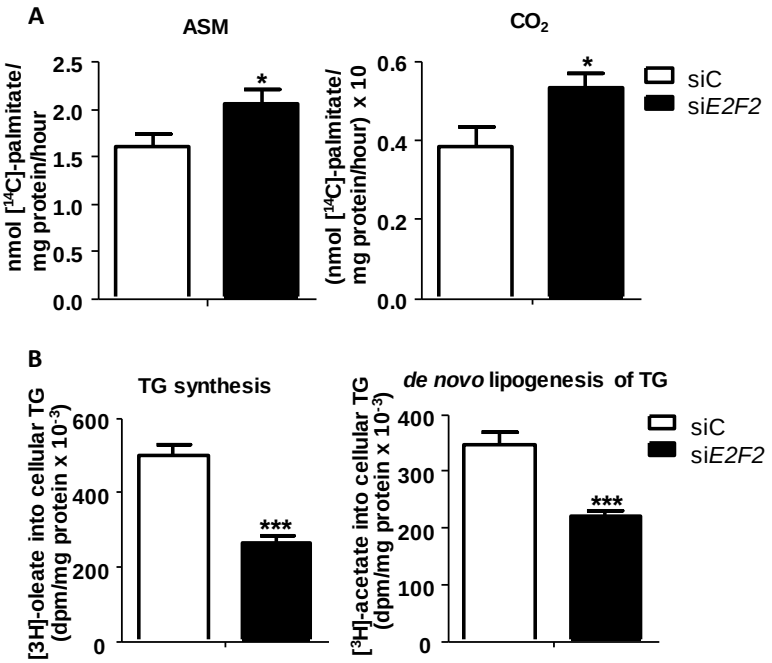

Figure E22. *E2F2* knock-down regulates lipid oxidation and synthesis in human hepatoma cells. *E2F2* transcription factor was silenced in HepG2 cell line by reverse transcription of specific siRNAs (si*E2F2*). Controls treated with a negative control siRNA (siC) were included in each assay. (A) Lipid oxidation rate was determined in the presence of 1mM oleate by measuring the amount of [^{14}C]-CO_2 (complete oxidation of [^{14}C]-palmitate) and [^{14}C]-labeled acid-soluble metabolites (ASM) (incomplete oxidation of [^{14}C]-palmitate) (n=4-5 plates per condition). (B) TG synthesis and *de novo* lipogenesis of TG was quantified by the amount of [^{3}H]-oleate or [^{3}H]-acetate incorporated into cellular TG (2 independent experiments each one with n=4-6 plates per group). Values are means ± SEM. Statistical analysis was determined by Student's two-tailed t-test. Significant differences between si*E2F2* and siC are indicated as *p <0.05, **p <0.01 and ***p <0.001.

3.2. E2f2 controls the metabolic pathways involved in lipid storage from the early stages of liver disease

We have already demonstrated that the absence in E2f2 protects mice from the obesity-linked HCC development and the associated liver lipid accumulation due to an increased FAO and decreased lipogenesis *(see Results section 3.1.2 and 3.1.4)*. These results were also validated in human hepatocellular carcinoma cells *(see Results section 3.1.5)*. Moreover, *E2f2* deficiency in mice also confers resistance to the hepatosteatosis at 3 months old *(see Results section 2.3.1)*. Then, we proposed that E2f2 could also regulate the lipid metabolism from the beginning of the disease. For that, metabolic fluxes involved in liver lipid input and output were analyzed in 3 month-old *E2f2*$^{-/-}$ and WT mice exposed to NAFLD induction treatment.

3.2.1. Liver lipid oxidation is stimulated in *E2f2* deficient mice

Firstly, liver lipid oxidation rate was determined. Like it was observed at 9 month-old, lipid oxidation rate was not altered in WT animals who developed NAFLD-HCC as demonstrated by the amount of [^{14}C]-ASM and [^{14}C]-CO_2 (*Figure E23.A)*. By contrast, NAFLD-HCC induction treatment induced FAO in *E2f2* depleted mice (*Figure E23.A)*, a response that was not associated with changes in the mRNA levels of genes related to β-oxidation chain reactions *(Figure E23.B)*. [^{14}C]-CO_2 quantity indicated that absence in *E2f2* also increased complete lipid oxidation in control conditions *(Figure E23.B)*.

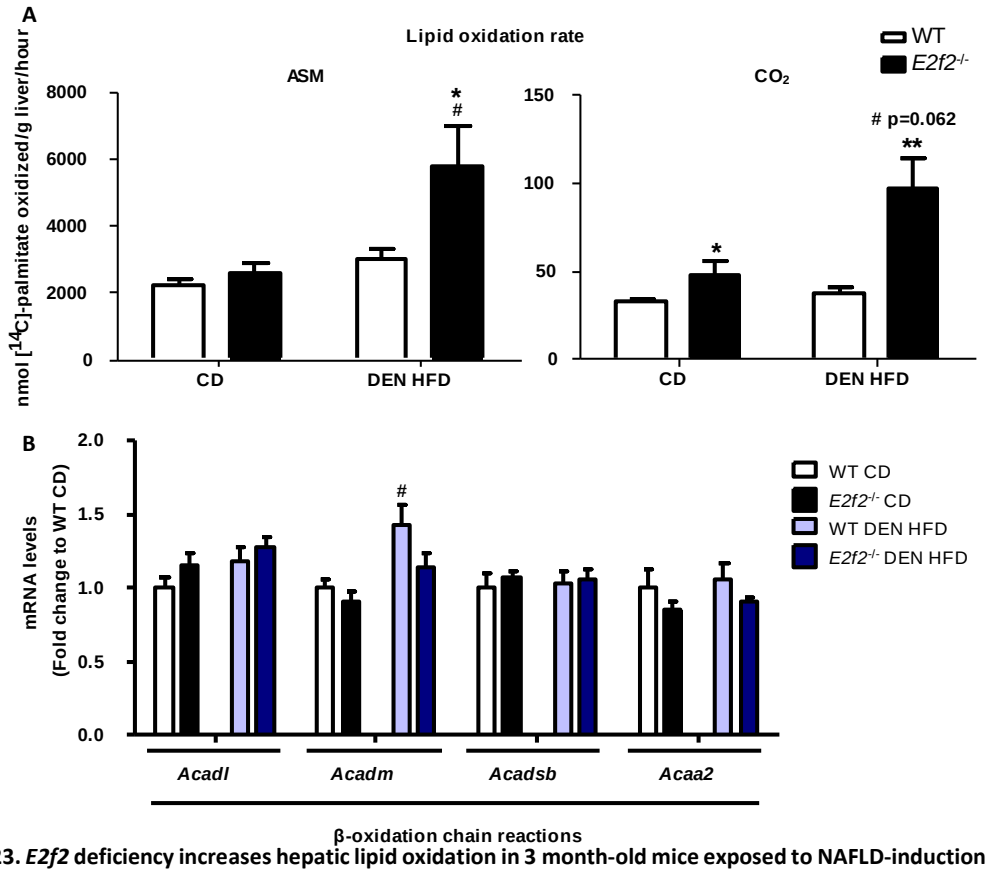

Figure E23. *E2f2* deficiency increases hepatic lipid oxidation in 3 month-old mice exposed to NAFLD-induction treatment. *E2f2* knockout (*E2f2*$^{-/-}$) and their control (WT) mice were injected the procarcinogenic compound diethylnitrosamine (DEN) (25 mg/kg of mice) or vehicle when they were 14 days old. After weaning, mice were kept on a high-fat diet (HFD) or a chow diet (CD) until they were sacrificed at 3 months old and livers were collected. (A) Lipid oxidation rate was determined in liver homogenates by measuring the amount of [^{14}C]-CO_2 (complete oxidation of [^{14}C]-palmitate) and [^{14}C]-labeled acid-soluble metabolites (ASM) (incomplete oxidation of [^{14}C]-palmitate) (n=3-4 per condition). (B) Hepatic mRNA levels of genes involved in β oxidation chain reactions were measured by rt-qPCR (n=7-8 per condition). Values are means ± SEM and statistical analysis was determined by Student's two-tailed t-test. Significant differences between *E2f2*$^{-/-}$ and WT mice are denoted as *p <0.05, **p <0.01 and ***p <0.001 and differences between DEN HFD and CD are determined by $^{\#}$p <0.05, $^{\#\#}$p <0.01 and $^{\#\#\#}$p <0.001. NAFLD, metabolic-dysfunction-associated fatty liver disease.

Consistent with the FAO rate in 3 month-old WT animals, no variations were observed in the gene expression of transcription factors that regulate lipid oxidation *(Figure E24.A)*. Linked with the increased FAO mediated by DEN HFD treatment, the expression of *Ppargc1b* and *Hnf4a* was increased in DEN HFD *E2f2*$^{-/-}$ mice livers as compared to their WT counterparts *(Figure E24.A)*, like it was shown in long-term DEN HFD. *Ppara* and *Rxra* were overexpressed in *E2f2*$^{-/-}$ mice in control conditions when compared to WT animals *(Figure E24.A)*, which could be related with the increased complete FAO.

The fact that liver lipid oxidation is increased in control conditions when *E2f2* is absent is also supported by the enhanced expression of certain genes involved in FA activation (*Acsm1*) and transport (*Cpt1, Cpt2*) in CD *E2f2*$^{-/-}$ mice *(Figure E24.B)*. Although FAO maintained unaltered in WT mice with NAFLD as compared to controls, DEN HFD treatment induced a mobilization of FA, as demonstrated by the increased the expression of *Acsm1, Acsm3, Cpt1* and *Cpt2 (Figure E24.B)*. Like it was observed at 9 months old, mRNA levels of *Acsl1* and *Cpt2* were elevated in 3 month-old *E2f2*$^{-/-}$ mice exposed to DEN HFD treatment *(Figure E24.B)*. Consistent with previous findings, NAFLD induction treatment also increased the expression of HNF4-α and CPT2 in *E2f2*$^{-/-}$ animals *(Figure E24.C)*.

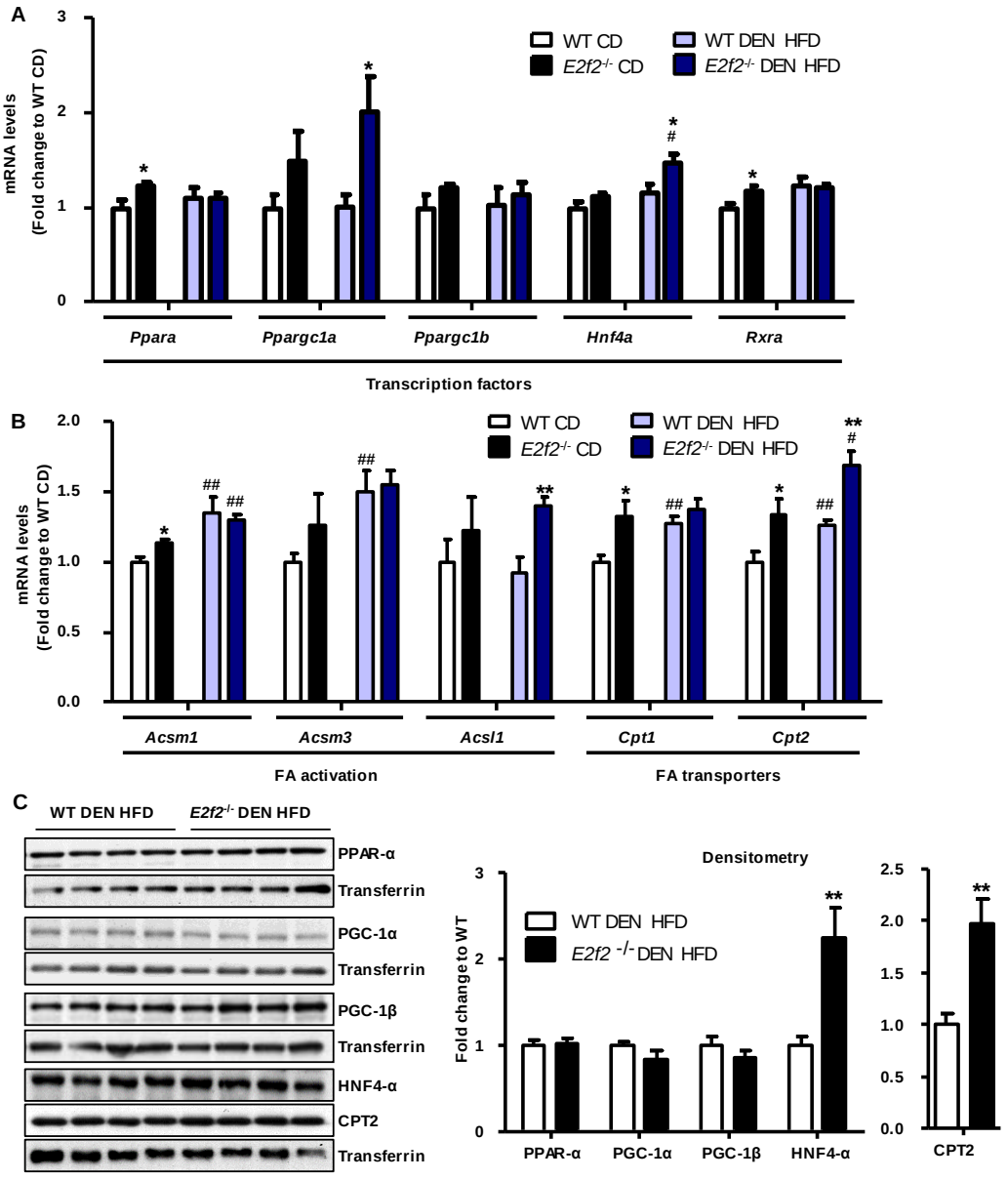

Figure E24. Liver expression of HNF4-α and CPT2 is enhanced in 3-month-old *E2f2*$^{-/-}$ mice exposed to DEN HFD. *E2f2* knockout (*E2f2*$^{-/-}$) and their control (WT) mice were injected the procarcinogenic compound diethylnitrosamine (DEN) (25 mg/kg of mice) or vehicle when they were 14 days old. After weaning, mice were kept on a high-fat diet (HFD) or a chow diet (CD) until they were sacrificed at 3 months old and livers were collected. Hepatic mRNA levels of (A) transcription factors and (B) genes involved in FA activation and transport were measured by rt-qPCR (n=7-8 per condition). (C) PPAR-α, PGC-1-α, PGC-1-β, HNF4-α and CPT2 proteins were assessed by immunoblotting in liver extracts (n=8 per condition). Transferrin was used as loading control. Representative immunoblots are shown. Values are means ± SEM and statistical analysis was determined by Student's two-tailed t-test. Significant differences between *E2f2*$^{-/-}$ and WT mice are denoted as *p <0.05, **p <0.01 and ***p <0.001 and differences between DEN HFD and CD are determined by $^{\#}$p <0.05, $^{\#\#}$p <0.01 and $^{\#\#\#}$p <0.001. CPT2, carnitine-O-palmitoyltransferase 2, FA, Fatty acid; HNF4-α, hepatocyte nuclear factor 4-alpha; PPAR-α, peroxisome proliferator-activated receptor alpha; PGC-1α, peroxisome proliferator-activated receptor gamma coactivator-1 alpha; PGC-1β, peroxisome proliferator-activated receptor gamma coactivator-1 beta.

Regarding the expression of genes who drive the oxphos, no differences were observed between WT and *E2f2*$^{-/-}$ mice exposed to DEN HFD treatment *(Figure E25)*.

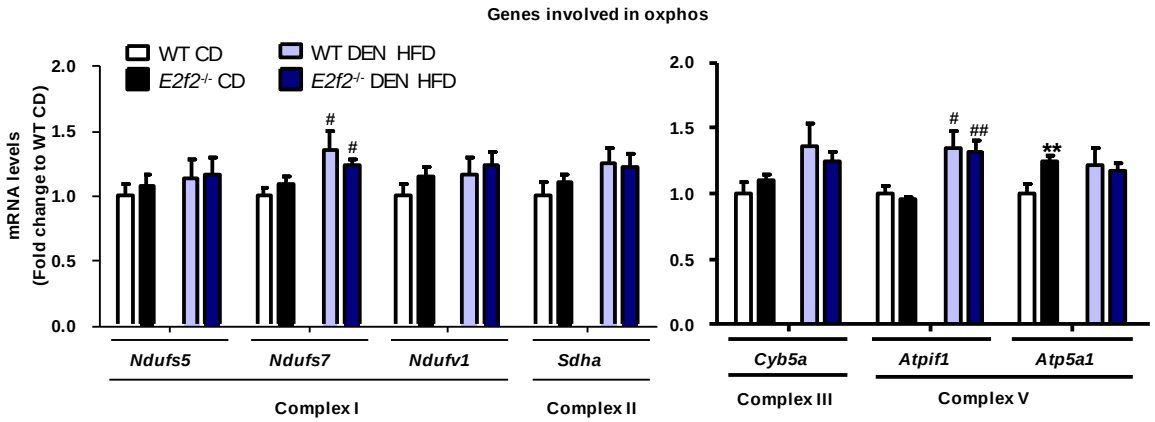

Figure E25. Expression of genes related to oxphos is not altered after exposition to NAFLD-induction treatment in *E2f2* depleted mice livers at 3 months old. *E2f2* knockout (*E2f2*$^{-/-}$) and their control (WT) mice were injected the procarcinogenic compound diethylnitrosamine (DEN) (25 mg/kg of mice) or vehicle when they were 14 days old. After weaning, mice were kept on a high-fat diet (HFD) or a chow diet (CD) until they were sacrificed at 3 months old and livers were collected. Hepatic mRNA levels of genes involved in oxphos were measured by rt-qPCR (n=7-8 per condition). Values are means ± SEM and statistical analysis was determined by Student's two-tailed t-test. Significant differences between *E2f2*$^{-/-}$ and WT mice are denoted as *p <0.05. NAFLD, non-alcoholic fatty liver disease.

All these results suggested that the absence in *E2f2* increases liver lipid oxidation through HNF4-α and CPT2 after exposition to DEN HFD, which could be associated with the resistance to develop hepatosteatosis.

3.2.2. Hypertriglyceridemia is prevented in *E2f2* knockout mice exposed to NAFLD-induction treatment

Like it was observed in 9 month-old mice *(see Results section 3.1.3)*, exposition to short-term DEN HFD treatment for 10 weeks also elevated circulating TG in WT animals when compared to controls *(Figure E26.A)*. On the contrary, serum FA concentration was not modified in WT mice who developed NAFLD *(Figure E26.A)*. Concerning *E2f2*$^{-/-}$ mice, circulating TG and FA concentration maintained lower than in their WT littermates after exposition to DEN HFD treatment *(Figure E26.A)*.

When VLDL catabolism in serum was inhibited by the administration of P-407 *in vivo*, a measure of the hepatic-TG secretion, DEN HFD treatment did not elevate serum TG levels in 3 month-old WT mice *(Figure E26.B)*, indicating that liver VLDL secretion was not the cause of the hypertriglyceridemia associated with hepatosteatosis. There were no differences in liver TG secretion rate of *E2f2*$^{-/-}$ mice *(Figure E26.B)*.

Accordingly, NAFLD-induction treatment did not alter the expression of genes related to VLDL metabolism (*Apob, Apoe, Lpl*) in WT or *E2f2*$^{-/-}$ animals *(Figure E26.C)*. Notably, decreased *Lpl* expression in *E2f2*$^{-/-}$ mice livers was observed in control conditions *(Figure E26.C)*.

Altogether, the results showed that the hypertriglyceridemia linked to NAFLD development is not due to an enhanced liver VLDL secretion, but it is prevented in absence of *E2f2*.

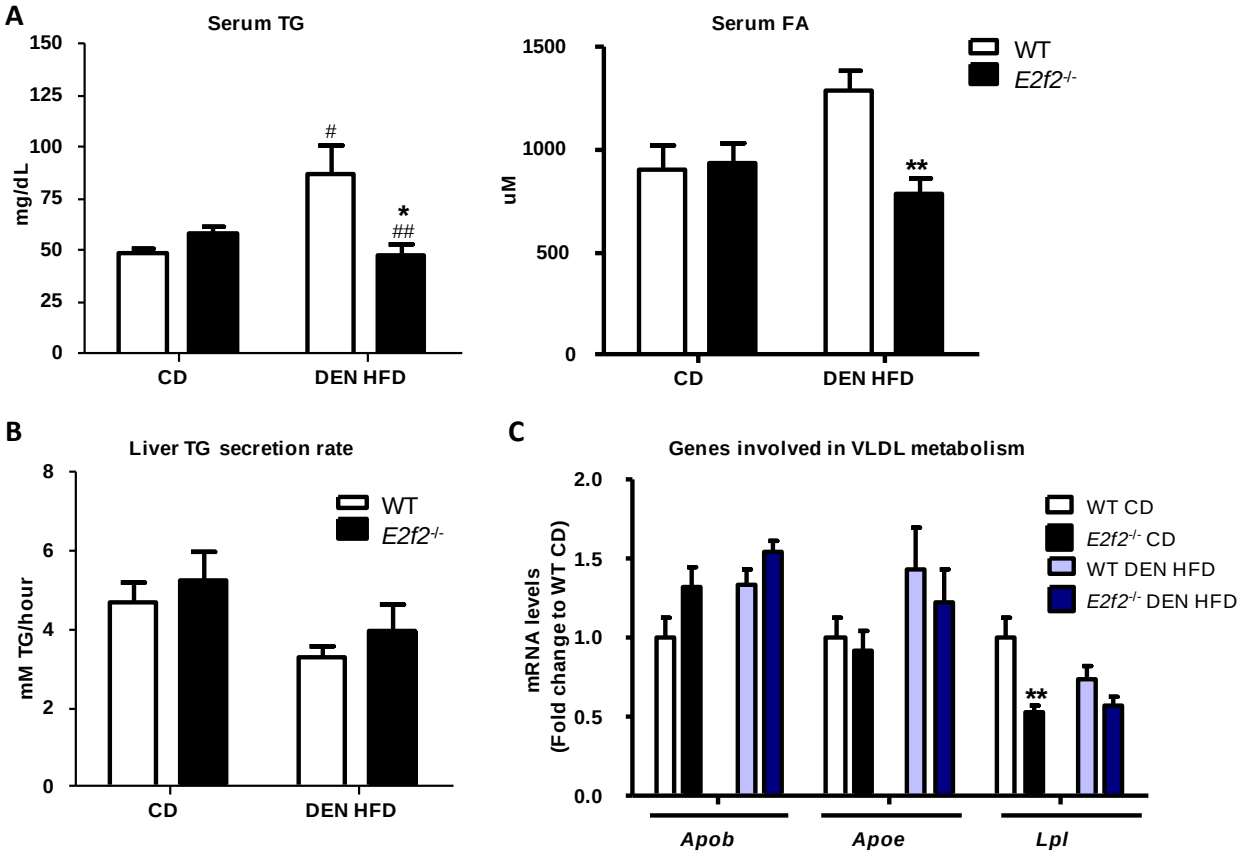

Figure E26. The absence in *E2f2* prevents the circulating TG increase associated to NAFLD-induction treatment. *E2f2* knockout (*E2f2*$^{-/-}$) and their control (WT) mice were injected the procarcinogenic compound diethylnitrosamine (DEN) (25 mg/kg of mice) or vehicle when they were 14 days old. After weaning, mice were kept on a high-fat diet (HFD) or a chow diet (CD) until they were sacrificed at 3 months old. Livers and serum were collected. (A) Circulating triglycerides (TG) and fatty acids (FA) were measured in serum obtained from mice in fed state as indicated in Materials and Methods (n=8 per condition). (B) Liver TG secretion, indicative of hepatic very-low density lipoproteins (VLDL) secretion, was calculated from the difference in serum of TG levels over the 6 hours following VLDL metabolism inhibition with P-407 (1 g/kg of mice) (n=4-5 per condition). (C) Hepatic mRNA levels of genes involved in VLDL metabolism were determined by rt-qPCR (n=7-8 per condition). Values are means ± SEM and statistical analysis was assessed by Student's two tailed t-test. Significant differences between *E2f2*$^{-/-}$ and WT mice are indicated as *p <0.05, **p <0.01 and ***p <0.001 and differences between DEN HFD and CD are denoted by $^{\#}$p <0.05, $^{\#\#}$p <0.01 and $^{\#\#\#}$p <0.001. NAFLD, non-alcoholic fatty liver disease.

3.2.3. E2f2 controls liver-lipid synthesis in obesity-related NAFLD

Regarding lipid input pathways in liver, [^{14}C]-glycerol incorporation into TG was decreased in 3 month-old *E2f2*$^{-/-}$ mice as compared to their WT littermates in control conditions *(Figure E27.A)*, suggesting that *E2f2* deficiency diminishes the synthesis of TG.

The results showed that the DEN HFD treatment induced the biosynthesis of TG in WT mice, which was prevented in *E2f2*$^{-/-}$ mice *(Figure E27.A)*. Concomitantly, PPAR-γ was overexpressed in WT mice who developed hepatosteatosis after exposition to DEN HFD treatment *(Figure E27.B)*, while maintained

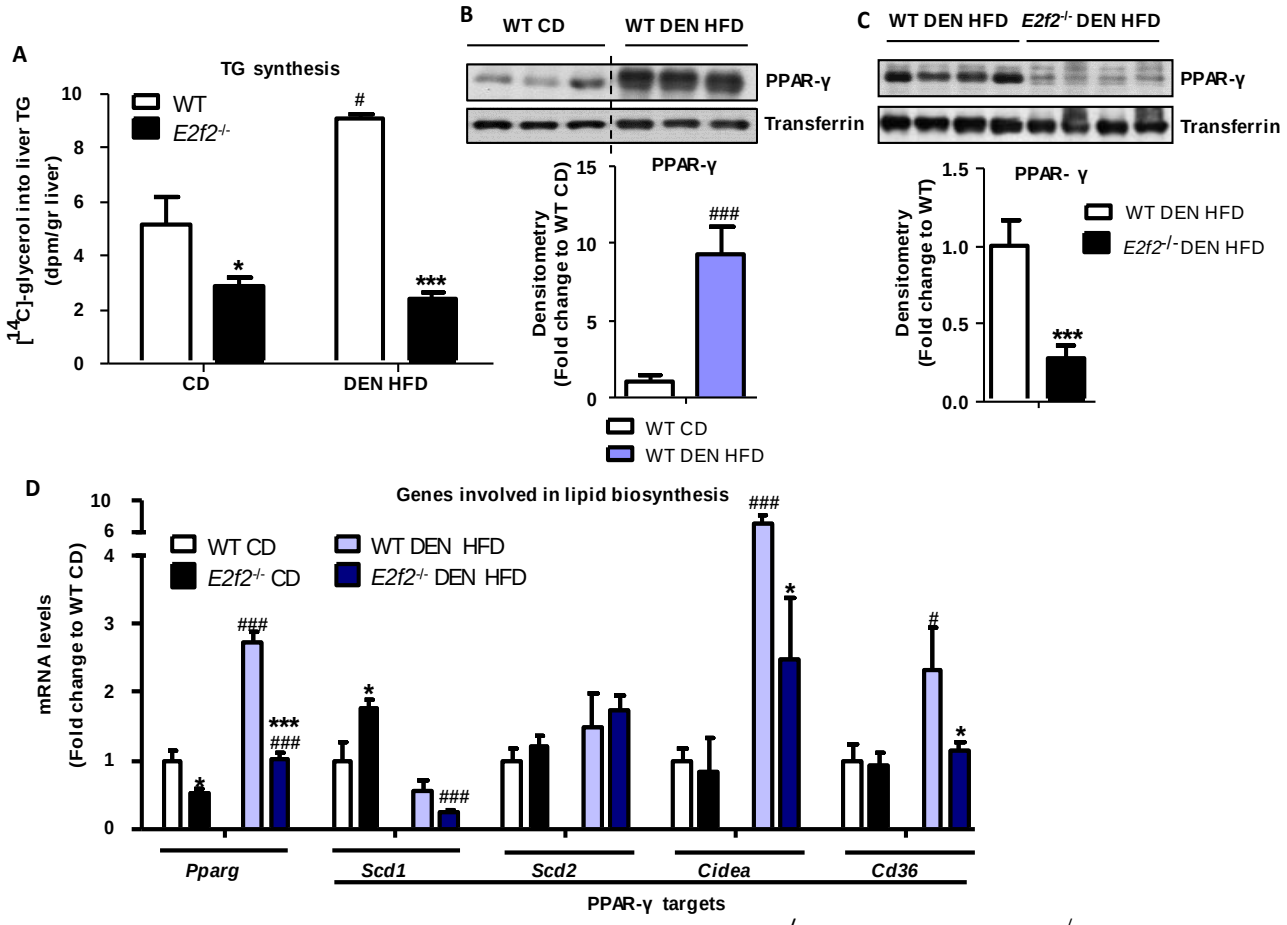

Figure E27. NAFLD-linked increase in liver TG biosynthesis is avoided in *E2f2*$^{-/-}$ mice. *E2f2* knockout (*E2f2*$^{-/-}$) and their control (WT) mice were injected the procarcinogenic compound diethylnitrosamine (DEN) (25 mg/kg of mice) or vehicle when they were 14 days old. After weaning, mice were kept on a high-fat diet (HFD) or a chow diet (CD) until they were sacrificed at 3 months old and livers were collected. (A) Biosynthesis of liver triglyceride (TG) was measured by the amount of [^{14}C] glycerol incorporated *in vivo* into TG (n=4 per condition). (B and C) Peroxisome proliferator-activated receptor gamma (PPAR-γ) liver content was assessed by immunoblotting using transferrin as loading control (n=8 per group). Representative immunoblots are shown. (D) Hepatic mRNA levels of genes involved in lipid synthesis were determined by rt-qPCR (n=8 per condition). Values are means ± SEM and statistical analysis was assessed by Student's two tailed t-test. Significant differences between *E2f2*$^{-/-}$ and WT mice are indicated as *p <0.05, **p <0.01 and ***p <0.001 and differences between DEN HFD and CD are denoted by $^{\#}$p <0.05, $^{\#\#}$p <0.01 and $^{\#\#\#}$p <0.001. NAFLD, non-alcoholic fatty liver disease.

decreased in *E2f2* depleted mice *(Figure E27.C)*. Expression of *Pparg* and its target genes involved in lipid store (*Cidea*) and transport (*Cd36*) was also enhanced in WT mice exposed to the NAFLD-induction treatment *(Figure E27.D)*. Consistent with the protein expression, *Pparg* was downregulated in *E2f2*$^{-/-}$ mice treated with DEN HFD, as well as *Scd1*, *Cidea* and *Cd36* *(Figure E27.D)*.

Next, we wondered if the reduced TG synthesis in absence of *E2f2* was due to a decreased DNL of FA. The results showed that, after exposition to the short-term DEN HFD treatment, DNL was not altered in *E2f2*$^{-/-}$ mice than in their WT littermates *(Figure E28.A)*. G6PDH and ME activities, the major sources of the reducing power needed for hepatic DNL, were decreased in *E2f2*$^{-/-}$ mice administered the NAFLD-induction treatment *(Figure E28.B)*. Those alterations did not result in a reduced expression of genes related to DNL (*Acaca, Fasn, G6pdx, Me2, Me3*) in *E2f2*$^{-/-}$ animals as exposed to DEN HFD as compared to their WT

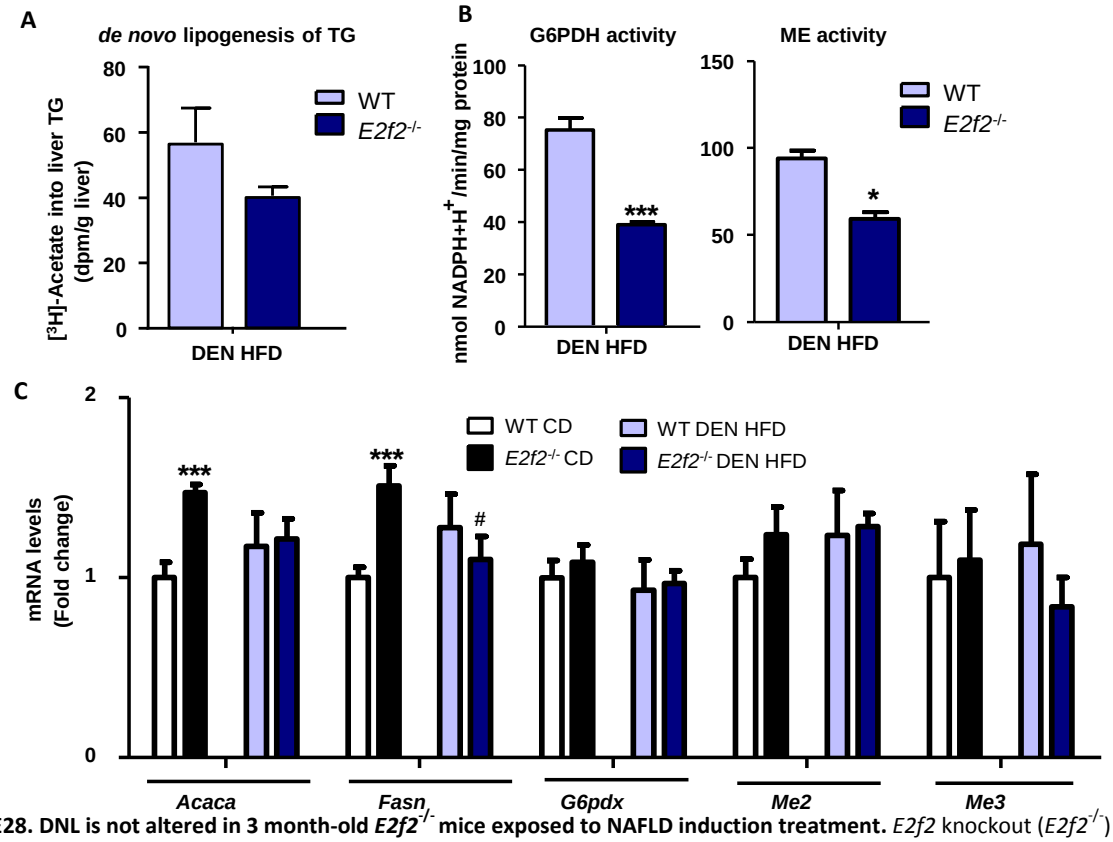

Figure E28. DNL is not altered in 3 month-old *E2f2*$^{-/-}$ mice exposed to NAFLD induction treatment. *E2f2* knockout (*E2f2*$^{-/-}$) and their control (WT) mice were injected the procarcinogenic compound diethylnitrosamine (DEN) (25 mg/kg of mice) or vehicle when they were 14 days old. After weaning, mice were kept on a high-fat diet (HFD) or a chow diet (CD) until they were sacrificed at 3 months old and livers were collected. (A) DNL of triglyceride (TG) was quantified by the amount of [^{3}H]-acetate incorporated into TG in freshly dissected liver slices (n=3-10 per condition). (B) Glucose-6-phosphate dehydrogenase (G6PD) and (C) malic enzyme (ME) activities were determined by spectrophotometry in liver homogenates (n=4 per group). (D) Hepatic mRNA levels of genes involved in *de novo* lipogenesis were determined by rt-qPCR (n=8 per condition). Values are means ± SEM and statistical analysis was assessed by Student's two tailed t-test. Significant differences between *E2f2*$^{-/-}$ and WT mice are indicated as *p <0.05, **p <0.01 and ***p <0.001 and differences between DEN HFD and CD are denoted by $^{\#}$p <0.05, $^{\#\#}$p <0.01 and $^{\#\#\#}$p <0.001. DNL, *de novo* lipogenesis; NAFLD, non-alcoholic fatty liver disease.

counterparts *(Figure E28.C)*. Notably, *Acaca* and *Fasn* expression were induced in *E2f2* deficiency in control conditions *(Figure E28.C)*.

Altogether, these data indicated that the decreased liver TG synthesis in *E2f2* deficient mice is mainly associated with the impaired esterification of TG rather than DNL, which results in a diminished TG storage. In proesteatotic conditions, the reduction of DNL is also involved in the prevention of NAFLD in absence of *E2f2*.

3.2.4. Decreased liver TG storage in *E2f2* knockout mice is not linked with diminished lipolysis of white adipose tissue

During a negative energy balance, WAT lipolysis is enhanced, so the TG stored in WAT is mobilized in order to provide energy to non-adipose tissues, including the liver. For that, TG is hydrolyzed and the released free FAs and glycerol are liberated into the circulation. Excessive circulating free FAs are involved in obesity-related NAFLD, since they can accumulate in the liver as TG and result in hepatic steatosis (Saponaro, Gaggini et al. 2015, Jung, Choi 2014).

Previous findings showed that WAT index was lower in 3 month-old *E2f2* deficient mice after NAFLD induction treatment than in WT animals *(see Results section 2.2, Table E3)*. Hence, we reasoned that WAT lipolysis could be enhanced in *E2f2*$^{-/-}$ mice exposed to DEN HFD. To prove this, the capability of WAT to hydrolyze TG was measured *ex vivo* in mice in basal and stimulated conditions, which resemble the fed and fasted state respectively.

In terms of released FA and glycerol levels, DEN HFD administration increased basal and, mainly, stimulated lipolysis in 3 month-old *E2f2*$^{-/-}$ mice when compared to their WT littermates *(Figure E29.A)*. However, gene expression analysis of key liver lipases (*Aadac, Lipc*) and FA transporters (*Slc27a1, Slc27a5*) did not show differences between both strains after exposition to DEN HFD treatment *(Figure E29.B)*.

Collectively, these results indicated that, although *E2f2* deficiency protected mice from the hepatic steatosis caused by DEN HFD at 3 months old, liver FA input is increased in *E2f2*$^{-/-}$ mice due to an enhanced lipolysis of WAT.

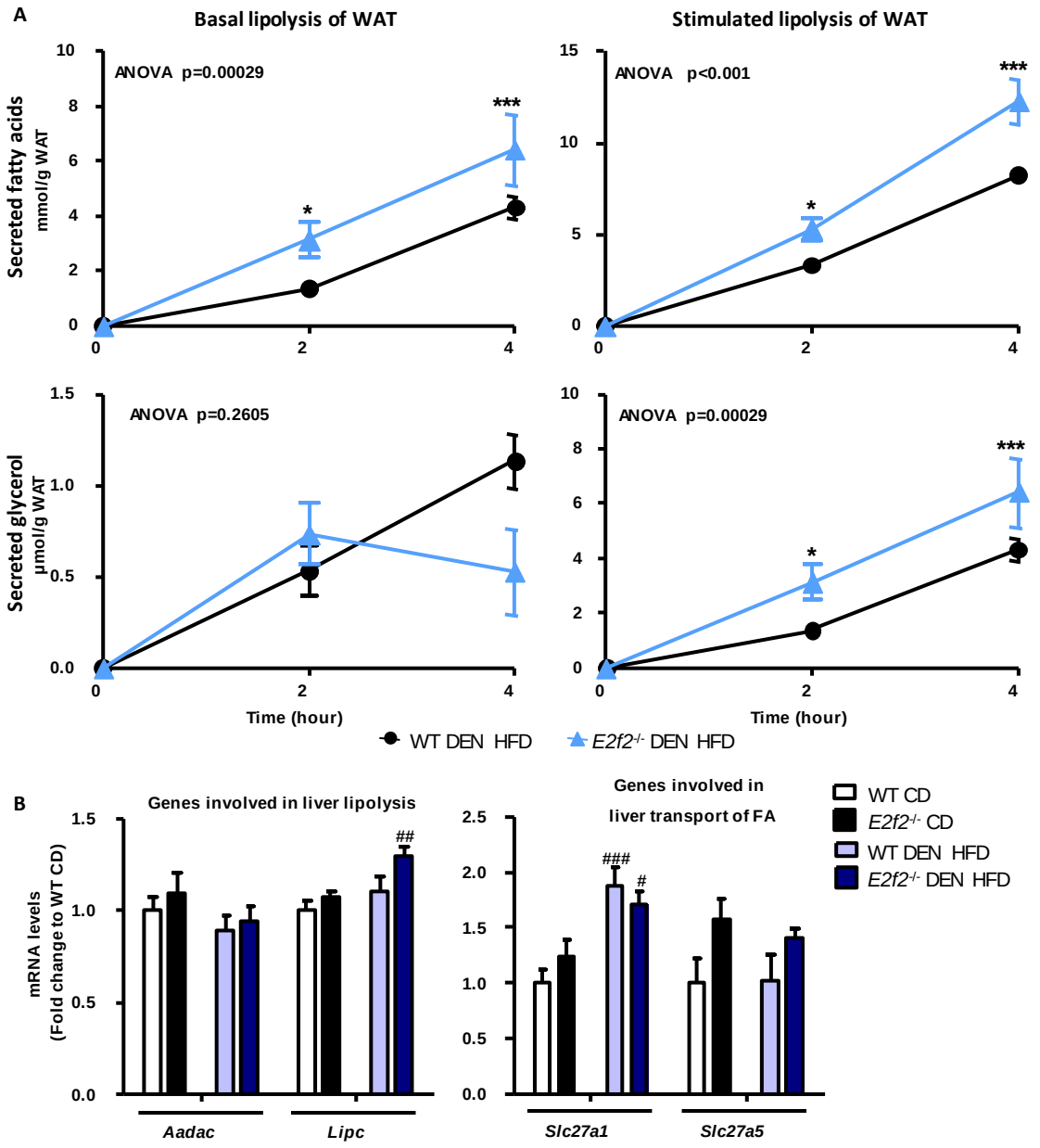

Figure E29. Depletion of *E2f2* enhances WAT lipolysis in mice exposed to NAFLD induction treatment. *E2f2* knockout (*E2f2*$^{-/-}$) and their control (WT) mice were injected the procarcinogenic compound diethylnitrosamine (DEN) (25 mg/kg of mice) or vehicle when they were 14 days old. After weaning, mice were kept on a high-fat diet (HFD) or a chow diet (CD) until they were sacrificed at 3 months old- Livers and white adipose tissues (WAT) were collected. (A) Basal and stimulated lipolysis of WAT was assessed in freshly isolated WAT by measuring the released fatty acids (FA) and glycerol to the media (n= 5 per condition). (B) Hepatic mRNA levels of genes involved in lipolysis and serum FA input were measured by rt-qPCR (n=7-8 per condition). Values are means ± SEM. Two-way ANOVA was performed to evaluate differences in FA and glycerol content and significance was determined by Bonferroni post-test. Student's two-tailed t-test was used to analyze differences in mRNA expression analysis. Significant differences between *E2f2*$^{-/-}$ and WT mice are indicated as *p <0.05, **p <0.01 and ***p <0.001 and differences between DEN HFD and CD are denoted by $^{\#}$p <0.05, $^{\#\#}$p <0.01 and $^{\#\#\#}$p <0.001. NAFLD, non-alcoholic fatty liver disease.

4. Involvement of E2f1 and E2f2 in the insulin resistance linked to NAFLD and NAFLD-HCC-induction treatments

As stated above, the metabolic complications of obesity and NAFLD include type II diabetes mellitus (T2DM), a condition that results from insulin resistance (IR) (Jung, Choi 2014). Raff *et al*. reported that T2MD increases the risk for HCC development in NAFLD patients (Raff, Kakati et al. 2015). In addition, it is already described that E2f1 maintains glucose homeostasis by regulation of the glucose-induced insulin secretion(Annicotte, Blanchet et al. 2009) and hepatic gluconeogenesis, which results in the prevention of the development of diabetes (Giralt, Denechaud et al. 2018). Thus, we wondered if the early stages of NAFLD and its progression to HCC would lead to IR and if E2f1 and/or E2f2 could be involved on it. To this end, IR was determined by glucose, insulin and pyruvate tolerance tests.

4.1. *E2f1* or *E2f2* depletion prevents the insulin resistance developed by exposition to short-term NAFLD-induction treatment

Serum glucose levels were higher in WT mice fed HFD for 10 weeks than in control animals when glucose *(Figure E30.A)* and insulin *(Figure E30.B)* tolerance tests were performed, but did not increase after pyruvate administration in fasting *(Figure E30.C)*. These results indicated that dietary obesity reduced the glucose and insulin sensitivity in mice without activating the gluconeogenesis.

By contrast, 3 month-old WT mice treated with DEN do not develop IR, as demonstrated by the unaltered glucose *(Figure E30.A)* and insulin *(Figure E30.B)* tolerance tests, as well as by the reduced glucose production from pyruvate in fasting *(Figure E30.C)*.

WT animals exposed to DEN HFD exhibited hyperglycemia during glucose tolerance test *(Figure E30.A)*, but did not show changes in the insulin tolerance test *(Figure E30.B)*, in which mice are treated with exogen insulin, showing that the IR presented is due to impairments in insulin secretion. Besides, *de novo* synthesis of glucose is activated in WT mice treated with DEN HFD after fasting *(Figure E30.C)*.

Collectively, these data suggested that HFD-induced obesity and NAFLD development are associated with IR in 3 month-old WT mice.

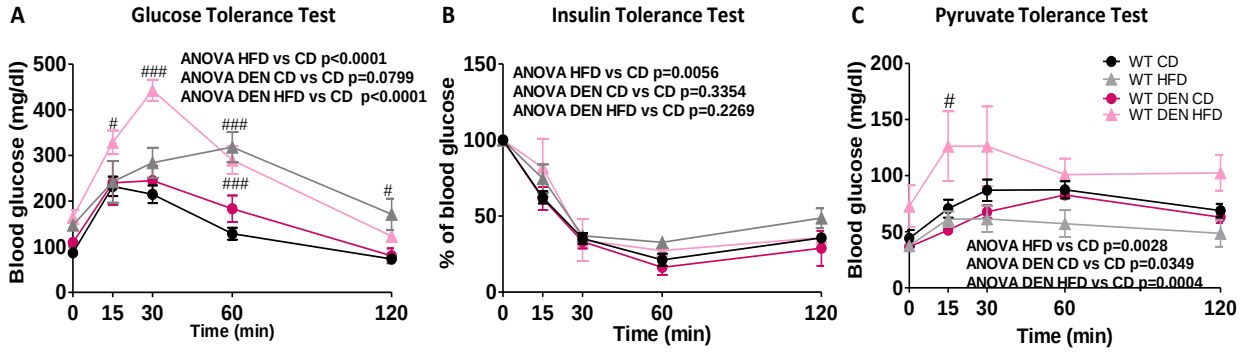

Figure E30. Obesity and NAFLD development are accompanied by IR in 3 month-old mice. Insulin resistance was evaluated by testing (A) glucose, (B) insulin and (C) pyruvate tolerance in 3-month-old wild type (WT) mice. Animals were injected the procarcinogenic compound diethylnitrosamine (DEN) (25 mg/kg of mice) or vehicle when they were 14 days old. After weaning, mice were kept on a high-fat diet (HFD) or a chow diet (CD) until the tests were done (n=8 for CD groups and n=4 for HFD, DEN CD and DEN HFD groups). Values are means ± SEM. Two-way ANOVA was performed to evaluate differences in serum glucose during tolerance tests and significance was determined by Bonferroni post-test. Significant differences between DEN CD or DEN HFD and CD are denoted by $^{\#}p < 0.05$, $^{\#\#}p < 0.01$ and $^{\#\#\#}p < 0.001$. IR, insulin resistance; NAFLD, non-alcoholic fatty liver disease.

Disrupted insulin secretion was evident in 3 month-old *E2f1*$^{-/-}$ mice, since they showed glucose intolerance and enhanced gluconeogenesis in comparison to their WT littermates in control conditions, with no alterations in the insulin tolerance *(Figure E31.A)*. *E2f2*$^{-/-}$ mice showed a slight improvement of the insulin sensitivity when compared to WT animals, which was not accompanied by changes in glucose or pyruvate tolerances *(Figure E31.A)*.

E2f1$^{-/-}$ mice treated with 10 weeks of HFD responded like WT animals to glucose and insulin tolerance tests *(Figure E31.B)*. Besides, they showed increased serum glucose concentration when pyruvate was administered after 13 hours of fasting *(Figure E31.B)*. These results indicate that the absence in *E2f1* does not protect mice from the IR caused by obesity. *E2f2*$^{-/-}$ mice presented better glucose tolerance and insulin sensitivity than their WT littermates, although serum glucose levels were elevated during the pyruvate tolerance test, which suggest that the lack of *E2f2* confers certain resistance to the obesity-related IR *(Figure E31.B)*.

Glucose tolerance improved in 3 month-old *E2f1*$^{-/-}$ and *E2f2*$^{-/-}$ mice treated with DEN HFD when compared to WT animals *(Figure E31.D)*. Moreover, *E2f1*$^{-/-}$ mice exhibited better insulin sensitivity during the corresponding tolerance test *(Figure E31.D)*. Exposition to DEN HFD treatment did not induced gluconeogenesis in *E2f1* or *E2f2* deficient mice *(Figure E31.D)*. In this context, *E2f1*$^{-/-}$ and *E2f2*$^{-/-}$ mice escaped from the IR linked to DEN HFD treatment.

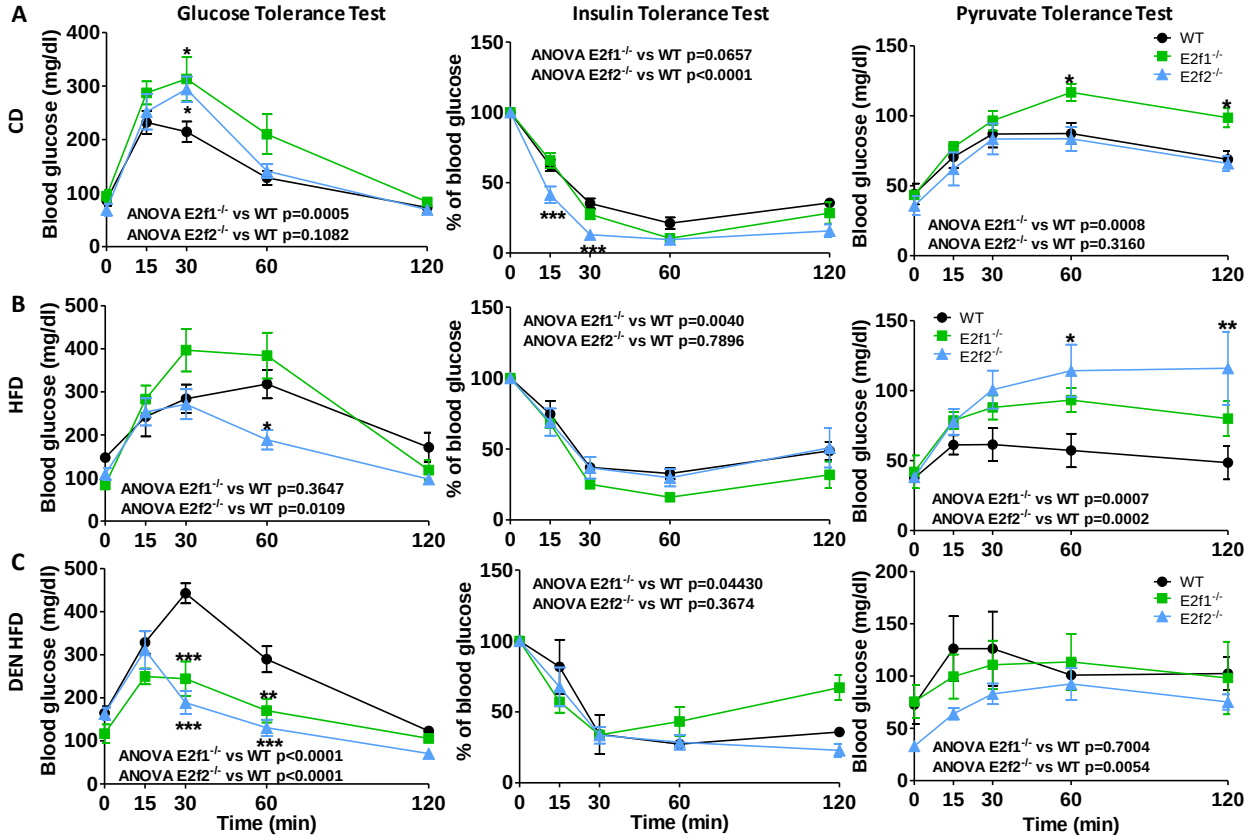

Figure E31. *E2f2* deficiency avoids better than *E2f1* deficiency the IR caused by NAFLD-induction treatment in 3 month-old mice. Insulin resistance was evaluated by testing glucose, insulin and pyruvate tolerance in 3-month-old wild type (WT), *E2f1* knockout (*E2f1*$^{-/-}$) and *E2f2* knockout (*E2f2*$^{-/-}$) mice with (A) CD treatment, as well as with (B) HFD treatment or (C) DEN HFD treatment. Animals were injected the procarcinogenic compound diethylnitrosamine (DEN) (25 mg/kg of mice) or vehicle when they were 14 days old. After weaning, mice were kept on a high-fat diet (HFD) or a chow diet (CD) until the tests were done (n=8 for CD groups and n=4 for HFD and DEN HFD groups). Values are means ± SEM. Two-way ANOVA was performed to evaluate differences in serum glucose during tolerance tests and significance was determined by Bonferroni post-test. Significant differences between *E2f1*$^{-/-}$ or *E2f2*$^{-/-}$ and WT mice are indicated as *p <0.05, **p <0.01 and ***p <0.001. IR, insulin resistance; NAFLD, non-alcoholic fatty liver disease.

Altogether, these results indicate that absence in *E2f2* protects mice better than the lack of *E2f1* against the IR provoked by a short-term HFD feeding regimen when combined or not with DEN.

4.2. Ablation of *E2f1* or *E2f2* in mice does not prevent the insulin resistance developed after long-term NAFLD-HCC induction treatments

Former results showed that IR was developed in WT obese mice with NAFLD exposed to a short-term HFD as well as DEN HFD, and that the absence in *E2f1* and *E2f2* avoided it *(see Results section 4.1)*. Thus, we wondered if IR was present in the latest stages of NAFLD and if the lack in *E2f1* or *E2f2* could prevent it.

NAFLD-HCC inducing treatments promoted IR, since blood glucose reached higher levels in 9 month-old WT mice administered HFD or DEN HFD during glucose *(Figure E32.A)* and insulin *(Figure E32.B)* tolerance tests as compared to control mice. DEN HFD treatment also activated the gluconeogenesis after 13 hours of fasting as demonstrated by the hyperglycemia in WT mice after the pyruvate tolerance test when compared to the control treatment *(Figure E32.C)*.

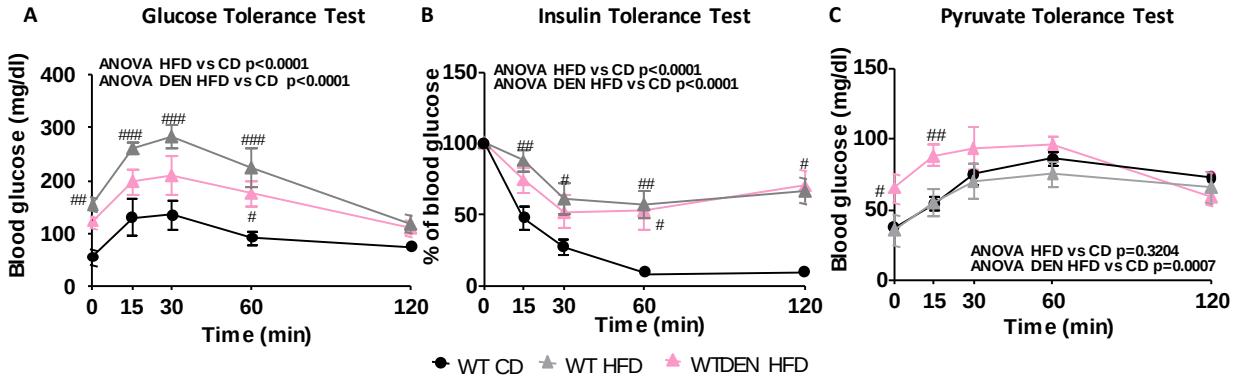

Figure E32. HCC development is associated with IR in obese 9 month-old WT mice. Insulin resistance was evaluated by testing (A) glucose, (B) insulin and (C) pyruvate tolerances in 9 month-old wild type (WT) mice. Animals were injected the procarcinogenic compound diethylnitrosamine (DEN) (25 mg/kg of mice) or vehicle when they were 14 days old. After weaning, mice were kept on a high-fat diet (HFD) or a chow diet (CD) until the tests were done at 9 months old (n=8 for CD group and n=4 for the rest of the groups). Values are means ± SEM. Two-way ANOVA was performed to analyze differences in serum glucose during tolerance tests and significance was determined by Bonferroni post-test. Significant differences between DEN CD or DEN HFD and CD are denoted by $^{\#}p < 0.05$, $^{\#\#}p < 0.01$ and $^{\#\#\#}p < 0.001$. HCC, hepatocarcinoma; IR, insulin resistance.

The combined treatment of DEN HFD caused a more aggravated hyperglycemia in *E2f1*$^{-/-}$ animals than in WT mice in glucose *(Figure E33.A)*, insulin *(Figure E33.B)* and pyruvate tolerance tests *(Figure E33.C)*. Besides, *E2f2*$^{-/-}$ animals showed the same IR level of WT mice after exposition to the combined treatment of DEN HFD *(Figure E33.A, B, C)*. Altogether, these results suggest that *E2f1* or *E2f2* deficiency in mice does not prevent the IR associated to NAFLD-HCC inductor treatment.

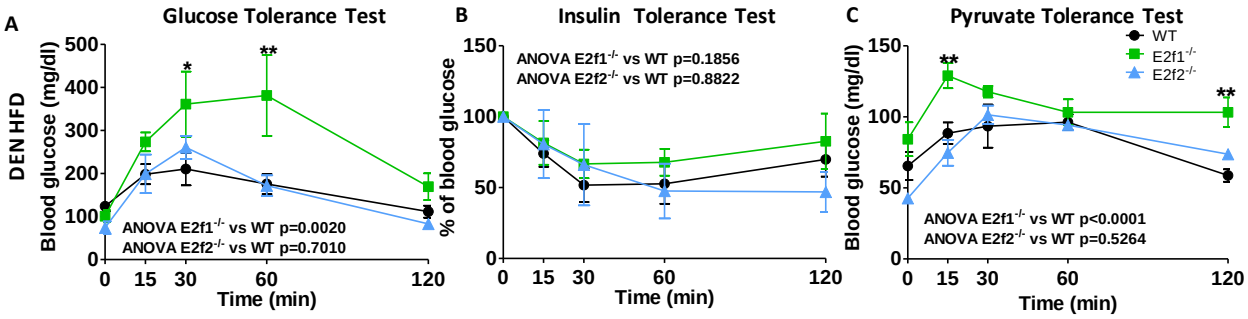

Figure E33. *E2f1* or *E2f2* deficiency does not protect against the IR induced by long-term DEN HFD treatment in 9 month-old mice. Insulin resistance was evaluated by testing (A) glucose, (B) insulin and (C) pyruvate tolerance in 3-month-old wild type (WT), *E2f1* knockout (*E2f1*$^{-/-}$) and *E2f2* knockout (*E2f2*$^{-/-}$) mice with DEN HFD treatment. Animals were injected the procarcinogenic compound diethylnitrosamine (DEN) (25 mg/kg of mice) when they were 14 days old. After weaning, mice were kept on a high-fat diet (HFD) until the tests were done (n=4 for DEN HFD group). Values are means ± SEM. Two-way ANOVA was performed to evaluate differences in serum glucose during tolerance tests and significance was determined by Bonferroni post-test. Significant differences between *E2f1*$^{-/-}$ or *E2f2*$^{-/-}$ and WT mice are indicated as *p <0.05, **p <0.01 and ***p <0.001. IR, insulin resistance.

Chapter E. DISCUSSION

Chapter E. DISCUSSION

E2F1 and E2F2 are transcriptions factors that belong to the E2F family. From the most classical definition, they are described as crucial regulators of the cell cycle and they act as tumor suppressors or proto-oncogenes in several types of cancer, including liver cancer (Chen, Tsai et al. 2009). Namely, E2F1 and E2F2 are upregulated in human HCC derived from several etiologies (Kent, Bae et al. 2017, Huang, Ning et al. 2019). Latest studies revealed that E2F1 and E2F2 transcription factors also modulate whole body metabolism and cell physiology (Denechaud, Lopez-Mejia et al. 2016), then, disorders in the E2F-Rb axis could lead to metabolic complications such as obesity and liver cancer.

Obesity is closely related to non-alcoholic fatty liver disease (NAFLD), the most prevalent chronic liver disease characterized by steatosis or excessive fat accumulation (Kumar, Priyadarshi et al. 2020, Alzahrani, Iseli et al. 2014). Since liver regulates organic glucose and lipid metabolism, a disproportionate lipid intake from diet overloads liver lipid sourcing pathways (Kawano, Cohen 2013). This situation cannot be balanced by elimination pathways and results in accumulation of lipids in liver and NAFLD. Obesity and NAFLD, major health problems worldwide, are considered predominant triggers of hepatocellular carcinoma (HCC) (Lauby-Secretan, Scoccianti et al. 2016, Bertot, Adams 2019). One of the main reasons for the increased carcinogenesis in obesity is the fact that metabolism is readapted in cancer cells for provision of new demands (energy, biomass) (Ward, Thompson 2012). Mainly, reprogramming of lipid metabolism acquires relevance in HCC when there is a lipid-rich setting like NAFLD (Beloribi-Djefaflia, Vasseur et al. 2016).

To date, therapeutical alternatives for NAFLD are based on diet and exercise, since there is no appropriate pharmacotherapy (Kumar, Priyadarshi et al. 2020). Due to the delayed diagnosis of HCC, curative therapies are not effective. Then, new treatments and novel diagnosis criteria are required for NAFLD-linked HCC. Targeting the metabolic rewiring could have promising role as disease management strategy. That is why, it is important to investigate if E2F1 and E2F2 are involved in the metabolic adaptation of NAFLD-HCC and if so, to consider them as potential biomarkers of the liver disease. In the first part of the study, we show that E2F1 and E2F2 transcription factors are required for obesity-related NAFLD and NAFLD-driven HCC. Then, we demonstrate that E2f2 coordinates the particular metabolic reprogramming of NAFLD-HCC even before cancer is developed.

1. E2F1 and E2F2 transcription factors drive obesity-related NAFLD and HCC development

Liver disease was previously induced in mice by exposition to different treatments, including administration of the procarcinogen diethylnitrosamine (DEN), feeding a high fat diet (HFD) or the combined exposition to DEN and HFD. Regarding the body weight and WAT index, HFD administration induced obesity in 3 month-old mice, a condition that was exacerbated when mice get older. Of note, body weight increase was not due to a higher consumption of food. Study of the lipid content revealed that this effect was accompanied by triglyceride (TG), diglyceride (DG) and cholesteryl ester (CE) accumulation in liver and, in fact, by NAFLD development. Although most of the mouse strains fail to develop advanced liver disease when placed only in HFD (Carlessi, Köhn-Gaone et al. 2019), exposition just to HFD also promoted the progression to NAFLD-HCC in our mice model of study. By contrary, the results showed that DEN-induced HCC is not linked to obesity or NAFLD development. Exposition only to HFD was the less carcinogenic treatment, nevertheless, feeding a lipid-rich diet exacerbates DEN-induced HCC concerning tumor quantity and size. In accordance with the histopathologic features, liver lipid accumulation in terms of TG and CE was evident in mice exposed to DEN HFD who developed NAFLD-HCC. The fact that mice treated with DEN HFD lost weight from the age of 6 months old onwards could be related with energy consumption needed for hepatocarcinogenesis development. Indeed, weight loss and cachexia are clinical symptom of HCC onset (Bialecki, Di Bisceglie 2005).

HCC pathogenesis is linked to an altered gene expression pattern, particularly in genes controlling the cell cycle (Li, Li et al. 2018). In case of E2F1 or E2F2 transcriptions factors, controversial roles have been described concerning HCC development. However, most of the evidences suggest that they act as oncogenes in the context of this type of liver cancer (Kent, Bae et al. 2017, He, Huang et al. 2020, Zhan, Huang et al. 2014, Hong, Eun et al. 2019). The results showed that liver E2f2 was only upregulated in mice with obesity-related NAFLD and NAFLD-HCC, indicating that E2f2 is induced since the early stages of the liver disease. This is in accordance with the enhanced expression of E2F1 and E2F2 in obese patients, even when they do not present NAFLD. Of note, E2F2 overexpression was more exacerbated once NAFLD was developed in obese patients. These patients should be classified as metabolically unhealthy obesity (MUO) cases, because they presented more than two criteria defining the metabolic dysregulation (Eslam,

Newsome et al. 2020), which would allow to differentiate MUO patients by E2F2 content. The fact that especially E2F2 could be associated with a metabolic dysregulation status could point out the value of E2F2 as predictor of the liver disease.

After determining that there is an involvement of E2F1 and E2F2 in obesity-related liver disease, given the effect of the metabolic status in E2F1 and E2F2 levels in liver of obese patients and mice, the role of E2F1 and E2F2 in the instauration and progression of NAFLD and NAFLD-HCC was investigated. As previously stated, steatosis or fat accumulation is the liver symptom of NAFLD (Kumar, Priyadarshi et al. 2020, Alzahrani, Iseli et al. 2014). The results indicate that *E2f1* and particularly *E2f2* deficiency protect mice from the hepatosteatosis associated to NAFLD and HCC, since total amounts of liver TG, DG and CE were not increased after exposition to the treatments. Similar metabolic profile was displayed in human HCC cell line when *E2F2* was silenced, but not in case of *E2F1* silencing.

Consistent with observations on liver lipid quantification and histology, gene expression analysis and Ki67 immunohistochemistry demonstrated that *E2f1* and *E2f2* deficient mice did not develop HCC in none of the conditions placed. We observed that cell cycle progression in obesity-driven HCC was promoted by increased *CycA2* and *Plk1* expression, biomarkers of human HBV-HCC or HCV-HCC (Bahnassy, Zekri et al. 2011, Petrelli, Perra et al. 2012), a condition prevented when *E2f1* or *E2f2* were absent. As expected, absence in *E2f1* or *E2f2* in mice also resulted in protection from hepatomegaly and liver injury, common characteristics of HCC (Bialecki, Di Bisceglie 2005).

Among its diverse functions, liver is responsible for the regulation of cholesterol metabolism (Arguello, Balboa et al. 2015). Under normal conditions, cholesterol homeostasis is carefully maintained, meanwhile, enhanced synthesis and accumulation is observed in NAFLD patients. One of the alternative metabolic pathway of free cholesterol (FC) is to form CE by esterification with a FA. The results showed that liver content in FC was not altered in obese mice with NAFLD, possibly because of the short-regimen of the diet, while it was markedly increased when the disease progressed to HCC. This profile was the same observed in liver CE content, suggesting that in NAFLD-HCC FC is deposited as CE and forms lipid droplets (LD). According to the fact that E2f1 regulates cholesterol (CHO) uptake from plasma and avoids its hepatic accumulation (Lai, Giralt et al. 2017), total amount of liver FC was not notably changed in *E2f1*$^{-/-}$ and *E2f2*$^{-/-}$ mice livers who escaped from obesity-related NAFLD development. Then, the reduction in CE content associated to the absence in *E2f1* or *E2f2* cannot be explained by alterations in FC levels. These results

indicate that the FA pool is not being derived to CE synthesis as an avoidance way of NAFLD development in *E2f1* or *E2f2* deficiency.

One of the most common histopathological features of human HCC are fibrosis and cirrhosis (Carlessi, Köhn-Gaone et al. 2019). Although fibrosis is not observed in HCC cases induced only by DEN (Carlessi, Köhn-Gaone et al. 2019), our mice model of NAFLD-linked HCC presented *Tfgb1*-mediated fibrosis. The fact that there is a causal relationship between obesity and fibrosis could explain that evidence (Chiang, Pritchard et al. 2011). Besides, it is already established the requirement of E2F1 in TGF-β signaling axis in human hepatoma cells and normal cells (Korah, Falah et al. 2012). We also observed that NAFLD-related tumor development was accompanied by inflammation, a condition that was evident since the onset of the liver disease. Instead of *Il6* and *Tnf*, in the obesity-related NAFLD-HCC, the central mediator of the inflammatory process was *Il1b*, which suggests that the oncogenic mechanism involved here is different to that described (Park, Lee et al. 2010). According to the prevention of progressive NAFLD, absence in *E2f1* or *E2f2* confers resistance to develop fibrosis or inflammation in mice liver.

As previously mentioned, a distinctive characteristic of HCC derived from NAFLD with respect to HCC cases from other etiologies is the fact that most of the patients also present type II diabetes mellitus (T2DM) (Dhamija, Paul et al. 2019), a circumstance evolved from insulin resistance (IR). Besides, T2DM is associated with comorbidities of the liver disease like obesity and NAFLD (Jung, Choi 2014). The corresponding tolerance tests revealed that IR was a sole domain of diet-induced obesity, as it was only presented in mice who developed liver disease by HFD regimen. The fact that 3 month-old mice exposed to DEN HFD showed glucose intolerance but responded correctly to exogenous insulin ascertains that insulin sensitivity is adequate but the secretion process is impaired in obese mice with NAFLD.

Although gluconeogenesis seems to be downregulated in HCC (Grasmann, Smolle et al. 2019), pyruvate tolerance experiments suggest that *de novo* glucose production in liver is enhanced by DEN administration in obese mice at 3 months old. Gluconeogenesis is suppressed in a postprandial state by insulin (Dong, Park et al. 2006). However, in a situation in which insulin signaling fails, like it is observed in mice with NAFLD, the following two events can occur at the same time: serum hyperglycemia and glucose deprivation in cells (Dong, Park et al. 2006). Then, genes involved in gluconeogenesis are induced. Given the possibility that glucose cellular concentration is low, it could be plausible an enhancement of the gluconeogenesis in our models of NAFLD. It is largely described that gluconeogenesis is active in NAFLD and NASH (Honma, Sawada et al. 2018), as well as in non-hepatic cancers under glucose deprivation (Grasmann, Smolle et al. 2019), where contributes to the synthesis of glycerolipids (Leithner, Triebl et al. 2018).

Deficiency in *E2f1* or *E2f2* did not prevent the development of the IR associated to HCC and *E2f1*$^{-/-}$ mice showed even a worse tolerance to glucose and pyruvate than WT animals. In contrast, in early stages of the liver disease, *E2f1* or *E2f2* deficiency prevented the IR related to obesity-induced NAFLD. Particularly, the fact that *E2f1*$^{-/-}$ mice showed certain intolerance to glucose but not to exogen insulin are in agreement with evidences supporting that E2f1 deficiency, together or not with *E2f2* deficiency, disrupts insulin secretion (Annicotte, Blanchet et al. 2009, Iglesias, Murga et al. 2004.)

Collectively, these observations demonstrate for the first time that E2F1 and, especially, E2F2 transcription factors are induced in obesity-linked NAFLD and NAFLD-HCC onset, which implies that, E2F1 and E2F2 are proesteatotic factors and have an oncogenic role. Absence in *E2f1* and, particularly, in *E2f2* prevents obesity-related liver disease and its progression, then, they are required for NAFLD and NAFLD-associated HCC development. Deficiency in *E2f1* and, specially, in *E2f2* also maintains lipid and glucose homeostasis in the early stages of the liver disease.

2. E2f2 coordinates the metabolic reprogramming of lipids required for NAFLD and NAFLD-HCC development

To date, it was established that metabolic rewiring observed in cancer was a side effect of mutations in proto-oncogenes or tumor suppressors (Ward, Thompson 2012). Nonetheless, recent observations endorse the idea that proto-oncogenes or tumor suppressors are indeed who directly regulate the metabolism even before tumorigenesis. This alternative proposal is based on the fact that they are involved not only in pathological conditions, but also in the maintenance of organic physiology. Under this context, we aimed to investigate the relation between E2f2 and the pathways that lead to the metabolic profile associated to progressive NAFLD.

Analysis of the transcriptional program related to prevention of NAFLD-related HCC in absence of *E2f2* showed that most significantly downregulated genes were clustered in pathways like platelet activation, signaling and aggregation, tool-like receptor (TLR) cascades, cell cycle and apoptosis. All those pathways are typically induced during HCC (Malehmir, Pfister et al. 2019, Lopes, Borges-Canha et al. 2016, Li, Li et al. 2018), then, their inactivation in absence of *E2f2* is in accordance with the prevention of obesity-linked hepatocarcinogenesis. In agreement with the observation that the lack of *E2f2* protected from lipid accumulation and obesity-related hepatoesteatosis, genes linked to lipid anabolism were also decreased in *E2f2*$^{-/-}$ mice who escaped from NAFLD-related HCC development, while those involved in lipid catabolism were increased. Notably, in steady-state, absence in *E2f2* perse attenuated immune system. Autoimmune disorders in extrahepatic tissues have been linked to both E2f2 depletion (Iglesias, Murga et al. 2004) and E2f2 induction (Zhang, Wang et al. 2018), indicating that the role of E2f2 in the immune system depends on the context. In our mice model of study, the results suggest that E2f2 was more related to promote hepatic immune response. Besides, hepatic lipid catabolism was enhanced in control conditions for *E2f2* deficient mice, which explains the low liver content in TG, DG and CE when E2f2 is absent.

Gene expression profile indicated that reprograming of lipid metabolism was of high relevance in obesity-linked HCC development. Therefore, we analyzed the routes involved in liver lipid acquisition and disposal during obesity-related NAFLD and its progression to HCC, as well as the impact that E2f2 could have on them.

Concerning lipid elimination pathways, deficiency in E2F2 was associated to high rates of fatty acid oxidation (FAO) in human tumoral cells and in mice livers, together with increased expression of genes related to several β-oxidation reactions and activation of FAs. Notably, gene and protein expression of CPT2, which participates in the rate limiting process of FAO and is promoter of hepatocarcinogenesis in obesity (Fujiwara, Nakagawa et al. 2018), was downregulated in mice models of NAFLD and NAFLD-HCC and upregulated when *E2f2* was deficient. Besides, contrary to that observed in NAFLD and NAFLD-HCC, absence in *E2f2* was also linked with upregulation of HNF4-α, a nuclear receptor that induces FAO and has a role in the inhibition of HCC (Walesky, Edwards et al. 2013). Hence, the results suggest that enhanced FAO, mediated by an increased channeling of fatty acids towards the mitochondria, was one of the main mechanism involved in the protection from the liver disease by E2f2. If more ATP is needed by cells, the reducing power obtained from FAO and TCA is derived to oxidative phosphorylation (oxphos) (Carracedo, Cantley et al. 2013). We observed that different genes related to this process had low expression in obesity-derived HCC, while they were induced in *E2f2* deficient mice livers. The expression pattern of PGC-1β, a factor that mediates oxphos and regulates obesity-driven steatosis (Sonoda, Mehl et al. 2007), was also similar.

As previously mentioned, lipid synthesis is a sourcing route of liver lipids. Increased esterification of [^{3}H]-glycerol and FA, together with the upregulated expression of PPAR-γ (gene and protein) and its target-genes involved in lipid transport and storage, indicates that TG biosynthesis was also a pathogenic mechanism promoting NAFLD and its progression to HCC. In *E2f2* depleted mice livers exposed to DEN HFD, all those parameters were decreased, which suggests that the absence in E2F2 prevented the lipogenesis induced by treatment. *de novo* lipogenesis (DNL) of TG assessed by [^{3}H]-acetate was not altered in *E2f2*$^{-/-}$ mice exposed to DEN HFD, which indicates that the reduced TG biosynthesis related to the lack of E2F2 was specifically due to a disruption of the esterification and not to a decreased DNL. Although their similarity (Kong, Chang et al. 2007), inhibition of the lipid synthesis in obesity seems to be a specific function of E2F2, since E2F1 is considered a lipogenic factor (Denechaud, Lopez-Mejia et al. 2016).

The results also suggest that dyslipidemia had an important role in NAFLD and its progression to HCC, since serum TG and FA were increased in mice exposed to DEN HFD. However, dyslipidemia is not caused by altered hepatic VLDL export, as liver VLDL secretion rate and *Apob* and *Apoe* expression maintained unaltered. Then, another mechanism must be involved on it, such as decreased WAT lipolysis coupled with decreased lipoprotein-TG catabolism. This process is the responsible for FA supply in liver and other non-adipose tissues if energy is required. Nevertheless, increased WAT index and the maintenance of

the gene expression involved in liver FA transport suggests that WAT lipolysis was not a route involved in the dyslipidemia associated to the liver disease. Despite the altered lipid serum profile in mice who developed NAFLD and NAFLD-HCC, increased *Lpl* expression suggests that hepatic catabolism of circulating TG was enhanced, a condition that leads to lipid accumulation in liver and HCC as it has been described elsewhere (Kim, Fillmore et al. 2001, Cao, Song et al. 2017). Concerning the role of E2f2, the results indicate that absence in *E2f2* proteced mice from the dyslipidemia and serum TG removal by liver, both routes involved in NAFLD and NAFLD-HCC development. Indeed, serum FA and TG were not increased in *E2f2*$^{-/-}$ mice exposed to proesteatotic conditions, although WAT lipolysis was enhanced, WAT index was diminished and liver expression of Lpl was downregulated.

Collectively, liver FAO, lipid synthesis and TG uptake, impaired routes in obesity-derived HCC, were also altered in early stages of the liver disease, a condition in which E2F2 was upregulated. Together with the fact that E2f2 depletion protected from the metabolic profile associated to progressive NAFLD *(Figure F1)*, we suggest that E2F2 is orchestrating the adaptive metabolism that precedes the NAFLD-related HCC. The relevance of this finding lies in the fact that E2F2 could be used as early biomarker of the obesity-related liver disease.

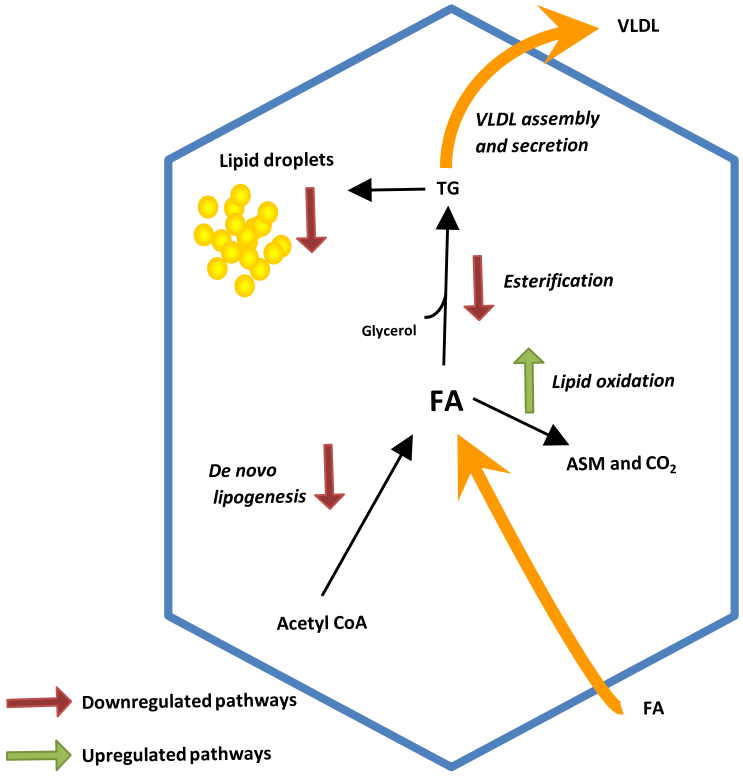

Figure F1. Schematic representation of FA metabolism in *E2f2*$^{-/-}$ mice liver to prevent obesity-related NAFLD and progression to HCC. ASM, Acid soluble metabolites; FA, Fatty acid; HCC, hepatocellular carcinoma; TG, triglyceride; NAFLD, non-alcoholic fatty liver disease.

Chapter F. CONCLUSIONS

Chapter F. CONCLUSIONS

1. **E2F1 and, especially, E2F2 transcription factors are involved in obesity-related NAFLD development and its progression to HCC.**
   1.1. Both E2F1 and E2F2 are overexpressed in obese patients with NAFLD and *E2f2* is also overexpressed in mice models of obesity-related NAFLD and NAFLD-related HCC, which implies that these transcription factors are proesteatotic and oncogenic factors in the liver disease.
   1.2. Absence in E2f1 and, particularly, in E2f2 prevent the development of obesity-related NAFLD. Mice lacking *E2f1* or *E2f2* do not present the hepatosteatosis neither liver inflammation caused by NAFLD-induction treatments, showing that these transcription factors are required for obesity-related NAFLD.
   1.3. *E2f1* and *E2f2* deficiency in mice confers resistance to NAFLD-related HCC development and the associated fibrosis and lipid storage, suggesting that both E2f1 and E2f2 are required in those processes.

2. **E2f2 transcription factor coordinates the metabolic reprogramming involved in obesity-related NAFLD development and its progression to HCC.**
   2.1. E2f2 controls the metabolic pathways involved in liver lipid storage from the early stages of the liver disease. As a protective mechanism, *E2f2* deficiency in mice prevents the dyslipemia and the increased liver TG synthesis and uptake linked to NAFLD and NAFLD-HCC. In addition, increased fatty acid oxidation, mediated by an increased channeling of fatty acids towards the mitochondria, contributes to the liver resistance to NAFLD and HCC development in *E2f2* knockout mice.
   2.2. In addition to the improvement of the lipid profile, *E2f2* deficiency in mice prevents the insulin resistance linked to early stages of the obesity-related NAFLD, but not that associated to NAFLD-HCC.

3. **E2F1 and, particularly, E2F2 are potential prognostic markers for the obesity-related NAFLD.** E2F1 and E2F2 are induced in obesity with and without NAFLD. Besides, the increase in E2F2 liver content is even more exacerbated once NAFLD is developed.

BIBLIOGRAFIA/BIBLIOGRAPHY

BIBLIOGRAFIA/BIBLIOGRAPHY

ABDELAAL, M., LE ROUX, C.W. and DOCHERTY, N.G., 2017. Morbidity and mortality associated with obesity. Annals of translational medicine, 5(7), pp. 161.

AGUILAR, V. and FAJAS, L., 2010. Cycling through metabolism. EMBO molecular medicine, 2(9), pp. 338-348.

AL-DAYYAT, H.M., RAYYAN, Y.M. and TAYYEM, R.F., 2018. Non-alcoholic fatty liver disease and associated dietary and lifestyle risk factors. Diabetes & metabolic syndrome.

ALZAHRANI, B., ISELI, T.J. and HEBBARD, L.W., 2014. Non-viral causes of liver cancer: does obesity led inflammation play a role? Cancer letters, 345(2), pp. 223-229.

ANNICOTTE, J.S., BLANCHET, E., CHAVEY, C., IANKOVA, I., COSTES, S., ASSOU, S., TEYSSIER, J., DALLE, S., SARDET, C. and FAJAS, L., 2009. The CDK4-pRB-E2F1 pathway controls insulin secretion. Nature cell biology, 11(8), pp. 1017-1023.

ARAB, J.P., KARPEN, S.J., DAWSON, P.A., ARRESE, M. and TRAUNER, M., 2017. Bile acids and nonalcoholic fatty liver disease: Molecular insights and therapeutic perspectives. Hepatology (Baltimore, Md.), 65(1), pp. 350-362.

ARANCETA-BARTRINA, J., PEREZ-RODRIGO, C., ALBERDI-ARESTI, G., RAMOS-CARRERA, N. and LAZARO-MASEDO, S., 2016. Prevalence of General Obesity and Abdominal Obesity in the Spanish Adult Population (Aged 25-64 Years) 2014-2015: The ENPE Study. Revista espanola de cardiologia (English ed.), 69(6), pp. 579-587.

ARGUELLO, G., BALBOA, E., ARRESE, M. and ZANLUNGO, S., 2015. Recent insights on the role of cholesterol in non-alcoholic fatty liver disease. Biochimica et biophysica acta, 1852(9), pp. 1765-1778.

ARIAS, I.M., WOLKOFF, A.W., BOYER, J.L., SHAFRITZ, D.A., FAUSTO, N., ALTER, H.J. and COHEN, D.E., eds, 2009. The liver: Biology and Pathobiology, 5th edition. ISBM 978-0-470-72313-5 edn.

ASPICHUETA, P., PEREZ, S., OCHOA, B. and FRESNEDO, O., 2005. Endotoxin promotes preferential periportal upregulation of VLDL secretion in the rat liver. Journal of lipid research, 46(5), pp. 1017-1026.

BAFFY, G., 2015. MicroRNAs in Nonalcoholic Fatty Liver Disease. J. Clin. Med., .

BAHNASSY, A.A., ZEKRI, A.R., LOUTFY, S.A., MOHAMED, W.S., MONEIM, A.A., SALEM, S.E., SHETA, M.M., OMAR, A. and AL-ZAWAHRY, H., 2011. The role of cyclins and cyclin dependent kinases in development and progression of hepatitis C virus-genotype 4-associated hepatitis and hepatocellular carcinoma. Experimental and molecular pathology, 91(2), pp. 643-652.

BANDARA, L.R., BUCK, V.M., ZAMANIAN, M., JOHNSTON, L.H. and LA THANGUE, N.B., 1993. Functional synergy between DP-1 and E2F-1 in the cell cycle-regulating transcription factor DRTF1/E2F. The EMBO journal, 12(11), pp. 4317-4324.

BARNUM, K.J. and O'CONNELL, M.J., 2014. Cell cycle regulation by checkpoints. Methods in molecular biology (Clifton, N.J.), 1170, pp. 29-40.

BELORIBI-DJEFAFLIA, S., VASSEUR, S. and GUILLAUMOND, F., 2016. Lipid metabolic reprogramming in cancer cells. Oncogenesis, 5, pp. e189.

BERKAN-KAWINSKA, A. and PIEKARSKA, A., 2020. Hepatocellular carcinoma in non-alcohol fatty liver disease - changing trends and specific challenges. Current medical research and opinion, 36(2), pp. 235-243.

BERNA, G. and ROMERO-GOMEZ, M., 2020. The role of nutrition in non-alcoholic fatty liver disease: Pathophysiology and management. Liver international: official journal of the International Association for the Study of the Liver, 40 Suppl 1, pp. 102-108.

BERNDT N, ECKSTEIN J, HEUCKE N, ET AL., 2019. Characterization of Lipid and Lipid Droplet Metabolism in Human HCC. Cells. 2019;8(5):512.

BERTOT, L.C. and ADAMS, L.A., 2019. Trends in hepatocellular carcinoma due to non-alcoholic fatty liver disease. Expert review of gastroenterology & hepatology, 13(2), pp. 179-187.

BETKE, K., BREWER, G.J., KIRKMAN, H.N, 1967. Standardization of procedures for the study of glucose-6-phosphate dehydrogenase. WHO Tech Rep Ser 1967, 366: 53.

BETTS, J.G., YOUNG, K.A., WISE, J.A., JOHNSON, E., POE, B., KRUSE, D.H., KOROL, O., JOHNSON, J.E., WOMBLE, M. and DESAIX, P., 2013. Metabolism and nutrition. Anatomy and Physiology. Houston, Texas: OpenStax.

BIALECKI, E.S. and DI BISCEGLIE, A.M., 2005. Clinical presentation and natural course of hepatocellular carcinoma. European journal of gastroenterology & hepatology, 17(5), pp. 485-489.

BJORNSON, E., MUKHOPADHYAY, B., ASPLUND, A., PRISTOVSEK, N., CINAR, R., ROMEO, S., UHLEN, M., KUNOS, G., NIELSEN, J. and MARDINOGLU, A., 2015. Stratification of Hepatocellular Carcinoma Patients Based on Acetate Utilization. Cell reports, 13(9), pp. 2014-2026.

BLANCHET, E., ANNICOTTE, J.S., LAGARRIGUE, S., AGUILAR, V., CLAPE, C., CHAVEY, C., FRITZ, V., CASAS, F., APPARAILLY, F., AUWERX, J. and FAJAS, L., 2011. E2F transcription factor-1 regulates oxidative metabolism. Nature cell biology, 13(9), pp. 1146-1152.

BLÜHER, M., 2019. Obesity: global epidemiology and pathogenesis. Nat Rev Endocrinol 15, 288–298.

BINDEA, G., MLECNIK, B., HACKL, H., CHAROENTONG, P., TOSOLINI, M., KIRILOVSKY, A., FRIDMAN, W.H., PAGES, F., TRAJANOSKI, Z. and GALON, J., 2009. ClueGO: a Cytoscape plug-in to decipher functionally grouped gene ontology and pathway annotation networks. Bioinformatics (Oxford, England), 25(8), pp. 1091-1093.

BRACKEN, A.P., CIRO, M., COCITO, A. and HELIN, K., 2004. E2F target genes: unraveling the biology. Trends in biochemical sciences, 29(8), pp. 409-417.

BRAY, F., FERLAY, J., SOERJOMATARAM, I., SIEGEL, R.L., TORRE, L.A. and JEMAL, A., 2018. Global cancer statistics 2018: GLOBOCAN estimates of incidence and mortality worldwide for 36 cancers in 185 countries. CA: a cancer journal for clinicians, 68(6), pp. 394-424.

BREMER, J., 1983. Carnitine--metabolism and functions. Physiological Reviews, 63(4), pp. 1420-1480.

CAMPANI, C., BENSI, C., MILANI, S., GALLI, A. and TAROCCHI, M., 2020. Resection of NAFLD-Associated HCC: Patient Selection and Reported Outcomes. Journal of hepatocellular carcinoma, 7, pp. 107-116.

CANCER GENOME ATLAS RESEARCH NETWORK. ELECTRONIC ADDRESS: WHEELER@BCM.EDU and CANCER GENOME ATLAS RESEARCH NETWORK, 2017. Comprehensive and Integrative Genomic Characterization of Hepatocellular Carcinoma. Cell, 169(7), pp. 1327-1341.e23.

CAO, A.R., RABINOVICH, R., XU, M., XU, X., JIN, V.X. and FARNHAM, P.J., 2011. Genome-wide analysis of transcription factor E2F1 mutant proteins reveals that N- and C-terminal protein interaction domains do not participate in targeting E2F1 to the human genome. The Journal of biological chemistry, 286(14), pp. 11985-11996.

CAO, D., SONG, X., CHE, L., LI, X., PILO, M.G., VIDILI, G., PORCU, A., SOLINAS, A., CIGLIANO, A., PES, G.M., RIBBACK, S., DOMBROWSKI, F., CHEN, X., LI, L. and CALVISI, D.F., 2017. Both de novo synthetized and exogenous fatty acids support the growth of hepatocellular carcinoma cells. Liver international: official journal of the International Association for the Study of the Liver, 37(1), pp. 80-89.

CARLESSI, R., KÖHN-GAONE, J., OLYNYK JK. and TIRNITZ-PARKER JEE., 2019. Chapter 4Mouse Models of Hepatocellular Carcinoma. In: TIRNITZ-PARKER JEE, ed, Hepatocellular Carcinoma.

CARRACEDO, A., CANTLEY, L.C. and PANDOLFI, P.P., 2013. Cancer metabolism: fatty acid oxidation in the limelight. Nature reviews.Cancer, 13(4), pp. 227-232.

CHEN, H.Z., TSAI, S.Y. and LEONE, G., 2009. Emerging roles of E2Fs in cancer: an exit from cell cycle control. Nature reviews.Cancer, 9(11), pp. 785-797.

CHIANG, D.J., PRITCHARD, M.T. and NAGY, L.E., 2011. Obesity, diabetes mellitus, and liver fibrosis. American journal of physiology.Gastrointestinal and liver physiology, 300(5), pp. G697-702.

CLEM, B.F. and CHESNEY, J., 2012. Molecular pathways: regulation of metabolism by RB. Clinical cancer research: an official journal of the American Association for Cancer Research, 18(22), pp. 6096-6100.

COOPER, G., 2000. The Cell: A Molecular Approach. 2nd edition. Sunderland (MA): Sinauer Associates.

CROFT, D., O'KELLY, G., WU, G., HAW, R., GILLESPIE, M., MATTHEWS, L., CAUDY, M., GARAPATI, P., GOPINATH, G., JASSAL, B., JUPE, S., KALATSKAYA, I., MAHAJAN, S., MAY, B., NDEGWA, N., SCHMIDT, E., SHAMOVSKY, V., YUNG, C., BIRNEY, E., HERMJAKOB, H., D'EUSTACHIO, P. and STEIN, L., 2011. Reactome: a database of reactions, pathways and biological processes. Nucleic acids research, 39(Database issue), pp. D691-7.

DALI-YOUCEF, N., MATAKI, C., COSTE, A., MESSADDEQ, N., GIROUD, S., BLANC, S., KOEHL, C., CHAMPY, M.F., CHAMBON, P., FAJAS, L., METZGER, D., SCHOONJANS, K. and AUWERX, J., 2007. Adipose tissue-specific inactivation of the retinoblastoma protein protects against diabesity because of increased energy expenditure. Proceedings of the National Academy of Sciences of the United States of America, 104(25), pp. 10703-10708.

DAVID, L.A., MAURICE, C.F., CARMODY, R.N., GOOTENBERG, D.B., BUTTON, J.E., WOLFE, B.E., LING, A.V., DEVLIN, A.S., VARMA, Y., FISCHBACH, M.A., BIDDINGER, S.B., DUTTON, R.J. and TURNBAUGH, P.J., 2014. Diet rapidly and reproducibly alters the human gut microbiome. Nature, 505(7484), pp. 559-563.

DE MATTEIS S., RAGUSA A., MARISI G. ET AL., 2018. Aberrant Metabolism in Hepatocellular Carcinoma Provides Diagnostic and Therapeutic Opportunities. Oxid Med Cell Longev. 2018;2018:7512159.

DE SPIEGELAERE, W., DERN-WIELOCH, J., WEIGEL, R., SCHUMACHER, V., SCHORLE, H., NETTERSHEIM, D., BERGMANN, M., BREHM, R., KLIESCH, S., VANDEKERCKHOVE, L. and FINK, C., 2015. Reference gene validation for RT-qPCR, a note on different available software packages. PloS one, 10(3), pp. e0122515.

DEGREGORI, J. and JOHNSON, D.G., 2006. Distinct and Overlapping Roles for E2F Family Members in Transcription, Proliferation and Apoptosis. Current Molecular Medicine, 6(7), pp. 739-748.

DELGADO, I., FRESNEDO, O., IGLESIAS, A., RUEDA, Y., SYN, W.K., ZUBIAGA, A.M. and OCHOA, B., 2011. A role for transcription factor E2F2 in hepatocyte proliferation and timely liver regeneration. American journal of physiology.Gastrointestinal and liver physiology, 301(1), pp. G20-31.

DENECHAUD, P.D., LOPEZ-MEJIA, I.C., GIRALT, A., LAI, Q., BLANCHET, E., DELACUISINE, B., NICOLAY, B.N., DYSON, N.J., BONNER, C., PATTOU, F., ANNICOTTE, J.S. and FAJAS, L., 2016. E2F1 mediates sustained lipogenesis and contributes to hepatic steatosis. The Journal of clinical investigation, 126(1), pp. 137-150.

DHAMIJA, E., PAUL, S.B. and KEDIA, S., 2019. Non-alcoholic fatty liver disease associated with hepatocellular carcinoma: An increasing concern. The Indian journal of medical research, 149(1), pp. 9-17.

DI STEFANO, L., JENSEN, M.R. and HELIN, K., 2003. E2F7, a novel E2F featuring DP-independent repression of a subset of E2F-regulated genes. The EMBO journal, 22(23), pp. 6289-6298.

DIMOVA, D.K. and DYSON, N.J., 2005. The E2F transcriptional network: old acquaintances with new faces. Oncogene, 24(17), pp. 2810-2826.

DONG, X., PARK, S., LIN, X., COPPS, K., YI, X. and WHITE, M.F., 2006. Irs1 and Irs2 signaling is essential for hepatic glucose homeostasis and systemic growth. The Journal of clinical investigation, 116(1), pp. 101-114.

DONNELLY KL, SMITH CI, SCHWARZENBERG SJ, JESSURUN J, BOLDT MD, PARKS EJ, 2005. Sources of fatty acids stored in liver and secreted via lipoproteins in patients with nonalcoholic fatty liver disease. J. Clin. Invest. 115:1343–135.

DYSON, N., 1998. The regulation of E2F by pRB-family proteins. Genes & development, 12(15), pp. 2245-2262.

ESLAM, M., NEWSOME, P.N., SARIN, S.K., ANSTEE, Q.M., TARGHER, G., ROMERO-GOMEZ, M., ZELBER-SAGI, S., WAI-SUN WONG, V., DUFOUR, J.F., SCHATTENBERG, J.M., KAWAGUCHI, T., ARRESE, M., VALENTI, L., SHIHA, G., TIRIBELLI, C., YKI-JARVINEN, H., FAN, J.G., GRONBAEK, H., YILMAZ, Y., CORTEZ-PINTO, H., OLIVEIRA, C.P., BEDOSSA, P., ADAMS, L.A., ZHENG, M.H., FOUAD, Y., CHAN, W.K., MENDEZ-SANCHEZ, N., AHN, S.H., CASTERA, L., BUGIANESI, E., RATZIU, V. and GEORGE, J., 2020. A new definition for metabolic dysfunction-associated fatty liver disease: An international expert consensus statement. Journal of hepatology.

ESLAM, M., SANYAL, A.J., GEORGE, J. and INTERNATIONAL CONSENSUS PANEL, 2020. MAFLD: A Consensus-Driven Proposed Nomenclature for Metabolic Associated Fatty Liver Disease. Gastroenterology.

ESLAM, M., VALENTI, L. and ROMEO, S., 2018. Genetics and epigenetics of NAFLD and NASH: Clinical impact. Journal of hepatology, 68(2), pp. 268-279.

ESTES, C., RAZAVI, H., LOOMBA, R., YOUNOSSI, Z. and SANYAL, A.J., 2018. Modeling the epidemic of nonalcoholic fatty liver disease demonstrates an exponential increase in burden of disease. Hepatology (Baltimore, Md.), 67(1), pp. 123-133.

FABBRINI, E., MOHAMMED, B.S., MAGKOS, F., KORENBLAT, K.M., PATTERSON, B.W. and KLEIN, S., 2008. Alterations in adipose tissue and hepatic lipid kinetics in obese men and women with nonalcoholic fatty liver disease. Gastroenterology, 134(2), pp. 424-431.

FABBRINI, E., SULLIVAN, S. and KLEIN, S., 2010. Obesity and nonalcoholic fatty liver disease: biochemical, metabolic, and clinical implications. Hepatology (Baltimore, Md.), 51(2), pp. 679-689.

FABREGAT, I., MORENO-CACERES, J., SANCHEZ, A., DOOLEY, S., DEWIDAR, B., GIANNELLI, G., TEN DIJKE, P. and IT-LIVER CONSORTIUM, 2016. TGF-beta signalling and liver disease. The FEBS journal, 283(12), pp. 2219-2232.

FAJAS, L., ANNICOTTE, J.S., MIARD, S., SARRUF, D., WATANABE, M. and AUWERX, J., 2004. Impaired pancreatic growth, beta cell mass, and beta cell function in E2F1 (-/-)mice. The Journal of clinical investigation, 113(9), pp. 1288-1295.

FAJAS, L., LANDSBERG, R.L., HUSS-GARCIA, Y., SARDET, C., LEES, J.A. and AUWERX, J., 2002. E2Fs regulate adipocyte differentiation. Developmental cell, 3(1), pp. 39-49.

FINCK, B.N. and KELLY, D.P., 2006. PGC-1 coactivators: inducible regulators of energy metabolism in health and disease. The Journal of clinical investigation, 116(3), pp. 615-622.

FOLCH, J., LEES, M. and SLOANE STANLEY, G.H., 1957. A simple method for the isolation and purification of total lipides from animal tissues. The Journal of biological chemistry, 226(1), pp. 497-509.

FOLK, W.P., KUMARI, A., IWASAKI, T., PYNDIAH, S., JOHNSON, J.C., CASSIMERE, E.K., ABDULOVIC-CUI, A.L. and SAKAMURO, D., 2019. Loss of the tumor suppressor BIN1 enables ATM Ser/Thr kinase activation by the nuclear protein E2F1 and renders cancer cells resistant to cisplatin. The Journal of biological chemistry, 294(14), pp. 5700-5719.

FOUAD, Y., ELWAKIL, R., ELSAHHAR, M., SAID, E., BAZEED, S., ALI GOMAA, A., HASHIM, A., KAMAL, E., MEHREZ, M. and ATTIA, D., 2021. The NAFLD-MAFLD debate: Eminence vs evidence. Liver international: official journal of the International Association for the Study of the Liver, 41(2), pp. 255-260.

FREEDMAN, J.A., CHANG, J.T., JAKOI, L. and NEVINS, J.R., 2009. A combinatorial mechanism for determining the specificity of E2F activation and repression. Oncogene, 28(32), pp. 2873-2881.

FRIEDMAN, S.L., NEUSCHWANDER-TETRI, B.A., RINELLA, M. and SANYAL, A.J., 2018. Mechanisms of NAFLD development and therapeutic strategies. Nature medicine.

FUJIWARA, N., NAKAGAWA, H., ENOOKU, K., KUDO, Y., HAYATA, Y., NAKATSUKA, T., TANAKA, Y., TATEISHI, R., HIKIBA, Y., MISUMI, K., TANAKA, M., HAYASHI, A., SHIBAHARA, J., FUKAYAMA, M., ARITA, J., HASEGAWA, K., HIRSCHFIELD, H., HOSHIDA, Y., HIRATA, Y., OTSUKA, M., TATEISHI, K. and KOIKE, K., 2018. CPT2 downregulation adapts HCC to lipid-rich environment and promotes carcinogenesis via acylcarnitine accumulation in obesity. Gut, 67(8), pp. 1493-1504.

FUKUI, H., 2019. Role of Gut Dysbiosis in Liver Diseases: What Have We Learned So Far? Diseases (Basel, Switzerland), 7(4), pp. 10.3390/diseases7040058.

GAO, X., VAN DER VEEN, J.N., HERMANSSON, M., ORDONEZ, M., GOMEZ-MUNOZ, A., VANCE, D.E. and JACOBS, R.L., 2015. Decreased lipogenesis in white adipose tissue contributes to the resistance to high fat diet-induced obesity in phosphatidylethanolamine N-methyltransferase-deficient mice. Biochimica et biophysica acta, 1851(2), pp. 152-162.

GAVRILOVA, O., HALUZIK, M., MATSUSUE, K., CUTSON, J.J., JOHNSON, L., DIETZ, K.R., NICOL, C.J., VINSON, C., GONZALEZ, F.J. and REITMAN, M.L., 2003. Liver peroxisome proliferator-activated receptor gamma contributes to hepatic steatosis, triglyceride clearance, and regulation of body fat mass. The Journal of biological chemistry, 278(36), pp. 34268-34276.

GERARD, C. and GOLDBETER, A., 2009. Temporal self-organization of the cyclin/Cdk network driving the mammalian cell cycle. Proceedings of the National Academy of Sciences of the United States of America, 106(51), pp. 21643-21648.

GERDES, J., LEMKE, H., BAISCH, H., WACKER, H.H., SCHWAB, U. and STEIN, H., 1984. Cell cycle analysis of a cell proliferation-associated human nuclear antigen defined by the monoclonal antibody Ki-67. Journal of immunology (Baltimore, Md.: 1950), 133(4), pp. 1710-1715.

GETZ, G.S. and REARDON, C.A., 2009. Apoprotein E as a lipid transport and signaling protein in the blood, liver, and artery wall. Journal of lipid research, 50 Suppl, pp. S156-61.

GIRALT, A., DENECHAUD, P.D., LOPEZ-MEJIA, I.C., DELACUISINE, B., BLANCHET, E., BONNER, C., PATTOU, F., ANNICOTTE, J.S. and FAJAS, L., 2018. E2F1 promotes hepatic gluconeogenesis and contributes to hyperglycemia during diabetes. Molecular metabolism, 11, pp. 104-112.

GOLABI, P., RHEA, L., HENRY, L. and YOUNOSSI, Z.M., 2019. Hepatocellular carcinoma and non-alcoholic fatty liver disease. Hepatology international, 13(6), pp. 688-694.

GONZALEZ-ROMERO, F., MESTRE, D., AURREKOETXEA, I., O'ROURKE, C.J., ANDERSEN, J.B., WOODHOO, A., TAMAYO-CARO, M., VARELA-REY, M., PALOMO-IRIGOYEN, M., GOMEZ-SANTOS, B., DE URTURI, D.S., NUNEZ-GARCIA, M., GARCIA-RODRIGUEZ, J.L., FERNANDEZ-ARES, L., BUQUE, X., IGLESIAS-ARA, A., BERNALES, I., DE JUAN, V.G., DELGADO, T.C., GOIKOETXEA-USANDIZAGA, N., LEE, R., BHANOT, S., DELGADO, I., PERUGORRIA, M.J., ERRAZTI, G., MOSTEIRO, L., GAZTAMBIDE, S., MARTINEZ DE LA PISCINA, I., IRUZUBIETA, P., CRESPO, J., BANALES, J.M., MARTINEZ-CHANTAR, M.L., CASTANO, L., ZUBIAGA, A.M. and ASPICHUETA, P., 2021. E2F1 and E2F2-Mediated Repression of CPT2 Establishes a Lipid-Rich Tumor-Promoting Environment. Cancer research, 81(11), pp. 2874-2887.

GRANDER, D., 1998. How do mutated oncogenes and tumor suppressor genes cause cancer? Medical oncology (Northwood, London, England), 15(1), pp. 20-26.

GRASMANN, G., SMOLLE, E., OLSCHEWSKI, H. and LEITHNER, K., 2019. Gluconeogenesis in cancer cells - Repurposing of a starvation-induced metabolic pathway? Biochimica et biophysica acta.Reviews on cancer, 1872(1), pp. 24-36.

GRECO, D., KOTRONEN, A., WESTERBACKA, J., PUIG, O., ARKKILA, P., KIVILUOTO, T., LAITINEN, S., KOLAK, M., FISHER, R.M., HAMSTEN, A., AUVINEN, P. and YKI-JARVINEN, H., 2008. Gene expression in human NAFLD. American journal of physiology.Gastrointestinal and liver physiology, 294(5), pp. G1281-7.

HAIM, Y., BLUHER, M., SLUTSKY, N., GOLDSTEIN, N., KLOTING, N., HARMAN-BOEHM, I., KIRSHTEIN, B., GINSBERG, D., GERICKE, M., GUIU JURADO, E., KOVSAN, J., TARNOVSCKI, T., KACHKO, L., BASHAN, N., GEPNER, Y., SHAI, I. and RUDICH, A., 2015. Elevated autophagy gene expression in adipose tissue of obese humans: A potential non-cell-cycle-dependent function of E2F1. Autophagy, 11(11), pp. 2074-2088.

HALLSTROM, T.C. and NEVINS, J.R., 2003. Specificity in the activation and control of transcription factor E2F-dependent apoptosis. Proceedings of the National Academy of Sciences of the United States of America, 100(19), pp. 10848-10853.

HATEBOER, G., KERKHOVEN, R.M., SHVARTS, A., BERNARDS, R. and BEIJERSBERGEN, R.L., 1996. Degradation of E2F by the ubiquitin-proteasome pathway: regulation by retinoblastoma family proteins and adenovirus transforming proteins. Genes & development, 10(23), pp. 2960-2970.

HE, Y., HUANG, S., CHENG, T., WANG, Y., ZHOU, S.J., ZHANG, Y.M. and YU, P., 2020. High glucose may promote the proliferation and metastasis of hepatocellular carcinoma via E2F1/RRBP1 pathway. Life Sciences, 252, pp. 117656.

HELIN, K., WU, C.L., FATTAEY, A.R., LEES, J.A., DYNLACHT, B.D., NGWU, C. and HARLOW, E., 1993. Heterodimerization of the transcription factors E2F-1 and DP-1 leads to cooperative trans-activation. Genes & development, 7(10), pp. 1850-1861.

HONG S., EUN J., CHOI S., SHEN Q., CHOI W., HAN J., NAM S., YOU J., Epigenetic reader BRD4 inhibition as a therapeutic strategy to suppress E2F2-cell cycle regulation circuit in liver cancer. Oncotarget. 2016; 7: 32628-32640.

HONMA, M., SAWADA, S., UENO, Y., MURAKAMI, K., YAMADA, T., GAO, J., KODAMA, S., IZUMI, T., TAKAHASHI, K., TSUKITA, S., UNO, K., IMAI, J., KAKAZU, E., KONDO, Y., MIZUNO, K., KAWAGISHI, N., SHIMOSEGAWA, T. and KATAGIRI, H., 2018. Selective insulin resistance with differential expressions of IRS-1 and IRS-2 in human NAFLD livers. International journal of obesity (2005), 42(9), pp. 1544-1555.

HSIAO, K.M., MCMAHON, S.L. and FARNHAM, P.J., 1994. Multiple DNA elements are required for the growth regulation of the mouse E2F1 promoter. Genes & development, 8(13), pp. 1526-1537.

HSIEH, M.C., DAS, D., SAMBANDAM, N., ZHANG, M.Q. and NAHLE, Z., 2008. Regulation of the PDK4 isozyme by the Rb-E2F1 complex. The Journal of biological chemistry, 283(41), pp. 27410-27417.

HU, B., LIN, J.Z., YANG, X.B. and SANG, X.T., 2020. Aberrant lipid metabolism in hepatocellular carcinoma cells as well as immune microenvironment: A review. Cell proliferation, 53(3), pp. e12772.

HUANG, Y.L., NING, G., CHEN, L.B., LIAN, Y.F., GU, Y.R., WANG, J.L., CHEN, D.M., WEI, H. and HUANG, Y.H., 2019. Promising diagnostic and prognostic value of E2Fs in human hepatocellular carcinoma. Cancer management and research, 11, pp. 1725-1740.

HUBER, H.E., EDWARDS, G., GOODHART, P.J., PATRICK, D.R., HUANG, P.S., IVEY-HOYLE, M., BARNETT, S.F., OLIFF, A. and HEIMBROOK, D.C., 1993. Transcription factor E2F binds DNA as a heterodimer. Proceedings of the National Academy of Sciences of the United States of America, 90(8), pp. 3525-3529.

HUNTINGTON, J.T., TANG, X., KENT, L.N., SCHMIDT, C.R. and LEONE, G., 2016. The Spectrum of E2F in Liver Disease--Mediated Regulation in Biology and Cancer. Journal of cellular physiology, 231(7), pp. 1438-1449.

HSU RY, L.H., 1967. Pigeon Liver Malic Enzyme. II. Isolation, Crystallization, and Some Properties. J Biol Chem. 1967;242(3):520-526.,

HUYNH, F.K., GREEN, M.F., KOVES, T.R. and HIRSCHEY, M.D., 2014. Measurement of fatty acid oxidation rates in animal tissues and cell lines. Methods in enzymology, 542, pp. 391-405.

IGLESIAS, A., MURGA, M., LARESGOITI, U., SKOUDY, A., BERNALES, I., FULLAONDO, A., MORENO, B., LLORETA, J., FIELD, S.J., REAL, F.X. and ZUBIAGA, A.M., 2004. Diabetes and exocrine pancreatic insufficiency in E2F1/E2F2 double-mutant mice. The Journal of clinical investigation, 113(10), pp. 1398-1407.

IGLESIAS-ARA, A., ZENARRUZABEITIA, O., BUELTA, L., MERINO, J. and ZUBIAGA, A.M., 2015. E2F1 and E2F2 prevent replicative stress and subsequent p53-dependent organ involution. Cell death and differentiation, 22(10), pp. 1577-1589.

IPSEN, D.H., LYKKESFELDT, J. and TVEDEN-NYBORG, P., 2018. Molecular mechanisms of hepatic lipid accumulation in non-alcoholic fatty liver disease. Cellular and molecular life sciences : CMLS, .

JAMWAL R, KRISHNAN V, KUSHWAHA DS & KHURANA R, 2020. Hepatocellular carcinoma in non cirrhotic versus cirrhotic liver: a clinico radiological comparative analysis. Abdominal Radiology.

JOHNSON, D.G., OHTANI, K. and NEVINS, J.R., 1994. Autoregulatory control of E2F1 expression in response to positive and negative regulators of cell cycle progression. Genes & development, 8(13), pp. 1514-1525.

JONES, J.G., 2016. Hepatic glucose and lipid metabolism. Diabetologia, 59(6), pp. 1098-1103.

JULIUS, U., 2003. Influence of plasma free fatty acids on lipoprotein synthesis and diabetic dyslipidemia. Experimental and clinical endocrinology & diabetes : official journal, German Society of Endocrinology [and] German Diabetes Association, 111(5), pp. 246-250.

JUNG, U.J. and CHOI, M.S., 2014. Obesity and its metabolic complications: the role of adipokines and the relationship between obesity, inflammation, insulin resistance, dyslipidemia and nonalcoholic fatty liver disease. International journal of molecular sciences, 15(4), pp. 6184-6223.

JUZA, R.M. and PAULI, E.M., 2014. Clinical and surgical anatomy of the liver: a review for clinicians. Clinical anatomy (New York, N.Y.), 27(5), pp. 764-769.

KATSIKI, N., MIKHAILIDIS, D.P. and MANTZOROS, C.S., 2016. Non-alcoholic fatty liver disease and dyslipidemia: An update. Metabolism: clinical and experimental, 65(8), pp. 1109-1123.

KAWANO, Y. and COHEN, D.E., 2013. Mechanisms of hepatic triglyceride accumulation in non-alcoholic fatty liver disease. Journal of gastroenterology, 48(4), pp. 434-441.

KENT, L.N., BAE, S., TSAI, S.Y., TANG, X., SRIVASTAVA, A., KOIVISTO, C., MARTIN, C.K., RIDOLFI, E., MILLER, G.C., ZORKO, S.M., PLEVRIS, E., HADJIYANNIS, Y., PEREZ, M., NOLAN, E., KLADNEY, R., WESTENDORP, B., DE BRUIN, A., FERNANDEZ, S., ROSOL, T.J., POHAR, K.S., PIPAS, J.M. and LEONE, G., 2017. Dosage-dependent copy number gains in E2f1 and E2f3 drive hepatocellular carcinoma. The Journal of clinical investigation, 127(3), pp. 830-842.

KIM, J.K., FILLMORE, J.J., CHEN, Y., YU, C., MOORE, I.K., PYPAERT, M., LUTZ, E.P., KAKO, Y., VELEZ-CARRASCO, W., GOLDBERG, I.J., BRESLOW, J.L. and SHULMAN, G.I., 2001. Tissue-specific overexpression of lipoprotein lipase causes tissue-specific insulin resistance. Proceedings of the National Academy of Sciences of the United States of America, 98(13), pp. 7522-7527.

KIM, J.U., SHARIFF, M.I., CROSSEY, M.M., GOMEZ-ROMERO, M., HOLMES, E., COX, I.J., FYE, H.K., NJIE, R. and TAYLOR-ROBINSON, S.D., 2016. Hepatocellular carcinoma: Review of disease and tumor biomarkers. World journal of hepatology, 8(10), pp. 471-484.

KISHIDA, N., MATSUDA, S., ITANO, O., SHINODA, M., KITAGO, M., YAGI, H., ABE, Y., HIBI, T., MASUGI, Y., AIURA, K., SAKAMOTO, M. and KITAGAWA, Y., 2016. Development of a novel mouse model of hepatocellular carcinoma with nonalcoholic steatohepatitis using a high-fat, choline-deficient diet and intraperitoneal injection of diethylnitrosamine. BMC gastroenterology, 16(1), pp. 61-016-0477-5.

KLEINER, D.E., BRUNT, E.M., VAN NATTA, M., BEHLING, C., CONTOS, M.J., CUMMINGS, O.W., FERRELL, L.D., LIU, Y.C., TORBENSON, M.S., UNALP-ARIDA, A., YEH, M., MCCULLOUGH, A.J., SANYAL, A.J. and NONALCOHOLIC STEATOHEPATITIS CLINICAL RESEARCH NETWORK, 2005. Design and validation of a histological scoring system for nonalcoholic fatty liver disease. Hepatology (Baltimore, Md.), 41(6), pp. 1313-1321.

KONG, L.J., CHANG, J.T., BILD, A.H. and NEVINS, J.R., 2007. Compensation and specificity of function within the E2F family. Oncogene, 26(3), pp. 321-327.

KORAH, J., FALAH, N., LACERTE, A. and LEBRUN, J.J., 2012. A transcriptionally active pRb-E2F1-P/CAF signaling pathway is central to TGFbeta-mediated apoptosis. Cell death & disease, 3, pp. e407.

KOVESDI, I., REICHEL, R. and NEVINS, J.R., 1986a. E1A transcription induction: enhanced binding of a factor to upstream promoter sequences. Science (New York, N.Y.), 231(4739), pp. 719-722.

KOVESDI, I., REICHEL, R. and NEVINS, J.R., 1986b. Identification of a cellular transcription factor involved in E1A trans-activation. Cell, 45(2), pp. 219-228.

KREK, W., LIVINGSTON, D.M. and SHIRODKAR, S., 1993. Binding to DNA and the retinoblastoma gene product promoted by complex formation of different E2F family members. Science (New York, N.Y.), 262(5139), pp. 1557-1560.

KUMAR, R., PRIYADARSHI, R.N. and ANAND, U., 2020. Non-alcoholic Fatty Liver Disease: Growing Burden, Adverse Outcomes and Associations. Journal of clinical and translational hepatology, 8(1), pp. 76-86.

LAEMMLI, U.K., 1970. Cleavage of structural proteins during the assembly of the head of bacteriophage T4. Nature, 227(5259), pp. 680-685.

LAI, Q., GIRALT, A., LE MAY, C., ZHANG, L., CARIOU, B., DENECHAUD, P.D. and FAJAS, L., 2017. E2F1 inhibits circulating cholesterol clearance by regulating Pcsk9 expression in the liver. JCI insight, 2(10), pp. 10.1172/jci.insight.89729.

LAUBY-SECRETAN, B., SCOCCIANTI, C., LOOMIS, D., GROSSE, Y., BIANCHINI, F., STRAIF, K. and INTERNATIONAL AGENCY FOR RESEARCH ON CANCER HANDBOOK WORKING GROUP, 2016. Body Fatness and Cancer--Viewpoint of the IARC Working Group. The New England journal of medicine, 375(8), pp. 794-798.

LEE, G., JEONG, Y.S., KIM, D.W., KWAK, M.J., KOH, J., JOO, E.W., LEE, J.S., KAH, S., SIM, Y.E. and YIM, S.Y., 2018. Clinical significance of APOB inactivation in hepatocellular carcinoma. Experimental & molecular medicine, 50(11), pp. 1-12.

LEE, J.S., YOO, J.E., KIM, H., RHEE, H., KOH, M.J., NAHM, J.H., CHOI, J.S., LEE, K.H. and PARK, Y.N., 2017. Tumor stroma with senescence-associated secretory phenotype in steatohepatitic hepatocellular carcinoma. PloS one, 12(3), pp. e0171922.

LEITHNER, K., TRIEBL, A., TROTZMULLER, M., HINTEREGGER, B., LEKO, P., WIESER, B.I., GRASMANN, G., BERTSCH, A.L., ZULLIG, T., STACHER, E., VALLI, A., PRASSL, R., OLSCHEWSKI, A., HARRIS, A.L., KOFELER, H.C., OLSCHEWSKI, H. and HRZENJAK, A., 2018. The glycerol backbone of phospholipids derives from noncarbohydrate precursors in starved lung cancer cells. Proceedings of the National Academy of Sciences of the United States of America, 115(24), pp. 6225-6230.

LI, N., LI, L. and CHEN, Y., 2018. The Identification of Core Gene Expression Signature in Hepatocellular Carcinoma. Oxidative medicine and cellular longevity, 2018, pp. 3478305.

LINDENMEYER, C.C. and MCCULLOUGH, A.J., 2018. The Natural History of Nonalcoholic Fatty Liver Disease-An Evolving View. Clinics in liver disease, 22(1), pp. 11-21.

LIU, G., XU, J.N., LIU, D., DING, Q., LIU, M.N., CHEN, R., FAN, M., ZHANG, Y., ZHENG, C., ZOU, D.J., LYU, J. and ZHANG, W.J., 2016. Regulation of plasma lipid homeostasis by hepatic lipoprotein lipase in adult mice. Journal of lipid research, 57(7), pp. 1155-1161.

LIU, H.X., FANG, Y., HU, Y., GONZALEZ, F.J., FANG, J. and WAN, Y.J., 2013. PPARbeta Regulates Liver Regeneration by Modulating Akt and E2f Signaling. PloS one, 8(6), pp. e65644.

LOPES, J.A., BORGES-CANHA, M. and PIMENTEL-NUNES, P., 2016. Innate immunity and hepatocarcinoma: Can toll-like receptors open the door to oncogenesis? World journal of hepatology, 8(3), pp. 162-182.

LUKAS, E.R., BARTLEY, S.M., GRAVEEL, C.R., DIAZ, Z.M., DYSON, N., HARLOW, E., YAMASAKI, L. and FARNHAM, P.J., 1999. No effect of loss of E2F1 on liver regeneration or hepatocarcinogenesis in C57BL/6J or C3H/HeJ mice. Molecular carcinogenesis, 25(4), pp. 295-303.

MALARKEY, D.E., JOHNSON, K., RYAN, L., BOORMAN, G. and MARONPOT, R.R., 2005. New insights into functional aspects of liver morphology. Toxicologic pathology, 33(1), pp. 27-34.

MALDONADO, E.N., DELGADO, I., FURLAND, N.E., BUQUE, X., IGLESIAS, A., AVELDANO, M.I., ZUBIAGA, A., FRESNEDO, O. and OCHOA, B., 2014. The E2F2 transcription factor sustains hepatic glycerophospholipid homeostasis in mice. PloS one, 9(11), pp. e112620.

MALEHMIR, M., PFISTER, D., GALLAGE, S., SZYDLOWSKA, M., INVERSO, D., KOTSILITI, E., LEONE, V., PEISELER, M., SUREWAARD, B.G.J., RATH, D., ALI, A., WOLF, M.J., DRESCHER, H., HEALY, M.E., DAUCH, D., KROY, D., KRENKEL, O., KOHLHEPP, M., ENGLEITNER, T., OLKUS, A., SIJMONSMA, T., VOLZ, J., DEPPERMANN, C., STEGNER, D., HELBLING, P., NOMBELA-ARRIETA, C., RAFIEI, A., HINTERLEITNER, M., RALL, M., BAKU, F., BORST, O., WILSON, C.L., LESLIE, J., O'CONNOR, T., WESTON, C.J., ADAMS, D.H., SHERIFF, L., TEIJEIRO, A., PRINZ, M., BOGESKA, R., ANSTEE, N., BONGERS, M.N., NOTOHAMIPRODJO, M., GEISLER, T., WITHERS, D.J., WARE, J., MANN, D.A., AUGUSTIN, H.G., VEGIOPOULOS, A., MILSOM, M.D., ROSE, A.J., LALOR, P.F., LLOVET, J.M., PINYOL, R., TACKE, F., RAD, R., MATTER, M., DJOUDER, N., KUBES, P., KNOLLE, P.A., UNGER, K., ZENDER, L., NIESWANDT, B., GAWAZ, M., WEBER, A. and HEIKENWALDER, M., 2019. Platelet GPIbalpha is a mediator and potential interventional target for NASH and subsequent liver cancer. Nature medicine, 25(4), pp. 641-655.

MALUMBRES, M. and BARBACID, M., 2009. Cell cycle, CDKs and cancer: a changing paradigm. Nature reviews.Cancer, 9(3), pp. 153-166.

MALUMBRES, M. and BARBACID, M., 2005. Mammalian cyclin-dependent kinases. Trends in biochemical sciences, 30(11), pp. 630-641.

MAO, S.A., GLORIOSO, J.M. and NYBERG, S.L., 2014. Liver regeneration. Translational research: the journal of laboratory and clinical medicine, 163(4), pp. 352-362.

MARTIN, B.T. and STREBHARDT, K., 2006. Polo-like kinase 1: target and regulator of transcriptional control. Cell cycle (Georgetown, Tex.), 5(24), pp. 2881-2885.

MAZHAR K., 2019. The Future of Nonalcoholic Fatty Liver Disease Treatment. Med Clin North Am. 103(1):57-69.

MCGARRY, J.D. and FOSTER, D.W., 1980. Regulation of hepatic fatty acid oxidation and ketone body production. Annual Review of Biochemistry, 49, pp. 395-420.

MEHLEM, A., HAGBERG, C.E., MUHL, L., ERIKSSON, U. and FALKEVALL, A., 2013. Imaging of neutral lipids by oil red O for analyzing the metabolic status in health and disease. Nature protocols, 8(6), pp. 1149-1154.

MICHELOTTI, G.A., MACHADO, M.V. and DIEHL, A.M., 2013. NAFLD, NASH and liver cancer. Nature reviews.Gastroenterology & hepatology, 10(11), pp. 656-665.

MILLAR, J.S., CROMLEY, D.A., MCCOY, M.G., RADER, D.J. and BILLHEIMER, J.T., 2005. Determining hepatic triglyceride production in mice: comparison of poloxamer 407 with Triton WR-1339. Journal of lipid research, 46(9), pp. 2023-2028.

MITXELENA, J., OSINALDE, N., ARIZMENDI, J., FULLAONDO, A. and ZUBIAGA, A., 2012. Proteomic Approaches to Unraveling the RB/E2F Regulatory Pathway. Man,T.K. and Flores,R.J. (eds), Proteomics—Human Diseases and Protein Functions. INTECH Open Access Publisher, .

MOLINA-SANCHEZ, P., RUIZ DE GALARRETA, M., YAO, M.A., LINDBLAD, K.E., BRESNAHAN, E., BITTERMAN, E., MARTIN, T.C., RUBENSTEIN, T., NIE, K., GOLAS, J., CHOUDHARY, S., BARCENA-VARELA, M., ELMAS, A., MIGUELA, V., DING, Y., KAN, Z., GRINSPAN, L.T., HUANG, K.L., PARSONS, R.E., SHIELDS, D.J., ROLLINS, R.A. and LUJAMBIO, A., 2020. Cooperation Between Distinct Cancer Driver Genes Underlies Intertumor Heterogeneity in Hepatocellular Carcinoma. Gastroenterology, 159(6), pp. 2203-2220.e14.

MORRIS, L., ALLEN, K.E. and LA THANGUE, N.B., 2000. Regulation of E2F transcription by cyclin E-Cdk2 kinase mediated through p300/CBP co-activators. Nature cell biology, 2(4), pp. 232-239.

MURANAKA, H., HAYASHI, A., MINAMI, K. ET AL., 2017. A distinct function of the retinoblastoma protein in the control of lipid composition identified by lipidomic profiling. Oncogenesis 6, e350, .

NAHON, P., ALLAIRE, M., NAULT, J.C. and PARADIS, V., 2020. Characterizing the mechanism behind the progression of NAFLD to hepatocellular carcinoma. Hepatic oncology, 7(4), pp. HEP36-2020-0017.

NAKAGAWA H, HAYATA Y, KAWAMURA S, YAMADA T, FUJIWARA N, KOIKE K., 2018. Lipid Metabolic Reprogramming in Hepatocellular Carcinoma Cancers (Basel). 2018;10(11):447., .

NEUMAN, E., FLEMINGTON, E.K., SELLERS, W.R. and KAELIN, W.G.,Jr, 1995. Transcription of the E2F-1 gene is rendered cell cycle dependent by E2F DNA-binding sites within its promoter. Molecular and cellular biology, 15(8), pp. 4660.

NEVINS, J.R., 1992. E2F: a link between the Rb tumor suppressor protein and viral oncoproteins. Science (New York, N.Y.), 258(5081), pp. 424-429.

NIEBERGALL, L.J., JACOBS, R.L., CHABA, T. and VANCE, D.E., 2011. Phosphatidylcholine protects against steatosis in mice but not non-alcoholic steatohepatitis. Biochimica et biophysica acta, 1811(12), pp. 1177-1185.

NOUREDDIN, M. and SANYAL, A.J., 2018. Pathogenesis of NASH: The Impact of Multiple Pathways. Current hepatology reports, 17(4), pp. 350-360.

O'CONNOR, C., 2008. Cell Division: Stages of Mitosis. Nature Education 1(1):188.

PAIS, R. and MAUREL, T., 2021. Natural History of NAFLD. Journal of clinical medicine, 10(6), pp. 10.3390/jcm10061161.

PALAIOLOGOU, M., KOSKINAS, J., KARANIKOLAS, M., FATOUROU, E. and TINIAKOS, D.G., 2012. E2F-1 is overexpressed and pro-apoptotic in human hepatocellular carcinoma. Virchows Archiv : an international journal of pathology, 460(5), pp. 439-446.

PARADIS V, ZALINSKI S, CHELBI E, GUEDJ N, DEGOS F, VILGRAIN V, ET AL., 2009. Hepatocellular carcinomas in patients with metabolic syndrome often develop without significant liver fibrosis: a pathological analysis. Hepatology; 49:851–859.

PARK, E.J., LEE, J.H., YU, G.Y., HE, G., ALI, S.R., HOLZER, R.G., OSTERREICHER, C.H., TAKAHASHI, H. and KARIN, M., 2010. Dietary and genetic obesity promote liver inflammation and tumorigenesis by enhancing IL-6 and TNF expression. Cell, 140(2), pp. 197-208.

PEDRO CARRERA-BASTOS1 MAELAN FONTES-VILLALBA1 JAMES H O'KEEFE2 STAFFAN LINDEBERG1 LOREN CORDAIN3, The western diet and lifestyle and diseases of civilization. Research Reports in Clinical Cardiology 2011:2 15–35, .

PETRELLI, A., PERRA, A., SCHERNHUBER, K., CARGNELUTTI, M., SALVI, A., MIGLIORE, C., GHISO, E., BENETTI, A., BARLATI, S., LEDDA-COLUMBANO, G.M., PORTOLANI, N., DE PETRO, G., COLUMBANO, A. and GIORDANO, S., 2012. Sequential analysis of multistage hepatocarcinogenesis reveals that miR-100 and PLK1 dysregulation is an early event maintained along tumor progression. Oncogene, 31(42), pp. 4517-4526.

PETTINELLI, P. and VIDELA, L.A., 2011. Up-regulation of PPAR-gamma mRNA expression in the liver of obese patients: an additional reinforcing lipogenic mechanism to SREBP-1c induction. The Journal of clinical endocrinology and metabolism, 96(5), pp. 1424-1430.

PUCHALSKA, P. and CRAWFORD, P.A., 2017. Multi-dimensional Roles of Ketone Bodies in Fuel Metabolism, Signaling, and Therapeutics. Cell metabolism, 25(2), pp. 262-284.

RABINOVICH, A., JIN, V.X., RABINOVICH, R., XU, X. and FARNHAM, P.J., 2008. E2F in vivo binding specificity: comparison of consensus versus nonconsensus binding sites. Genome research, 18(11), pp. 1763-1777.

RAFF, E.J., KAKATI, D., BLOOMER, J.R., SHOREIBAH, M., RASHEED, K. and SINGAL, A.K., 2015. Diabetes Mellitus Predicts Occurrence of Cirrhosis and Hepatocellular Cancer in Alcoholic Liver and Non-alcoholic Fatty Liver Diseases. Journal of clinical and translational hepatology, 3(1), pp. 9-16.

RANGEL-HUERTA, O.D., PASTOR-VILLAESCUSA, B. and GIL, A., 2019. Are we close to defining a metabolomic signature of human obesity? A systematic review of metabolomics studies. Metabolomics: Official journal of the Metabolomic Society, 15(6), pp. 93-019-1553-y.

REEVES, H.L., ZAKI, M.Y. and DAY, C.P., 2016. Hepatocellular Carcinoma in Obesity, Type 2 Diabetes, and NAFLD. Digestive diseases and sciences, 61(5), pp. 1234-1245.

RHIND, N. and RUSSELL, P., 2012. Signaling pathways that regulate cell division. Cold Spring Harbor perspectives in biology, 4(10), pp. 10.1101/cshperspect.a005942.

RIBAS, V., GARCIA-RUIZ, C. and FERNANDEZ-CHECA, J.C., 2016. Mitochondria, cholesterol and cancer cell metabolism. Clinical and translational medicine, 5(1), pp. 22-016-0106-5. Epub 2016 Jul 25.

RUI, L., 2014. Energy metabolism in the liver. Comprehensive Physiology, 4(1), pp. 177-197.

RUIZ, J.I. and OCHOA, B., 1997. Quantification in the subnanomolar range of phospholipids and neutral lipids by monodimensional thin-layer chromatography and image analysis. Journal of lipid research, 38(7), pp. 1482-1489.

SALOMAO M, REMOTTI H, VAUGHAN R, SIEGEL AB, LEFKOWITCH JH, MOREIRA RK., 2012. The steatohepatitic variant of hepatocellular carcinoma and its association with underlying steatohepatitis. . Hum Pathol.;43(5):737-746., .

SALOMAO, M., YU, W.M., BROWN, R.S.,Jr, EMOND, J.C. and LEFKOWITCH, J.H., 2010. Steatohepatitic hepatocellular carcinoma (SH-HCC): a distinctive histological variant of HCC in hepatitis C virus-related cirrhosis with associated NAFLD/NASH. The American Journal of Surgical Pathology, 34(11), pp. 1630-1636.

SANTONI-RUGIU, E., JENSEN, M.R. and THORGEIRSSON, S.S., 1998. Disruption of the pRb/E2F pathway and inhibition of apoptosis are major oncogenic events in liver constitutively expressing c-myc and transforming growth factor alpha. Cancer research, 58(1), pp. 123-134.

SAPONARO, C., GAGGINI, M., CARLI, F. and GASTALDELLI, A., 2015. The Subtle Balance between Lipolysis and Lipogenesis: A Critical Point in Metabolic Homeostasis. Nutrients, 7(11), pp. 9453-9474.

SCHREURS, M., KUIPERS, F. and VAN DER LEIJ, F.R., 2010. Regulatory enzymes of mitochondrial beta-oxidation as targets for treatment of the metabolic syndrome. Obesity reviews: an official journal of the International Association for the Study of Obesity, 11(5), pp. 380-388.

SCHULZE, K., IMBEAUD, S., LETOUZE, E., ALEXANDROV, L.B., CALDERARO, J., REBOUISSOU, S., COUCHY, G., MEILLER, C., SHINDE, J., SOYSOUVANH, F., CALATAYUD, A.L., PINYOL, R., PELLETIER, L., BALABAUD, C., LAURENT, A., BLANC, J.F., MAZZAFERRO, V., CALVO, F., VILLANUEVA, A., NAULT, J.C., BIOULAC-SAGE, P., STRATTON, M.R., LLOVET, J.M. and ZUCMAN-ROSSI, J., 2015. Exome sequencing of hepatocellular carcinomas identifies new mutational signatures and potential therapeutic targets. Nature genetics, 47(5), pp. 505-511.

SCHULZE, M., 2019. Metabolic health in normal-weight and obese individuals. Diabetologia volume 62, pages 558–566,

SENNI, N., SAVALL, M., CABRERIZO GRANADOS, D., ALVES-GUERRA, M.C., SARTOR, C., LAGOUTTE, I., GOUGELET, A., TERRIS, B., GILGENKRANTZ, H., PERRET, C., COLNOT, S. and BOSSARD, P., 2019. Beta-Catenin-Activated Hepatocellular Carcinomas are Addicted to Fatty Acids. Gut, 68(2), pp. 322-334.

SHI, Y., WANG, Q., SUN, Y., ZHAO, X., KONG, Y., OU, X., JIA, J., WU, S. and YOU, H., 2020. The Prevalence of Lean/Nonobese Nonalcoholic Fatty Liver Disease: A Systematic Review and Meta-Analysis. Journal of clinical gastroenterology, 54(4), pp. 378-387.

SHIBAHARA, J., ANDO, S., SAKAMOTO, Y., KOKUDO, N. and FUKAYAMA, M., 2014. Hepatocellular carcinoma with steatohepatitic features: a clinicopathological study of Japanese patients. Histopathology, 64(7), pp. 951-962.

SMYTH, G.K., 2004. Linear models and empirical bayes methods for assessing differential expression in microarray experiments. Statistical applications in genetics and molecular biology, 3, pp. Article3-6115.1027. Epub 2004 Feb 12.

SONG, P., KIM, J.H., GHIM, J., YOON, J.H., LEE, A., KWON, Y., HYUN, H., MOON, H.Y., CHOI, H.S., BERGGREN, P.O., SUH, P.G. and RYU, S.H., 2013. Emodin regulates glucose utilization by activating AMP-activated protein kinase. The Journal of biological chemistry, 288(8), pp. 5732-5742.

SONODA, J., MEHL, I., CHONG, L., NOFSINGER, R. and EVANS, R., 2007. PGC-1β controls mitochondrial metabolism to modulate circadian activity, adaptive thermogenesis, and hepatic steatosis. Pnas vol. 104 no. 12 5223-5228

STEFAN, N., HARING, H.U., HU, F.B. and SCHULZE, M.B., 2013. Metabolically healthy obesity: epidemiology, mechanisms, and clinical implications. The lancet.Diabetes & endocrinology, 1(2), pp. 152-162.

SUN, Y. and ZHANG, Z., 2020. In Silico Identification of Crucial Genes and Specific Pathways in Hepatocellular Cancer. Genetic testing and molecular biomarkers, 24(5), pp. 296-308.

SZABO, G. and CSAK, T., 2012. Inflammasomes in liver diseases. Journal of hepatology, 57(3), pp. 642-654.

TOTOKI, Y., TATSUNO, K., YAMAMOTO, S., ARAI, Y., HOSODA, F., ISHIKAWA, S., TSUTSUMI, S., SONODA, K., TOTSUKA, H., SHIRAKIHARA, T., SAKAMOTO, H., WANG, L., OJIMA, H., SHIMADA, K., KOSUGE, T., OKUSAKA, T., KATO, K., KUSUDA, J., YOSHIDA, T., ABURATANI, H. and SHIBATA, T., 2011. High-resolution characterization of a hepatocellular carcinoma genome. Nature genetics, 43(5), pp. 464-469.

TREMMEL, M., GERDTHAM, U.G., NILSSON, P.M. and SAHA, S., 2017. Economic Burden of Obesity: A Systematic Literature Review. International journal of environmental research and public health, 14(4), pp. 10.3390/ijerph14040435.

TSATSOULIS, A & PASCHOU, SA, 2020. Metabolically Healthy Obesity: Criteria, Epidemiology, Controversies, and Consequences. Curr Obes Rep (2020), .

VANDER HEIDEN, M.G., CANTLEY, L.C. and THOMPSON, C.B., 2009. Understanding the Warburg effect: the metabolic requirements of cell proliferation. Science (New York, N.Y.), 324(5930), pp. 1029-1033.

VERMEULEN, K., VAN BOCKSTAELE, D.R. and BERNEMAN, Z.N., 2003. The cell cycle: a review of regulation, deregulation and therapeutic targets in cancer. Cell proliferation, 36(3), pp. 131-149.

VERONA, R., MOBERG, K., ESTES, S., STARZ, M., VERNON, J.P. and LEES, J.A., 1997. E2F activity is regulated by cell cycle-dependent changes in subcellular localization. Molecular and cellular biology, 17(12), pp. 7268-7282.

WALESKY, C., EDWARDS, G., BORUDE, P., GUNEWARDENA, S., O'NEIL, M., YOO, B. and APTE, U., 2013. Hepatocyte nuclear factor 4 alpha deletion promotes diethylnitrosamine-induced hepatocellular carcinoma in rodents. Hepatology (Baltimore, Md.), 57(6), pp. 2480-2490.

WANG, C., RAUSCHER, F.J.,3rd, CRESS, W.D. and CHEN, J., 2007. Regulation of E2F1 function by the nuclear corepressor KAP1. The Journal of biological chemistry, 282(41), pp. 29902-29909.

WARD PS. and THOMPSON CB., 2012. Metabolic reprogramming: a cancer hallmark even warburg did not anticipate. Cancer Cell. 2012 Mar 20;21(3):297-308.

WATKINS, P.A., 1997. Fatty acid activation. Progress in lipid research, 36(1), pp. 55-83.

WEINBERG, R.A., 1995. The retinoblastoma protein and cell cycle control. Cell, 81(3), pp. 323-330.

WENZEL, E.S. and SINGH, A.T.K., 2018. Cell-cycle Checkpoints and Aneuploidy on the Path to Cancer. In vivo (Athens, Greece), 32(1), pp. 1-5.

WISE EM, B.E., 1964. Malic enzyme and lipogenesis. Proc Natl Acad Sci U S A.;52(5):1255-1263,.

World Health Organization data repository. https://www.who.int/topics/obesity; accesed 30 April 2020.

WU, L., TIMMERS, C., MAITI, B., SAAVEDRA, H.I., SANG, L., CHONG, G.T., NUCKOLLS, F., GIANGRANDE, P., WRIGHT, F.A., FIELD, S.J., GREENBERG, M.E., ORKIN, S., NEVINS, J.R., ROBINSON, M.L. and LEONE, G., 2001. The E2F1-3 transcription factors are essential for cellular proliferation. Nature, 414(6862), pp. 457-462.

YAO, G., 2014. Modelling mammalian cellular quiescence. Interface focus, 4(3), pp. 20130074.

YATA, Y., GOTWALS, P., KOTELIANSKY, V. and ROCKEY, D.C., 2002. Dose-dependent inhibition of hepatic fibrosis in mice by a TGF-beta soluble receptor: implications for antifibrotic therapy. Hepatology (Baltimore, Md.), 35(5), pp. 1022-1030.

YOUNES, R. and BUGIANESI, E., 2017. Should we undertake surveillance for HCC in patients with NAFLD? Journal of hepatology.

YOUNOSSI, Z.M., RINELLA, M.E., SANYAL, A.J., HARRISON, S.A., BRUNT, E.M., GOODMAN, Z., COHEN, D.E. and LOOMBA, R., 2021. From NAFLD to MAFLD: Implications of a Premature Change in Terminology. Hepatology (Baltimore, Md.), 73(3), pp. 1194-1198.

YOUNOSSI, Z., TACKE, F., ARRESE, M., CHANDER SHARMA, B., MOSTAFA, I., BUGIANESI, E., WAI-SUN WONG, V., YILMAZ, Y., GEORGE, J., FAN, J. and VOS, M.B., 2019. Global Perspectives on Nonalcoholic Fatty Liver Disease and Nonalcoholic Steatohepatitis. Hepatology (Baltimore, Md.), 69(6), pp. 2672-2682.

ZARRINPAR, A., 2017. Metabolic Pathway Inhibition in Liver Cancer. SLAS technology, 22(3), pp. 237-244.

ZHAN, L., HUANG, C., MENG, X.M., SONG, Y., WU, X.Q., MIU, C.G., ZHAN, X.S. and LI, J., 2014. Promising roles of mammalian E2Fs in hepatocellular carcinoma. Cellular signalling, 26(5), pp. 1075-1081.

ZHANG, R., WANG, L., PAN, J. ET AL., 2018. A critical role of E2F transcription factor 2 in proinflammatory cytokines-dependent proliferation and invasiveness of fibroblast-like synoviocytes in rheumatoid Arthritis. Sci Rep 8, 2623.

ZHANG, Y., XU, N., XU, J., KONG, B., COPPLE, B., GUO, G.L. and WANG, L., 2014. E2F1 is a novel fibrogenic gene that regulates cholestatic liver fibrosis through the Egr-1/SHP/EID1 network. Hepatology (Baltimore, Md.), 60(3), pp. 919-930.

ZHIVOTOVSKY, B. and ORRENIUS, S., 2010. Cell cycle and cell death in disease: past, present and future. Journal of internal medicine, 268(5), pp. 395-409.

.

BASQUE VERSION

LABURPENA

LABURPENA

1. Sarrera eta helburuak

Munduko Osasun Erakundearen (OME) arabera, obesitatea osasun-egoeraren kontrako arriskua da, zeinak gorputzean gehiegizko gantz-pilaketa duen bereizgarritzat eta zeinaren munduko prebalentzia ia hirukoiztu egin den azken 40 urteetan, bai garatutako bai garatu-gabeko herrialdeetan. Gibeleko metabolismoaren asaldurekin lotuta dago, zeinak gibel lipidoen metaketan eta gibel koipetsuaren gaixotasun ez-alkoholikoaren (NAFLD) progresioa ahalbidetzen duten.

NAFLDaren ezaugarria esteatosia edo gibel koipetsu ez-alkoholikoa da, egoera bat zeinean gibeleko TG eduki altua lipidoen pilaketan (batez ere, serumeko gantz azidoen (GA) barneratzea eta *de novo* lipogenesia edo DNL) eta deuseztatze bideen (batik bat, lipidoen oxidazioa edo GAOa eta dentsitate oso baxuko lipoproteinen edo VLDLren kanporaketa) arteko konpentsazio ezak bideratzen duen. Egun, NAFLDa kartzinoma hepatozelularraren (HCC) arrisku-faktore garrantzitsua da. Esteatosiaren baitan garatzen den HCCak **NAFLDarekin loturiko HCC**a izena du eta ezaugarri bereizgarriak ditu (lipido metaketa eta hantura, esaterako) beste etiologia batzuetatik garatutako HCCekin alderatuz gero. HCCan gene-gidari asko daude, tumore-histologiari, zelularen seinalizazio-bidezidorrei eta berprogramazio metabolikoari dagokion ezaugarri hain heterogeneoak azaltzen dituena. NAFLDarekin loturiko HCCaren fenotipoari dagokionez, nabarmentzekoa da obesitateak, berez, asaldura metabolikoak ahalbidetzen dituela, metabolikoki osasuntsua (MHO) den eta ez-osasuntsua den paziente obesoen (MUO) arteko bereizmena egiten duen sinadura metaboliko batekin erlazionatu baita.

E2F trankripzio faktoreen familia, tipikoki ziklo zelularraren erregulatzailea dena, aldaketa metabolikoen arduraduna da ere, zeinak gibeleko egoera patologikoetan eta horri loturiko konplikazio metabolikoetan (obesitatea eta diabetesa, adibidez) gertatzen diren. E2F faktoreetako nahasmenduak deskribatu dira HCCan, gibeleko minbizian duten garrantzia nabarmentzen duena. Ikerketa gehienak E2F1ean oinarritzen dira, azterlanaren arabera, onkogene edo tumore-ezabatzaile moduan deskribatzen dena. E2F2aren kasuan, gehienetan E2F1aren antzekotasun funtzionalarekin erlazionatu izan da. Alabaina, hainbat ikerketek ezagutzera eman dute prozesu batzuk konpartitzen dituzten arren, funtzio batzuk batarenak edo bestearenak direla bakarrik. Ikerkuntza gehiago behar da E2F1 eta E2F2ren arteko

mekanismo komunak eta propioak bereiztu ahal izateko, baita NAFLDarekin loturiko HCCan duten eragina zehazteko ere.

Hori dena kontuan hartuta, proposatu genuen **E2F1ak eta E2F2ak obesitateari loturiko NAFLDaren garapenean eta HCCrako bilakaeran parte hartzen duten bidezidor metabolikoak erregulatzen dituztela**. Testuinguru horretan, lan honen xede nagusiak izan ziren: 1) Ikertzea E2F1ak edota E2F2ak parte hartzen duten obesitarearekin loturiko NAFLDaren garapenean eta HCCaren bilakaeran; 2) E2F1ak edota E2F2ak gidatzen dituzten asaldura metabolikoen mekanismoak identifikatzea NAFLDaren garapenean eta HCCrako bilakaeran; 3) E2F1 eta E2F2 obesitatearekin erlazionatutako NAFLDaren biomarkatzaile goiztiar moduan baliozkotzea.

2. Prozedura esperimentalak

Animalia ereduak *E2f1* knockout (*E2f1*$^{-/-}$), *E2f2* knockout (*E2f2*$^{-/-}$) eta zegokien sagu basati (WT) (129/Sv x C57BL/6) arrak izan ziren. Gibelarentzako kartzinogenikoa den dietilnitrosamina (DEN) intraperitonealki ziztatu zitzaien jaio-osteko 14. egunean eta, titia kendu ondoren, gantzetan aberatsa den dietarekin (HFD) (DEN HFD izeneko taldea) edo oinarrizko dietarekin (DEN CD izeneko taldea) elikatu ziren sakrifikatu ziren arte 3 hilabeterekin NAFLDa ikertzeko edo 9 hilabeterekin HCCa ikertzeko. *E2f1* eta *E2f2* geneen gibeleko adierazpena analizatu zen gibeleko gaixotasunaren fase ezberdinetan WT saguetan. Ikerketa-talde guztietan, gorputzeko hainbat parametro eta janari kontsumoa jaso ziren, gibeleko mina neurtu zen, gibeleko eta serumeko profil lipidikoa analizatu zen, baita gibeleko histologia, fibrosi maila, ziklo zelularraren aktibazioa eta intsulinarekiko erresistentzia (IR). 9 hilabetetako *E2f2*$^{-/-}$ saguetan, gene adierazpenaren profila ebaluatu zen eta, bai 3 bai 9 hilabetetako *E2f2*$^{-/-}$ saguetan, gibeleko lipidoen hornitzean eta eliminazioan parte hartzen duten bidezidorren fluxu metabolikoak analizatu ziren baita ere.

E2F1 eta *E2F2* siRNA bidez isilarazi zen **HepG2 giza hepatoma zelula-lerroan**, triglizerido (TG) edukia eta bere sintesian eta degradazioko fluxu metabolikoak neurtzeko.

Azkenik, E2F1 eta E2F2aren adierazpena ebaluatu zen pazienteen gibel-biopsietan, aurretik histologikoki gibel normala (NL) edo NAFLDa zuten taldeetan klasifikatu zirenak.

3. Emaitzak

Gorputzeko pisuaren neurketak eta gantz ehun zuriaren (GEZ) indizeak erakutsi zuten HFD dietak obesitatea induzitu zuela 3 hilabetetako saguetan eta baldintza hori areagotu zela saguak zaharragoak ziren heinean. Bereziki, gorputz-pisuaren handitzea ez zen janari-kontsumoa areagotzearen ondoriozkoa izan. Lipido-edukiaren azterketak erakutsi zuen efektu hori gibeleko triglizerido (TG), diglizerido (DG) eta kolesteril esterren (CE) pilaketarekin bat zetorrela, hots, NAFLDaren garapenarekin. HFD elikatzeak NAFLD-HCCren bilakaera ere sustatu zuen sagu-ereduetan. Aitzitik, emaitzek erakutsi zuten DENek induzitutako HCCa ez zegoela obesitatearekin edo NAFLDaren garapenarekin lotuta. Bakarrik HFDa ematea tratamendu kartzinogenikorik txikiena izan zen, hala ere, lipidoetan aberatsa den dieta batekin elikatzeak DENak induzitutako HCCa areagotu zuen tumore kantitateari eta tamainari dagokionez. Ezaugarri histopatologikoekin bat, gibeleko lipidoen metaketa (TG eta CE moduan) nabaria zen NAFLD-HCCa garatu zuten eta DEN HFD ezarri zitzaien saguetan.

Emaitzek erakutsi zutenez, E2f2ak goranzko erregulazioa izan zuen obesitatearekin loturiko NAFLD eta NAFLD-HCC garatu zuten saguetan bakarrik, E2f2 obesitatean induzitzen dela adieraziz gibeleko gaixotasunaren hasierako faseetatik. Hori gibeleko E2F1 eta E2F2ak paziente obesoetan zuten adierazpen areagotuarekin erlazionatzen da, gibeleko gaixotasuna ez zutenean ere ematen den egoera. Horrela, E2F1 eta E2F2ak gibeleko gaixotasunaren iragarletzat duten balioa aditzera ematen da. Nabarmenki, E2F2aren gainadierazpena oraindik handiagoa izan zen behin NAFLDa garatuta zegoela paziente obesoetan, zeinak MUO bezala sailkatzeko irizpideak betetzen zituzten eta beraz, MUO pazienteak E2F2 edukiaren bidez ezberdintzea baimenduko luke.

E2f1 eta E2f2ak obesitatearekin loturiko gibelaren gaixotasunean eginkizun bat zutela zehaztu ondoren (E2F1 eta E2F2aren mailak paziente obesoen eta saguen egoera metabolikoan zuten efektuaren bidez), E2f1 eta E2f2aren zereginak ikertu ziren NAFLDaren eta NAFLD-HCCaren agerpenean eta bilakaeran. *E2f1*$^{-/-}$ eta bereziki *E2f2*$^{-/-}$ saguek tratamendu guztiengatik induzitutako tumoreen garapena ia guztiz ekidin zutela behatu genuen, *E2f1* eta, batik bat, *E2f2*ren absentziak tratamenduek induzitutako hepatokartzinogenesiarekiko babesa ematen dutela adieraziz. Analisi histokimikoak eta lipidoen kuantifikazioak frogatu zutenez, *E2f1* eta *E2f2*aren faltak gibeleko lipidoen metaketa ekidin zuen HCC induzitzeko tratamenduei erantzunez. Antzeko profil metabolikoa nabarmendu zen giza-HCCaren zelula lerroetan *E2F2* isilarazi zenean, baina ez *E2F1* isilaraztean. *E2f1* eta bereziki *E2f2*ren defizientziak 3 hilabetetan garatutako hepatoesteatositik babestu zituen saguak baita ere, ziklo zelularra aktibo ez

zegoenean, E2f1 eta E2f2ren eginkizun metabolikoa aditzera ematen duena. NAFLD aurrerakoiaren prebentzioarekin bat, gene adierazpenak eta analisi histokimikoak jakinarazi zuten *E2f1* eta *E2f2*ren absentziak eragozten zituela bai *Tfgb1*-bidezko fibrosia bai *Il1b*-bidezko hantura, zeinak obesitatearekin loturiko NAFLD eta NAFLD HCCaren azterketa-ereduetan nabarmen ziren.

E2f2ren parte-hartzea obesitatearekin loturiko gibel-gaixotasunaren garapenean E2f1arena baino garrantzitsuagoa izan zen, beraz, E2f2ren absentziak zuen NAFLD-HCCa garatzeko erresistentziarekin loturiko transkripzio-programa ikertu genuen. Bertatik ezagutu genuen esanguratsuki gehien gainadierazi ziren geneak lipidoen katabolismoan eta energia ekoizpenean taldekatzen zirela, HCCan tipikoki induzitzen diren bidezidorrak hain zuzen ere. Bestalde, beheranzko adierazpena zuten *locus*ak ziklo zelularrarekin, apoptosiarekin eta lipidoen sintesiarekin erlazionatzen ziren. Hori guztia bat dator *E2f2*ren absentziak NAFLDa eta erlazionatutako HCCa ez garatzeko saguetan ematen duen babesarekin.

*Mikroarray*eko datuetan oinarrituz, gibeleko lipidoen sustatzean eta irteeran jarduten duten bidezidorrak analizatu ziren. Lipidoen deuseztatze-bideei dagokienez, E2F2ren defizientzia GAen oxidazio (GAO) maila altuekin erlazionatu zen giza-tumore zeluletan eta saguen gibeletan, β-oxidazioaren erreakzioetako eta GAen aktibazioko geneen handitutako adierazpenarekin batera. Bereziki, GAOren pausu mugatzailean parte hartzen duen eta obesitatean hepatokartzinogenesiaren sustatzaile den CTP2 gene eta proteinaren adierazpenak beheranzko erregulazioa zuen NAFLD eta NAFLD-HCCaren sagu-ereduetan eta goranzko erregulazioa zuen *E2f2* defizientea zenean. Gainera, NAFLDan eta NAFLD-HCCan gertatzen denaren kontrara, *E2f2*ren absentzia HNF4-α-ren gainadierazpenarekin erlazionatuta zegoen, hartzaile nuklear bat zeina GAOa eragiten duen eta HCCaren inhibizioan zeregin bat duen. Hortaz, emaitzek iradokitzen dute E2f2ak gibel-gaixotasuna garatzetik eskaintzen duen babesean jarduten duen mekanismo nagusietako bat areagotutako GAOa dela, zeina handitutako mitokondrioarekiko GAen garraioaren bidez ematen den. Zelulek ATP gehiago behar izatekotan, GAOtik eta azido trikarboxilikoaren ziklotik (ATZ) eskuratutako ahalmen erreduzitzailea fosforilazio oxidatzailera (oxphos) bideratzen da. Prozesu horrekin erlazionatutako hainbat genek adierazpen baxua zutela behatu genuen obesitatearekin lotutako HCCan eta induzituta zeudela *E2f2*an defizienteak ziren saguen gibeletan. *Oxphos*a gidatzen duen eta obesitateak induzitutako esteatosia erregulatzen duen PGC-1β-ren adierazpen patroia antzekoa zen.

Lipidoen hornitze bideei dagokionez, [^{3}H]-glizerolaren eta GAen esterifikazioaren emendapenak, PPAR-γ gene eta proteinaren baita lipidoen garraioan eta biltzean jarduten duten bere itu geneen

gainadierazpenarekin batera, adierazten dute TGaren biosintesia NAFLDa eta HCCarekiko bilakaera sustatzen duen beste mekanismo bat dela. DEN HFD tratamendua ezarritako *E2f2* gabeko saguen gibeletan, parametro guzti horiek gutxiegituta zeuden, iradokitzen duenak *E2f2*ren absentziak tratamenduak induzitutako lipogenesia galarazten duela. [^{3}H]-azetatoarekin ebaluatutako TGaren *de novo* lipogenesia (DNL) ez zegoen aldatuta DEN HFD ezarritako *E2f2*$^{-/-}$ saguetan, *E2f2*ren faltarekin erlazionatutako TGaren biosintesi murriztua esterifikazioaren asalduragatik izan zela adieraziz eta ez DNL gutxiagotzeagatik.

Emaitzek iradoki zuten dislipemiak garrantzia handia zuela NAFLDan eta HCCarekiko bere bilakaeran, izan ere, TG eta GA serikoen maila handiagotua zegoen DEN HFD ezarritako saguetan. Aitzitik, dislipemia ez zuen VLDLren gibeleko kanporaketaren asaldurak eragin, gibeleko VLDL jariapena baita *Apob* eta *Apoe*ren adierazpenak aldatu gabe mantendu zirelako. GEZaren lipolisia, energia premian gibelaren eta gantz-ehunak ez direnen GA hornitzailea, ez zen parte-hartzen zuen bidezidorra ezta ere, GEZaren indizea handituta baitzegoen obesitatearekin loturiko NAFLDa zuten WT saguetan kontrolekin alderatuz gero. NAFLD eta NAFLD-HCCa garatu zuten saguetan serumeko lipido-profila asaldatuta egon arren, goratutako *Lpl* adierazpenak iradokitzen du serumeko TGaren gibeleko katabolismoa handituta zegoela, gibelean lipido metaketa eta HCCa garatzea ahalbidetzen duen egoera. E2F2ren zereginari dagokionez, emaitzek adierazten dute *E2f2*ren absentziak saguak dislipemiatik eta odol-TGaren gibeleko ezabatzetik babesten dituela. Izan ere, GA eta TG serikoen maila ez zen altua baldintza proesteatotikoak ezarritako *E2f2*$^{-/-}$ saguetan, nahiz eta GEZaren lipolisia handituta egon, GEZ indizea txikiagotua eta gibeleko *Lpl* adierazpenaren erregulazioa baxuagoa izan.

Orohar, gibeleko GAOa, lipidoen sintesia eta TGen xurgapena, obesitatearekin loturiko HCCan nahasita dauden bidezidorrak dira eta asaldatuta daude gibeleko gaixotasunaren fase goiztiarretan baita ere, E2F2 gainadierazita dagoen egoera hain zuzen. Jakinik *E2f2*ren ezabatzeak NAFLD aurrerakoiarekin erlazionatutako profil metabolikotik saguak babesten zituela (1. Irudia), iradokitzen dugu E2F2ak NAFLDari loturiko HCCa baino lehenago gertatzen den metabolismoaren moldaketa gidatzen duela. Aurkikuntza

honen garrantzia E2F2 obesitatearekin erlazionatutako gibel-gaixotasunaren biomarkatzaile goiztiarra izatean datza.

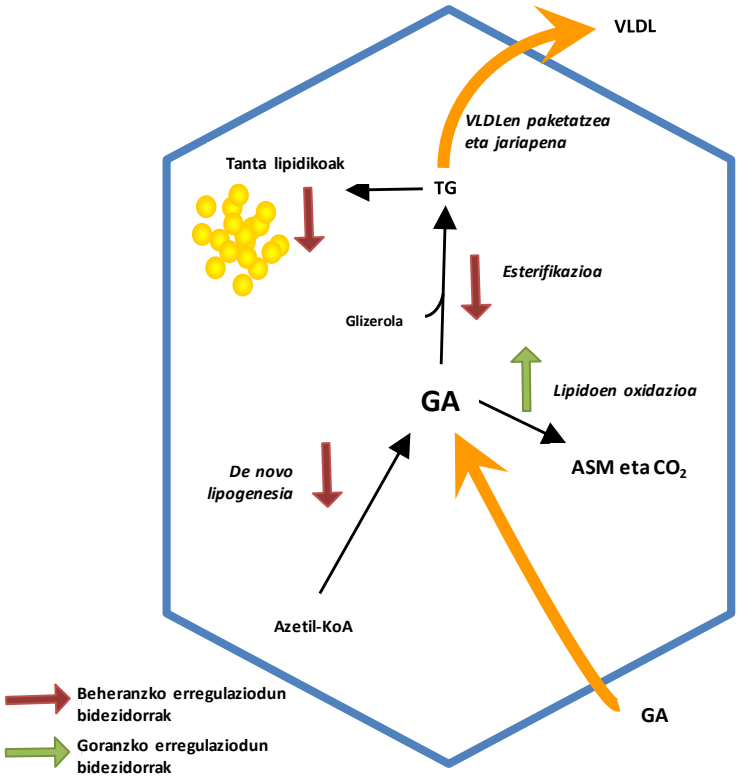

1. irudia. Obesitatearekin lotutako NAFLDa eta HCCrako bilakaera ekiditeko *E2f2*$^{-/-}$ saguaren gibelean ematen den GAen metabolismoaren irudikapen eskematikoa. ASM, metabolito solugarri azidoak; GA, gantz azidoa; HCC, kartzinoma hepatozelularra; TG, triglizeridoa; NAFLD, gibel koipetsuaren gaixotasun ez-alkoholikoa.

Azkenik, obesitatearen eta NAFLDaren konplikazio metabolikoek II motako diabetes mellitusa (IIMDM) barruan hartzen dute, zeina intsulinarekiko erresistentziatik (IR) eratortzen den eta NAFLD pazienteetan HCCa pairatzeko arriskua handitzen duen egoera. Gainera, jadanik deskribatuta dago E2F1ak glukosaren homeostasia mantentzean eta diabetesa ekiditean jarduten duela. Beraz, jakin nahi izan genuen NAFLDaren fase goiztiarrean eta HCCrako bilakaerak IRa ahalbidetzen bazuen eta E2f1 edota E2f2ak horretan zereginik bazuten. Dagokien tolerantzia testek erakutsi zuten IRa garatu zela DENarekin konbinaturiko edo ez konbinaturiko HFD dieta laburra ezartzeagatik NAFLDa zuten WT sagu obesoetan, dietak-induzitutako egoera dela adieraziz. *E2f1* eta *E2f2*ren absentziak NAFLDa induzitzeko tratamentuari loturiko IRa garatzea saihestu zuten saguetan, baina ez NAFLD-HCCa induzitzeko tratamenduari erlazionaturikoa.

4. Ondorioak

1. **E2F1 eta, bereziki, E2F2 transkripzio faktoreek obesitateari loturiko NAFLDaren garapenean eta HCCrako bilakaeran jarduten dute.**
   1.1. Bai E2F1 bai E2F2 gainadierazita daude NAFLDa duten paziente obesoetan eta *E2f2* gainadierazita dago baita ere obesitatearekin erlazionatutako NAFLDaren eta NAFLDari loturiko HCCaren sagu-ereduetan, zeinak transkripzio faktore hauek proesteatotikoak eta onkogenikoak direla iradokitzen duen.
   1.2. E2f1 eta, batik bat, E2f2aren absentziak obesitatearekin loturiko NAFLDaren garapena prebenitzen du. *E2f1* edo *E2f2* faltan duten saguek ez dute hepatoesteatosirik ezta NAFLDren indukzio-tratamenduek eragindako gibel-hanturarik, transkripzio faktore hauek obesitatearekin lotutako NAFLDan premiazkoak direla erakutsiz.
   1.3. *E2f1* eta E2f2aren defizientziak erresistentzia ematen du NAFLDarekin loturiko HCCarekiko eta horrekin erlazionatutako fibrosiarekiko eta lipido metaketarekiko, bai E2f1 bai E2f2a prozesu horietan beharrezkoak direla adieraziz.
2. **E2f2 transkripzio faktoreak obesitatearekin loturiko NAFLDaren garapenean eta HCCarekiko bilakaeran ematen den berprogramazio metabolikoa koordinatzen du.**
   2.1. E2f2ak gibeleko lipido-biltegiratzean ekiten duten bidezidor metabolikoak kontrolatzen ditu gibel-gaixotasunaren fase goiztiarretik. Babes mekanismo bezala, saguetako *E2f2*aren defizientziak NAFLD eta NAFLD-HCCarekin lotutako dislipemia eta areagotutako TGen sintesia baita xurgapena saihesten ditu. Bestalde, handitutako GAOak NAFLDarekiko eta HCCarekiko erresistentzia ahalbidetzen du *E2f2* knockout saguetan, areagotutako mitokondrioarekiko GAen garraioaren bidez.
   2.2.Profil lipidikoa hobetzeaz gain, *E2f2*aren defizientziak obesitatearekin lotutako NAFLDaren fase goiztiarretako IRa prebenitzen du saguetan, baina ez NAFLD-HCCarekin erlazionaturikoa.

3. **E2F1 eta, batez ere, E2F2a obesitatearekin lotutako NAFLDaren markatzaile prognostiko eta potentzialak dira.** E2F1 eta E2F2 NAFLDa duen ala ez duen obesitatean induzitzen dira. Gainera, gibeleko E2F2 edukiaren handitzea oraindik ere nabarmenagoa da NAFLD garatzen denean.

A atala. SARRERA

A. SARRERA

1.Gibela

1.1. Gibelaren egitura eta anatomia

Gibela giza gorputzaren bigarren organo eta guruinik handiena da eta gorputzaren pisuaren %2,5 dauka (Juza, Pauli 2014). Diafragma behean kokatzen da, abdomen-barrunbearen goi-eskuinaldean, digestio-hodi eta gorputz osoko odol-fluxuaren ondoan hain zuzen ere. Gibelak daukan kokapen estrategikoak metabolismo organikoa erregulatzea ahalbidetzen dio.

Parenkima gibelaren egitura funtzionala da eta lau lobuluk osatzen dute (eskuinekoak, ezkerrekoak, lauak eta kaudalak edo Spiegel lobuluak) (Arias, Wolkoff et al. 2009, Malarkey, Johnson et al. 2005) (*B1.A irudia*). Glissonen kapsulak, parenkima inguratzen duen ehun konektibozko geruzak, lobulu bakoitza **lobuluxka** deritzon egitura hexagonaleko unitateetan banatzen du (*B1.B irudia*). Lobuluxkek zain hepatiko zentral bat daukate eta ertzean, triada portala izeneko egitura bat, porta zainaren adar batek, arteria hepatikoaren adar batek eta behazun-duktoaren adar batek osatzen dutena. Erdiko zaina eta porta triadaren artean sinusoide eta hepatozito ilarak daude (Remak trabekulak edo lerroak), eta ilara hauen artean, zelula endotelialak eta Disse espazio perisinusoidala aurkitzen dira.

Gibeleko unitate funtzionala eta mikrozirkulatzailea **azino hepatikoa** da (*B1.D irudia*), bi erdiko zainen artean hedatzen den eta porta triada bi lotzen dituen espazio parenkimala. Triadarekiko dagoen distantziaren arabera, oxigeno-kontzentrazio gradiente bat ezartzen da eta beraz, azino hepatikoa hiru eskualdetan banatzen da: periportala (1), bitartekoa (2) eta peribenosoa (3).

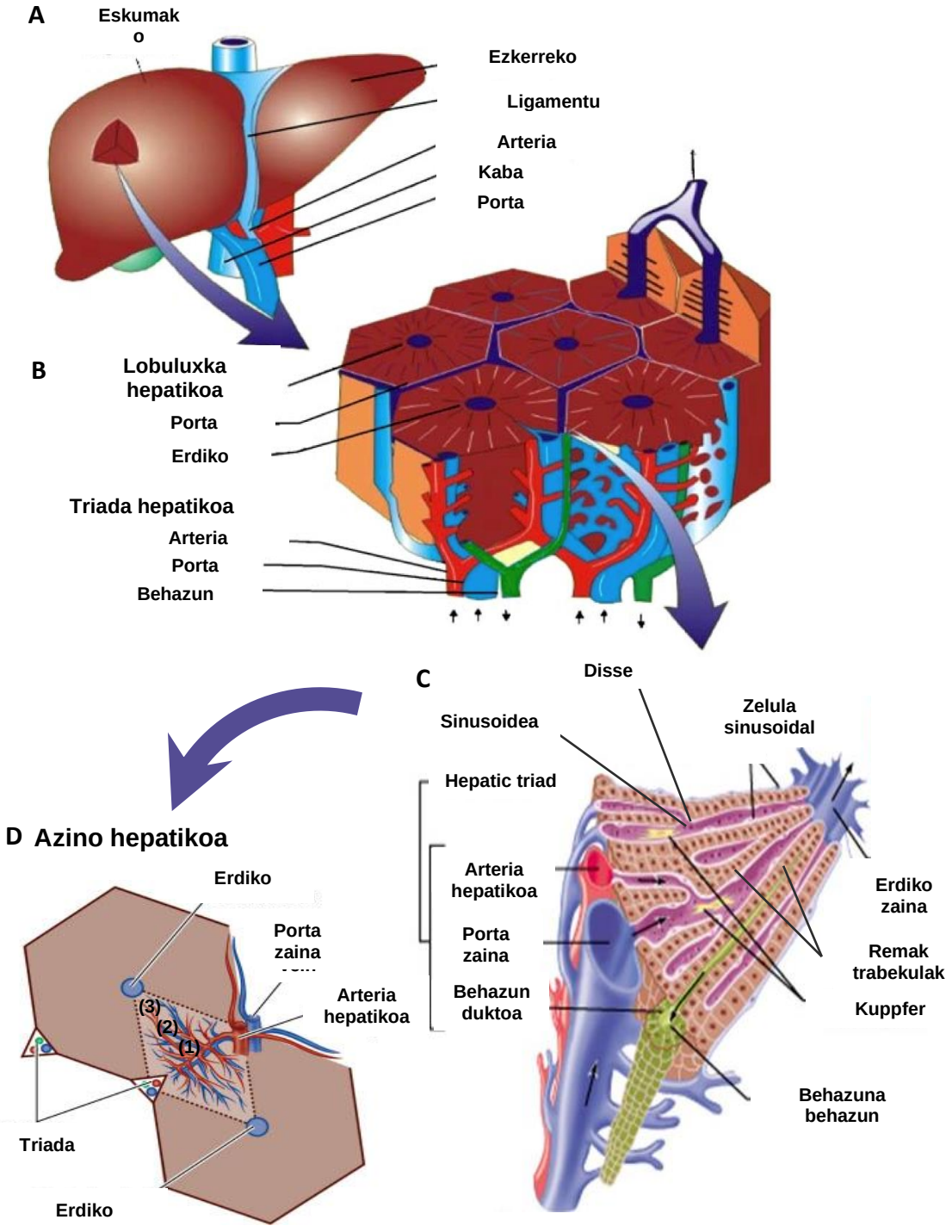

B1 irudia. Gibela (A) era bere unitate estrukturala (B, C) eta funtzionala (D): lobuluxka eta azinoa. Azino hepatikoa puntudun lerro batez adierazita dago. Eskualdeak horrela adierazita daude: (1) periportala, (2) bitartekoa and (3) peribenosoa. Irudia https://bio.mox.polimi.it/nanomedicine/perfusion-characteristics-liver-tissue/ eta https://medicine.academic.ru/99185/hepatic_acinus webgunetatik moldatuta dago.

Gibela bi taldetan banatzen diren zenbait **zelulaz** osatuta dago: zelula parenkimalak eta zelula ez-parenkimalak. Zelula parenkimalak edo **hepatozitoak** gibeleko bolumen osoaren %80a osatzen dute eta ehunaren funtzio sintetiko eta metaboliko askoren arduradunak dira (*B2 irudia*). Hiru espezialitate molekularren arabera, domeinuka polarizatzen dira. Domeinu kanalikularra edo apikala behazunaren jariaketan espezializatua dago eta domeinu basolaterala edo sinusoidala, aldiz, odolaren eta hepatozitoen arteko substantzien trukaketa gertatzen den tokia da, adibidez, lipidoen jariaketa. Alboko domeinuari dagokionez, zelulen atxikiduraren arduraduna da. Betetzen dituzten funtzio metabolikoak ugariak direnez, hepatozitoek organulu kopuru handia dute zitoplasman.

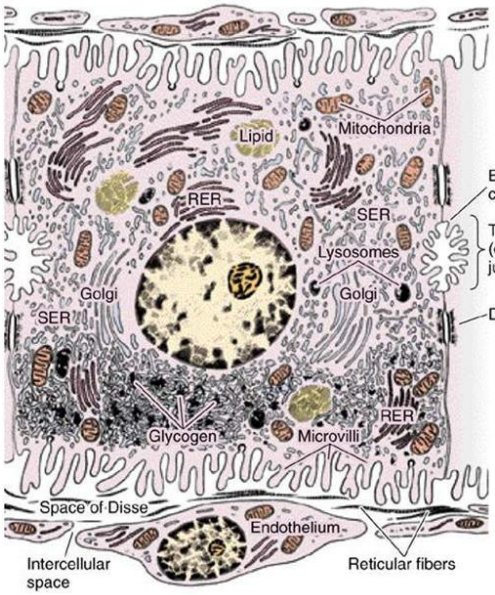

B2 irudia. Hepatozitoaren irudikapen eskematikoa. RER, erretikulu endoplasmatiko pikortsua; SER, erretikulu endoplasmatiko leuna. http://intranet.tdmu.edu.ua/data/kafedra/internal/histolog/classes_stud/en/stomat/ptn/1/17%20Digestive%20system.htm webgunetik moldatutako irudia.

Zelula ez-parenkimalak edo **sinusoidalak** hurrengokoak dira: 1) zelula endotelialak (porta aldeko odolaren eta hepatozitoen arteko substantzien elkartrukean parte hartzen dute), 2) Kupffer zelulak (sortzetiko inmunitate sisteman parte hartzen duten makrofago fagozitikoak), 3) zelula estelatuak edo Ito zelulak (gantz-biltegi zelulak dira eta matrize extrazelularraren osagaiak jariatzen dituzte, fibrogenesian parte hartuz), 4) zelula linfoideak edo Pit zelulak (zelula hiltzaileak edo *natural killer* motako linfozitoak), 5) behazun epitelioa.

Egitura heterogeneoaz eta konplexutasun funtzionalaz gain, gibelak birsortzeko gaitasuna du, kalte zelularraren aurreko konpentsazio-mekanismoa dena (Mao, Glorioso et al. 2014). Bestelako prozesu metaboliko ugari ere burutzen dira gibelean: gorputz osoko amonioaren eta bikarbonatoaren

homeostasiaren mantentzea, xurgatutako nutrienteen eta xenobiotikoen prozesatzea, behazun-azidoaren sintesia eta behazunaren eraketa, plasma-proteina gehienen sintesia, seinale molekula eta hormonen biltegiratzea eta prozesatzea, baita organismoaren erantzun immunologiko akutuan parte-hartzea (Arias, Wolkoff et al. 2009, Malarkey, Johnson et al. 2005).

Gainera, gibelak funtsezko zeregina dauka **metabolismo energetikoaren** erregulazioan eta metabolikoki beste ehun batzuekin konektatuta dagoen ardatza da (Betts, Young et al. 2013, Rui 2014). Izan ere, gibela proteinak, lipidoak eta karbohidratoak sintetizatu, metabolizatu, deuseztatu eta banatzearen arduraduna da. **Oreka energetikoa positiboa** denean (egoera postprandiala), gibelak gorputzeko energia biltegiak berrezartzen ditu glikogeno eta triglizeridoekin (TG), bai gibelean bai gantz-ehun zurian (GEZ). Areagotzen diren beste bide kataboliko batzuk kolesterogenesia eta aminoazidoen sintesia dira. Aminoazidoak proteinen eta bestelako nitrogeno-konposatuen aitzindariak dira. Glukosaren oxidazio hepatikoa da erreakzio anaplerotiko horietarako beharrezko energia eta molekula erreduzitzaileen iturria. Bestalde, **oreka energetikoa negatiboa** denean (baraualdian edo jarduera fisikoa egiterakoan), gibelak glukosa eta gorputz zetonikoak (GZ) jariatzen ditu, funtsezko erregai metabolikoak direnak burmuina, giharrak eta bihotza bezalako ehun extraheptikoentzat. Horretarako energia-iturria gantz-azidoen (GA) oxidaziotik lortzen da. Biltegi hepatikoetatik askatzeaz gain, glukosa eta GAk gibelean sintetizatu egiten dira GEZetik eta giharretatik datozen aintzindarietatik abiatuz. Energia-metabolismoa gibelean zeharo erregulatuta dago hainbat hormonen, seinale neuronalen eta elikagaien bidez. Egoera postprandialeko erreakzioak intsulinak eta glukosak zuzentzen dituzte batez ere eta glukagonak, berriz, elikagai gabeziako koordinazio metabolikoaren ardura dauka. Energia-metabolismoaren kontrolean gertatutako edozein asaldura gaixotasun metabolikoekin lotuta egon daiteke, hala nola, gibel koipetsuaren gaixotasun ez-alkoholikoa (ingelesezko *non-alcoholic fatty liver disease* edo NAFLD) edota II motako diabetes mellitus (2MDM) (Jones 2016).

1.2.Lipidoen metabolismoa gibelean

Aipatu bezala, gibela gorputz osoaren metabolismoa modulatzen duen organo zentrala da eta metabolismo lipidikoaren erregulazioan funtsezko zeregina dauka. Baldintza fisiologikoetan, gibeleko lipido-edukiera maila baxuan eta konstantean mantentzen da lipido sintesiaren eta deuseztatzearen arteko oreka aproposa delako (Kawano, Cohen 2013). Gibelean lipidoak eskuratzeko bidezidor metaboliko nagusiak odoleko GA askeen xurgapena eta TGaren *de novo* lipogenesia (DNL) dira. Aldiz, GAen oxidazioaren bidezko TGaren degradazioa eta dentsitate oso txikiko lipoproteina (VLDL) bidezko TGaren jariaketa dira gibelean lipidoak deuseztatzeko biderik garrantzitsuenak (*B3 irudia*).

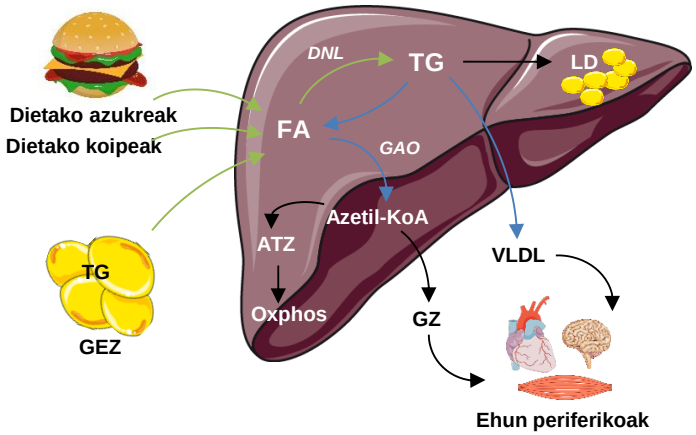

B3 irudia. Gibelean metabolismo lipidikoa erregulatzen duten bidezidor nagusiak. Lipido-horniketa bideak gezi berdeekin adieerazten dira eta lipidoen deuseztatzerako bideak gezi urdinekin. ATZ, azido trikarboxilikoaren zikloa; DNL, *de novo* lipogenesia; GA, gantz azidoak; GAO, gantz azidoen oxidazioa; GEZ, gantz-ehun zuria GZ, gorputz zetonikoak; LD, tanta lipidikoak; Oxphos, fosforilazio oxidatzailea; TG, triglizeridoa; VLDL, dentsitate oso baxuko lipoproteina.

Gibeleko **GAen xurgapen-tasa** odoleko GAen kontzentrazioaren araberakoa da, zeina GEZaren lipolisiaren menpekoa den aldi berean (Kawano, Cohen 2013). GEZa eukariotoen funtsezko TG biltegia da eta lipolisi izeneko prozesua organo honetan gertatzen da hain zuzen ere. Prozesu horretan, TGaren hidrolisia gauzatzen da eta produktuak diren GA-ak eta glizerol molekulak zirkulaziora askatzen dira (Duncan 2007). GEZaren liposia baraualdian areagotzen den bidezidorra da batik bat, izan ere, gainerako ehunek GA-ak eta glizerol molekulak energia-iturri moduan erabiltzen dituzte. GAen absortzioa hepatozitoek duten GA-ak xurgatzeko ahalmenaren araberako ere bada, FATP5 izeneko mintz plasmatikoko garraiatzailearen edota CD36 glikoproteinaren bidez burutzen den prozesua (Kawano, Cohen 2013).

Lipido hepatikoen bigarren iturri nagusia **DNL**a da. Dieta-azukreak (glukosa eta, batez ere, fruktosa) GA berriak sintetizatzeko erabiltzen da. Glikolisiaren eta pirubatoaren oxidazioaren bidez, glukosa katabolizatu egiten da azetil-KoA molekula eman arte (Kawano, Cohen 2013). Orduan, azetil-KoA karboxilasak (ACC), bidezidorraren entzima mugatzailea dena, azetil-KoA molekula karboxilatuko du eta bertatik eratzen den malonil-KoA molekula, ostean, palmitatora eraldatuko da GA sintasa (GAS) entzimaren bidez. Ondoren, kate luzeko GAen elongasa 6 (ELOVL6) eta estearil-KoA desaturasa (SCD1, SCD2) entzimei esker, palmitatoa GA-an bihurtzen da. Azkenean, aziltransferasek hainbat erreakzio burutzen dituzte. Horietan, sintetizatu berri diren hiru GA glizerol-3-fosfatoarekin esterifikatzen dira, hurrenez-hurren, azido fosfatikoa, diglizeridoa (DG) eta TGa eratuz. DNLrako behar den ahalmen erreduzitzailea (NADPH eta $FADH_2$) glukosa-6-fosfato-dehidrogenasak (G6PDH) eta entzima malikoak (ME) katalizatutako erreakzioetatik hornitzen da (Wise EM 1964). NADPHaren eraketak ez du GAen sintesia kontrolatzen. DNLa transkripzio mailan erregulatzen da nagusiki karbohidratoekiko erantzun-elementuei lotzen den proteinaren (ChREBP) eta esterolagatik erregulatutako elementura lotzen den 1c proteinaren (SREBP1c) bidez. Bi proteina horiek glukosak eta intsulinak induzitzen ditu. Horrez gain, peroxisoma proliferatzaileagatik aktibatutako γ hartzaileak (PPAR-γ) gene lipogenikoak ere erregulatzen ditu (Gavrilova, Haluzik et al. 2003).

TG hepatikoaren ezabatze-bide nagusietako bat **β-oxidazio mitokondrialaren** (GAO) bidezko GAen katabolismoa da (Kawano, Cohen 2013). Prozesu horrek, ATPa ekoizteko energia-iturria eskaintzen du odoleko glukosa maila baxua denean. Lehenik, erreaktibotasuna lor dezaten, GAk aktibatu egin behar dira haien A-koentzima eratorriak eratuz. Horretarako, azil-KoA sintetasak (esaterako, Acsm1, Acsm2, Acsl1), seguraski FATPeekin elkarlanean, GAen eraldaketa katalizatzen du gantz azil-KoA motako molekuletara. Ondoren, karnitina palmitoiltransferasek (CPT1 eta CPT2) gantz azil-KoA molekulak matrize mitokondrialera garraiatzen dituzte eta, bertan daudela, GAO zikloan sartzen dira, non azetil-KoA molekulak izan arte zatitzen diren. Ziklo horrek lau entzima mota behar ditu: azil-KoA dehidrogenasak (adibidez, Acadl, Acadm, Acadsb), 2-enoil-KoA hidratasak, 3-hidroxiacil-KoA dehidrogenasak eta 3-oxoacil-KoA tiolasak (Acaa2 esaterako). Ondoren, azetil-KoA molekulak oxidatu egiten dira azido trikarboxiloen zikloan (ATZ) eta eraturiko NADH eta $FADH_2$ molekulak ATPa sortzeko erabiltzen dira fosforilazio oxidatzailean (*oxphos*). Azetil-KoAren gainkarga GZen sintesira bideratzen da, oso oxidatzaileak diren ehun extrahepatikoen (garuna eta bihotza batez ere) erregai alternatiboa baitira barauan (Puchalska, Crawford 2017).

Janondoko egoeran, intsulinaren efektuak GAOa inhibitzen du. Aitzitik, glukagonak GAOa sustatzen du barauan funtsezkoak diren hainbat entzima erregulatuz: AMPagatik aktibatzen den proteina kinasa (AMPK), ACC eta CPT (Kawano, Cohen 2013, Schreurs, Kuipers et al. 2010). Erregulazio transkripzionalari

dagokionez, PPAR-α molekulak paper garrantzitsu bat duela deskribatu da (Kawano, Cohen 2013). Aktibo dagoen PPAR-α molekula X erretinoidearen hartzailearekin (RXR) elkartzen da heterodimeroak eratzeko eta peroxisoma areagotzeilearen erantzun elementuetara (PPREs) lotzeko. PPAR-α molekulak 1α eta 1β motako PPAR-γ-koaktibatzaileekin (PGC) ere elkarrekiten du, zeinak GAOa, *oxphos*a eta mitokondrio-biogenesiaren sustapenean inplikatuak dauden (Finck, Kelly 2006).

Lipido hepatikoaren edukia **VLDL partikulen** bidezko TGaren esportazioak ere oreka dezake (Kawano, Cohen 2013, Ipsen, Lykkesfeldt et al. 2018). VLDL partikula TG eta kolesteril esterretan aberatsa den nukleo hidrofobiko batez osatuta dago. Nukleo hori fosfolipidoz eta kolesterol askeaz konposatutako geruza hidrofiliko batek inguratzen du. VLDL partikula bakoitza B apolipoproteina (ApoB) molekula batekin lotuta dago, gibeletik kanporatu ahal izateko. Horrez gain, E apolipoproteina (ApoE) partikulak ere VLDLtan biltzen dira, odoleko VLDL jariapena eta argitzea erregulatzeko (Getz, Reardon 2009). Behin plasman, VLDL partikulak muskulu eskeletikoa, gantz-ehuna eta bihotza bezalako ehun periferikoak hornitzeko erabiltzen dira. Horretarako, TGa hidrolizatzen da lipoproteina lipasa (Lpl) entzimaren eraginez. VLDL partikula-hondarrak gibelera itzultzen dira, non Lpl hepatikoak beraien xurgapena erregulatzen duen (Liu, G., Xu et al. 2016).

2. *Gibel koipetsuaren gaixotasun ez-alkoholikoa (NAFLD)*

NAFLDaren ezaugarria esteatosia edo gibel koipetsu ez-alkoholikoa da, hau da, hepatozitoen %5ean gutxienez alkohol/medikazio kontsumoaren edota beste gaixotasun batzuen (esaterako, hepatitis birala, lipodistrofia) ondoriozkoa ez den gehiegizko gantz-metaketa. Baldintza-espektro zabala hartzen du, potentzialki progresiboa ez den esteatositik potentzialki progresiboa den esteatohepatitisera edo esteatohepatitis ez-alkoholikora (ingelesezko *non-alcoholic steatohepatitis* edo NASH) hedatzen dena. Aldi berean ematen diren hanturak eta kalte zelularrak (hepatozitoen balonizazioa) determinatzen du NASH. Fibrosi gradu ezberdinak ere bateratu daitezke egoera horretan. Fase larriagoetan, gibeleko gaixotasuna zirrosira edo kartzinoma hepatozelularrera (ingelesezko *hepatocellular carcinoma* edo HCC) bilakatu daiteke (Al-Dayyat, Rayyan et al. 2018). Gibel osasuntsu baten irudikapena, NAFLDaren patogenesiaren fase nagusiekin batera, B4 irudian erakusten da.

B4 irudia. Gibel osasuntsu baten eta NAFLD patogenesiaren fase desberdinen irudikapena. NAFLD, gibel koipetsuaren gaixotasun ez-alkoholikoa; HCC, kartzinoma hepatozelularra. (Baffy 2015) erreferentzian oinarritua.

Kontzeptualizazio hobea lortzeko, adituen nazioarteko kontsentsu batek eritasuna izenez aldatzea proposatu du oraintsu, bada, **disfuntzio metabolikoarekin loturiko gibel koipetsuaren gaixotasunera** (ingelesezko *metabolic-dysfunction-associated fatty liver disease* edo MAFLD) (Eslam, Newsome et al. 2020). Era horretan, MAFLDa sistema anitzeko gaixotasun baten agerpen hepatikotzat hartzen da, gorputz osoko erregulazio metabolikoaren asalduran oinarritzen dena. Gibeleko esteatosiaz gain, MAFLDaren diagnostiko positibo batek honako irizpide bat hartzen du bere baitan: gehiegizko pisua/obesitatea, 2MDM edo erregulazio metabolikoaren asaldura gaixo ez-obesoetan (*B5 irudia*) (Eslam, Newsome et al. 2020). Erregulazio metabolikoaren asalduraren kontzeptua 2.2.1. ataleko B1 taulan zehazten da. MAFLDa beste nahasmendu hepatiko batekin aldiberekotu daiteke, hala nola, hantura, hepatozitoen balonizazioa edota fibrosia (Eslam, Newsome et al. 2020). NAFLDak ez bezala, definizio berriak ez ditu gaixotasun

konkomitanteak edo alkoholaren kontsumoa baztertzen (Eslam, Sanyal et al. 2020). Nolanahi ere, nagusiki alkoholikoak diren zirrosidun pazienteek ez dute entseguetan parte hartzen.

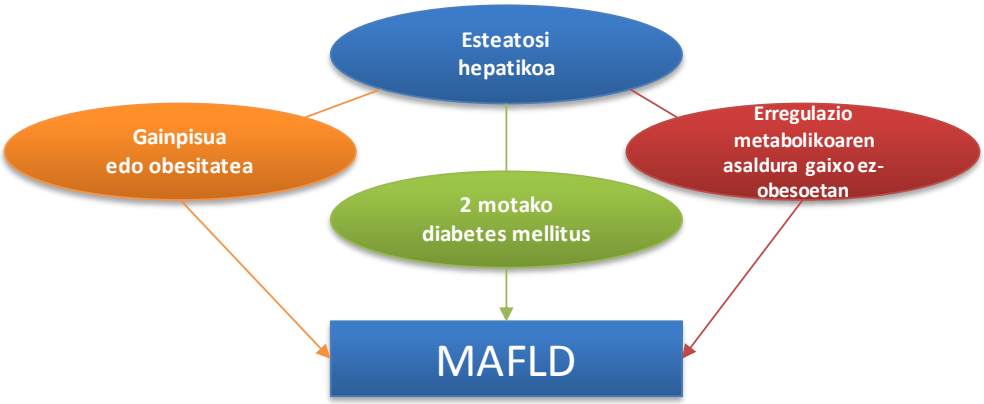

B5 irudia. MAFLDa diagnostikatzeko diagrama. MAFLD, disfuntzio metabolikoarekin loturiko gibel koipetsuaren gaixotasuna. Eslam M. *et al.*, 2020 zitan oinarritua (Eslam, Newsome et al. 2020).

Definizio aldaketak eztabaida handia eragin du. Alde batetik, termino berriak metabolismoaren rola gorentzen duela kontsideratzen da, gaixotasunaren heterogeneotasuna barne hartzen duela (Fouad, Elwakil et al. 2021) eta baliagarritasun klinikoa duela paziente kohorte desberdinetan (Eslam, Newsome et al. 2020). Beste aditu batzuen ustez, ordea, gaixotasunaren patogenesia hobeto ulertzeko balio ez duen termino anbiguoa da. Osasun arloko langileenganako eta politikarenganako kontzientzia oztopatu dezake, zeinak negatiboki eragin baitiezaioke diagnostiko-metodoei eta sendagaien aurkikuntzari buruzko gaixotasunaren kudeaketari (Younossi 2021). Egoera gehiago argitu arte, NAFLD terminoa erabiltzea erabaki zen lan honetan.

NAFLDan ematen den gantz-metaketa modu fidagarrian **diagnostikatu** daiteke zauri txikiko/ odolik gabeko teknikekin (irudi-teknikak, odoleko biomarkatzaileak) edo analisi histologikoekin, gibel-biopsia burutzea beharrezko duena. Alabaina, biopsia da oraingoz dagoen erreminta bakarra NAFLD pazienteetan hepatoesteatosiaren eta NASH egoeren arteko bereizketa zehatza egiteko. Bada, patologo batek aktibitate maila edo NAFLD-aktibitatearen puntuazioa (NAS puntuazioa) neurtu dezake ondorengokoak kontuan hartuz: esteatosi maila, hantura, hepatozito-balonizazioa eta fibrosia (Lindenmeyer, McCullough 2018, Kleiner, Brunt et al. 2005).

Lehen aipatu den bezala, esteatosia **kalte zelularrarekin** batera eman daiteke, NASH egoera deritzona (Noureddin, Sanyal 2018). Gibeleko kaltea hainbat gertaera paralelok eragin dezakete. Lipotoxikotasuna da gidari nagusietako bat, zenbait lipidoren (GA-ak, zeramidak, lisofosfatidilkolina,

kolesterol askea) kontzentrazio altuak erretikulu endoplasmikoaren (ER) estresa eta disfuntzio mitokondriala eragiten baitu. Bi prozesu horiek direla eta, oxigeno espezie erreaktiboak (ROS) eratzen dira, estres oxidatzailea eta hantura sortaraziz. Ondorioz, inflamasoma aktibatzen da, proteina anitzez osaturiko konplexu zitoplasmatikoa zeina arriskuari loturiko eredu molekularrei erantzuten dion. Horrek 1β interleukina (IL1β) eta nekrosi tumoralaren α faktorea (TNF-α) bezalako zitokina hanturarazleen aktibazioa dakar eta ondorioz, zelula-apoptosia (Szabo, Csak 2012). Proteina-konplexu horren aktibitatea NASHarekin lotuta dago, baina ez dago baldintza esteatotikoarekin berez erlazionatuta. Badaude hantura eragin dezaketen kanpo faktore batzuk ere (Noureddin, Sanyal 2018). Adibidez, NASHarekin loturiko gaixotasun metabolikoetan, GEZko intsulinarekiko erresistentziak (IR) 6 motako interleukina (IL6) edo adipokinen askatzea dakar eta heste-mikrobiomaren alterazioak gibeleko efektu hanturarazleak eragiten ditu. Izan ere, hesteetako disbiosiak eragindako hanturak gibeleko lesio kronikoa izatea errazten du NAFLD gaixoengan (Fukui 2019).

Berez, gibeleko kalteak eta hanturak tumore-hazkunderako β faktorearen (TGF- β) seinalizazioa aktibatzen dute, Kupffer zelulak aktibarazten dituena eta ondorioz, zelula estelatuak miofibroblastoetan bereiztea ahalbidetzen duena (Fabregat, Moreno-Caceres et al. Or.). Gero, zelula kanpoko matrizea soberan eratu eta gibelean metatzen da, **fibrosia** eta **zirrosia** eraginez. Azkenik, zirrosiak HCCren garapen edo gibel-hutsegiterako aurrejarrera ezartzen du pazienteengan (Kumar, Priyadarshi et al. 2020).

Ondo definituta dago esteatosia NAFLDa garatzeko beharrezko baldintza dela (Lindenmeyer, McCullough 2018). Historikoki, itzulgarria den egoeratzat hartu izan da eta paziente gehienak hamarkadak diraute asintomatiko, konplikazio klinikorik gabe. Duela gutxi argitaratu den meta-analisi baten arabera, NAFLDak mundu osoko populazio helduaren %25ari erasaten dio eta beraz, gibeleko gaixotasun kronikorik arruntena da, baita osasun arazo garrantzitsua (Kumar, Priyadarshi et al. 2020). NAFLDa zirrosia edota HCC bezalako gibel-eritasun ez-itzulgarriak pairatzeko arrisku-faktore bat da ere. Kasu gehienek ez dute hanturarik izaten inoiz edo denbora-tarte jakin batean izaten dute bakarrik, hala ere, esteatosidun pazienteen %20a NASH moduan sailkatuta dago (Estes, Razavi et al. 2018). NASH kasu batzuk fibrosira azkar eboluzionatzen duten bitartean, beste batzuk ez dute horrelako bilakaerarik izaten. Hantura edo fibrosia duten pazienteek zirrosia edo gibeleko minbizia izateko sentiberatasun handiagoa dutela deskribatu den arren, esteatosidun pazienteen %10ak bakarrik izaten du zirrosia (Kumar, Priyadarshi et al. 2020). Gainera, hepatokartzinogenesia zirrosirik ez baina esteatosia duten gibeletan ager daiteke (Eslam, Sanyal et al. 2020, Reeves, Zaki et al. 2016), gibeleko lipido-metaketaren ahalmen onkogenikoa nabarmenarazten duena (2.3.1. sekzioan deskribatua).

2.1. Lipido-metabolismoaren desoreka NAFLDan

Aipatu bezala, gibeleko metabolismo lipidikoa erabat kontrolpean dago. Beraz, bide hori erregulatzen duten prozeduretan gerta daitekeen edozein desorekak gehiegizko lipido pilaketa eragin dezake eta NAFLDa ahalbidetu. Konkretuki, handitutako TG edukia lipido metaketa- eta eliminazio-prozesuen arteko oreka haustean ematen da.

Jakina da gibeleko TGaren %60a **odoleko GA**etatik datorrela NAFLDan (Donnelly, Smith et al. 2005). Obesitatea edo gainelikadura moduko egoera patogenikoetan, gorputzeko gantz-masa handitzen da eta bai IR bai hantura ematen dira sarritan. Baldintza horiek GEZko TG lipolisia handitzea sustatzen dute eta ondorioz, GA-ak odolera jariatzen dira. Hori lotuta egon daiteke NAFLD pazienteetan agertzen den odoleko GAen igoerarekin (Fabbrini, Mohammed et al. 2008) eta FATP5 baita CD36 proteinen adierazpen hepatiko areagotuarekin (Greco, Kotronen et al. 2008).

Lipidoen hornitze-bide nagusietako bat ez den arren, gibeleko TGaren %14a **dietako gantzetatik** eratortzen da NAFLD-dun pazienteetan (Donnelly, Smith et al. 2005). Hesteetan xurgatutako lipidoak kilomikron izeneko lipoproteinetan garraiatzen dira zirkulazio-sisteman zehar ehun periferikoak hornitu daitezen. Ondoren, gibelak kilomikroi-hondarrak zirkulaziotik deuseztatzen ditu.

DNLa NAFLDa pairatzen duten pertsonengan handitua dagoen prozesu bat da eta gibeleko TG biltegiaren %26a hornitzen du *(*Donnelly, Smith et al. 2005). PPAR-γ proteinak gene lipogenikoak erregulatzen dituenez, NAFLDa garatzen laguntzen du baita ere (Gavrilova, Haluzik et al. 2003).

Emaitza eztabaidagarriak argitaratu dira **oxidazio lipidikoak** gibeleko gaixotasunarengain duen eraginari dagokionez (Ipsen, Lykkesfeldt et al. 2018). GAOaren ikerketek erakutsi dute bidezidor metaboliko hori handituta, aldatu gabe edota txikituta egon daitekeela esteatosia edo NASHa duten pazienteetan. GAOaren nahasmenduez gain, mitokondrioaren egitura eta funtzio aldaketak NAFLD-dun pazienteen ezaugarri dira (Friedman, Neuschwander-Tetri et al. 2018).

Azkenik, desegokiak diren **VLDL**ren muntaiak eta sekrezioak esteatosi hepatikoa ahalbidetzen dute (Ipsen, Lykkesfeldt et al. 2018). Ordea, hipertriglidizemiarekin erlazionatuta daude bai NAFLD-dun pazienteen ezaugarria den VLDLren gehiegizko ekoizpena bai TGetan aberatsagoak diren VLDL partikulen jariapena. Arrunta da baita ere APOBn alterazio genetikoak aurkitzea NAFLD-dun pazienteen artean.

2.2. NAFLDari loturiko arrisku-faktoreak

NAFLDa zenbait **eritasun extrahepatiko**ekin hertsiki erlazionaturik dago, esaterako, sindrome metabolikoa eta bere osagaiak diren obesitatea, dislipemia, hipertentsioa eta 2MDMa (Al-Dayyat, Rayyan et al. 2018). Izan ere, NAFLDaren prebalentzia %90ean dago pertsona obesoetan edo hiperlipidemia dutenetan eta hipertentsioa duten indibiduoen %50ak pairatzen du NAFLDa (Friedman, Neuschwander-Tetri et al. 2018). 2MDMdun pazienteen %70ak baino gehiagok ere NAFLDa dauka (Al-Dayyat, Rayyan et al. 2018). Gainera, munduko NAFLDaren tasa igotzen ari da, obesitatea edo 2MDM, bizimodu sedentarioa eta jarduera fisiko ezaren handitzearekin batera. Egoera horrek gibelari lotutako, kardiobaskular edo edozein kausako heriotz-tasaren handitzea dakar NAFLD-dun pazienteetan (Younossi, Tacke et al. 2019). Nabarmenki, metabolikoki ez-osasuntsua den fenotipoa deskribatu da gorputzeko masaren indizearen (GMI) arabera pisu normala duten indibiduoetan (ingelesezko *metabollically unhealthy phenotype in individuals with normal weight* edo MUHNW) (Schulze 2019). Hain zuzen ere, NAFLD-dun pazienteen %10a argala da eta NAFLDaren prebalentzia obesoak ez diren pazienteetan %16koa da (Shi, Wang et al. 2020).

NAFLDaren klinika eta progresioa heterogeneoak dira eta horietan eragina duten **faktore** ugari existitzen dira (B6 irudia). Gainera, aurrejoera genetikoak, ingurune-faktoreak eta sindrome metabolikoaren elementuak bata bestearekin elkarrekiten dute eta faktore horien kantitatea baita larritasuna zenbat eta handiagoa izan, orduan eta zorrotzagoa izango da NAFLDaren garapen klinikoa (Pais, Maurel 2021). Adibidez, dietak eta mikrobiotak homeostasi metabolikoarengan eragina dute. Dietak, batez ere gantzetan/fruktosan aberatsa den “ekialdeko dieta”, erlazionatuta dago erregulazio metabolikoaren asaldurarekin (Carrera-Bastos, Fonte et al. 2011) eta NAFLDa eboluzionatzeko arriskuaren handipenarekin (Berna, Romero-Gomez 2020). Izan ere, heste-flora eta heste-permeabilitatea erraz alda dezake, behazun-azidoaren metabolismoa erregulatzen delarik (David, Maurice et al. 2014), eta ondorioz, glukosaren eta lipidoen metabolismoa baita energia homeostasia ere modulatzen da (Arab, Karpen et al. 2017).

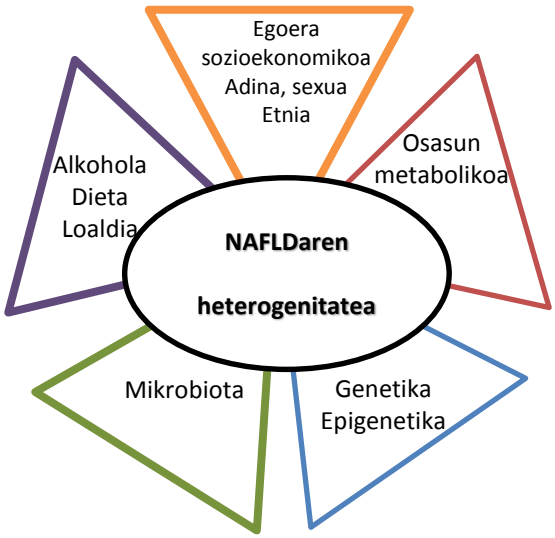

Figure B6. NAFLDaren bilakaera klinikoan eragina duten faktoreak. NAFLD, gibel koipetsuaren gaixotasun ez-alkoholikoa. Pais eta kolaboratzaileen artikuluan oinarritua (Pais, Maurel 2021).

NAFLDaren suszeptibilitateari eta progresioari loturiko gene-loci anitz daude eta gehienek metabolismo lipidikoarekin erlazionaturiko proteinak kodetzen dituzte (Eslam, Valenti et al. 2018). PNPLA3 genean ematen den I148M polimorfismoa da NAFLDaren inguruan hoberen erreplikatuta dagoen aldaera genetikoa. Gene horrek baltsa lipidikoen (LD) birmoldaketan parte hartzen du. APOB edo UCP2 lokusetako aldaerak ere deskribatu dira NAFLDa izateko aurrejoeran. Aldaketa epigenetikoei dagokionez, besteak beste, miR-122ren beheranzko erregulazioa NASH eta HCCren garapenarekin lotu da.

Gaur gaurkoz, ez dago NAFLDa tratatzeko terapia espezifikorik eta pazienteen kudeaketa-estrategiak bizimodu aldaketan eta komorbiditateendako tratamendu farmakologikoan (esaterako, intsulina sentikortasuna tratatzeko, estatinak) oinarritzen dira (Mazhar K. 2019).

2.2.1. Obesitatea: NAFLDari loturiko arrisku-faktore nagusia

Munduko Osasun Erakundearen (OME) arabera, **obesitatea** osasun-egoeraren kontrako arriskua da, zeinak gorputzean gehiegizko gantz-pilaketa duen bereizgarritzat. Egun, GMIa gainpisua eta obesitatea sailkatzeko erabiltzen den tresna da pertsona helduetan eta gorputzeko pisuaren eta altueraren berbidura arteko zatiketaren bidez kalkulatzen da (kg / m^2). Hori horrela izanik, gainpisua GMI ≥ 25 denean eta obesitatea GMI ≥ 30 denean definitzen dira.

Obesitatearen eta gainpisuaren tasak epidemia mailara iritsi dira eta, OMEaren datu-basearen arabera, munduko prebalentzia ia hirukoiztu egin da 1975 eta 2016 urteen bitartean. 2016an, 18 urte eta helduagoen %39ak gainpisua zuen eta %13a obesoa zen *(B7 irudia)* (World Health Organization data repository. https://www.who.int/topics/obesity; accesed 30 April 2020). Intzidentziari dagokionez, osasun-arazo bat dela kontsideratzen da. Izan ere, intzidentziak horrela jarraitzen badu, munduko populazioaren %50ak gainpisua izango duela estimatu da 2030ean (Tremmel, Gerdtham et al. 2017). Gainera, osasun-auzi horrek zama ekonomiko nabarmena suposatzen du, munduko barne-produktu gordinaren %2.8a izan zela estimatu baitzen 2014an.

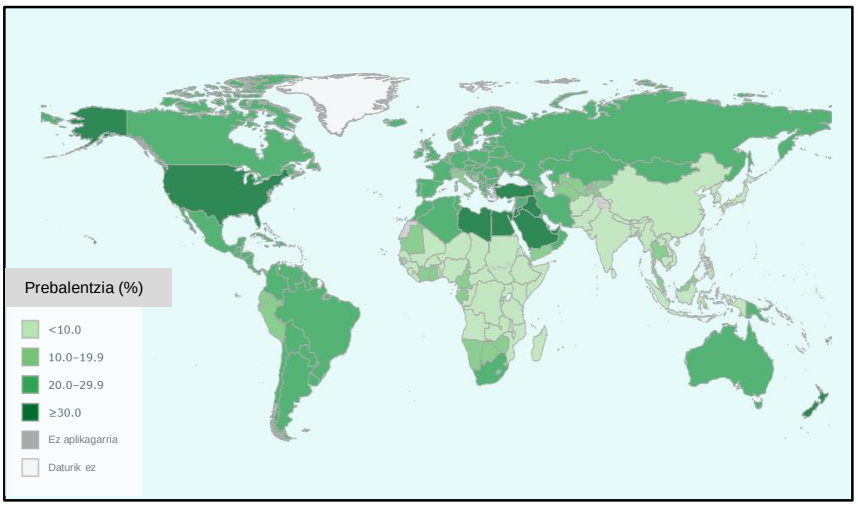

B7 irudia. Obesitatearen prebalentzia globala helduetan. Obesotzat definituta dauden 18 urteko eta helduagoen portzentaia herrialdeka 2016an. Munduko Osasun Erakundetik eraldatutako irudia (World Health Organization data repository. https://www.who.int/topics/obesity; accesed 30 April 2020.)

Orain arte, obesitateak garatutako herrialdeetan soilik erasaten zuela uste izan da, alabaina, gainpisu- eta obesitate-tasak garatu gabeko baita erdi-garatutako herrialdeetan ere handitzen ari dira (World Health Organization data repository. https://www.who.int/topics/obesity; accesed 30 April 2020). Mundu mailan, osasun-arazo honen bi kausa nagusiak dira: gantzetan aberatsa den dieta jatearen areagotzea eta bizimodu sedentarioari loturiko jarduera fisikoaren jaitsiera. Badaude biologiarekin, ingurumenarekin eta gizartearekin zerikusia duten faktoreak baita ere zeinak gainpisua eta obesitatea izateko suszeptibilitatearengan eragiten duten (Blüher 2019).

2MDM, gaixotasun kardiobaskularra (GKB), NAFLDa eta minbizia bezalako komorbilitateengatik hiltzeko arriskuaren handiagotzearekin dago erlazionatuta obesitatea (Abdelaal, le Roux et al. 2017). Aipatzekoa da metabolikoki osasuntsu diren paziente obesoen azpitalde bat deskribatu dela (Stefan, Haring

et al. 2013). Hau da, ez dute GKB izateko arrisku handiagorik pisu normala duten pertsonekin alderatzean, gorputzeko gantz-banaketa egokia delako, batez ere, zonalde abdominalean.

GMIak gorputzean gantza nola metatzen denari buruzko informazio ematen ez duenez, obesitatearen definizioa okerra izan daiteke. Hori horrela izanik, obesitatea bi taldetan banatu da: metabolikoki osasuntsua dena (ingelesezko *metabolically healthy obesity*, MHO) eta metabolikoki ez-osasuntsua dena (ingelesezko *metabolically unhealthy obesity*, MUO) (Tsatsoulis, A & Paschou, SA 2020). MHO taldeak GKB pairatzeko arriskurik ez duten pazienteak hartzen ditu barruan. Bizimodua eta adina gorabehera, MUOra eboluzionatu dezakeen baldintza iragankorra dela kontsideratzen da. MUO fenotipoan ohikoa da gantz-ehunaren disfuntzioa eta IR izatea, sindrome metabolikoaren elementuak direnak hain zuzen. Osasun metabolikoaren kontzeptua oraindik eztabaidagarria den arren, gutxienez B1 taulan espezifikaturiko bi baldintza metaboliko arriskutsuen presentziak definitzen du (Eslam, Newsome et al. 2020).

2.3. NAFLDari loturiko kartzinoma hepatozelularra

Gibeleko minbizia gaixotze- eta hilkortasun-arrazoi nagusietako bat da mundu mailan. Munduko Minbiziaren Estatistika Erakundearen (ingelesezko *Global Cancer Statistics*) arabera, seigarren neoplasmarik arruntena eta minbiziagatiko laugarren heriotza-kausa izan zen 2018an (Bray, Ferlay et al. 2018). Urte bakoitzeko 841 000 kasu berri estimatzen dira, zeinetatik 782 000 heriotz-kasu diren. 2030. urterako, gibel-

B1 taula. Erregulazio metabolikoaren asaldua pairatzeko arriskua definitzen dituzten irizpideak. Eslam M. *et al.*, 2020(Eslam, Newsome et al. 2020) erreferentziatik eraldatua.

Gutxienez hurrengoko bi baldintzen presentzia
• Gerri zirkunferentzia ≥ 102/88 cm gizon/emakume kaukasiarretan edo ≥ 90/80 cm gizon/emakume asiarretan. • Odol presioa ≥ 130/85 mmHg edo botika tratamendu espezifikoa. • Plasma TG ≥ 150 mg/dl edo botika tratamendu espezifikoa. • Plasma CHO-HDL < 40/50 mg/l gizon/emakumetan edo botika tratamendu espezifikoa • Prediabetes: baraualdiko glukosa maila 100 eta 125 mg/dl bitartekoa, elikatu eta bi ordu osteko glukosa maila 140 eta 199 mg/dl bitartekoa edo HbA1c 5.7 % eta 6.4 % bitartekoa. • HOMA-IR puntuazioa ≥ 2.5. • Plasma hs-CRP maila > 2 mg/l.

CHO, kolesterola; HbA1c; hemoglobina A1c; HDL, dentsitate altuko lipoproteina; HOMA-IR, intsulinaren erresistentzia homeostatiokoaren eredua; hs-CRP, sentsibilitate altuko C proteina erreaktiboa; TG, triglizeridoa.

minbiziaren intzidentzia %137a handitzea estimatzen den bitartean, prebalentzia %146a igoko dela kalkulatu da (Estes, Razavi et al. 2018). Bestalde, intzidentzia- eta heriotza-tasa 2 edo 3 aldiz handiagoa da gizonezkoetan emakumezkoetan baino (Bray, Ferlay et al. 2018). Gibel-minbizi mota ezberdinen artean, neoplasia gaizto primarioen %90a **HCCa** da.

Pronostiko edo prognosi txarra izateaz gain, HCCaren garapenak biziraupen baxua dakar (batezbesteko biziraupena 11 urtekoa da eta 5-urteko biziraupen tasa %18koa da), batik bat, tumorearen bersortzea eta metastasia dela eta (Berkan-Kawinska, Piekarska 2020, Sun, Zhang 2020). HCCaren abiarazle etiologiko ugari daude eta izan daitezke bai birikoak (B, C eta D hepatitisen birusak; HBV, HCV eta HDV hurrenez-hurren) bai faktore ez-infekziosoak: toxikoak (alkohola, erretzea, aflatoxina), immunologikoa (hepatitis autoimmunea, hepatitis biliar primarioa) eta gaixotasun metabolikoak (diabetesa, hemokromatosia eta NAFLDa) De Matteis, Ragusa et al. 2018). Historikoki, HBVa eta HCVa izan dira HCCren eragileak (Bertot, Adams 2019). Ordea, HCVren terapiaren hobekuntzak eta NAFLDaren prebalentziaren handiagotzeak adierazten dute NAFLDari loturiko HCCk bestelako etiologiekin erlazionaturiko HCCak gainditzen dituela. Hortaz, NAFLDa HCC eragiten duten etiologia nagusietako bat da. Izan ere, Ameriketako Estatu Batuetan, HCC kasuen %32ak NAFLDa jatorritzat duten heinean, kasuen %20a HCVari egozten zaio.

HCC esteatohepatitikoa (HCC-SH) edo **NAFLDari lorturiko HCC** izena du esteatosia iturburu duen HCCak eta ezaugarri bereizgarriak ditu bestelako jatorridun HCCekin alderatuz gero (Salomao, Remotti et al. 2012). Gainera, sindrome metabolikoarekin erlazionatuta dago, obesitatea, 2MDM, dislipemia eta hipertentsioaren prebalentzia NAFLD-HCCa duten pazienteetan gainerako HCC kasuetan baino handiagoa baita (Dhamija, Paul et al. 2019, Shibahara, Ando et al. 2014, Salomao, Remotti et al. 2012, Salomao, Yu et al. 2010). Aipatzekoa da ere NAFLDa iturburu duen HCCa pertsona zaharragoetan garatzen dela (Campani, Bensi et al. 2020).

Histopatologiari dagokionez, NAFLD-HCCko tumoreek ondorengo ezaugarriak dituzte: LD handietan metatutako lipidoak, hantura, Mallory-Denk izeneko inklusio-gorputzak eta balonizazioa (Park, Lee et al. 2010, Shibahara, Ando et al. 2014, Salomao, Remotti et al. 2012, Salomao, Yu et al. 2010, Lee, Yoo et al. 2017) (B8 irudia). Diagnosirako erabiltzen diren kriterio morfologikoak ezberdinak izanik, gainerako HCC azpiklaseekin alderatzerakoan, NAFLD-HCC kasuetan askotariko proportzioak deskribatu dira prebalentzia, tumoreen tamaina eta bereizmena, fibrosiaren presentzia eta minbiziaren oldarkortasunari dagokionez (Nahon, Allaire et al. 2020). Gibeleko zirrosia HCCa garatzeko arrisku-faktore nagusietako bat den arren, HCC kasuen %23-65a NAFLDa duten paziente ez-zirrotikoetan ematen da (Bertot, Adams 2019, Paradis, Zalinski et al. 2009).

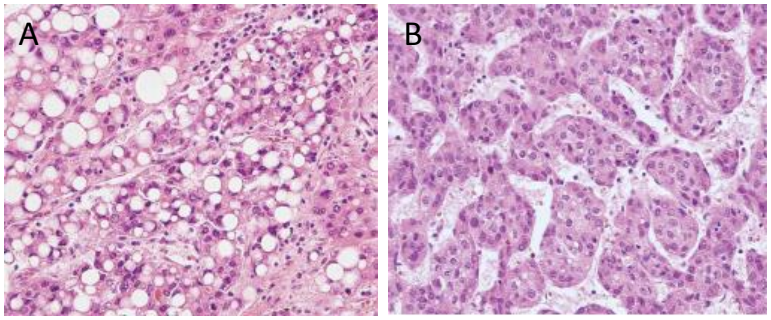

B8 irudia. (A) HCC-SHaren eta (B) ohiko HCCaren ezaugarri histologikoak. HCC, kartzinoma hepatozelularra; HCC-SH, kartzinoma hepatozelular esteatohepatitikoa. (Lee, J. S., Yoo et al. 2017) erreferentziatik moldatua.

Daukan iragarpen txarrarekin loturik, HCCa eboluzio-aldi aurreratuetan diagnostikatu ohi da eta ondorioz, tratamendu-aukerak mugatuak dira Paziente gehienetan gibel-transplanteak, erauzketak edota bestelako tratamenduek ez dute arrakastarik izaten eta beraz, zainketa aringarriak jasotzen dituzte (Golabi, Rhea et al. 2019). NAFLDa jatorritzat duen HCCak kontsentsudun definizio bat ez izateak (Nahon, Allaire et al. 2020) oraindik gehiago eragozten du bere detekzioa. Horregatik, beharrezkoa da definizio-irizpide berriak ezartzea (Jamwal, Krishnan et al. 2020).

2.3.1. Kartzinoma hepatozelularraren berprogramazio metabolikoa

Gibela gorputz osoko glukosaren eta lipidoen metabolismoa erregulatzen duen organoa da. Nahasmendu metaboliko asko deskribatu dira NAFLDa bezalako gibeleko baldintza patologiko ugaritan. HCCa zirrosirik ez duten gibeletan sortu ahal dela jakin denetik (Zarrinpar 2017), asaldura metabolikoek garrantzia hartu dute hepatokartzinogenesian. Hala ere, profil metabolikoari buruzko informazio gutxi dagoenez gaur egun, ez da guztiz ezagutzen obesitateak edota NAFLDak HCCarengan nolako eragina duten azaltzen dituzten mekanismoak.

Onkogeneen aktibazioa eta gene tumore-ezabatzaileen galera suposatzen duten gertaerez gain, badaude mikroinguruneari eta metabolismoari loturiko faktore batzuk zeinak hepatokartzinogenesia bultzatzen duten eta NAFLDaren garapenaren berdinak diren: IR bidezko hiperintsulinemia, oxidazio eta ER estresagatik induzitutako zitokina hanturarazleen igoera, adipokinen erregulazioaren galera eta asaldutako heste-mikrobiota (Nakagawa, Hayata et al. 2018). Gainera, **berprogramazio metabolikoak**, hots, minbizi-zeluletan berez gertatzen diren aldaketa metabolikoak, obesitatean kartzinogenesia garatzen laguntzen du (Ward, Thompson et al. 2012). Zelula proliferatiboetako eta kieszenteetako metabolismoa ezberdina da, izan ere, tumoreetako zelulen kontrol gabeko ugalketak energia, biomasa eta erredox orekaren mantentzea du behar. Betekizun horiek guztiak berprogramazio metabolikoari esker egiten dira. Eta ez hori bakarrik, baizik eta moldaketa metabolikoan eratutako metabolitoek ere minbizia sorraraztea ahalbidetzen dute seinale-bidezidorrak, egoera epigenetikoak eta zelula-bereizmena erregulatuz.

Glukosaren metabolismoari dagokionez, Warburg efektua edo glukolisi aerobikoa da gehien ikertu den adaptazio-gertakizuna, non glukosa laktatoa ekoizteko bideratzen den, TZA ziklora eta *oxphos*era metabolizatu beharrean (Vander Heiden, Cantley et al. 2009). Fenomeno hori oxigenoaren presentzian edo mitokondrio funtzionalak izan arren gertatzen da baita ere. Handitutako glukosaren xurgatzearekin bat, HCCdun pazienteetan glukolisi aerobikoa gertatzen dela behatu da (De Matteis, Ragusa et al. 2018). Bestalde, Bjornson *et al*.-ek glukoneogenesia hepatokartzinogenesian ezabatu egiten dela deskribatu zuten, prozesu horretako entzima mugatzaileen beheranzko erregulazioa ematen zelako (Bjornson, Mukhopadhyay et al. 2015).

Azkenengo ikerketek **metabolismo lipidikoaren adaptazioak** minbizi zeluletan duen garrantzia ezagutzera eman dute. Energia-erreserba eta konposatuen biltegiak izateaz gain, lipidoek egitura-funtzioak dituzte eta mintz-jariakortasuna baita proteinen dinamika ere erregulatu ditzakete konposaketaren eta oparotasunaren arabera (Beloribi-Djefaflia, Vasseur et al. 2016). Zelula-hazkuntza, migrazioa edo metastasia moduko prozesu gaiztoetako seinale-kaskadak gidatzen dituztenez, lipidoek funtzio ugari betetzen dituzte kartzinogenesian ere. Gaur gaurkoz, lipidoen metabolismoa hepatokartzinogenesiaren bereizgarria dela kontsideratzen da, esteatositik garatzen denean bereziki, lipidotan aberatsa den egoera baita.

Nakagawa eta kolaboratzaileek frogatu zuten **DNLa** unibertsalki areagotuta dagoela HCCan (Nakagawa, Hayata et al. 2018). HCCaren adierazpen profilean behatu denez, lipido-biosintesian parte hartzen duten geneen goranzko erregulazioa ematen da zelula ez-tumoralekin alderatzerakoan (Bjornson, Mukhopadhyay et al. 2015). Gainera, GAS genearen (GASN) gainadierazpena HCCaren prognosi txarrarekin erlazionatuta dago (De Matteis, Ragusa et al. 2018), SCD-sarea hepatokartzinogenesia eta

pazientearenganako emaitzekin lotuta dago (De Matteis, Ragusa et al. 2018), eta SBREBP1-bidezko lipogenesiaren aktibazioa deskribatu da HCCan (Nakagawa, Hayata et al. 2018). G6PDH eta EM bezalako NADPHren ekoizpenarekin erlazionaturiko entzimak baita ere goranzko erregulazioa dute mota horretako gibel-tumoreetan (De Matteis, Ragusa et al. 2018). Nabarmenki, DNLaren inhibitzaile kimiko asko daude minbizia eta HCCa tratatzeko terapiaren saiakuntza aurreklinikoetan eta klinikoetan (Nakagawa, Hayata et al. 2018).

Zelula ez-proliferatiboek lipido exogenoak erabili ohi dituztenez, HCCaren garapena ahalbidetzen duen beste bidezidor nagusi bat handitutako gibel-LPL bidezko **odoleko GAen xurgapena** izan daiteke (Cao, Song et al. 2017). Hain zuzen ere, Cao eta kolaboratzaileek jakinarazi zuten serumeko GAen kontsumoaren ardura LPLren gainadierazpenarengan zegoela HCCan. Bestalde, GAen translokasak (CD36), garraiatzaileak (FATP2, FATP5) eta FABP familiako hainbat kide (1, 4, 5) GAen eskuratze eta gibelerako garraioarekin erlazionatzen dira HCCan (Hu, Lin et al. 2020). Aipatu bezala, hori bereziki garrantzitsua da gehiegizko elikaduragatiko obesitatean, non, GEZko lipolisia eta dieta iturri izanik, GAen odoleko kontzentrazioa handitua dagoen (Fabbrini, Mohammed et al. 2008).

Datu eztabaidagarriak aurkeztu dira **lipidoen deuseztatze-bide** nagusiek HCCan duten paperari dagokionez. Bidezidor horien portaera GAen jatorriaren araberakoa izan daiteke (Berndt, Eckstein et al. 2019). PPAR-α eta CTP2ren gainadierazpena, **FAO**aren areagotzearekin batera, β-katenina bidezko HCCaren energia iturria direla deskribatu da (Senni, Savall et al. 2019, Hu, Lin et al. 2020). Aldiz, beste ikerketa batzuen arabera, Cpt2ren beheranzko erregulazioaren bidezko FAOaren ezabatzea ematen da HCCan lipidoetan aberatsa den inguruari egokitzeko (Nakagawa, Hayata et al. 2018, Berndt, Eckstein et al. 2019). Edozein kasutan, asaldura mitokondrialak HCCaren gertakari goiztiarrak direla kontsideratzen da (De Matteis, Ragusa et al. 2018).

Lehen esan bezala, **VLDL jariaketaren** eteteak gibeleko lipidoen metaketa ahalbidetzen du. Minbizirik ez duen ehunarekin alderatuz, VLDLeen kanpo-garraioan parte hartzen duten gene nagusiak beherantz erregulatuta daude HCCan (Bjornson, Mukhopadhyay et al. 2015). Konkretuki, HCCan gertatzen den APOB genearen ablazioa pazientearen etorkizun txarrarekin erlazionatzen da (Lee, G., Jeong et al. 2018). Hala ere, VLDLeen esportazioa areagotuta dagoela deskribatu da HCC duten pazienteetan (Berndt, Eckstein et al. 2019). Momentuz, ez da ezer argitaratu TGaren gibeleko mobilizazioari dagokionez NAFLD-HCC azpiklasean.

Funtsean, berprogramazio metabolikoa premiazkoa da HCCan tumorearen hazkuntzarako eta progresiorako. Hori horrela izanik, asaldatutako bidezidorren kontrolak hepatokartzinogenesian inplikazio

kliniko garrantzitsuak izan ditzake (De Matteis, Ragusa et al. 2018). Orain arte uste izan da tumore-ezabatzaileetako edo proto-onkogenetako mutazioek lehendabizi ziklo zelularra erregulatu, proliferazioa sostengatu eta hazkuntza-supresioa edota zelula-heriotza ekiditen zutela (Ward, Thompson et al. 2012). Beraz, minbizi-zeluletan dagoen egokitutako metabolismoa aldaketa horietako erantzun pasiboa zela kontsideratzen zen. Alabaina, frogek ez-ohiko kontzeptu bat erakusten dute zeinean proto-onkogeneak eta tumore-ezabatzaileak metabolismoa kontrolatzeko eboluzionatu duten eta hori bera baiten kartzinogenesian duten lehen rola.

Minbizia gidatzen duten geneek HCC mota aldarazten dute, berezko tumore-biologia erakutsiz (Molina-Sanchez, Ruiz de Galarreta et al. 2020). Beraien adierazpen-mailan, aktibitatean eta beraien arteko kooperazio-patroietan gerta daitezkeen aldaketek tumoreen arteko heterogenitatea dakartzate histologiari, fenotipo immunologikoari, transkriptomari eta terapiarekiko erantzunari dagokionez. Esaterako, NAFLDan eman daitekeen HCCa garatzeko arriskua PNPLA3 geneko zenbait aleloren bidez estratifikatzeko eta aurreikusteko aukera dago, beti ere HCCaren beste hainbat faktoreekin (gizonezko generoa, adin zaharra eta obesitatea izatea) konbinatuz gero (Nahon, Allaire et al. 2020). Hala ere, exoma espezifikoen, genomaren eta RNA sekuentziazioaren inguruko ikerketek ez dute NAFLD-HCCaren genomarentzako berezko patroirik aurkitu. E2F motako transkripzio-faktoreek, ziklo zelularraren erregulatzaile nagusiak izanik, prozesu guzti horietan eginkizun bat izan dezakete, metabolismo fisiologikoaren eta patologikoaren kontrolean parte hartzen baitute (3.3 sekzioan deskribatuta).

3. Ziklo zelularra eta E2F transkripzio-faktoreak

3.1. Ziklo zelularra eta bere erregulazioa

Ziklo zelularra oso kontserbatuta dagoen prozesu bat da zeinak proliferazio zelularra ahalbidetzen duen. Zelula-ugalketan, zelula bat genetikoki berdin-berdina diren bi alaba-zelulatan banatzen da. Mekanismo hau beharrezkoa da organismo eukariotoen zelula-hazkuntzan, garapenean eta ezberdintzapenean (Wenzel, Singh 2018, Vermeulen, Van Bockstaele et al. 2003). Hertsiki erlazionatuta dago zelula-heriotzarekin ere, bi prozesuak helduen ehun-homeostasiaren arduradunak baitira (Zhivotovsky, Orrenius 2010). Hortaz, ziklo zelularraren erregulazioan zehar gerta daitezkeen asaldurek minbizia (Wenzel, Singh 2018, Vermeulen, Van Bockstaele et al. 2003), gaixotasun metabolikoak edo kardiobaskularrak eta eritasun neurodegeneratiboak (Zhivotovsky, Orrenius 2010). bezalako patologiak ahalbidetzen dituzte.

Zelula-zatiketak jarraiak diren lau **fase** ditu: Gap1 (G_1) edo hazkuntza- fasea; sintesi-fasea (S) edo DNAren sintesi fasea, Gap2 (G_2) fasea, non zelula mitosirako prestatzen den, eta fase mitotikoa (M), non zelula zatitzen den *(B9 irudia)* (Wenzel, Singh 2018). G_1 fasean dauden zelulak G_0 deritzon fase ez-ugalkor batean sar daitezke. Zelula seneszenteak ez bezala, atseden-fase hori itzulgarria da zelula kieszenteentzat, ziklo zelularrean ugaltzeko berriz sartu baitaitezke hazkuntza-faktore fisiologikoei erantzunez (Yao 2014). Mitosi aurreko periodoak (G_1, S, G_2) interfasea du izena eta ziklo zelularraren %95a bertan ematen da (Cooper 2000).

Osotasun genomikoa eta zatiketa egokia gauzatu behar da alaba-zelulatan. Horretarako, kontrol-puntu edo ingelesezko ***checkpoints*** deritzon kontrol-mekanismo zorrotzak daude *(B9 irudia)*. Kontrol-puntu horiek ziklo zelularra noranzko bakarrekoa dela segurtatzen dute eta hurrengoko gertaerak gauzatzen dituzte behin aurreko faseak era egokian bete direnean, ziklo zelularraren trantsizioa era ordenatuan gertatzen delarik (Rhind, Russell 2012). G_1/S edo errestrikzioaren kontrol-puntua (R) garrantzitsuena da eta zelula zatiketarako prest dagoela ziurtatzen du (Gerard, Goldbeter 2009). Itzulgarria ez den puntu bat da eta, behin gaindituta, zatiketa zelularra era ezeztaezinean burutuko da, hazkuntza-faktorerik behar izan gabe. Beste hiru kontrol-puntu daude: S-barrukoa, G_2/M eta M edo ardatz mitotikoaren kontrol-puntua (Barnum, O'Connell 2014). Erregulazio-ziklo guzti horiek seinale positiboak eta negatiboak dauzkate, batik bat, zelula-tamaina, DNAren kaltearekiko erantzuna eta kromosomen segregazioa kontrolatzen dituztenak. Akatsak modu egokian zuzentzen diren arte, kontrol-puntuen aktibazioak ziklo zelularraren gelditzea dakar.

Zuzenketa oker bat ematen bada, zelula seneszentzian sartuko da edo apoptosia burutuko du (Malumbres, Barbacid 2009).

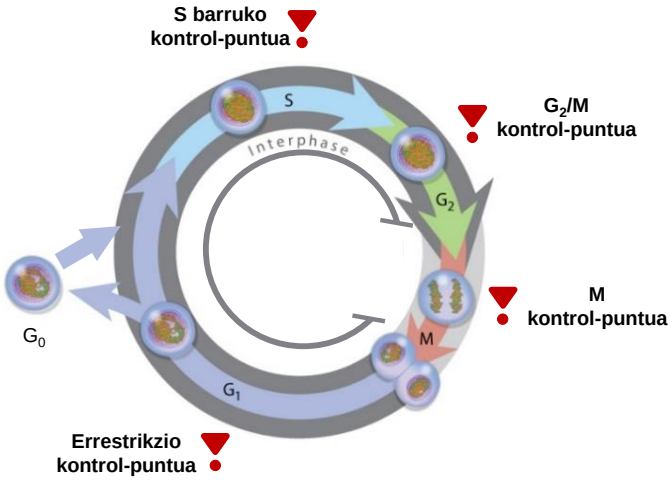

B9 irudia. Ziklo zelularraren irudikapen eskematikoa. Ziklo zelularraren faseak eta kontrol-puntuak erakusten dira. G_0, fase ez-ugalkorra; G1, Gap1 fasea; G2, Gap2 fasea; Interphase, interfasea; M, fase mitotikoa; S, sintesi-fasea. O'Connor et al., 2008 erreferentziatik moldatua.

Kinasa-menpeko ziklinak (CDK) serina/treonina motako kinasak dira, zeinak ziklo zelularraren dinamika kontrolatzen duten aktibazio jarrai eta iragankorren bidez (Malumbres, Barbacid 2005). Adierazpen konstitutiboa duten arren, CDK proteinek beharrezkoa dute erregulazio-azpiunitateak diren ziklinekin lotzea aktibitate biologikoa izateko. CDK-k ez bezala, ziklinak ziklo zelularrean zehar era ziklikoan sintetizatu eta suntsitzen dira. CDKn kinasa aktibitatea beste hainbat modutan ere erregulatzen da, hala nola, inhibitzaileetara (CKI) lotuz, fosforilazio/desfosforilazio bidez, baita tolesketa eta lokalizazio zelularraren arabera.

Espezifikoak diren CDK-ziklina konplexu heterodimerikoak dihardute zelula-zatiketaren fase bakoitzean eta gakoak diren substratuak fosforilatzen dituzte **ziklo zelularra garatu** dadin (Malumbres, Barbacid 2005). G_1 fase goiztiarrean, 4,6 CDK/D ziklina konplexuak erretinoblastomaren (Rb) tumore-ezabatzaile proteina inaktibatzen du fosforilazio bidez. Rb-ren inaktibazioa 2 CDK/E ziklina konplexuari esker betetzen da. Uste da 3 CDK /C ziklina konplexuak Rb fosforilatzen duela baita ere zelula kieszenteen G_0/G_1 trantsizioan. Rb inaktiboak **E2F transkripzio-faktore** funtzionalaren askatzea ahalbidetzen du eta horrek baimentzen du zelulak errestrikzio kontrol-puntua gainditzea eta S fasean sartzea (Nevins 1992, Weinberg 1995). 2 CDK/E ziklina konplexua G_1/S trantsizioan da garrantzitsua. Azkenik, S fasearen betetzea eta irteera

2 CDK/A ziklina konplexuaren bidez gauzatzen da, 1 CDK/A,B ziklina konplexuak S/G_2 eta G_2/M trantsizioan parte hartzen duten bitartean.

3.2. E2F transkripzio-faktoreen familia

E2 faktorea (E2F) E2 promotore adenobiralaren aktibaziorako beharrezko zelula-faktore gisa identifikatu zen lehen aldiz (Kovesdi, Reichel et al. 1986a, Kovesdi, Reichel et al. 1986b). Geroztik, ugaztunetan E2F familia etengabe hazten joan da kide berriak gehitu direlarik (Dimova, Dyson 2005).

E2F **transkripzio-faktoreen** familia bat da zeina funtsezkoa den **ziklo zelularraren garapenean**. E2Fek ziklo zelularraren hainbat erregulatzaile nagusi induzitzen dituzte (E ziklina, A ziklina, Rb), baita nukleotidoen biosintesian (Tk, Ts, Dhrf), DNAren erreplikazioan (Orc1, Cdc6 eta Mcm-ko zenbait kide) (Dyson 1998) edota mitosian (Plk1) (Martin, Strebhardt 2006) dihardutenak ere. Gainera, E2Fren beste itu batzuk barnean hartzen dituzte DNAren konponketan, apoptosian, diferentziazioan eta garapenean parte hartzen duten geneak (Bracken, Ciro et al. 2004).

Egunera arte, zortzi E2F **loci kromosomiko** (E2F1-8) daude ugaztunetan, zeinak 10 gene-produktu ezberdin kodetzen dituzten (E2F1, E2F2, E2F3a, E3F3b, E2F4, E2F5, E2F6, E2F7a, E2F7b, E2F8) (DeGregori, Johnson 2006, Chen, Tsai et al. 2009) *(B10 irudia)*. E2F3a eta E2F3b ekoizteko desberdinak diren bi promotore erabiltzen diren bitartean, E2F7a eta E2F7b transkripto primarioaren ordezko *splicing*aren bidez lortzen dira (Di Stefano, Jensen et al. 2003).

E2F familiako kide guztiek kontserbatua dagoen hego-helize motako **DNAra lotzeko domeinu** (DBD) bat daukate gutxienez (Chen, Tsai et al. 2009). E2F kideen arteko homologia gradu altua domeinu honetan datza, 5'-TTTSSCGC-3' kontsentsu-motibora lotzea ahalbidetzen duena, non S hizkia G edo C izan daitekeen. E2F1-6k **dimerizazio domeinu** bat daukate baita ere, dimerizazio-kide proteinak (DP) lotzen diren lekua. E2Fren eta DPren (DP1, DP2 eta DP3/4 *Homo sapiens*en) arteko heterodimerizazioak DNAra lotzeko afinitatea eta aktibitate transkripzionala modulatzen ditu (Helin, Wu et al. 1993, Bandara, Buck et al. 1993, Huber, Edwards et al. 1993, Krek, Livingston et al. 1993), eta leuzina kremailera (LZ) eta marka-kutxa (MB) motiboen bidez ematen da. E2F7-8k ez dute domeinu hori eta DNAra homodimero bezala lotzen dira DPrekiko era independiente batean (Chen, Tsai et al. 2009). E2F1-5en **karboxi-terminalak** transaktibazio

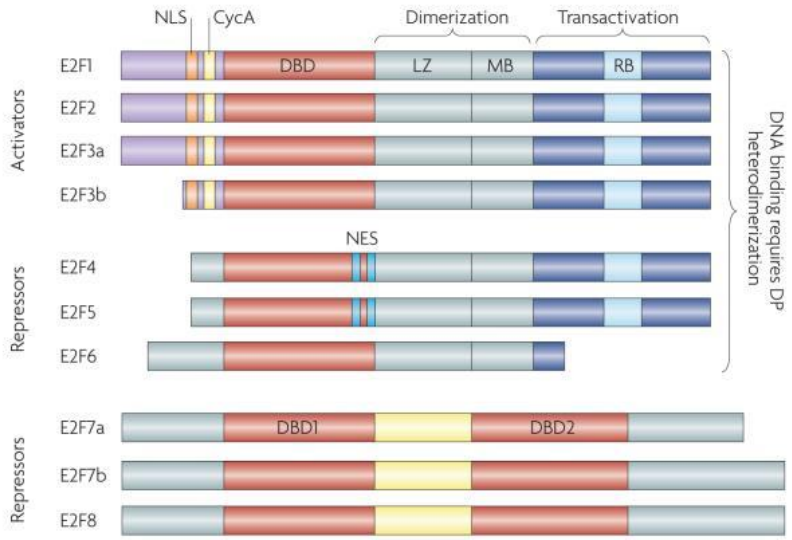

B10 irudia. Ugaztunen E2F proteinen irudikapen eskematikoa. CycA, A ziklina lotzeko lekua; DBD, DNA lotzeko domeinua; NES, nukleotik esportatzeko seinalea; NLS, nukleoan lokalizatzeko seinalea; MB, marka-kutxa; LZ, leuzina kremailera; RB, Rb lotzeko domeinua. Chen, Tsai et al. 2009 erreferentziatik moldatua.

domeinu bat dauka, zeinak Rb familiako kideekin edo poltsiko proteinekin (Rb, p107, p130) interakzio espezifikoa izatea ahalbidetzen duen. E2F6-8k ez dute trantsaktibazio domeinurik, hortaz, Rb-rekiko modu independientean dihardute. Bestalde, **amino-terminalean** E2F1-3-k A ziklina/2 CDK lotzeko lekua eta nukleoan kokatzeko seinalea (NSL) dituzte eta E2F4-5-ek nukleotik esportatzeko alderdi biko seinalea (NES) daukate.

Bere homologian eta *in vitro*ko propietate funtzionaletan oinarrituz, E2F familiako kideak tradizionalki izan daitezke: aktibatzaileak (E2F1-3a), zeinak zelula-hazkuntza eta zikloan zehar erregulatzen diren, edo errepresoreak (E2F3b-6) eta ez-ohiko errepresoreak (E2F7-8), zeinak konstitutiboki adierazita dauden (Kong, Chang et al. 2007). Hala ere, ikerketa askok rol konplexuagoak ezagutarazi dituzte, izan ere, testuinguruaren arabera aktibatzaileak errepresore moduan jardun dezakete eta alderantziz (Mitxelena, Osinalde et al. 2012). Egun, sailkapen hori ez-zehatza eta sinplifikatuegia dela kontsideratzen da (Huntington, Tang et al. 2016).Daukaten antzekotasuna dela eta, E2F kideek bat datozen **funtzioak** dituzte, izan ere, kide baten funtzio-galera gertatzen denean, beste kideen bidezko konpentsazioak organismo baten biziraupena segurtatzen du (Kong, Chang et al. 2007). Gene-talde espezifikoen erregulazioaren bidez, kide bakoitzak bere rol propioak eta bakarrak dituzte. Esaterako, E2F1-3 S fasean sartzeko beharrezkoak dira (Wu, Timmers et al. 2001, Kong, Chang et al. 2007), baina E2F3 da beharrezkoa den bakarra hazkuntza-zelulak ziklo zelularrean behin eta berriz sartzeko (Kong, Chang et al. 2007) eta E2F1 da apoptosia induzitzen duen bakarra estimulu proliferatiboen absentzian (Hallstrom, Nevins 2003). DNAra lotzeko kontsentsu-

motiboa ez da itu-geneen **transkripzio-kontrolaren espezifizitatean** parte hartzen duen mekanismo bakarra, E2F lotzeko *in vivo* gune gehienek kontsentsu-motibo hori ez dutelako (Rabinovich, Jin et al. 2008, Cao, Rabinovich et al. 2011). Gainera, E2F1 orokorrean GCn aberatsa den eta giza-promotore gehienetan dagoen sekuentzia batera lotzen da eta zuzenean eta proteina-proteina bidezko interakzioan errekrutatu ahal da (Cao, Rabinovich et al. 2011). Beste E2F kide batzuek hainbat transkripzio faktoreekin eta transkripzio-makinariako hainbat proteinekin elkarrekin dezakete baita ere (Mitxelena, Osinalde et al. 2012). Beraz, lotura-espezifizitea itu-gene bakoitzaren promotorean ematen den E2Fren eta beste transkripzio faktoreen arteko lankidetzan oinarritzen da (Mitxelena, Osinalde et al. 2012). Gene-erregulazio konbinatorioak ahalbidetzen du E2F kide ezberdinek rol funtzional propioak izatea, E2Fak barnean hartzen dituzten itu-gene ezberdinak erregulatuz (Freedman, Chang et al. 2009).

Funtzio-espezifitatea hurrengoko faktoreetan oinarritzen da baita ere: E2F-ren sintesian (Chen, Tsai et al. 2009) eta ubikitina-proteasoma makinaria bidezko degradazioan (Hateboer, Kerkhoven et al. 1996), Rb kide jakinetarako loturan (Chen, Tsai et al. 2009), CDKren fosforilazio zuzenean (Morris, Allen et al. 2000) edota aldaketa epigenetikoetan (Chen, Tsai et al. 2009). Lehen aipatu bezala, E2F familiak bere burua erregulatu dezake baita ere, E2Fak lotzeko lekuak baitituzte euren promotoreetan (Johnson, Ohtani et al. 1994, Hsiao, McMahon et al. 1994, Neuman, Flemington et al. 1995). Bestalde, funtzioa lokalizazio zelularraren araberako izan daiteke (Verona, Moberg et al. 1997).

3.3. E2F transkripzio-faktoreak erregulatzaile metaboliko gisa

Zelula-garapenean eta minbizian ematen diren egokitze metabolikoek ziklo zelularraren eta metabolismoaren arteko lotura bat ezartzen dute. Ohiko funtzioez gain, ziklo zelularraren hainbat erregulatzaileek metabolismoaren kontrolean daukaten parte-hartzea ezagutzera eman da azken hamarkadan, bai baldintza fisiologikoetan bai patologikoetan. Hori dela eta, ziklo zelularraren modulatzaileak minbizian ematen den metabolismoaren aldaketaren arduradunak direla proposatu da.

3.3.1. CDK-E2F ardatzaren eginkizuna metabolismo fisiologikoaren erregulazioan

Ziklo zelularraren erregulatzaileak homeostasi metaboliko osoan laguntzen dute prankreasa, gantz-ehuna, giharrak edo gibela bezalako organo metaboliko garrantzitsuen garapenean eta diferentziazioan parte hartuz (Denechaud, Lopez-Mejia et al. 2016). Ziklo zelularraren modulatzaileak metabolismoaren kontrolean daukaten eginkizuna sagu mutanteen fenotipoaren behaketan nabarmentzen da (Aguilar, Fajas 2010). Adibidez, ziklo zelularra erregulatzen duten geneetan (D1 ziklina, CDK edo CKI batzuk) eman

daitezkeen aberrazio genetikoek **gorputzaren tamaina** aldaketa suposatzen dute. Alabaina, *E2f1*$^{-/-}$ eta *E2f2*$^{-/-}$ saguek garapen normala daukate, segur aski, gainontzeko kideen bidezko konpentsazioa dela eta (Denechaud, Lopez-Mejia et al. 2016).

Askotan frogatu izan da E2F familiako kide batzuek **adipogenesian** parte hartzen dutela. E2f1 eta E2f3ak *Pparg*ren adierazpena aktibatzen dute eta adipozitoen diferentziazioa induzitzen dute (Fajas, Landsberg et al. 2002). Konkretuki, E2f1 *Pparg*ren promotorera lotzen da *in vivo*. E2f4ak, ordea, adipogenesia negatiboki erregulatzen du *Pparg* promotorera espezifikoki lotzen delarik (Fajas, Landsberg et al. 2002).

Gibelean, 4 CDK-Rb-E2f1 bidezidorrak DNLa aktibatzen du intsulinari erantzunez eta E2f1ak betetze funtzionala dauka *Fasn*, *Scd1* eta *Srebp1* promotoreetan, gakoak diren gene lipogenikoak (Denechaud, Lopez-Mejia et al. 2016). Gainera, E2f1ak kolesterolaren homeostasia mantentzen du gibelean, bere knock-down bidezko ezabatzeak LDLren handitutako xurgapena eta kolesterolaren pilaketa ahalbidetzen baitu (Lai, Giralt et al. 2017). Aldiz, saguen enbrio-fibroblastoetan egindako ikerketek frogatu dute Rb-ren inaktibazioak GAen sintesia eta GAen konposaketaren aldaketa areagotzen dutela, E2f eta Srebp1-ek koordinatzen duten *Elovl6* eta *Scd1*-en erregulazio transkripzionalaren bidez (Muranaka, Hayashi et al. 2017).

Lipido-metabolismoaz gain, E2F familia glukosaren homeostasiaren kontrolarekin erlazionatu izan da ere, **pankreaseko β-zelulen ugalketa** erregulatzen duelarik. β-zelulen kopuru baxuagoa deskribatu da *E2f1*n defizienteak diren saguetan, glukosaren-menpeko intsulinaren jariapena asaldatzen duena (Fajas, Annicotte et al. 2004). Hala ere, sagu horiek ez dute diabetesik, ehun periferikoetan intsulinarekiko sentikortasuna handia delako (Fajas, Annicotte et al. 2004).

β-zelulen funtzioaren erregulazioan ere parte hartzen du E2f1ek, glukosa eta intsulinarekiko erantzun metabolikoa pizten duelarik. Nabarmenki, E2f1ak glukosaren menpeko intsulinaren jariapena induzitzen du Kir6.2 gene adierazpena aktibatuz irla-pankreatikoetan, ATParekiko sentikorra den potasio-kanala (Annicotte, Blanchet et al. 2009). Izan ere, glukosak 4 CDK-D2 ziklinaren aktibitatea areagotzen du, ondoriotzat Rb-ren inaktibazioa dakarrena eta jarraian, E2f1aren aktibazioa. Bidezidor hori intsulinaren efektu autokrinoaren bidez induzitzen da baita ere. Beste ikerketa batzuek iradokitzen dute E2f1ak gibeleko glukosaren sintesia erregulatu dezakeela. Konkretuki, glukoneogenesi hepatikoa asaldatuta dago *E2f1*$^{-/-}$

saguetan (Giralt, Denechaud et al. 2018), zeinak fluxu glukolitiko baxua duten gibeleko glukogeno edukia murriztua dagoelako (Denechaud, Lopez-Mejia et al. 2016).

Badaude ziklo zelularraren modulatzaileak **metabolismo oxidatiboa** kontrolatzen dutela baieztatzen duten ikerketak. Bereziki, Rb-ren inaktibazioak glukolisi anaerobikoa areagotzen du (Clem, Chesney 2012) eta mitokondrien aktibitatea eta kantitatea handitzen du adipozitoetan (Aguilar, Fajas 2010). Horrek adierazten du Rb-k metabolismo oxidatibotik glikolitikora ematen den aldaketa modulatu dezakeela, minbizi-zelulen ezaugarria dena hain zuzen ere. Berriz, beste ikerketa batzuek erakutsi dute Rb-ren delezioak aktibitate mitokondriala areagotzen duela bihotzean eta *oxphos*a asaldatzen duela giharrean (Denechaud, Lopez-Mejia et al. 2016). Rb-E2f1 bidezidorrak miokardioko glukosaren oxidazioa eragiten du, pirubato deshidrogenasaren lipoamida kinasa 4 isozima (PDK4) aktibatzen duelarik, diabetes eta obesitatean gainadierazita dagoen eta gakoa den elikagai-sentsorea (Hsieh, Das et al. 2008). Gainera, GEAn eta gihar eskeletikoan, Rb-E2f1 ardatzak metabolismo oxidatiboa pizten du jarduera fisikoari, hotz-baldintzei eta murriztutako elikagai-eskuragarritasunari erantzuteko (Blanchet, Annicotte et al. 2011). Azken ikerketek agerian utzi dute Rb-E2f ardatzaren bidezko metabolismo oxidatiboaren kontrola testuinguruaren araberakoa dela.

Nabarmenki, E2f1ak baditu zenbait funtzio zeinetan Rb-k parte hartzen ez duen. Hala nola, E2F1 fisikoki erreprimitzen dute BIN1ak ziklo zelularra moteltzeko (Folk, Kumari et al. 2019) eta KAP1ak apoptosia saihesteko DNAren kalte-erantzuna emateko (Wang, Rauscher et al. 2007).

Ebidentzia horiek finkatzen dute, ziklo zelularraren kontrolaz gain, E2f transkripzio-faktoreen familiak eta bereziki E2f1ak zelula-fisiologia modulatzen dutela, Rb-ren menpe edo ez. Lipidoen eta glukosaren homeostasiaren mantentzean parte hartzen du, baita energia gastuaren erregulazioan oso metabolikoak diren ehunetan.

3.3.2. Ziklo zelularraren erregulatzaileen parte-hartzea gibeleko konplikazio metabolikoetan eta kartzinoma hepatozelularrean

Lehen aipatu denez, jakina da transkripzio-faktoreen E2F familia aldaketa metaboliko ugariren arduraduna dela minbizia garatu ez den arren. Proposamen berri horiek zera dute oinarri: ziklo zelularraren erregulatzaileetan gertatzen diren asalduak gibeleko baldintza patologikoekin eta loturiko konplikazio metabolikoekin erlazionatzen dira, bereziki obesitatea eta diabetesa.

Hainbat eta hainbat ebidentzia daude ziklo zelularraren erregulatzaileek **obesitatean** duten parte-hartzea frogatzen dutenak. Adibidez, adipozitoetako Rb-ren inaktibazio espezifikoak saguak elikadura jatorri duen obesitatetik babesten ditu, bai gastu energetikoa bai GEZaren arretzea (ingelesezko *WAT browning*) areagotzen direlarik (Dali-Youcef, Mataki et al. 2007). Horren harira, *E2f1*$^{-/-}$ saguek dietak induzitutako obesitatearekiko erresistentzia dute (Fajas, Landsberg et al. 2002) eta bere absentziak hiperglizemia txikiagotzen du sagu diabetikoetan (Giralt, Denechaud et al. 2018). Gainera, E2F1 gainadierazita dago abdomen-adipositatea, odoleko GA aske altuak eta IR duten paziente obesoen (GMI > 30) erraietako gantz-ehunean (Haim, Bluher et al. 2015). E2F1aren adierazpena handitua dago baita ere GMI > 40 eta glukosarekiko intolerantzia duten pazienteen gibel-laginetan (Denechaud, Lopez-Mejia et al. 2016).

Gibeleko gaixotasunean E2F familiak duen eginkizunari dagokionez, deskribatu da *E2f1*aren defizientziak sagu diabetikoetan garatutako esteatosia hobetzen duela, nahiz eta saguak ez dauden obesitatearengandik ezta hiperglizemiarengandik babestuta (Denechaud, Lopez-Mejia et al. 2016). E2F1 fibrosiarekin erlazionatuta egon daiteke ere, zirrosia-NASH duten paziente eta saguetan gainadierazita baitago (Zhang, Xu et al. 2014).

PPAR-β-k duen E2f1, 2, 7 eta 8ren gaineko erregulazioa beharrezkoa da **gibelaren birsortze** egokia gerta dadin (Liu, H. X., Fang et al. 2013). Kontrara, beste ikerketa batzuek E2f1 gibelaren birsortze prozesuan ezinbestezkoa ez dela frogatu dute (Lukas, Bartley et al. 1999). Beste alde batetik, jakina da E2f2ak hepatektomia partzialaren osteko gibelaren hazkuntza egokian laguntzen duela (Delgado, Fresnedo et al. 2011), segur aski fosfatidilkolinaren (PC) eta fosfatidiletanolaminaren (PE) homeostasia mantentzeagatik (Maldonado, Delgado et al. 2014).

Ziklo zelularraren garapenean duten garrantzia kontuan harturik, Rb-E2F bidezidorreko mutazioak **minbizi** mota ugaritan gertatzen dira (Chen, Tsai et al. 2009). Ikuspegi tradizionalean oinarrituz, Rb-E2F bidezidorrak tumorogenesia induzitzen du RBren galera eta ondorengoko E2Fren estimulazioa dakartzaten alterazio genetikoen bidez, zelula-proliferazioaren erregulazioaren asaldua ematen delarik. Beraz, aktibatzaileak diren E2Fak onkogene jarrera izatea espero da eta beraien alterazioek barnean hartuko lituzkete funtzio-irabazi motako mutazioak, anplifikazioak eta gainadierazpenak. Bestalde, errepresoreak diren E2Fak tumore ezabatzaile moduan jardungo lukete eta funtzio-galera motako mutazioekin, delezio kromosomikoekin eta minbiziko epigenetika-isiltzearekin erlazionatuko lirateke. Nolanahi ere, inguruaren eta ehunaren arabera, E2F berdinek onkogene edo tumore-ezabatzaile moduan ekin dezaketela egiaztatu da (Chen, Tsai et al. 2009).

HCCari dagokionez, Rb funtzioaren inaktibazioa mekanismo genetiko, epigenetiko eta birikoengatik izaten da eta mutazio zuzenen bidez edo eraldatutako CDKen aktibitatearen bidez gertatzen da (Huntington, Tang et al. 2016). Izan ere, pRb-ren maila baxuak deskribatu dira giza-HCC kasu gehienetan, prognosi txarrarekin erlazionatzen dena (Palaiologou, Koskinas et al. 2012).

E2Ftako alterazioak ere behatu dira HCCn, portaera ikerketaren araberakoa den arren. Orokorrean, ikerketa gehienak E2F1ean oinarritzen dira, gehien aztertutako kidea. **E2f1**aren rol onkogenikoa finkatzen duen ebidentzia garrantzitsu bat da bere absentziak saguak DEN bidez induzitutako kartzinogenesiarengandik babesten dituela (Kent, Bae et al. 2017). Gainera, aurreratutako edota minbizi goiztiarra duten pazienteetan, *E2F1*aren adierazpena areagotuta dago eta *E2f1* kopien kantitatearen irabaziak HCCaren garapen espontaneoa ahalbidetzen du saguetan DNAren integritatea mantentzen duten itu-geneen aktibazio transkripzionalaren bidez (Kent, Bae et al. 2017). Bestalde, *E2F1*en gainadirazpena glukosan aberatsa den inguruan, zeina Warburg efektuarekiko antzekotasuna duen, handitutako ugalketarekin eta metastasiarekin erlazionaturik dago giza-HCCaren zelula-lerroetan (He, Huang et al. 2020). E2F1 apoptosiaren kontrako faktorea dela frogatu da giza eta sagu-HCCan (Zhan, Huang et al. 2014). Horren kontra, beste ikerketa batzuek egiaztatu dute E2f1k tumore-ezabatzaile moduan jardun dezakeela HCCn apoptosia induzitzen baitu (Palaiologou, Koskinas et al. 2012).

Askoz gutxiago dakigu gainerako E2F kideek HCCan duten eginkizunari buruz. Konkretuki, **E2F2**a E2F1aren rolekin erlazionatu izan da daukaten funtzio-antzekotasuna dela eta. Izan ere, E2F2ren adierazpena areagotuta dago HCC kohorteetan eta HCCaren zelula-lerroetan, zeina ondorio txarrekin erlazionatzen den (Zhan, Huang et al. 2014, Hong, Eun et al. 2019). Hala ere, giza-HCCan behatu den *E2F2*aren kopia kantitatearen galerak ezagutzera ematen du tumore-ezabatzaile moduan ekin dezakeela baita ere (Kent, Bae et al. 2017).

E2F8a ezik, rol bikoitza duena, gainerako E2F familiako kideek (E2F3-6) gibel-onkogenesian laguntzen dutela uste da, HCCan goranzko erregulazioa baitute (Zhan, Huang et al. 2014, Kent, Bae et al. 2017, Huang, Ning et al. 2019).

Transkripzio-faktoreen E2F familiak ziklo zelularraren garapen aproposa eta gorputz osoaren homeostasia sustatzen duenez, bidezidor honetako asalduek tumorogenesia eta eritasun metabolikoak dakartzate. Hala ere, E2F aktibatzaileen eta errepresoreen ikuspuntu kanonikoa ez dator bat behatutako E2Fren funtzio konplexuarekin, bereziki E2F1 eta E2F2ak HCCan duten eginkizunaren kasuan. Hori horrela

izanik, ikerketa gehiago behar da E2F1 eta E2F2ren arteko mekanismo komunak eta propioak bereizteko, baita obesitatearekin erlazionaturiko HCCarengan duten eragina ezartzeko ere.

B atala. HELBURUAK

B. HELBURUAK

Munduko Osasun Erakundearen (OME) datu-basearen arabera, obesitatearen prebalentzia hirukoiztu egin da azken 40 urteetan. Osasun-arazo honek ez du eragina garatutako herrialdeetan bakarrik, baizik eta gainpisuaren eta obesitatearen ratioak egun handitzen daude garatu gabeko herrialdeetan baita ere.

Obesitatea gibeleko asaldura metabolikoekin erlazionatuta dago, zeinak gibeleko lipido-metaketa eta gibel koipetsuaren gaixotasun ez-alkoholikoaren (ingelesezko *non-alcoholic fatty liver* disease, NAFLD) garapena ahalbidetzen dituen (Alzahrani, Iseli et al. 2014). Izan ere, paziente obesoen %90a baino gehiagok NAFLDa pairatzen du (Kumar, Priyadarshi et al. 2020). Ikerketa epidemiologikoek jakinarazi dute obesitatea organo ezberdinetan minbizia garatzeko arrisku-faktore bat dela, gibela kasu (Lauby-Secretan, Scoccianti et al. 2016). Kartzinoma hepatozelularra (HCC), gibel-minbizi primarioa, mundu mailan seigarren neoplasia gaizto arruntena da eta obesitatearekin loturiko minbiziagatiko heriotzen arrazoi nagusietako bat da (Michelotti, Machado et al. 2013). Mendebaldeko herrialdeetan, HCC kasuen %4-22a NAFLD-dun pazienteetan ematen da (Michelotti, Machado et al. 2013). Alabaina, NAFLDa jatorri duen HCCa induzitzen duten mekanismoak ez dira guztiz ezagutzen eta horrek gaixotasunaren diagnostiko goiztiarra mugatzen du.

Tumorearen eraketa eta garapena kontrol gabeko zelula-zatiketarengatik gertatzen da, zeina ondorengo nahasdura genetikoek ahalbidetzen duten: 1) onkogeneen funtzio-irabaztea edo 2) tumore-ezabatzaile diren geneen funtzio-galera (Grander 1998). Deskribatu denez (Schulze, Imbeaud et al. 2015, Cancer Genome Atlas Research Network. Electronic address: http://wheeler@bcm.edu, Cancer Genome Atlas Research Network 2017, Totoki, Tatsuno et al. 2011), HCCaren hainbat eta hainbat gidari daude, HCCaren ezaugarri heterogeneoak azaltzen dituena, neurri batean behintzat. Horietan gerta daitezkeen aldaerek (adierazpen mailan, aktibitatean eta asalduren arteko konbinaketan) tumore arteko heterogeneitatea eragiten dute tumorearen histologiari edota zelula-seinaleen bidezidorrei dagokionez (Molina-Sanchez, Ruiz de Galarreta et al. 2020). NAFLDari loturiko HCCaren fenotipoa analizatzerako orduan kontuan hartu beharko litzateke obesitateak, berez, nahasdura metabolikoak abiatzen dituela. Izan ere, obesitatea ezaugarri metaboliko jakinekin erlazionatzen da, zeinak metabolikoki osasuntsua den obesitatea (ingelesezko *metabolically healthy obesity*, MHO) eta metabolikoki ez-osasuntsua den obesitatea (ingelesezko *metabolically unhealthy obesity*, MUO) duten pazienteen arteko desberdintasuna ezartzen duten (Rangel-Huerta, Pastor-Villaescusa et al. 2019). Behin tumorea eratuta dagoela, minbizi-zeluletan

metabolismoa berprogramatzen da energia eta aitzindari-biosintetikoen beharrak ase daitezen (Grander 1998).

Transkripzio-faktoreen E2F familia berebizikoa da ziklo zelularra aurrera eramateko eta onkogene edo tumore-ezabatzaile moduan jardun dezake inguruaren eta zelula-motaren arabera (Huntington, Tang et al. 2016). E2Fen adierazpen handia dago gibel-ehun tumoralean, gibel-minbizian duten garrantzia aditzera ematen duena (Huang, Ning et al. 2019). Gainera, geroz eta ikerlan gehiago dago ezagutzera ematen ari direnak E2F1ak metabolismoan duen eginkizuna, zeina zelula-zikloarekiko independentea den. Hala ere, orain arte ez da jakin E2F1ak eta E2F2ak duten eragina gibel-gaixotasunaren garapenean eta kartzinogenesiaren indukzioan NAFLDan.

Aurrekari horiek kontuan hartuz, proposatu genuen **E2F1ak eta E2F2ak obesitateari loturiko NAFLDaren garapenean eta HCCrako bilakaeran parte hartzen duten bidezidor metabolikoak erregulatzen dituztela**. Testuinguru horretan, tesi honen xede konkretuak hurrengoak izan ziren:

1. helburua. Ikertzea E2F1ek edota E2F2k parte hartzen duten NAFLDaren garapenean eta HCCaren bilakaeran.

1.1. E2F1 edota E2F2 obesitateari-loturiko gibel-laginetan gainadierazita dagoen argitzea eta hori horrela bada, NAFLDaren garapenarekin erlazionatzen den ezagutzea.

1.2. Ikertzea *E2f1* edota *E2f2*aren defizientziak obesitateari loturiko NAFLDtik eta HCCtik babesten duen.

2. helburua. E2F1ak edota E2F2ak gidatzen dituzten asaldura metabolikoen mekanismoak identifikatzea obesitateari loturiko NAFLDaren garapenean eta HCCrako bilakaeran.

2.1. Ikertzea *E2f1*aren edota *E2f2*aren defizientziak egokitutako metabolismo lipidokoa saihesten duen obesitatean gertatzen den NAFLDan eta HCCan.

2.2. Argitzea *E2f1*aren edota *E2f2*aren absentziak obesitateari loturiko NAFLDan eta HCCan gertatzen den intsulinarekiko erresistentziatik babesten duen.

3. helburua. E2F1 eta E2F2 obesitatearekin erlazionatutako NAFLDaren biomarkatzaile goiztiar moduan baliozkotzea.

C atala. MATERIALAK ETA METODOAK

1. Materialak

1.1 Tanpoiak eta medioak

1.1.1 Zitokimika eta histokimikarako tanpoiak

- **Inmunohistokimikarako zitrato tanpoia.** %0.37 (p/b) azido zitriko monohidratoa eta %0.29 (p/b) sodio zitrato dihidratoa ur distilatuan (dH_2O); pH 6.
- **Sirius red tindaketarako I soluzioa.** %0.01 (p/b) Fast Green FCF saturatutako azido pikrikoan (Panreac, Espainia).
- **Sirius red tindaketarako II soluzioa**. %0.04 (p/b) Fast Green FCF, %0.1 (p/b) Sirius redean saturatutako azido pikrikoan (Panreac, Espainia).
- **Oil red O soluzioa. %**0.5 (p/b) Direct Red isopropanolean (Scharlau Chemicals, Espainia).

1.1.2 Gene adierazpenerako tanpoiak

- **RNA elektroforesirako karga-tanpoia (6 x).** %40 (p/b) sukrosa; %0.25 (p/b) bromofenol urdina; %0.25 (p/b) xileno zianola.
- **Tris-Acetato-EDTA (TAE) tanpoia. %**0.4 (b/b) azido azetiko glaziala (Panreac, Espainia); 10 mM EDTA; 40 mM Tris-HCl miliQ-H_2On; pH 8.5.

1.1.3 Aktibitate metabolikoetarako tanpoiak eta medioak

[^{3}H]-oleatoaren esterifikazioa triglizeridoan (TG):

- **Medioa**. 5 µCi/ml [^{3}H]-azido oleikoa (PerkinElmer, AEB) 20 µM azido oleiko hotzarekin 1 g/L glukosa duen eta ATCC etxekoa (AEB) den *Eagle's minimum essential* izeneko medioan (EMEM), 2 mM L- glutamina eta %0.5 (p/b) gantz-azido (GA) askerik gabeko behi seroalbumina (BSA) (Roche, Suitza) gehigarri.

β-oxidazio ratioaren saioa:

- **Homogeneizazio tanpoia.** 25 mM Tris-HCl, 500 nM sukrosa (Panreac, Espainia), 1 mM EDTA-Na_2 (Merck-Millipore, Alemania); pH 7.4.
- **Gibel-ehunean egindako β-oxidazio saiorako medioa**. 0.5 µCi/ml [1-^{14}C]-palmitatoa (PerkinElmer, AEB) eta 0.2 mM azido palmitikoa, 115 mM NaCl, 2.8 mM KCl, 10 mM Tris-HCl, 1.2 mM KH_2PO_4, 10 mM $NaHCO_2$,

0.2 mM EDTA-Na_2, %0.3 (p/b) gantz azido (GA) askerik gabeko BSA, 2 mM L-karnitina, 5 mM ATP, 0.5 mM malato eta 0.1 mM CoA gehigarri.

- **Zelula-kulturan egindako β-oxidazio saiorako medioa.** 0.5 µCi/ml [1-^{14}C]-palmitatoa (PerkinElmer, AEB) eta 0.2 mM azido palmitikoa 1 g/L glukosa duen EMEM medioan, %0.5 (p/b) GA askedun BSA gehigarri.

***De novo* lipogenesia (DNL):**

- **Gibel ehunean egindako DNLrako medioa.** 20 µCi/ml [^{3}H]-azido azetikoa (PerkinElmer, AEB) eta 20 µM sodio azetato hotza (Merck-Millipore, Alemania) 1 g/L *Dulbecco's Modified Eagle* (DMEM) izeneko medioan, zeinak 4 g/L glukosa eta 150 nM insulina (Novo Nordisc, Danimarka) duen.
- **Zelula kulturan egindako DNLrako medioa.** 20 µCi/ml [^{3}H]-azido azetikoa (PerkinElmer, AEB) 20 µM azido azetiko hotzarekin 2 g/L glukosa duen EMEM medioan, 2 mM L- glutamina eta 84 nM insulina gehigarri.

Glucose-6-fosfato dehidrogenasa (G6PDH) eta entzima malikoaren (ME) aktibitate-saioak:

- **Homogeneizazio tanpoia.** 150 mM KCl, 1 mM $MgCl_2$, 0.5 mM ditiotreitol (DTT) (Roche, Suitza), 10 mM N-azetilzisteina; pH 7.6.
- **Inkubazio tanpoia G6PDHren aktibitate-saiorako** 100 mM gizilglizina, 10 mM $NADP^+$ (Merck-Millipore, Alemania); 150 mM $MgSO_4$; 30 mM glucosa-6-fosfatoa; 2.4 mM NADPH (Merck-Millipore, Alemania); pH 8.
- **Inkubazio tanpoia MEren aktibitate-saiorako**. 0.4 M trietanolamina (TEA), 3.4 mM $NADP^+$ (Merck-Millipore, Alemania); 0.12 M $MnCl_2$; pH 7.4.

Lipolisia:

- **Lipolisirako medioa.** %4 (p/b) GA aske gabeko BSA duen 1 g/L DMEM (lipolisi basalerako), 20 µM isoproterenol bitartratoa gehigarri (estimulatutako lipolisirako).

1.1.4 *Western blotting*erako (WB) tanpoiak

- **Homogeneizazio tanpoia**. 10 mM NaF, %1 (b/b) NP-40, 2 mM Na_3VO_4, 150 mM NaCl, 50 mM azido 4-(2-hidroxietil)-1-piperazinoetanosulfonikoa (HEPES), %10 (b/b) glizerol (Merck-Millipore, Alemania), 10 mM $Na_4P_2O_7$, 2 mM EDTA-Na_2, 2 mM fenilmetanosulfonil fluoride (PMSF), 0.1 mM leupeptina (Fisher Scientific, AEB); pH 7.4.
- **Karga-tanpoia SDS-PAGErako (5 x)**. 300 mM Tris-HCl, %50 (b/b) glizerol; %10 (p/b) SDS; %25 (b/b) 2-merkaptoetanol, %0.04 (p/b) bromofenol urdina; pH 6.8

- **Nitrozelulosa-mintzean proteinak transferitzeko tanpoia.** 76.8 mM glizina, %0.04 (p/b) SDS, 10 mM Tris-HCl, %20 (b/b) metanol (Panreac, Espainia).
- **SDS-PAGE tanpoia.** 25 mM Tris-HCl; 192 mM glizina, %0.1 (p/b) SDS; pH 8.3
- **Tris-arekin indargetutako gatz disoluzioa, Tween 20 duena (TBST)**. 0.15 M NaCl, 20 mM Tris-HCl, %0.05 (b/b) Tween 20 dH_2On; pH 7.5.

1.1.5 Beste tanpoi batzuk

- **Bradford saiorako nahastea. %**0.01 (p/b) Coomassie Brilliant Blue G, %5 (b/b) etanol (Panreac, Espainia), %10 (p/b) H_3PO_4 dH_2On.
- **Fosfatoarekin indargetutako gatz-disoluzioa (PBS).** 0.14 mM NaCl, 3 mM KCl, 10 mM Na_2HPO_4, 1.2 mM KH_2PO_4 miliQ H_2On; pH 7.4
- **Nahaste kromikoa. %**50 (b/b) H_2SO_4 (Fluka Chemical, AEB), %0.5 (p/b) $K_2Cr_2O_7$ (Probus, Espainia).
- **Serum fisiologikoa (PS). %**0.9 (p/b) NaCl dH_2On.

1.1.6 Beste medio batzuk

- **Gene isilpenerako medioa.** 1 g/L glukosa duen EMEM, 2 mM L- glutamina eta %10 (b/b) behi-fetalaren serumarekin (FBS).
- **Zelulak mantentzeko medioa.** 1 g/L glukosa duen EMEM medioa, zeinak 100 IU/ml penicillina, 100 µg/ml estreptomizina, 2 mM L-glutamina eta ATCC etxeko (AEB) %10 (b/b) FBS duen.

Bestela zehaztu ezik, erreaktibo guztiak Sigma-Aldrich etxekoak dira (AEB).

1.2. Ekipamendua

Balantzak	Mettler PJ400 eta Mettler AT231 Delta rang
Berogailua	P Selecta Theroven (200 °C)
CO_2 inkubatzaileak	Thermo Scientific HeraCell 150
Dentsitometroa	Bio-Rad GS-800 eta Molecular Imager FX
Elektroforesi bertikala	Bio-Rad Mini Protean II
Elektroforesi horizontalak	Bio-Rad Sub-Cell GT agarose Gel Electrophoresis System
Elektroforesientzako energia-iturria	Bio-Rad Power 1000
Elektrotransferentzia kamera	Bio-Rad Trans-Blot Cell
Elikatzeko instrumentua	Instech Laboratories 20 GA 25 mm-ko herdoilgailtza den elikatzeko hodia
Espektrofotometroak	Nanodrop ND-1000 Spectophotometer eta Biotek Synergy™ HT plaka irakurgailua
Esposizio kamera	FUJI EC-AWU (18 x 24 cm^2)
Esterilizazioa	Biologia Zelularra eta Histologia Departamentuko zerbitzuko esterilizazio-makinaria, EHUko Medikuntza eta Erizaintzako Fakultatea
Glukometroa	Arkray Glucocard M
Hodi irabiagailuak	Heidolph REAX 2000 eta Duomax 1030
Homogeneizatzaileak	Kinematica Polytron PT 1200 C, B.Braun Biotech International eta Elvejhem Potter S
II motako segurtasun biologikorako kabinak	Thermo Scientific MSC-Advantage
Irabiagailudun bainu termostatikoa	P-Selecta Unitronic 320 OR
Izarniadura-kontagailua	PerkinElmer Tri-Carb 2810 TR
Kontzentradore-lurrungailua	Thermo Scientific Savant SC250EXP
Mikroskopio konfokala	Olympus Fluoviwe FV500
Mikroskopio optikoa	Carl Zeiss AG, Nikon Eclipse 50i eta Jenoptik ProgRes® CapturePro kamera
Mikrotomoa	Biologia Zelularra eta Histologia Departamentuko zerbitzua, EHUko Medikuntza eta Erizaintzako Fakultatea

Mikrozentrifugak	Heraeus Biofuge primoR eta Biofuge Fresco
pHmetroa	Crison GLP 21
Termozikladorea	Biometra T-Gradient Thermoblock
TLC kamera	Desaga
Ultracentrifugaren errotorea	Beckman Coulter 50.4 Ti
Ultrasoinuen sorgailua	Soniprep 150
Ultrazentrifuga	Beckman Coulter Optima™ L-100 XP
Zelulen kontagailu automatikoa	Bio-Rad TC 20™
Zentrifuga	Sorvall RT 7 (RTH-750 errotorea)

2. Ikerketa ereduak

2.1. Giza laginak

2.1.1. Giza laginen ebaluazio klinikoa eta laborategi-azterketa

Ikerketa honetan 80 gibel lagin erabili ziren. 18 lagin istripu zerebrobaskularraz hildako gibel-emaileenak ziren, Javier Crespo Dk.-k emandakoak, Marqués de Valdecilla Unibertsitate Ospitalea, Santander, Espainia. Gibel-biopsiak frogatu zuen laginak histologikoki normalak (NL) zirela eta ez zutela hepatitisaren B birusik (HBV), hepatitisaren C birusik (HCV) ezta giza inmunoeskasiaren birusik (GIB). Gorputzaren masa-indizea (GMI) 30 kg/m^2 baino baxuagoa zen gibel-emaile horietan.

62 paziente GMIa 30 kg/m^2 baino handiagoa duten paziente obesoak ziren, zeinei gibel-biopsia egin zitzaien diagnostiko bat lortzeko. Horietatik 15 pazientek NL zuten eta 47 pazienteei gibel koipetsuaren gaixotasun ez-alkoholikoa (NAFLD) diagnostikatu zitzaien Kleinerren irizpideen arabera (Kleiner, Brunt et al. 2005). Paziente obesoentzako inklusio-irizpideek kontutan hartzen zuten baita ere alkohol (< 20 g eguneko) edo potentzialki hepatotoxikoak diren sendagaien absentzia. HBV, HCV eta GIBaren serum testetan emaitza negatiboa zuten eta inork ez zuen eritasun autoimmunerik.

Ikerketa-lana bat zetorren Helsinki Adierazpenarekin baita lege lokal eta nazionalekin. Ospitale bakoitzeko eta Euskal Herriko Unibertsitateko (EHU) Giza Etikaren batzordeek ikerketa-prozedura guztiak onartu zituzten eta idatzizko baimen informatuak eskuratu ziren ikerketan parte hartu aurretik.

2.2. Animalia-ereduak

3 edo 9 hilabetetako *E2f1* knockout (*E2f1*$^{-/-}$), *E2f2* knockout (*E2f2*$^{-/-}$) eta dagokien sagu basati (ingelesezko *wild type* edo WT) (129/Sv x C57BL/6 anduia) arrak Ana Zubiaga Dk-aren laborategian ekoiztu ziren (Genetika, Antropologia Fisikoa eta Animalia Fisiologiako Departamentua, Zientzia eta Teknologia Fakultatea, EHU). *E2f1* eta *E2f2*ren ezabapena (ingelesezko *knock-down*) western blotting (WB) bidez frogatu zen (prozedura Materialak eta Metodoak, 3.9. atala behatu) (D1 irudia).

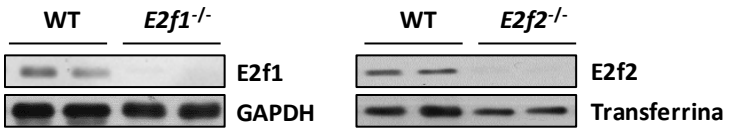

D1 irudia. E2f *knock-down*aren baliozkotzea 3 hilabetetako *E2f*$^{-/-}$ saguen gibelean. *E2f1* knockout (*E2f1*$^{-/-}$), *E2f2* knockout (*E2f2*$^{-/-}$) eta dagokien sagu basatiak (WT) erabili ziren. Saguak hiru hilabete zituzteneak sakrifikatu ziren eta gibela jaso zen. Gibeleko E2f1 eta E2f2 edukiera neurtu zen immunoblotting bidez glizeraldehido-3-fosfato deshidrogenasa (GAPDH) edo transferrina karga-kontrol moduan erabiliz (n=8 taldeko) (behatu prozedura Materialak eta Metodoak ataleko 3.9. sekzioan). Immunoblot adierazgarriak erakusten dira.

5-6 sagu ipini ziren kutxa bakoitzean. 22 °C-tan mantendu ziren, 12 ordu argi artifiziala (8:00tatik 20:00tara)/12 ordu iluntasun zikloarekin. Janaria eta txorrotako ura *ad libitum* eman zitzaien. Gorputz-masa eta jandako elikagai kantitatea bi astero neurtu zen. Jandako elikagai kantitatea determinatu zen egun bakoitzean sagu bakoitzak kontsumitutako gramoak bezala.

EHUko Animalien Ongizatearen Etika Batzordeak animaliekin egindako prozedurak onartu zituen eta bat zetozen Europar Batasuneko animaliekin ikertzeko araudiarekin.

2.2.1. Kartzinoma hepatozelularraren eta gibel koipetsuaren gaixotasun ez-alkoholikoaren garatu araztea

Park et al.-ek deskribatu zuten moduan, kartzinoma hepatozelularra (HCC) garatuarazi zen gibelarentzako kartzinogenikoa den dietilnitrosamina (DEN) emanez, gantzetan aberatsa den dietarekin (%60 gantz-kaloriadun F3282 sagu-dieta, Bio-Serv, AEB) (HFD) edo oinarrizko dietarekin konbinatuz (%20 proteinadun saguentzako F4031 kontrol-dieta, Bio-Serv, AEB) (CD) (Park, Lee et al. 2010) (D2 irudia). DEN (25 mg/sagu kg-ko, Sigma-Aldrich, AEB) intraperitonealki ziztatu zitzaien jaio osteko 14. egunean. Titia kendu eta gero, hilabete bateko adina zutenean, saguak HFDarekin (DEN HFD izeneko taldea) edo CDarekin (DEN CD izeneko taldea) elikatzen hasi ziren 32 astez eta 9 hilabeterekin (9m) sakrifikatu ziren. Adin berdineko beste talde batzuei serum fisiologikoa (ingelesezko *physiologic serum*, PS) eman zitzaien, CDarekin (CD izeneko taldea) edo HFDarekin (HFD izeneko taldea) konbinatuz.

NAFLD 3 hilabetetako (3m) saguetan ikertu zen. Horretarako, DEN edo PSa lehen deskribatu den bezala eman zitzaien eta saguak CD edo HFDarekin 10 astez elikatu ziren.

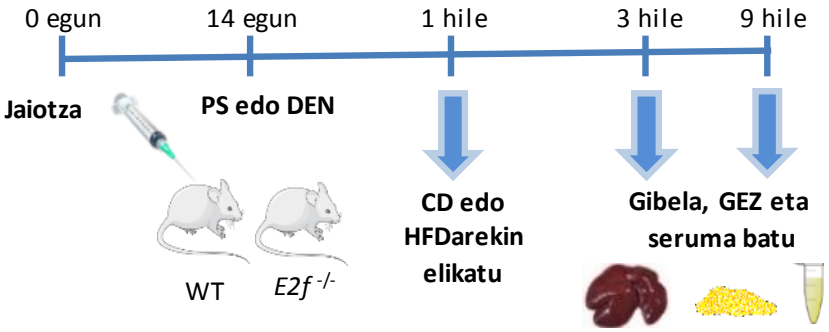

D2 irudia. HCC eta NAFLD saguetan gararazteko tratamenduak. Gibelarentzako kartzinogenikoa den 25 mg/sagu kg-ko dietilnitrosamina (DEN) dosia edo serum fisiologikoa (PS) intraperitonealki eman zitzaien 2 asteko adineko *E2f1* knockout (*E2f1*$^{-/-}$) eta *E2f2* knockout saguetan (*E2f2*$^{-/-}$) baita sagu basatietan (WT). Animaliei titia kendu zitzaien bi aste geroago eta oinarrizko dietan (CD) edo gantzetan aberatsa den dietan (HFD) mantendu ziren 3 edo 9 hilabeterekin sakrifikatu ziren arte. Orduan, seruma, gibela eta GEZa batu ziren. GEZ, gantz-ehun zuria; HCC, kartzinoma hepatozelularra; NAFLD, gibel-koipetsuaren gaixotasun ez-alkoholikoa.

2.2.2. Ehunen eta serumaren biltzea

Bestela espezifikatzen ez bada, saguek 4 orduko baraualdian egon ziren eta intraperitonealki injektatutako sodio pentobarbitalarekin (Abbott Laboratorios, Espainia) (60 mg/sagu kg-ko PSn) burutu zen eutanasia.

Beheko kaba zainan edo buztaneko zainan ziztatuz atera zen odola eta giro-tenperaturan (GT) koagulatzen utzi zen 30 minutuz. Seruma lortzeko, odola zentrifugatu zen 2,000 xg-tan 30 minutuz 4 °C-tan. Edozein frakzio zelular deuseztatzeko, gainjalkina berriz ere zentrifugatu zen 10,000 xg-tan 10 minutuz 4 °C-tan. Seruma jaso zen eta -80 °C-tan gorde zen analisiak egin ziren arte.

Gibela eta gantz-ehun zuria (GEZ) batu ziren eta PBS hotzetan garbitu. Ehunak azkar-azkar pisatu ziren eta gibeleko tumoreak zenbatu eta kalibragailu batekin neurtu ziren. Ondoren, ehunak zatitan moztu ziren segituan eta zatiak hurrengokoetarako erabili ziren: saio metabolikoetarako, formalinan (Sigma-Aldrich, AEB) edo Tissue-Tek® O.C.T. Compound-ean (VWR-Avantor, AEB) fixatzeko analisi histologikoetarako eta nitrogeno likidoan izoztu eta -80 °C-tan gordetzeko analisi biokimikoa egin arte.

2.3. Zelula-lerroak

Giza-hepatomaren HepG2 zelula-lerroa ATCC etxean erosi zen. Zelulak mantentze-medioan kultibatu ziren (Materialak eta Metodoak, 1.1.6 atala) 37 °C-tan eta %5 CO_2-n.

2.3.1. *E2F1* edo *E2F2*aren *knock-down*a

Isiltze edo *Knock-down* esperimentuak siRNA oligonukleotidoen alderantzizko transfekzioaren bidez burutu ziren. Balidatutako *E2F1*en kontrako siRNA (si*E2F1*) eta aurre-diseinatutako *E2F2*ren kontrako siRNA (si*E2F2*) (denak Ambion etxekoak, AEB) erabili ziren. Kontrol negatiboak ipini ziren saio bakoitzean Silencer™ Select Negative Control siRNA (siC) erabiliz (Ambion, AEB). siRNA bakoitzaren nukleotido-sekuentzia D1 taulan jasotzen dira.

D1 taula. HepG2 zeluletan geneak isiltzeko erabilitako siRNAen sekuentziak.

siRNA	Espeziea	Zentzuduna	Zentzu-kontrakoa
si***E2F1***	*Homo sapiens*	5'-GUCACGCUAUGAGACCUCATT-3'	5'-UGAGGUCUCAUAGCGUGACTT-3'
si***E2F2***	*Homo sapiens*	5'-GCCUCAUGGUUCUAGUAAATT-3'	5'-UUUACUAGAACCAUGAGGCCT-3'

Liofilizatutako siRNAk nukleasarik gabeko eta esterilizatutako urarekin (Ambion, AEB) nahastu ziren 50 mM-tan. Biltegiratzeko soluzio horiek -20 °C-tan gorde ziren. Lanerako soluzioak momentuan erabiltzeko prestatu ziren 1 mM-rreko kontzentrazioan. Zelulak saio bakoitzerako aproposak ziren plaketan hazi ziren. Baldintzak D2 taulan zehazten dira. siRNA, OptiMEM Reduced Serum (Gibco, AEB) eta RNAiMAX lipofektamina (Invitrogen, AEB) plaketan inkubatu ziren 20 minutuz GTn. Gero, gene-isilpenerako medioan (1.1.6. atala) zeuden HepG2 zelulak gehitu ziren siRNAk zituzten plaketan eta 48 orduz kultibatu ziren. Dagokion atalean deskribatzen da ikerketa metabolikoak nola egin ziren.

D2 taula. HepG2 zeluletan siRNAn alderantzizko transfekzioa egiteko baldintzak.

	Zitokimika	WB mRNA adierazpena	TG edukiaren neurtzea Erradioisopoen saioak
Plaka	24 putzukoa	6 putzukoa	60 mm-ko diametrokoa
siRNA nM	12	12	18
siRNA lan-soluzioa ul	6	30	53
RNAiMAX lipofektamina ul	1	5	9
OptiMEM ul	100	500	875
Zelulak	7.5 x 10^4 zelula 0.4 ml mediotan	4 x 10^5 zelula 2 ml mediotan	7.5 x 10^5 zelula 2 ml mediotan

Gene isilpenaren efizientzia RNA adierazpenaren analisiaren bidez (3.11 atala) konfirmatu zen (D5 irudia).

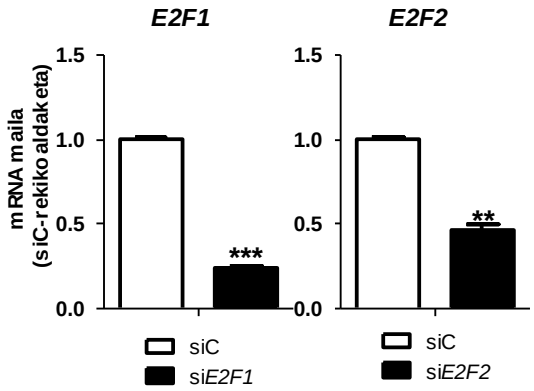

D5 irudia. Giza-tumore zeluletan *E2F1* edo *E2F2* isilpenaren baliozkotzea. *E2F1* (si*E2F1*) edo *E2F2* (si*E2F2*) HepG2 zelula-lerroan isildu ziren siRNA espezifikoen alderantzizko transkripzioaren bidez. Kontrol negatiboak (siC) erabili ziren saio guztietan. *E2F1* eta *E2F2*ren mRNA adierazpena analizatu zen rt-q-PCR bidez. Prozedura hori Materialak eta Metodoak, 3.11. atalean azaltzen da. Balioak 5 experimenturen batez bestekoak ± errore estandarra dira. si*E2F* eta siC arteko aldaketa esanguratsuak **p<0.001 eta *** p<0.0001 moduan adierazten dira (Student t-testa).

3. Prozedura esperimentalak

3.1. Histokimika eta zitokimika

3.1.1. Gibel-laginen prestaketa

Bestela zehazten ez bada, gibel zatiak indargetu gabeko %10 (b/b) formalinatan (Sigma-Aldrich, AEB) fixatu ziren 24 orduz 4 °C-tan eta %50 (b/b) etanoletan (Scharlau Chemicals, Espainia) mantendu ziren parafinizatu arte.

Parafina blokeak prestatu eta 5 µm-ko lodiko xafletan moztu ziren mikrotomoarekin. Xaflak polilisinarekin trataturiko mikroskopiorako portetan (Thermo Scientific, AEB) jaso ziren eta gau guztia fixatzen utzi ziren.

3.1.2. Hematoxilina eta eosina tindaketa

Parafinan txertatutako xafla xilenoan (Sigma-Aldrich, AEB) desparafinizatu zen, etanol (Scharlau Chemicals, Espainia) kontzentrazio murriztu mailakatuan doazen soluzioen bidez berridratatu zen eta ur destilatuarekin (dH_2O) garbitu zen. Ondoren, Shandon™ Harris Hematoxilinarekin (Thermo Scientific, AEB) tindatu zen 2.5 minutuz eta dH_2O-rekin garbitu. Laginari kolorea kendu zitzaion %0.5 (b/b) HCl-an (Merck-Millipore, Alemania) hondoratuz eta dH_2O-rekin garbituz. Ondoren, ehuna bertindatu zen Eosin-Y Alcoholic-arekin (Thermo Scientific, AEB) 25 segundoz, garbitu eta deshidratatu zen etanol kontzentrazioaren emendapen mailakatudun nahasketekin. Azkenik, laginak DPX Sigma-Aldrich, AEB) muntai-medioarekin muntatu ziren.

Mikrografia adierazgarriak hartu ziren 20 x objetiboarekin eta mikroskopio bertikalarekin.

3.1.3. Sirius red tindaketa

Fibrogenesia kolageno zuntzak Sirius redarekin tindatuz neurtu zen (Yata, Gotwals et al. 2002).

Parafinan txertatutako xafla desparafinizatu eta berridratatu zen. Behin hidratatuta, xafla Sirius red tindaketarako I soluzioan (1.1.1 atala) sartu zen 15 minutuz eta Sirius red tindaketarako II soluzioan (1.1.1 atala) beste 15 minutuz. Ondoren, %100 etanoletan (Scharlau Chemicals, Espainia) deshidratatu

zen eta Histo-Clear-ekin (National Diagnostics, AEB) garbitu. Azkenik, xafla muntatu zen DPX muntai-medioarekin (Sigma-Aldrich, AEB).

Mikrografiak digitalki hartu ziren 20 x objetiboarekin lehen esan bezala. Tindatutako kolageno-azalera FRIDA softwarearekin kuantifikatu zen gibel-xafla bakoitzean zoriz aukeratutako 5 eremutan.

3.1.4. Oil red O tindaketa

Esteatosi hepatikoa gibel-ehunean analizatu zen Oil red O tindaketaren bidez, zeinak lipido neutralak tindatzen dituen (Mehlem, Hagberg et al. 2013).

8 µm-ko lodieradun eta OCTn izoztutako ehun-xaflak moztu eta fixatu ziren %10 (b/b) indargetu gabeko formalinatan (Sigma-Aldrich, AEB) 2 minutuz. Ondoren, xafla %60 (b/b) isopropanolarekin (Scharlau Chemicals, Espainia) busti zen eta momentuan prestatutako Oil red O soluzioarekin (1.1.1 atala) tindatu zen. Gero, laginak %60 (b/b) isopropanoletan (Scharlau Chemicals, Espainia) ipini ziren eta Mayer Hematoxilinarekin (Sigma-Aldrich, AEB) bertindatu ziren minutu batez. Azkenik, urtsua den muntai-medioarekin (Dako, Danimarka) muntatu ziren laginak.

Mikrografia adierazgarriak 40 x objetiboarekin hartu ziren lehenago deskribatu bezala.

3.1.5. Ki67, E2F1 eta E2F2 analisi immunohistokimikoa

Immunohistokimika mota guztietan, gibel-xaflak desparafinizatu, berridratatu eta PBSrekin garbitu ziren. Ondoren, antigenoak berreskuratzeko, laginak zitrato tanpoian (1.1.4 atala) utzi ziren 20 minutuz 97 °C-tan eta irakin ez zezaten. Behin antigenoa berreskuratuta, xaflak blokeatu ziren %3 H_2O_2-PBStan egindako nahasketarekin 10 minutuz GTn. Atzealdeko zarata murrizteko, xaflak berriz ere blokeatu ziren 30 minutuz GTn. Ondoren, laginak antigorputz primarioarekin inkubatu ziren kamera umel batean. Antigorputz bakoitzari dagokion ber-blokeoa eta inkubazio baldintzak D3 taulan jasotzen dira. Jarraian, xaflak ImmPRESS™ untxi-kontrako eta errefau minaren peroxidasa (ingelesezko *horseradish peroxidase*, HRP) konjugaturiko antigorputz sekundarioan (Vector laboratories, AEB) inkubatu ziren 30 minutuz GTn. Detekzio kolorimetrikoa Vector VIP kromogeno morearekin (Vector laboratories, AEB) egin zen. Azkenik, laginak Mayer Hematoxilinarekin (Sigma-Aldrich, AEB) tindatu, txorrotako urarekin garbitu, deshidratatu eta DPX muntaia-medioarekin (Sigma-Aldrich, AEB) muntatu ziren lehenago deskribatu den bezala.

Mikrografiak digitalki hartu ziren 40 x objetiboarekin. Ki67 tindaketak, ziklo zelularraren progresioa S fasera ebaluatzen duena (Gerdes, Lemke et al. 1984), CellProfiler softwarearekin kuantifikatu zen, gibel xafla bakoitzean zoriz aukeratutako 5 eremutan positiboak ziren nukleoak zenbatuz. E2F1 edo E2F2rekin tindatutako nukleoko azalera FRIDA softwarearekin kalkulatu zen, paziente bakoitzerako ausazko 5 eremutan.

D3 taula. Analisi immunohistokimikoetan erabilitako antigorputz primarioen erreferentziak, ber-blokeorako nahasketak eta inkubazio baldintzak.

	Etxe komertziala	Katalogoko zenbakia	Ber-blokeorako nahasketak	Antigorputza inkubatzeko baldintzak	Ostalaria
Ki67	Abcam	AB66155	%10 ahuntz seruma PBSn	1:2000 (b/b) %2 (p/b) BSA-PBS Ordu 1 GTn	Untxia
E2F1	Abcam	AB94888	%5 ImmPRESS™ ahuntz seruma (Vector)	1:100 (b/b) Antigorputz diluentean (Dako) Gau osoz 4 °C-tan + ordu 1 37 °C-tan	Untxia
E2F2	Invitrogen	PA5-41473	%5 ImmPRESS™ ahuntz seruma (Vector)	1:100 (b/b) Antigorutz diluentean (Dako) 2 ordu 37 °C-tan	Untxia

BSA, behi seroalbumina; Dako, Dako (Danimarka); GT, Giro tenperatura; Invitrogen, Invitrogen (AEB); PBS, fosfatoarekin indargetutako gatz-disoluzioa; Vector, Vector Laboratories (AEB).

3.1.6. Lipido neutralen zitokimika

7.5 x 10^4 zelula esterilizatutako eta zirkularrak diren kristaletan hazi ziren, 24 putzuko plaka batean 2.3.1 atalean deskribatu den bezala. Gene-isiltzearen ostean, zelulak hiru aldiz garbitu ziren PBSarekin eta PBSn diluituriko %3.7 (b/b) (Panreac, Espainia) formaldehido nahasketarekin fixatu ziren. Zelula-iragazkortasuna lortzeko, lagina PBSn diluituriko %0.25 (b/b) Triton (Sigma-Aldrich, AEB) nahasketan inkubatu zen 5 minutuz GTn. Ondoren, 3 garbiketa egin ziren eta zelulak PBSan prestatutako %10 (b/b) FBS (Biochrom, EB) soluzioarekin blokeatu ziren 15 minutuz GTn.

Lipido baltsa neutralak Bodipy 493/503 tindagai fluoreszente berdearekin (1:200 PBSn) (Invitrogen, AEB) tindatu ziren 2 orduz GTn. Gero, kristalak garbitu egin ziren hiru aldiz soberako tindagaia kentzeko eta zelulen nukleoak DAPI tindagai urdin fluoreszentearekin (Sigma-Aldrich, AEB) (1:1000 PBSn) tindatu ziren 5 minutuz GTn. Azkenik, kristalak muntai-media urtsuarekin muntatu ziren (Dako, Danimarka). Irudi optikoak Olympus Fluoviwe FV500 mikroskopio konfokalarekin hartu ziren EHUko SGIker Mikroskopio Zerbitzuan.

3.2. Serumaren analisia

Neurtu nahi zen parametroaren arabera, odola buztaneko zainetik edo beheko kaba zainetik atera zen. Gero, seruma isolatu zen 2.2.2 atalean adierazten den bezala.

3.2.1.Transaminasa, lipido eta glukosaren kuantifikazioa

Serum alanina aminotransferasa (ALT), triglizerido (TG) totala, gantz azidoak (GA) eta glukosa eskuragarri dauden kit komertzialen bidezko metodo kolorimetrikoen saioekin kuantifikatu ziren. Horretarako, 96-putzuko plakak erabili ziren eta laginen bina aplikazio egin ziren saio bakoitzean.

ALT 4 orduko baraualdia egin ostean sakrifikatutako saguen beheko kaba zainetik ateratako serumean neurtu zen etxe komertzialaren gomendioak jarraituz. Laburki, serumaren 12 µl 15 µl-ko bolumenean diluitu ziren dH_2O-rekin. Gero, lagina 200 µl erreaktiborekin nahastu zen (R1:R2, 4:1) (Spinreact, Espainia) eta minutu batez inkubatu zen 37 °C-tan. Absorbantzia 340 nm-tan neurtu zen, minutu bateko tarteetan, 30 minutuz. 10 eta 20. minutuen arteko tartea aukeratu zen ATLren kontzentrazioa neurtzeko. Kalibrazio-zuzenerako erabili zen erreferentzia-tartea 129 eta 1548 µU bitartekoa izan zen. Datuak serum litroko dauden nazioarteko unitateetan adierazi ziren

Serum **TG**aren neurketa 13 orduko baraualdia egindako saguen buztaneko zainetik ateratako odolean egin zen, beti etxe komertzialeko argibideak jarraituz. Laburki, serumaren 7 µl 15 µl-ko bolumenean diluitu ziren dH_2O-rekin. Gero, erreaktiboaren 200 µl (Menarini Diagnostics, Italy) gehitu ziren laginera eta 5 minutuz inkubatu zen 37 °C-tan. Absorbantzia 500 nm-tan neurtu zen. Kalibrazio-kurba multikalibratzaile batekin egin zen (1.2- µg TG-tik 35.2 µg TG-ra) (Menarini Diagnostics, Italy) eta emaitzak serum dL-ko dagoen TG mg-tan adierazi ziren.

GAen determinazioa etxe komertzialaren gomendioen arabera burutu zen. Laburki, 13 orduko baraualdiaren ostean ateratako 3 µl serum 15 µl-ko bolumenera eraman ziren. R1 erreaktiboaren 160 µl (Wako Life Sciences, AEB) gehitu ziren serumera eta 2 minutuz inkubatu 37 °C-tan. Zuria den neurketa 546 nm-tan egin zen. Gero, R2 erreaktiboaren 80 µl gehitu ziren eta absorbantzia neurtu zen 37 °C-tan 4 minutuko inkubazioa egin ostean. GA kontzentrazioa zuriaren absorbantziaren balioa kenduz kalkulatu zen. Kalibrazio-zuzenerako erabili zen erreferentzia-tartea 0.5 eta 15 nmol bitartekoa izan zen. Emaitzak GAen µM bezala adierazi ziren.

Glukosaren kontzentrazioa glukometro batekin (Arkray Factory, Japonia) neurtu zen buztaneko zainetik ateratako odolean. Serum dL-ko glukosa mg bezala adierazi ziren datuak.

3.3. Tolerantzia testak

Intsulinarekiko erresistentzia (IR) glukosa, intsulina eta pirubatoarekiko tolerantzia testen bidez ebaluatu zen saguetan.

3.3.1. Glukosarekiko tolerantzia testa (GTT)

4 orduko baraualdia eta gero, saguei txorrotako urarekin prestatutako glukosa soluzio bat (2 g/sagu kg-ko) eman zitzaien saguei ahotik elikatzeko instrumentu aproposarekin (Instech Laboratories, AEB) (Andrikopoulos, Blair et al. 2008). Odoleko glukosa maila neurtu zen (3.2.1. atalean azaltzen den bezala) glukosarekin elikatu baino lehenago baita 15, 30, 60 eta 120 minutu beranduago.

3.3.2. Intsulinarekiko tolerantzia testa (ITT)

Intsulinarekiko sentikortasuna aztertzeko, saguak 4 orduko baraualdian mantendu ziren. Gero, PBStan diluitutako 0.75 U intsulina/sagu kg-ko injekzio intraperitonala jaso zuten (Sun, Miller et al. 2012). Glukosa maila GTTn bezala monitorizatu zen.

3.3.3. Pirubatoarekiko tolerantzia testa

Pirubatoarekiko tolerantzia testa egin zen glukogenesiaren aktibazioa determinatzeko, hots, pirubatotik abiatutako glukosaren biosintesia. Saguak 13 orduz mantendu ziren barauan eta PBSn disolbaturiko sodio pirubatozko nahasketa bat (2 g/sagu kg-ko) ziztatu zitzaien intraperitonealki (Song, Kim et al. 2013). Glukosa maila GTTn eta ITTn adierazten den bezala monitorizatu zen.

3.4. Gibeleko eta zeluletako lipidoen kuantifikazioa

3.4.1. Laginen prestaketa

Lipidoak **gibeletik** erauzteko, ehunaren 30 mg mekanikoki homogeneizatu ziren hotz zegoen PBSaren 10 bolumenetan beirazko Potter Elvehjem homogenizatzailearekin 20 kolpe emanez 700 rev/minuko abiaduran eta 4 °C-tan zegoen izotzeko bainu batean. Gero, 3.1.1 atalean adierazten denez, proteina kontzentrazioa neurtu zen.

Lipidoak **zeluletatikn** erauzteko, zelulak birritan garbitu ziren PBSarekin eta PBSren 1 ml-tan jaso ziren. 2,000 xg-tan zentrifugatu ziren 5 minutuz 4 °C-tan eta 1 ml dH_2O-tan berreseki. Laginek izozketa-desizozketa ziklo bina jasan zituzten zelula-apurketa segurtatzeko. Ondoren, proteina kontzentrazioa neurtu zen (3.10.1 atala behatu).

3.4.2. Lipido erauzketa

Lipidoak Folch metodoaren arabera erauzi ziren (FOLCH, LEES et al. 1957) gibel homogenatuko 1.5 mg proteinatik edo lagin zelularreko 1 mg proteinatik abiatuz. Kutsadura biologikoa ekiditeko, aurretik nahasketa kromikoarekin garbitutako beirazko materiala erabili zen.

Laginak 1.5 ml-tara diluitu ziren dH_2O-rekin eta kloroformo:metanol:HCl soluzioaren (1:2:0.0075, b/b/v) (Scharlau Chemicals, Espainia) 8 ml gehitu ziren. Hodiak irmo irabiatu ziren irabiatzaile batekin 2 minutuz. Ondoren, hodiak 2,000 xg-tan zentrifugatu ziren 12 minutuz 4 °C-tan, fase urtsua (gainekoa) eta fase organikoa (behekoa) bereizteko. Lipidodun fase kloroformikoa (behekoa) beste hodi batera transferitu zen beirazko Pasteur pipeta bat erabiliz. Ondoren, gainerako lipidoak berriz ere erauzi ziren fase urtsutik. Horretarako, kloroformo:metanol:HCl soluzioaren (1:2:0.0075, b/b/v) (Scharlau Chemicals, Espainia) 4 ml gehitu ziren eta aurretik deskribatu den bezala, hodiak irabiatu eta zentrifugatu ziren. Bereizitako fase organikoa jaso eta aurrekoari gehitu zitzaion. Gera zitekeen kutsadura urtsua deuseztatzeko, fase organikoa garbitu egin zen bolumen guztiaren hirurenean %0.88 (p/b) KCl nahasketa gehituz. Hodiak indar handiz irabiatu ziren irabiagailua batean minutu batez eta 2,000 xg-tan zentrifugatu ziren 12 minutuz 4 °C-tan. Ondoren, beheko fasea beste hodi batera transferitu zen.

Azkenik, laginak lehortu arte lurrundu ziren kontzentradore-lurrungailu batekin 45 °C-tan 1.5 orduz. Gibel edo zelula laginetik eratorritako lipido erauzkina 100 µl toluenotan (Scharlau Chemicals, Espainia) disolbatu zen eta N_2 atmosferarekin biltegiratu zen beirazko hoditxoetan -20 °C-tan analisiak egin zirene arte.

3.4.3. Lipido banaketa geruza fineko kromatografia bidez

Lipido erauzkina geruza fineko kromatografia (TLC) bidez banatu zen 6 garapenen bidez (Ruiz, Ochoa 1997).

Lehenik eta behin, 20 x 20 cm-ko silika-gelezko plakak (Pre-coated TLC-plates SIL-G25, Macherey-Nagel, Alemania) 1 mM EDTA-Na_2-rekin aurretratatu ziren 5 orduz gutxienez eta lehortzen utzi ziren gau osoan. Ondoren, ezpurutasunak deuseztatu ziren plakak kloroformo:metanol:HCl soluzioarekin (60:40:10, b/b/v) garbituz gau osoan zehar. Plakak 100 °C-tan 30 minutuz ipini ziren aktiba zitezen TLCa egin behar zen egun berean.

Lipido purudun patroien 3 µl (Avanti Polar Lipids and Sigma-Aldrich, AEB) eta lipido erauzkinen 3 µl ziztatu ziren plakaren beheko aldetik 1.5 cm-ra. Ondoren, jarraiko sei garapen kromatografiko desberdin burutu ziren polaritate murriztu mailakatua duten nahasketekin, D4 taulan erakusten den moduan. Garapen bakoitzaren ondoren, plakak lehortu egin ziren aire beroarekin.

Fase mugikorraren konposizioa	Proportzioa (v:v)	Distantzia abiapuntutik (cm)
Kloroformo:metanol:dH_2O	60:40:10	1.8
Kloroformo:metanol:dH_2O	65:40:5	2.3
Etil azetatoa: etanol:isopropanol: methanol:kloroformo:%0.25 KCl	35:20:5:15:22:9	5.5
Tolueno:dietil eter:etanol	60:40:3	8.5
n-heptano: dietil eter	94:8	12
n-heptano	100	13

D4 taula. Sei garapeneko geruza fineko kromatografian erabiltzen diren disolbatzaileen nahasketa lipido neutralak eta fosfolipidoak banatzeko.

3.4.4. Lipidoen ikusaraztea eta kuantifikazioa

Bereizketa kromatografiko guztiak egin eta gero, lipidoak kiskaldu egin ziren plaka %10 $CuSO_4$ (p/b) %8 H_3PO_4-an (b/b) prestaturiko nahasketan hondoratuz 10 segundoz. Jarraian, plaka aire beroarekin sikatu zen lehendabiziko lipido-puntuak nabarmendu ziren arte eta segituan plaka 200 °C-tan erre zen 3 minutuz.

TLC plakaren irudi bat digitalizatu zen GS-800 dentsitometroarekin (Bio-Rad Laboratories, AEB) (D2 irudia) eta kuantifikazioa Quantity One softwarearekin (Bio-Rad Laboratories, AEB) egin zen. Lipido-puntu bakoitzaren dentsitate optiko integratua (IOD), atzealdeko zarata kendu ostean, kalibrazio-kurbaren IOD balioetan interpolatu zen. Kalibraziorako lipidoen kantitate-tarteak (nmol) ondorengoak ziren: CE (0.09-1.45), TG (0.27-17), DG (0.15-3), FC (0.36-3.6), CL (0.02-0.3), PE (0.33-3.91), PI (0.1-1.72), PS (0.13-2.22) eta PC (0.63-7.63). Lortutako emaitzak mg proteinako nmol-etan adierazi ziren.

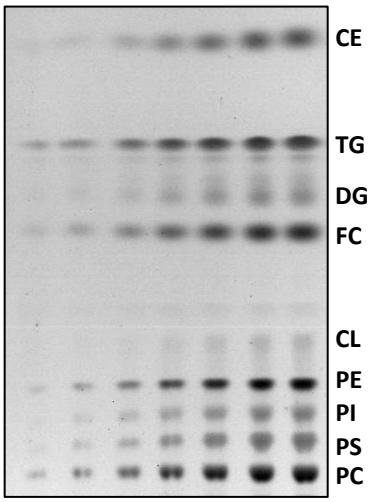

D2 irudia. 9 lipido purudun patroien TLC irudia. CE, kolesteril ester; CL, cardiolipina; DG, diazilglizeridoa; FC, kolesterol askea; PC, fosfatidilkolina; PE, fosfatidiletanolamina; PI, fosfatidilinositol; PS, fosfatidilserina eta TG, triglizeridoa.

3.4.5. Triglizerido kontzentrazioaren neurketa

Gibeleko eta zeluletako TGa neurtzeko, 3.2.1 atalean azaldutako saio entzimatikoa erabili zen.

Lipidoak erauzi (3.4.2 atala) eta 100 µl isopropanoletan (Scharlau Chemicals, Espainia) disolbatu ziren. Gibel-homogenatuko 5 µl edo zelula-esekiduraren 20 µl lipido-erauzkin erabili ziren. Isopropanol bolumen egokia gehitu zen kalibrazio kurbara. Lortutako emaitzak mg proteinako nmol-etan adierazi ziren.

3.5. Gibel-triglizeridoaren jariapen-ratioaren analisia

Gibeleko TGaren jariapena, oso dentsitate txikiko lipoproteinen (VLDL) gibel-ekoizpenaren ratioa adierazten duena, saguetan *in vivo* neurtu zen. Horretarako, animaliak 2 orduz baraualdian mantendu ziren esperimentua egin aurretik, odolean garraiatu dezaketen kilomikroiak deuseztatzeko asmoz.

VLDLren katabolismoa inhibitu zen PSan (1.1.5 atala) prestaturiko Pluronic F-127 (Poloxamer P-407) (Invitrogen, AEB) intraperitonealki ziztatuz 1 g/sagu kg-ko dosian, lipoproteina lipasaren inhibitzailea dena (Millar, Cromley et al. 2005). Injekzioa baino justu lehenago eta 6 ordu beranduago, odol laginak atera ziren eta TG kontzentrazioa neurtu zen komertzialki eskuragarriak diren kitak erabiliz (3.2.1 atala).

VLDLren gibeleko jariapen-ratioa kalkulatu zen Poloxamer ziztatu ondoren iragandako 6 orduetara zegoen serumeko TG mailaren desberdintasunetik. Lortutako emaitzak orduko mM bezala adierazi ziren.

3.6. Fluxu metabolikoen analisia erradioisotopoak erabiliz

Fluxu metabolikoak erradioisotopoen barneratzearen bidez kuantifikatu ziren. Esperimentu horiek *in vitro* HepG2 zeluletan, *in vivo* saguetan eta *ex vivo* gibel-ehunean burutu ziren.

3.6.1. Triglizeridoaren sintesia

TGaren sintesia bi eratan analizatu zen, ikertu nahi zen pausuaren arabera. Glizerolaren eta GAen arteko esterifikazioa analizatu zen TGan barneratutako [^{14}C]-glizerola edo [^{3}H]-oleatoa neurtuz eta TGaren *de novo* sintesia analizatu zen TGra barneratutako [^{3}H]-azetatoa neurtuz (D3 irudia).

D3 irudia. [^{3}H]-azetatotik edo [^{14}C]-glizeroletik abiatzen den eta TGra doan aztarna erradiaktiboa, zeina TGren sintesia neurtzeko den. ACC, azetil-KoA karboxilasa; Elovl, gantz-azil-KoA elongasak; GA, gantz-azidoa; GAS, GA sintasa; SCD, estearoil-KoA desaturasak; TG, triglizeridoa.

3.6.1.1. [^{14}C]-glizerolaren *in vivo* esterifikazioa triglizeridoan

Bi orduko baraualdiaren ostean, animaliei [^{14}C]-glizerol nahasketa (1.1.3 atala) ziztatu zitzaien intraperitonealki (Niebergall, Jacobs et al. 2011). 2 ordu beranduago, gibela jaso zen eta lipidoak erauzteko eta banatzeko erabili zen.

750 mg gibel homogeneizatu ziren 3.4.1 atalean deskribatzen den eran. Lipidoak erauzi ziren homogenatu bakoitzetik. Lipido erauzkina 200 µl toluenotan (Scharlau Chemicals, Espainia) disolbatu zen eta TLC bidez banandu zen (3.4.3 atala) jarraian azaltzen diren zenbait aldaerarekin. Kasu horretan, lagin bakoitzaren 30 µl aplikatu ziren aurre-tratamendurik gabeko plaketan eta TLCa 4 garapenekin burutu zen.

Metodo kromatografiko horrek hurrengoko lipidoak banatu zituen: PC, PE, FC, DG, TG eta CE. Fase mugikorreko disolbatzaile nahasketak D5 taulan adierazten dira.

D5 taula. Bost garapeneko geruza fineko kromatografian erabiltzen diren disolbatzaileen nahasketa lipido neutralak eta fosfolipidoak banatzeko.

Fase mugikorraren konposizioa	Proportzioa (v:v)	Distantzia abiapuntutik (cm)
Kloroformo:metanol:dH_2O	60:40:10	1.8
Kloroformo:metanol:dH_2O	65:40:5	2.3
Etil azetatoa: etanol:isopropanol: methanol:kloroformo:%0.25 KCl	35:20:5:15:22:9	5.5
n-heptano:diisopropileter:azido azetikoa	70:30:3	15
n-heptano	100	16

TLCa egin ondoren, lipidoak iodo lurrunekin tindatu ziren. Horretarako, iodo kristalak zituen kamera kromatografiko bat erabili zen. Plaka bertan sartu zen lipidoen banda horiak agertu ziren arte. TGari zegokion silika-banda jaso eta 4 ml Coctail BioGreen 3 izarniadura likidoa (Scharlau Chemicals, Espainia) zuten hodietan bota zen. Erradioaktibitatea izarniadura kontagailuan neurtu zen. Azkenik, lortutako emaitzak gibel-ehun gramoko dpm-tan adierazi ziren.

3.6.1.2. Triglizeridoan esterifikatutako [^{3}H]-oleatoa zelula-kulturan

Oleatotik abiatutako TGaren sintesia [^{3}H]-oleato bidez neurtu zen HepG2 zeluletan (Aspichueta, Perez et al. 2005). *E2F2* RNA knock-downaren ostean (2.3.1 atala), zelulak [^{3}H]-azido oleikoa zuten 1.5 ml medioan (1.1.3 atala) inkubatu ziren 120 minutuz 37 °C-tan eta %5 CO_2-tan. Gero, zelulak 5 aldiz garbitu ziren PBS hotzarekin eta 1 ml PBStan jaso ziren. Zelula-esekiduraren 100 µl proteina neurtzeko erabili ziren 3.10.1 atalean deskribatzen den moduan.

Lipidoak gainerako laginetik erauzi ziren (3.4.2. atala) eta TLC bidez bereizi (3.4.3 atala) jarraian azaltzen diren zenbait aldaketekin. Erauzkin lipidiko osoa 50 µl of toluenotan (Scharlau Chemicals, Espainia) disolbatu zen eta aurre-tratamendu gabeko plaketan aplikatu zen. Lipido guztiak hartu zirela segurtatzeko, beste 30 µl tolueno gehitu ziren laginak zeuden hodietara eta plakan aplikatu ziren. Hiru garapen kromatografiko egin ziren, ondorengo lipido espezieak banatzen zituenak: fosfolipidoak (PL), FC, DG, TG eta EC. Garapen bakoitzean erabili zen disolbatzaile nahasketa D6 taulan adierazten da.

D6 taula. Hiru garapeneko geruza fineko kromatografian erabiltzen diren disolbatzaileen nahasketa lipido neutralak eta fosfolipidoak banatzeko.

Fase mugikorraren konposizioa	Proportzioa (v:v)	Distantzia abiapuntutik (cm)
Kloroformo:metanol:dH_2O	60:40:10	1.8
n-heptano:diisopropileter:azido azetikoa	70:30:3	15
n-heptano	100	16

TGan barneraturiko [^{3}H]-oleatoaren kantitatea 3.6.1.1. atalean deskribatu den bezala neurtu zen. Lorturiko emaitzak zelula-proteinaren gramoko dpm-tan adierazi ziren.

3.6.1.3. Triglizeridoaren *de novo* lipogenesia

Lipidoen *de novo* lipogenesia (DNL) Aspichueta et al.-ek deskribatu zuten moduan (Aspichueta, Perez et al. 2005) analizatu zen zelula-kulturan edo gibel-ehunean.

DNLa **zeluletan** neurtu zenean, aurretik gene-isilpena eginda zuten HepG2 zelulak (2.3.1. atala) markatutako substratudun medio egokian (1.1.3. atala) inkubatu ziren 120 minutuz 37 °C-tan eta %5 CO_2-tan. Ondoren, 3.6.1.2 atalean adierazten denez, zelulak batu eta garbitu ziren, proteina neurtu zen eta lipidoak erauzi ziren.

DNLa **gibel-ehunean** analizatu zenean, saguak 3 orduz mantendu ziren baraualdian gibela batzeko sakrifikatu baino lehenago. Atera-berriko gibelaren 40 mg-ko ehun-zatiak inkubatu ziren [^{3}H]-azido azetikodun 700 µl DNL mediotan (1.1.3 atala) 4 orduz 37 °C-tan. Gero, ehun-zatiak 5 aldiz garbitu ziren PBS hotzarekin eta segituan izoztu ziren nitrogeno likidoarekin eta -80 °C-tan biltegiratu analizatu arte. Ehuna homogeneizatu zen (3.4.1. atala) eta lipidoak homogenatu guztitik erauzi ziren (3.4.2. atala).

Bi kasuetan, lipidoak TLC bidez bereizi ziren 3.6.1.2. atalean deskribatzen den eran.

TGan barneratutako [^{3}H] aztarna nola neurtu 3.6.1.1. atalean azaltzen da. Jasotako emaitzak zelula-proteinako edo gibel-ehun gramoko dpm-tan adierazi ziren.

3.6.2. Gantz-azidoen β-oxidazioaren ratioa

GAen β-oxidazioaren ratioa determinatu zen bi prozedura hauek neurtuz: [^{14}C]-palmitatoaren CO_2-rainoko oxidazioa totala eta [^{14}C]-palmitatoaren metabolito azido disolbagarrietarainoko (ASM) oxidazio partziala (Huynh, Green et al. 2014) (D4 irudia). ASMek barnean hartzen dituzte hurrengoko molekulak: azetil-KoA, azetil-karnitinak, gorputz zetonikoak (GZ) eta azido trikarboxilikoaren (ATZ) bitartekariak.

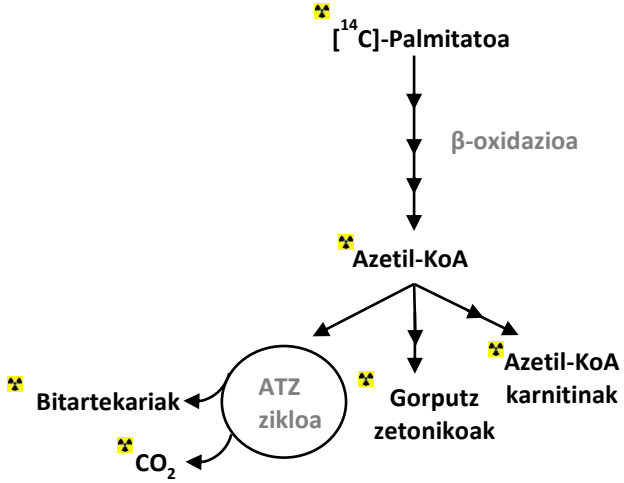

D4 irudia. Metabolito azido disolbagarrietan eta CO_2-an barnetaratzen den [^{14}C]-palmitatoaren aztarna erradiaktiboa. ATZ; azido trikarboxilikoaren zikloa.

Saioa **gibel-ehun** xafletan *ex vivo* egin zenean, saguek 3 orduko baraualdia izan zuten sakrifizioaren aurretik. Batu-berriko gibelaren 60 mg-ko zatiak homogeneizazio tanpoi (1.1.2. atala) hotzarekin homogeneizatu ziren (3.4.1. atala) beirazko Potter Elvehjem homogeneizatzailean 5 kolpe emanez. Gero, homogenatuak ultrasoinuekin tratatu ziren 6 mikroi-ko potentziarekin 10 segundoz izotzezko bainu batean eta 500 xg-tan zentrifugatu ziren 10 minutuz 4 °C-tan. Homogenatuaren gainjalkineko 500 µg proteina erabili ziren saioan 200 µl-ko bolumenean. Erreakzioa [1-^{14}C]-azido palmitikoa duen 400 µl saio-medio (1.1.3 atala) gehituz hasi zen. Laginak ordu batez inkubatu ziren 37 °C-tan 1.5 ml-tako hodietan, zeinak tapan disko formako Whatman kromatografia-papera (GE Healthcare, EB) zuzten. Erreakzioa 300 µl azido perkloriko (Scharlau Chemicals, Espainia) gehituz gelditu zen. Horrela, disoluzioan dauden gainerako ASMak eta oxidatu gabeko palmitato kateak soluziotik prezipitatzen dira. Erreakzioa gelditu baino justu lehenago, disko-paperak 1 M NaOH-rekin (Sigma-Aldrich, AEB) busti ziren,

zeinak TCA zikloan azetil-KoA oxidatzetik askatzen den CO_2 harrapatzea ahalbidetzen duen. Laginak GT 2 orduz inkubatu ziren.

Zelula-kulturan, aurretik gene-isilpena egin zitzaien HepG2 zelulak (2.3.1. atala) medio aproposaren (1.1.3. atala) 1.5 ml-tan inkubatu ziren 4 orduz 37 °C-tan eta %5 CO_2-an. Ondoren, medioa batu zen eta zentrifugatu zen 5000 xg-tan 5 minutuz. Gainjalkinaren 1000 µl beste hodi batzuetara transferitu zen. 1 M NaOH-rekin bustitako disko-papera ipini zen tapa bakoitzean eta erreakzioa gelditu zen lehenago deskribatu den bezala. Ondoren, laginak 2 orduz inkubatu ziren 37 °C-tan irmo irabiatzen zirelarik.

Inkubatu ostean, bi kasuetan, disko-paperak Optiphase HISAFE 2 izarniadura likidoaren (PerkinElmer, AEB) 4 ml zituzten beirazko hoditxoetara pasatu ziren. Disoluzio azidoa 21,000 xg-tan zentrifugatu zen 10 minutuz 4 °C-tan. Gainjalkinaren 400 µl Hionic Fluor izarniadura likidoaren (PerkinElmer, AEB) 4 ml zituzten plastikozko hoditxoetara pasatu ziren. CO_2 eta ASMetara loturiko erradioaktibitatea izarniadura-kontagailu batean neurtu zen. Erreakzioaren aktibitate espezifikoa kalkulatu ahal izateko, [^{14}C]-palmitatoaren aztarna inkubatu gabeko saio-medioan ere neurtu zen Coctail BioGreen 3 izarniadura likidoaren (Scharlau Chemicals, Espainia) 4 ml-rekin. [1-^{14}C]-palmitatoaren oxidatutako molak aktibitate espezifikoaren balioarekin determinatu ziren. Jasotako emaitzak gibel gramoko eta orduko oxidatu den [1-^{14}C]-palmitato nmol bezala adierazi ziren.

3.7. Gantz-ehun zuriaren lipolisia

Gantz-ehun zuriak (GEZ) TGa GA askeetan eta glizerolean hidrolizatzeko duen ahalmena neurtu zen 3 orduko baraualdian egon ziren saguen GEZ zati batu-berrietan (Gao, van der Veen et al. 2015).

Laburki, GEZaren 20 mg-ko zatiak lipolisi medio egokiaren (1.1.3. atala) 100 µl-tan inkubatu ziren 2 orduz. Jarraian, kultura-medioa berriztatu zen eta beste bi orduz inkubatu ziren ehunak. Kultura-medioak jaso ziren eta askatutako GA eta glizerola komertzialki eskuragarri dauden kit-ekin determinatu ziren. Medioaren 10 µl erabili ziren GAk neurtzeko (3.2.1. atala) eta 15 µl glizerola determinatzeko, azken hau 3.2.1. atalean adierazten den TGa kuantifikatzeko kit-aren bidez, zeinak glizerol askera neurtzen duen. Horretarako, balioak etxe komertzialaren argibideak jarraituz zuzendu ziren eta datuak GEZ gramoko µmol-etan adierazi ziren.

3.8. Glukosa-6-fosfato deshidrogenasaren eta entzima malikoaren aktibitateen analisia

Glukosa-6-fosfato deshidrogenasaren (G6PDH) (Betke, K., Brewer, G.J., Kirkman, H.N 1967) eta entzima malikoaren (ME) (Hsu RY 1967) aktibitateak espektrofotometria bidez neurtu ziren, behealdean adierazten den bezala, entzima hauek katalizatzen dituzten erreakzioetan ekoizten den NADPHa neurtuz:

$$\text{Glukosa-6-P} + \text{NADP}^+ \xrightarrow{G6PDH} \text{6-fosfoglukono-}\delta\text{-laktona} + \text{NADPH} + \text{H}^+$$

$$\text{L-Malato} + \text{NADP}^+ \xrightarrow{ME} \text{Pirubato} + \text{CO}_2 + \text{NADPH} + \text{H}^+$$

Neurketa hauetarako, gibelaren 40 mg homogeneizatu ziren (3.4.1. atala) homogeneizazio tanpoi aproposean (1.1.3. atala). Gero, homogenatua 105,000 xg-tan zentrifugatu zen ordu batez 4 °C-tan eta gainjalkina, frakzio zitosolikoari dagokiona, jaso zen (Buque, Martinez et al. 2010). G6PDH eta MEren aktibitateak neurtzeko, erauzkin zitosolikoen 60 eta 250 µg proteina erabili ziren hurrenez hurren, zeinak 1 µg/µl-ko kontzentraziora eraman ziren. Laginaren proteina totala Bradford saioaren bidez neurtu zen (3.10.2 atala).

G6PDHren 900 µl inkubazio-tanpoi eta MEren 400 µl inkubazio-tanpoi (1.1.3 atala) zituzten saio-hodiak aurreinkubatu ziren 5 minutuz 37 °C-tan. Erreakzioa saio-hodietara lagin kantitate egokia gehituz hasi zen. 5 minutu 37 °C-tan eta irabiatzen egon ondoren, erreakzioa hodiak izotzetan sartuz gelditu zen. Azkenik, ekoiztutako NADPH+H$^+$ neurtu zen 340 nm-tan.

Kalibrazio-kurbarako erabili zen patroien tartea 19 eta 84 nmol NADPH bitartekoa izan zen G6PDHren saiorako eta 28.8 eta 180 nmol NADPH bitartekoa MEren saiorako. Zuriari, lagina gehitu beharrean, dH_2O gehitu zitzaion eta NADPHren absentzian egin zen. Aktibitateak proteina mg-ko eta minutuko ekoiztu den NADPH nmol-etan adierazi ziren.

3.9. Western blotting

Gibel-ehuna 3.4.1 atalean azaltzen den eran homogeneizatu zen, horretarako aproposa den homogeneizazio tanpoia erabiliz (1.1.4 atala). Homogenatuak izotzetan irabiatzen mantendu ziren 30 minutuz proteinak disolbatu zitezen. Ondoren, laginak 16,000 xg-tan zentrifugatu ziren 30 minutuz 4 °C-

tan eta gainjalkina batu zen. Proteina totala gainjalkinetan neurtu zen (3.10.1 atala) eta laginak -20 °C-tan biltegiratu ziren analizatu arte.

Laginak 2 µg/µl-tan diluitu ziren karga-tanpoiarekin (1.1.4 atala) eta dH_2O-rekin, eta desnaturalizatu egin ziren 95 °C-tan berotuz 5 minutuz. Erauzkinaren 20 µg proteina banandu ziren %10 sodio dodezil sulfato- poliakrilamida gel elektroforesiaren (SDS-PAGE) bidez, baldintza desnaturalizatzailetan eta erreduzitzaileetan (Laemmli 1970), Mini Protean II electroforesi-makinaria bertikala (Bio-Rad, AEB) erabiliz 100 v-tan. PageRuler Plus Protein Ladder (ThermoFisher Scientific, AEB) erabili zen pisu molekularraren markatzaile moduan. Banatutako proteinak nitrozeluloasazko mintzetara (Amersham™ Protean™, 0.2 µm, GE HealthCare, EB) transferitu eta finkatu ziren elektroblot umelaren bidez Mini Trans-Blot cell (Bio-Rad, AEB) makinaria erabiliz 2 orduz 100 v-tan.

Jarraian, mintzak blokeatu ziren blokeo-tanpoiarekin ordu batez GTn eta antigorputz primario komertzialarekin inkubatu ziren gau osoa 4 °C-tan. Inkubazio-baldintza optimoak D7 taulan jasotzen dira. hurrengo egunean, mintzak 3 aldiz garbitu ziren Tween 20 gehigarri duen Tris-arekin indargetutako gatz soluzioarekin (TBST) (1.1.4 atala) eta HRP konjokatua duen antigorputz sekundarioarekin (TBSTn disolbaturiko %5 BSA (p/b) nahasketan prestatua) inkubatu zen ordu batez GTn (D7 taula). Beste hiru garbiketa ostean, proteina immunoerreaktiboak detektatu ziren ECL Western blotting detekziorako erreaktibo kimioluminiszentearekin (GE Healthcare, EB). RX-N X-Ray argazki-filmetan (Fujifilm, Japan) egin zen esposizioa esposizio-kasete bat erabiliz. Ondoren, filma errebelatu eta fixatu argazki-likidoekin (AGFA, Belgika) zen. Azkenik, digitalizazioa eta kuantifikazioa burutu ziren erreflexio bidezko dentsitometria bidimentsionala erabiiliz GS-800 dentsitometroa eta Quantity One softwarearekin (Bio-Rad, AEB).

D7 taula. Western blottingean erabilitako antigorputzen erreferentziak eta inkubazio-baldintzak.

	Itua	Etxea	Katalogo Zb.	Blokeo-tanpoia	Diluzioa	Ostalaria
Antigorputz primarioak	**E2f1**	SC	Sc-251	%5 NFDM-TBSTn	1:1,000	Sagua
	E2f2	SC	Sc-9967	%5 NFDM-TBSTn	1:1,000	Sagua
	PPAR-α	SC	Sc-9000	%5 NFDM-TBSTn	1:1,000	Untxia
	PPAR-γ	SC	Sc-7273	%5 NFDM-TBSTn	1:1,000	Sagua
	PGC-1α	SC	Sc-13067	%5 NFDM-TBSTn	1:1,000	Untxia
	PGC-1β	Abcam	Ab176328	%5 NFDM-TBSTn	1:1,000	Untxia
	CPT2	Abcam	Ab181114	%5 BSA-TBSTn	1:1,000	Untxia
	HNF4-α	Abcam	Ab201460	%5 BSA-TBSTn	1:1,000	Untxia
	GAPDH	Abcam	Ab8245	%5 BSA-TBSTn	1:20,000	Sagua

	Transferrina	SC	sc-22597	%5 NFDM in TBST	1:1,000	Ahuntza
Antigorputz sekundarioak (HRP-konjokatudunak)	**Sagu-kontrako IgG**	CST	7076	%5 BSA-TBSTn	1:2,000	Zaldia
	Untxi-kontrako IgG	CST	7074	%5 BSA-TBSTn	1:2,000	Zaldia
	Ahuntz-kontrako IgG	Thermo	31400	%5 BSA-TBSTn	1:10,000	Sagua

E2f1, E2f 1 transkripzio-faktorea; E2f2, E2f 2 transkripzio-faktorea; PPAR-α, peroxisoma proliferatzaileagatik aktibatutako alpha hartzailea; PPAR-γ, peroxisoma proliferatzaileagatik aktibatutako gamma hartzailea; PGC-1α, PPAR-γ-ren alpha koaktibatzailea; PGC-1β, PPAR-γ-ren beta koaktibatzailea; CPT2, karnitina 2 palmitoiltransferasa; HNF4-α, 4 alpha faktore nuklear hepatikoa; GAPDH, glizeraldehido-3-fosfato deshidrogenasa; Ig, immunoglobulina; HRP, Errefau minaren peroxidase, ingelesezko *Horseradish peroxidase*; CST, Cell Signaling Technology; SC, Santa Cruz; Thermo, Thermo Fisher Scientific; BSA, behi seroalbumina; NFDM, non-fat dried milk edo gantzik gabeko esne hautsa; TBST, Tris-arekin indargetutako salinoa Tween-20 gehigarri.

3.10. Proteina totalaren kontzentrazioaren determinazioa

Proteina totalaren kontzentrazioa detekzio kolorimetriko bidez neurtu zen. Jarraian burutu beharreko teknika gorabehera, azido bizinkoninikoan (BCA) oinarritutako teknika edo Bradford saioa erabili zen. Bi kasuetan, mikrosaioak birritan egin ziren 96 putzuko plaketan.

3.10.1. Azido bizinkoninikoan oinarritutako metodoa

Komertzialki eskuragarria den BCA erreaktiboa (ThermoFisher Scientific, AEB) erabili zen eta etxe komertzialaren gomendioak jarraitu ziren.

Gibel-homogenatutik eratorriko laginak ultrasoinuz aurre-tratatu ziren ehuna guztiz apurtu zedin. Horretarako, Soniprep-150 ultrasoinuen sorgailua erabili zen 6 micron-eko potentzian (3 ziklo, 30 segundo ON + 15 segundo OFF), beti laginak 4 °C-tan mantentzen zirelarik izotz-bainu batean beroa ekiditeko.

Saioan, gibel-homogenatuaren 0.15 µl edo zelula-esekiduraren 10 µl erabili ziren. Laginak H_2O-rekin diluitu ziren 100 µl arte. Ondoren, kit-eko A eta B substratuen nahasketaren (50:1) 100 µl gehitu ziren. Erreakzioa ilunpean inkubatu zen 37 °C-tan 30 minutuz eta absorbantzia 562 nm-tan neurtu zen.

Laginaren proteina kontzentrazioa kalkulatu zen BSArekin eraikitako kalibrazio-kurbaren (0-15 µg) absorbantzia-balioetan interpolatuz.

3.10.2. Bradford saioa

G6PDH edo MEren aktibitatearen analisirako (3.8 atala), proteina totalaren kontzentrazioa Bradford saioaren bidez kuantifikatu zen gibel-ehuna homogeneizatu eta gero, homogeneizazio tanpoiek BCA kit-arekin interferitzen duten sustantziak baitituzte.

Horretarako, 25 µl-ko bolumenean zegoen laginaren 2 µl aplikatu ziren birritan. Bradford erreaktiboaren nahasketaren (1.1.5 atala) 250 µl gehitu ziren eta ilunpean inkubatu zen 10 minutuz GTn. Absorbantzia 595 nm-tan neurtu zen eta 0 eta 7.5 µg BSA bitartekoa izan zen erabilitako kalibrazio-kurba.

3.11. Gene-adierazpenaren analisia

3.11.1. RNA erauzketa

RNA totala Trizol erreaktiboa (Invitrogen, AEB) erabiliz eta etxe komertzialaren argibideak jarraituz erauzi zen. Material guztiari kutsadura kendu zitzaion RNaseZap® soluzioarekin (Invitrogen, AEB) garbituz.

Gibel-laginetan, ehunaren 30 mg homogeneizatu ziren Trizol erreaktiboaren 1 ml-tan Polytron PT 1200 homogeneizatzailearen bidez, 30 segundoz 5 abiaduran eta izotz-bainu batean. Zelula-laginetan, gene-isilpena jasandako HepG2 zelulak zuzenean Trizol erreaktiboaren 1 ml-rekin askatu ziren kultura-plakatik.

Bi kasuetan, RNA erauzi eta DNasa (Invitrogen, AEB) tratamendua egin zitzaion DNA kutsadura ekiditeko asmoz. RNA kontzentrazioa neurtu zen absorbantzia 260 nm-tan neurtuz Nanodrop ND-1000 espektrofotometroan. 280 nm-tako absorbantzia neurtu zen baita ere, proteina kutsaduraren adierazlea. RNA lagina purua zela kontsideratu zen 260/280 ratioa 1.85 baino handiagoa zenean.

RNA kalitatea ere analizatu zen elektroforesi bidez. Karga-tanpoiarekin (1.1.2 atala) nahasturiko RNA laginaren 1 µg banatu zen Tris-azetato-EDTA (TAE) nahasketan disolbaturiko %1 (p/b) agarosazko (Laboratorios CONDA, Espainia) gela erabiliz elektroforesi-makinaria bertikalean (Bio-Rad, AEB). RNA 1:25 (b/b) Sybr safe™ DNA gelaren tindatzailearekin (ThermoFisher Scientific, AEB) ikustarazi zen.

3.11.2. Mikroarray analisia

Saguei emandako HCC-indukzio tratamenduaren bidez eraldatu ziren bidezidorren ikuspegi biologikoaz jabetzeko, gene-adierazpen profila burutu zen mikroarray bat eginez 9 hilabetetako *E2f2*$^{-/-}$ eta WT saguen gibeletan, zeinak DEN HFD edo kontrol tratamenduak jasan zituzten (n=4 baldintza bakoitzean).

Horretarako, RNA laginak erabili ziren. Lehenik eta behin, RNAren integritatea analizatu zen Agilent 2100 Bioanalizatzailean Agilent RNA 6000 Nano chip-ekin (Agilent Technologies, AEB), 28S/18S (RNA erribosomikoak) ratioa eta RNAren integritate-zenbakia (RIN balioa) estimatzen dituena.

RNA laginak markatu ziren eta hibridatu ziren “One-Color Microarray-Based Gene Expression analysis (Low Input Quick Amp Labeling)" 6.5 bertsioaren protokoloa (Agilent Technologies, AEB) erabiliz. Horretarako, RNA totalaren 50 ng erretrotranskribatu ziren AffinityScript alderantzizko transkriptasarekin (Agilent Technologies, AEB) T7 promotorera loturiko Oligo dT primerrak erabiliz. Anplifikatutako eta markatutako cRNA ekoizteko, kate bikoitzeko AffinityScript erretrotranskripzio bidez sintetizatutako cDNA *in vitro* transkribatu zen T7 RNA polimesarasarekin Cy3-CTPen presentzian. Markatutako laginak purifikatu ziren silikan oinarritutako RNeasy spin zutabeak (Qiagen, Alemania) erabiliz. Erreakzio bakoitzaren etekina eta aktibitate espezifikoa determinatu zen cRNA kuantifikatuz NanoDrop 1000 espektrofotometroan. Etekina > 0.825 µg eta aktibitate espezifikoa 3 < 6 pmol/µg zuten laginak kontsideratu ziren baliagarri.

Laginak analizatu ziren Agilent SurePrint G3 Mouse GE 8x60K (Diseinuaren 028005 identifikazioa) (Agilent Technologies, AEB) plataformaren bidez, zeinean saguaren 55,681 ezaugarri ordezkaturik dauden. Markatutako cRNA laginen 600 ng hibridatu ziren 65 ℃–tan 20 orduz. G2565CA DNA mikroarray eskanerrean eskaneatu ziren arrrayak eta irudiak Agilent Feature Extraction Softwarea (vs. 10.7.3.1) erabiliz prozesatu ziren.

Softwaretik ateratako datu gordinak GeneSpring GX 12.5 Softwarea (Agilent Technologies, AEB) erabiliz analizatu ziren. Datuak koantil normalizazioaz eta batez bestekoa erdiratuz normalizatu ziren, mikroarray guztietako gene-adierazpena konparagarria izatea ahalbidetzen duena. Kanpo utzi ziren ezaugarri uniformeak ez zituzten datuak, populazioz kanpokoak (ingelesezko *outliers*) edota datuak zeinetan ezaugarri-intentsitateek ez zuten gainditzen lagin guztien zarata-seinalea 4 baldintzetako batean.

Bi sagu-anduien arteko gene-adierazpen diferentziala LIMMA pakete estatistikoarekin analizatu zen (Smyth 2004) MultiExperiment Viewer (MeV) vs. 4.7.1 (http://www.tm4.org/mev/) aplikazioa erabiliz. Doitutako p-balioak (ingelesezko *adjusted p-values*, adj-p-value) Benjamini-Hochberg metodoa aplikatuz lortu ziren (False discovery rate, FDR) test-anizkoitzen zuzenketarako. Gero, DEN HFD eta CD tratamenduen arteko klase-anizkoitzeko konparaketa bat egin bi genotipoetan.

3.11.3. Mikroarrayaren analisi funtzionala

Gene-adierapen profilaren garrantzia biologikoa ezagutu zen bidezidorren aberastasun analisia eginez ClueGO (v2.3.3) aplikazioa erabiliz (Bindea, Mlecnik et al. 2009), Cytoscape plataformaren plugin bat (Shannon, Markiel et al. 2003) (http://www.cytoscape.org, v3.4.0). Geneak bidezidor biologikoetan biltzeko Reactome datu-basea (http://www.reactome.org) erabili zen (Croft, O'Kelly et al. 2011). Adierazpena aldatu zuten geneentzako inklusio irizpideak adj-p-value < 0.05 eta aldakuntza-tasa (ingelesezko *fold change*) > 1.35 izan ziren.

Mikroarray analisia, datuen aurreprozesamenduarekin eta analisi bioinformatikoarekin batera, EHUko SGIker zerbitzuko Gene adierazpenaren Unitatean burutu ziren.

3.11.4. cDNAren sintesia eta denbora errealean kuantifikatzailea den polimerasaren kate-erreakzioa (RT-qPCR)

Mikroarrayaren emaitzak balidatu egin ziren denbora errealean kuantifikatzailea den polimerasaren kate-erreakzioaren bidez (ingelesezko *real-time quantitative polymerase chain reaction*, RT-qPCR). Horretarako erretrotranskripzioa burutu zen RNA erauzkinaren 1.8 µg-tan SuperScript III First-Strand Synthesis System for RT-PCR kit-arekin (Invitrogen, AEB) etxe komertzialaren gomendioak jarraituz. Laginean RNA kutsadura ekiditeko, lehen cDNA katea zorizko primerren eta RNase OUT soluzioaren presentzian sintetizatu zen.

Aukeratutako geneen adierazpena (gainadierazitako batzuk, azpiadierazitako batzuk eta aldaketarik gabeko beste batzuk) EHUko SGIker zerbitzuko Gene adierazpenaren Unitatean neurtu zen BioMarkTM HD sistema eta *Dynamic Array Integrated Fluidic Circuits* (IFC) (Fluidigm Corporation, AEB) erabiliz. Protokoloa *Fluidigm's Fast Gene Expression Analysis* izan zen, EvaGreen aukeratuz BioMark HD sistemaren D1 bertsioan.

Itu-geneak espezifikoki aurreanplifikatu ziren Multiplex PCR Master kit-arekin (Qiagen, Alemania) (95 ˚C 15 minutu; 95 ˚C 15 segundoz eta 60 °C 4 minutuz duten 14 ziklo). Primerren 50 nM erabili ziren. Ondoren, soberako primerrak deuseztatu ziren Exo I kit-arekin (Thermo Scientific, AEB) etxe komertzialaren jarraibideen arabera. Laginak 1:5 diluitu ziren EDTA zuen Tris-EDTA tanpoiarekin eta 96.96 Dynamic Array IFC-an aplikatu ziren. SsoFastTM EvaGreen® Supermix kit-a Low ROX-arekin (Bio-Rad, AEB) erabili zen anplifikaziorako. GE Fast 96x96 PCR + Melt v2 protokoloa erabili zen PCRan.

Itu-geneak binaka aplikatu ziren. Kalibrazio-kurbarako kontrol laginen diluzio seriatuak aplikatu ziren, PCRaren anplifikazioa ebaluatzeko ere erabili zena. Azkenik, normalizaziorako gene-egonkortasuna NormFinder eta GeNorm algoritmoen bidez analizatu zen (De Spiegelaere, Dern-Wieloch et al. 2015) GenEx softwarea (MultiD 5.2 bertsioa) erabiliz. Sagutik eratorritako laginentzat, glizeraldehido-3-fosfato deshidrogenasa (Gapdh), TATA-kutxara lotzen den proteina (Tbp), A ziklofilina (Ppia) eta aktinaren (Actb) adierazpenak erabili

D8 taula. RT-qPCR analisian erabilitako oligonukleotidoak.

Bidezidorra	Genea	Espeziea	Sarrera zenbakia	Oligonukleotidoaren sekuentzia (5'- 3')	
DNA sintesia	***Tk***	*M. musculus*	NM_009387.2	F	CCACACATGATCGGAACACC
				R	GCCATCATTTCACAGAAATCCA
	Orc	*M. musculus*	NM_011015.2	F	TGGCCCTGTTCAGGTAGTGG
				R	GGCAGTGGTGCAAAGTCCTT
Mitosia	***Plk1***	*M. musculus*	NM_011121.4	F	TGTAGTTTTGGAGCTCTGTCG
				R	TCCCTGTGAATGACCTGATTG
E2F	***E2f1***	*M. musculus*	L21973.1	F	TGCCAAGAAGTCCAAGAATCA
				R	GCTTACCAATCCCCACCAT
	E2F1	*H. sapiens*	NM_005225.2	F	ATGTTTTCCTGTGCCCTGAG
				R	AGATGATGGTGGTGGTGACA
	E2f2	*M. musculus*	BC062101.1	F	AGGAGCTGAAGGAGCTGATG
				R	GGGAGCAACTCTGAATGAGC
	E2F2	*H. sapiens*	NM_004091.3	F	AGGCAGGGGAATGTTTGA
				R	TGCTCCGTGTTCATCAGC
Ziklinak	***Ccnd3***	*M. musculus*	U43844.2	F	ACTGGATGCTGGAGGTGTGTG
				R	CAATTGCGCCTTTCGGG
	Ccna2	*M. musculus*	NM_009828.3	F	GTTTCTCTTCTCAACCCACCAGA
				R	AAACTAAAACCCGACATAAAAACTGTACA
	Ccne1	*M. musculus*	NM_007633.2	F	GAAGGTGGCTCCGACCTTTC
				R	CATCCCAGGGCTGACTGCT
Lipido-oxidazioa	***Ppara***	*M. musculus*	NM_011144.6	F	GCAGTGCCCTGAACATCGAG
				R	CGTCTGATGAGCATGTCACTGTG
	Ppargc1a	*M. musculus*	NM_008904.2	F	AATGCAGCGGTCTTAGCACT
				R	ACGTCTTTGTGGCTTTTGCT
	Ppargc1b	*M. musculus*	NM_133249.2	F	CCTACCCACAAGGACAGCAT
				R	CTTTTACAGGACGCCAGGTC
	Rxra	*M. musculus*	NM_001290481.1	F	GTCAAGCAGCAGACAAGCAG
				R	TATGGAGCGGTGGGAGAA
	Acsl1	*M. musculus*	NM_007981.4	F	AGTGTGGGGTGGAAATCATC
				R	TTTGGGGTTGCCTGTAGTTC
	Acsm1	*M. musculus*	NM_054094.5	F	TGTGGCTTCTGAGTGTCCTG
				R	AGTATGGTCTGGGGATGCTG
	Acsm3	*M. musculus*	NM_212441.2	F	GGACACAAAACACGACGAGA

				R	ATCGGAGGCTATCAAATCCA
	Cpt1	*M. musculus*	NM_013495.2	F R	TCGAAAGCCCATGTTGTACAGC CATCAGTGGCCTCACAGACTCC
	Cpt2	*M. musculus*	NM_009949.2	F R	AATCCCTCAGAAATCCAGGCAC CTGCCCAGACATCTCGGTTC
	Acadl	*M. musculus*	NM_007381.4	F R	GTAAGAACGAACGCCAAAAGA TGATGAACACCTTGCTTCCA
	Acasb	*M. musculus*	NM_025826.4	F R	CGTTGCTCCTCTGGTTTCC CACCGATTTCTCCATTTTTGAG
	Acaa2	*M. musculus*	NM_177470.3	F R	CTTTTGCCCCTCAGTTCTTG GCCTCCACTCACATTGGTTT
Oxphos	***Ndufv1***	*M. musculus*	NM_133666.3	F R	ACGACAGCACCCAAGAAAAC TACCAGTCACCCCGTCTCA
	Ndufs7	*M. musculus*	NM_029272.3	F R	GCACGCTTACCAACAAGATG GTCACAGCCACGAACAACC
	Ndufs5	*M. musculus*	NM_001030274.1	F R	TCAAGAAACAGCGGGAGAAG TGAGGTGGAGGGGTGTATTT
	Sdha	*M. musculus*	NM_023281.1	F R	TATTGCTACTGGGGGCTACG TGGGGTGGAACTGAACAAAT
	Cyb5a	*M. musculus*	NM_025797.4	F R	CCTGGTGGAGAAGAAGTCCTAA TCCCCGATGATGTATGTTTTG
	Atpif1	*M. musculus*	NM_007512.4	F R	TCGGTGTCTGGGGTATGAAG TCAGCCTTTTCTCGTTTTCC
	Atp5a1	*M. musculus*	NM_007505.2	F R	TTTAGAGACAACGGCAAGCA CAGGCGGGAGTGTAGGTAGA
Lipogenesia	***Pparg***	*M. musculus*	AB644275	F R	CACTCGCATTCCTTTGACATC CGCACTTTGGTATTCTTCGAG
	Cd36	*M. musculus*	NM_001159558.1	F R	CCCTCCAGAATCCAGACAAC CACAGGCTTTCCTTCTTTGC
	G6pdx	*M. musculus*	NM_008062.2	F R	GGGAAGAGTTGTACCAGGGTG TTCAGGTAGAAGGCCATCCCG
	Scd1	*M. musculus*	NM_009127.4	F R	TGGCTGGGCAGGAACTAGTG TGTTCCCCAAGGGCTTCATC
	Scd2	*M. musculus*	NM_009128.2	F R	TTTGTACTATGTAATCAGCGCCC AGCCGTGCCTTGTATGTTCT
	Cidea	*M. musculus*	BC096649.1	F R	CTCGGCTGTCTCAATGTCAA GGAACTGTCCCGTCATCTGT
	Acaca	*M. musculus*	NJ5MYKM201R	F R	TGGTGCAGAGGTACCGAAGTG GTCGTAGTGGCCGTTCTGAAAG
	Fasn	*M. musculus*	NJ5SCE0G016	F R	GATCCTGGAACGAGAACACGATC GACATTTCCTGAAGTTTCCGCA
	Me2	*M. musculus*	NJ5TPBG1014	F R	TGCGACTTTTGAAGATGCAG TGGCTTTGATTACACCGTGA
	Me3	*M. musculus*	NJ5UDPPE016	F R	ATACTGGGCTTGGGAGACCT TAGCAGGACAGGAAGGCACT
Lipolisia	***Aadac***	*M. musculus*	AF306788.1	F R	CGTCTGATGAGCATGTCACTGTG TGAGAGCCATTGACTTTCTTTTGG
	Lipc	*M. musculus*	AY228765.1	F R	GGAAATCCCCTCCAAATCTCC CTCTGTTCCCACGCCTTGCT
GA garraioa	***Slc27a1***	*M. musculus*	BC028937.1	F R	CAGTGCCACCAACAAGAAGA CAGCTCGTCCATCACTAGCA
	Slc27a5	*M. musculus*	NM_009512.2	F R	TCATTGCTGACCCCCTCTAC TCCAGGTTCCTTCACACACA
VLDL metabolismoa	***Apob***	*M. musculus*	NM_009693.2	F R	GTGATCCCCACAGCAATAAGCA AGATTCCCAGGACCATGGAAAA
	Apoe	*M. musculus*	NM_009696.3	F R	TGGAGGCTAAGGACTTGTTTCG CTCGGCTAGGCATCCTGTCA
	Lpl	*M. musculus*	NM_008509.2	F R	GCCCAGCAACATTATCCAGT GGTCAGACTTCCTGCTACGC
Hantura	***Tnf***	*M. musculus*	NM_001278601.1	F R	ACGGCATGGATCTCAAAGAC GTGGGTGAGGAGCACGTAGT
	Il1b	*M. musculus*	NM_008361.4	F R	CAGGCAGGCAGTATCACTCA AGGTGCTCATGTCCTCATCC
	Il6	*M. musculus*	DQ788722.1	F R	TCCTTCCTACCCCAATTTCC GCCACTCCTTCTGTGACTCC

	Adgre1	*M. musculus*	NM_010130.4	F R	GAGCTTACGATGGAATTCTCCTTGTAT CACAGCAGGAAGGTGGCTATG
Fibrosia	***Tgfb1***	*M. musculus*	NM_011577.2	F R	CGCCATCTATGAGAAAACCA CCAAGGTAACGCCAGGAAT
	Acta2	*M. musculus*	NM_007392.3	F R	CCACCGCAAATGCTTCTAAGTC AGGAACTGGAGGCGCTGATC
	Col1a2	*M. musculus*	NM_007743.3	F R	AGGACACAGTGGTATGGATGG ACCTGGAGTTCCATTCTCTCC
	Col3a1	*M. musculus*	NM_009930.2	F R	AGAATGGGGAGACTGGACCT TGCCTTGTAATCCTTGTGGA
Gene normalizatzaileak	***Actb***	*M. musculus*	NM_007393	F R	ATCGCTGACAGGATGCAGAAG TCAGGAGGAGCAATGATCTTGA
	Gapdh	*M. musculus*	NM_001289726	F R	TATGACTCCACTCACGGCAAATT TCGCTCCTGGAAGATGGTGAT
	Tbp	*M. musculus*	NM_001004198	F R	AGCGGTTTGCTGCAGTCATC TCACTCTTGGCTCCTGTGCAC
	TBP	*H. sapiens*	BT019657.1	F R	TTCCGGGAGTCATGGCACCCT TCTTTGCAGTGACCCAGCAGCATC
	Ppia	*M. musculus*	NM_00890	F R	CCAAGACTGAGTGGCTGGATG GCTCCATGGCTTCCACAATG
	HBMS	*H. sapiens*	M95623.1	F R	CACCCACACACAGCCTACTT ACACTGTCCGTCTGTATGCG

ziren normalizazio-faktoreak kalkulatzeko. Zelula-laginetan, TATA-kutxara lotzen den proteina (TBP) eta hidroximetilbilano sintasa (HBMS) izan ziren normalizazio-geneak. Primerrak Primer3 softwarea erabiliz diseinatu ziren eta Invitrogen (AEB) enpresak sintetizatu zituen. Itu-geneak analizatzeko erabilitako primerrak D8 taulan jasotzen dira.

3.12. Analisi estatistikoa

Aurkeztutako emaitzak talde bakoitzeko “n” animalien batez besteko aritmetiko ± batez bestekoaren errore estandarra (ingelesezko *standard error of the mean* edo SEM) dira. Datuen analisi estatistikoa test desberdinen bidez egin zen GraphPad softwarean. Bi talderen arteko desberdintasunak parekatu gabeko Student t testaren bidez analizatu ziren. Bi bideko bariantzaren analisia (ANOVA) eta Bonferroniren post-testa erabili ziren bi talde baino gehiago alderatzeko.

Esangura estatistikoa horrela adierazi zen:

- *E2f1*$^{-/-}$ vs WT: * p<0.05, ** p<0.01 and *** p<0.001
- *E2f2*$^{-/-}$ vs WT: * p<0.05, ** p<0.01 and *** p<0.001

- DEN HFD vs CD: # p<0.05, ## p<0.01 and ### p<0.001
- DEN CD vs CD: # p<0.05, ## p<0.01 and ### p<0.001
- HFD vs CD: # p<0.05, ## p<0.01 and ### p<0.001

- si*E2F1* vs siC: * p<0.05, ** p<0.01 and *** p<0.001
- si*E2F2* vs siC: * p<0.05, ** p<0.01 and *** p<0.001

- NL ez-obesoak vs NL obesoak: * p<0.05, ** p<0.01 and *** p<0.001
- NL ez-obesoak vs NAFLD obesoak: * p<0.05, ** p<0.01 and *** p<0.001
- NL obesoak vs NAFLD obesoak: * p<0.05, ** p<0.01 and *** p<0.001

F atala. ONDORIOAK

F atala. ONDORIOAK

1. E2F1 eta, bereziki, E2F2 transkripzio faktoreek obesitateari loturiko NAFLDaren garapenean eta HCCrako bilakaeran jarduten dute.

1.1. Bai E2F1 bai E2F2 gainadierazita daude NAFLDa duten paziente obesoetan eta *E2f2* gainadierazita dago baita ere obesitatearekin erlazionatutako NAFLDaren eta NAFLDari loturiko HCCaren sagu-ereduetan, zeinak transkripzio faktore hauek proesteatotikoak eta onkogenikoak direla iradokitzen duen.

1.2. E2f1 eta, batik bat, E2f2aren absentziak obesitatearekin loturiko NAFLDaren garapena prebenitzen du. *E2f1* edo *E2f2* faltan duten saguek ez dute hepatoesteatosirik ezta NAFLDaren indukzio-tratamenduek eragindako gibel-hanturarik, transkripzio faktore hauek obesitatearekin lotutako NAFLDan premiazkoak direla erakutsiz.

1.3. *E2f1* eta E2f2aren defizientziak erresistentzia ematen du NAFLDarekin loturiko HCCarekiko eta horrekin erlazionatutako fibrosiarekiko eta lipido metaketarekiko, bai E2f1 bai E2f2a prozesu horietan beharrezkoak direla adieraziz.

2. E2f2 transkripzio faktoreak obesitatearekin loturiko NAFLDaren garapenean eta HCCarekiko bilakaeran ematen den berprogramazio metabolikoa koordinatzen du.

2.1. E2f2ak gibeleko lipido-biltegiratzean ekiten duten bidezidor metabolikoak kontrolatzen ditu gibel-gaixotasunaren fase goiztiarretik. Babes mekanismo bezala, saguetako *E2f2*aren defizientziak NAFLD eta NAFLD-HCCarekin lotutako dislipemia eta areagotutako TGen sintesia baita xurgapena saihesten ditu. Bestalde, handitutako gantz-azidoen (GA) oxidazioak (GAO) NAFLDarekiko eta HCCarekiko erresistentzia ahalbidetzen du *E2f2* knockout saguetan, areagotutako mitokondrioarekiko GAen garraioaren bidez.

2.2. Profil lipidikoa hobetzeaz gain, *E2f2*aren defizientziak obesitatearekin lotutako NAFLDaren fase goiztiarretako intsulinarekiko erresistentzia (IR) prebenitzen du saguetan, baina ez NAFLD-HCCarekin erlazionaturikoa.

3. *E2F1 eta, batez ere, E2F2a obesitatearekin lotutako NAFLDaren markatzaile prognostiko eta potentzialak dira.* *E2F1 eta E2F2 NAFLDa duen ala ez duen obesitatean induzitzen dira. Gainera, gibeleko E2F2 edukiaren handitzea oraindik ere nabarmenagoa da NAFLD garatzen denean.*